Towards an Understanding of the Mechanisms of Acellular Zone Formation in Sutured Tendons

A thesis submitted to The University of Manchester for the degree of
Doctor of Philosophy
in the Faculty of Medical and Human Sciences

2010

Sarah Al Youha

School of Medicine

CONTENTS

Final word count: 32,237

LIST OF FIGURES

LIST OF TABLES

Abstract

Fibrotic diseases account for an estimated 45% of the total number of deaths in the developed world (Wynn 2007). Tendons are an excellent model for studying the dysregulated response which leads to fibrosis, as tendons have an organized, parallel matrix, in which tissue defects could easily be distinguished. Wong et al. (2006b) demonstrated the presence of a bell-shaped region around sutures in tendons that was devoid of cells in histological sections. The mechanisms of the formation of this acellular zone, that was also noted in cornea and cartilage (Matsuda et al. 1999; Hunziker and Stähli 2008), were unknown. It was hypothesized that the acellular zone was formed by cell death and that suturing caused alterations to the extracellular matrix of sutured regions of tendon, which made the acellular zone refractory to cellular re-population.

The acellular zone was tracked in sutured tendons for up to a year to determine the temporal properties of the acellular zone. Electron microscopic and time lapse studies were carried out to determine if the acellular zone formed by cell migration or cell death. Microarray analysis was conduced to confirm this and to reveal potential molecular targets for future studies. The extracellular matrix of sutured tendons was studied by electron, atomic, scanning and polarized light microscopy and mechanical measurements were obtained using nanoindentation.

It was concluded that the acellular zone formed within 24 hours and persisted for up to a year. Tension and size of the suture's grasp were also shown to be important for acellular zone formation. Cell death was the main effector of acellular zone formation. Microarray analysis showed evidence of upregulation of inflammatory mediators and programmed necrosis pathways. The sutured extracellular matrix was denser, more disorganized and had a lower Young's modulus than unsutured regions of the same tendon. These differences in the properties of the extracellular matrix of sutured tendons may be the cause of the persistence of the acellular zone.

Declaration

I declare that no portion of the work referred to in the thesis has been submitted in support of an application for another degree or qualification of this or any other university or other institute of learning.

Copyright Statement

(i) The author of this thesis (including any appendices and/or schedules to this thesis) owns certain copyright or related rights in it (the Copyright) and s/he has given The University of Manchester certain rights to use such Copyright, including for administrative purposes.

(ii) Copies of this thesis, either in full or in extracts and whether in hard or electronic copy, may be made only in accordance with the Copyright, Designs and Patents Act 1988 (as amended) and regulations issued under it or, where appropriate, in accordance with licensing agreements which the University has from time to time. This page must form part of any such copies made.

(iii) The ownership of certain Copyright, patents, designs, trade marks and other intellectual property (the Intellectual Property) and any reproductions of copyright works in the thesis, for example graphs and tables (Reproductions), which may be described in this thesis, may not be owned by the author and may be owned by third parties. Such Intellectual Property and Reproductions cannot and must not be made available for use without the prior written permission of the owner(s) of the relevant Intellectual Property and/or Reproductions.

(iv) Further information on the conditions under which disclosure, publication and commercialisation of this thesis, the Copyright and any Intellectual Property and/or Reproductions described in it may take place is available in the University IP Policy (see http://www.campus.manchester.ac.uk/medialibrary/policies-/intellectual-property.pdf), in any relevant Thesis restriction declarations deposited in the University Library, The University Librarys regulations (see http://www.-manchester.ac.uk/library/aboutus/regulations) and in The Universitys policy on presentation of Theses.

Acknowledgements

I would like to express my deepest gratitude to my supervisors; Karl Kadler, Jason Wong and Gus McGrouther and my advisor John McLaughlin. Thank you for the opportunities, the mentorship, the guidance and encouragement.

To past and present members of the Kadler Lab: Chloé, Sue, Zoher, David, Hui, Nick, Marisa and Liz. Thank you for making being in the lab so enjoyable, yet educational! I really appreciate all the help and already miss the coffee breaks.

I would also like to thank: Mike Sherratt and David Holmes for providing guidance in my final year; Leo Zeef for help with the microarray; Samantha Forbes and Hui Lu for electron microscopy help; Emily from Manchester's BSF; Nigel Hodson for help with Atomic Force Microscopy; Riaz Akhtar and Alistaire Selby for help with nanoindentaiton; Xuegen Zhoa for help with scanning acoustic microscopy, Nawsheen Alam, for helping me in my first year and Jason Wong for help with the surgeries.

Thank you to my friends: Fay and Farah, Waleed, Ayoub, Lucie, Kirsty, Bader and Tariq for being so supportive.

Lastly but most importantly, thank you to my family: Noura, Nada, Mama and Baba for being so understanding and patient. I could not have survived the past three years without you.

Abbreviations

AFM	Atomic Force Microscopy
ANOVA	Aanalysis Of Variance
CCA	Congenital Contractural Arachnodactyly
CMAC	Cell-Matrix Adhesion Complex
CO_2	Carbon Dioxide
Cx	Connexon
DAVID	Database for Annotation, Visualization and Integrated Discovery
DMEM	Dulbecco's Modified Eagle's Medium
DNA	Deoxyribonucleic acid
ECM	Extracellular Matrix
EDTA	Ethylenediaminetetraacetic acid
EM	Electron Microscopy
FACIT	Fibril Associated Collagens with Interrupted Repeats
FDP	Flexor Digitorum Profundus
FDS	Flexor Digitorum Superficialis
H&E	Haematoxylin and Eosin
IMS	Industrial Methylated Spirit
KEGG	Kyoto Encyclopedia of Genes and Genomes
MAPG	Microfibrilar-associated glycoprotein
MAPK	Mitogen-activated protein kinase
MMP	Matrix Metalloproteases
NCCD	Nomenclature Committee on Cell Death
Nec-1	Necrostatin-1
OsO_4	Osmium Tetraoxide
PBS	Phosphate Buffered Soultion
PCA	Prinicipal Components Analysis

qPCR	Quantitive polymerase chain reaction
RIP	Receptor-interacting proteins
RNA	Ribonucleic Acid
S	Sutured
SAM	Scanning Acoustic Microscopy
SLRP	Small Leucine Rich Repeats
SPSS	Statistical Package for the Social Sciences
T	Under tension
TBE	Tris/Borate/EDTA
TEM	Transmission Electron Microscopy
TRITC	Tetramethyl Rhodamine Iso-Thiocyanate
TUNEL	Terminal deoxynucleotidyl transferase dUTP nick end labeling
UnS	Not sutured
UnT	Not under tension

Part I

Introduction

CHAPTER 1

INTRODUCTION

1.1 Scope of the Research

It has been estimated that 45% of the total number of deaths in the developed world are caused by some type of fibrotic disease (Wynn 2007). Fibrotic disease are characterized by the replacement of the normal extracellular matrix of tissues by an abnormal, disorganized, collagen-rich matrix. This abnormal matrix can form after any chronic injury, causing organ dysfunction, which can manifest as heart failure, pulmonary fibrosis, progressive kidney disease and liver cirrhosis (Wynn 2008). One area where this formation of excessive fibrotic scar tissue is problematic and has not been studied in detail, is after surgical repair. Although around 50 million surgeries are performed in the United States of America (USA) alone, the effects of surgical repair on tissue architecture have not been well characterized (Dubay and Franz 2003). Wound failure at the suture site can have serious consequences, giving rise to complications such as pseudoaneurysms, fascial dehiscence, incisional hernias and gastrointestinal anastomotic leaks, which can have mortality rates of almost 50% (Carlson 1997).

Tendons are an excellent model to study this dyregulated response to injury. Ten-

dons are cord-like structures, which connect muscle to bone, acting mainly as force transmitters (Benjamin et al. 2008). The organized extracellular matrix of tendons makes them an ideal candidate to study defects in the organization of the extacellular matrix. Tendons are also notorious for their poor healing capabilities. In one study, the mean rehabilitation time after a tendon injury was approximated to be 130 days (Chan et al. 2006). The lengthy treatment period associated with tendon injuries places a significant financial burden on society. It has been estimated that tendon injuries cost the USA's economy $30 billion per year. By elucidating the causes of the poor healing response of tendons after surgical repair insight can be gained, which can used to improve tissue healing.

A potential source of surgical repair failure has been identified by Wong et al. (2006b). who described a region devoid of cells around the suture site in tendons. The research presented in this thesis, shows that this acellular region in sutured tendons is caused by direct physical damage to the tendon cells by the suture. It was also found that this acellular region is refractory to healing, as it remains permanently acellular. The persistence of this acellular zone is most likely to be the result of the compressive forces of the tied suture causing compaction of the underlying extracellular matrix, making it too dense for cells and remodeling enzymes (e.g. matrix metalloproteinases) to penetrate. This injury model could be used to further examine the mechanisms of extracellular matrix disruption by mechanical injuries. Future studies can also be aimed at replacing the use of sutures with other methods to join injured tissue ends, thus avoiding compaction of tissue.

1.2 Tendons

1.2.1 The Extracellular Matrix

The extracellular matrix provides structure to tissues and a medium for cells and non-structural molecules to attach. The organization and composition of extracellular ma-

trix molecules, such as the protein collagen, are attributes that distinguish between different types of connective tissues. For example, collagen fibrils are arranged in parallel arrays in tendon, as lamellae in cornea and in a complex 3-dimensional weave in skin (Hulmes 2002).

1.2.1.1 Collagen

Collagen is the most abundant structural protein in vertebrates. There are many types of collagen, of which more than twenty types have been identified (Kadler et al. 1996). Different collagens can be grouped according to their structure. For example, there are fibrillar collagens (Types I-III, V, XI), collagens which have network-like structures (types IV, VIII, X) and fibril-associated collagens with interrupted triple helices (FACITs), that are located on the surface of collagen fibrils (IX, XII, XIV, XVI, XIX) (Prockop and Kivirikko 1995).

Type I Collagen Collagen fibrils account for 70-80% of tendon tissue. The main function of collagen fibrils is to provide strength and flexibility to tissues, and to provide a scaffold for cells and molecules to attach (Kadler 1995). The principal collagen in tendons is type I collagen, which is also the most abundant and widely distributed collagen (Prockop and Kivirikko 1995). Type I collagen fibrils are heterotrimers of three polypeptide chains, two α_1(I) chains and one α_2(I) chain. Each polypeptide chain is made up of the repeating motif Gly-X-Y, in which X and Y are most frequently occupied by the imino acids proline and hydroxyproline (Canty and Kadler 2002). Specific amino acid residues in the α chains undergo hydroxylation and glycosylation (Kadler 1995). The three polypeptide chains then form a triple helix intracellularly (Engel and Prockop 1991), which is flanked by *C*- and *N* telopeptides (Capaldi and Chapman 1982). Extracellularly, cleavage of the telopeptides by metalloproteinases results in the formation of collagen molecules. Collagen molecules have a diameter that is around 1.4 - 1.5 nm (Ananthanarayanan and Veis 1972) and a length that is approximately 300 nm (Miterová et al. 1989). Millions of collagen molecules combine via entropy-

driven fibrillar assembly (Kadler et al. 1987). These collagen fibrils are then covalently cross-linked, in reactions that are catalyzed by lysyl oxidase (Bailey et al. 1974).

In electron microscopic images, collagen fibrils appear to have a banded appearance. This appearance is the result of the collagen fibril molecules being regularly staggered (*D* period = 64 - 67 nm) in relation to one another (Doyle et al. 1974). The collagen diameter in tendons varies between 10-500nm. Early embryos have predominantly uniform narrow diameter collagen fibrils. Post-natal tendons tend to have a mixture of narrow diameter and large diameter collagen fibrils, exhibiting a bimodal distribution of fibril diameter (Parry et al. 1978). Collagen fibrils combine to form fibers, which aggregate to collagen fascicles that are surrounded by loose connective tissue. The fibrils are mainly orientated parallel to the long axis of the tendon (Birk and Trelstad 1986). Figure 1.1 provides an illustrative depiction of the organization of collagen in tendon.

1.2.1.2 Other Extracellular Matrix Molecules

The extracellular matrix is the primary source of the mechanical properties of tendons that are essential for its function. Hence, the extracellular matrix's architecture and composition may provide clues to the effects of injury and repair on the mechanical properties of tendons (Riley 2004). Although, collagen molecules are the main contributors to the tensile strength of tendons, other extracellular matrix, such as proteoglycans and elastic fibers also play a part (Kjaer et al. 2006).

Proteoglycans Proteoglycans are composed of a core protein that is covalently bound to one or more glycosaminoglycans chains. Vogel et al. (1993) and Berenson et al. (1996) both showed that in cadaveric human rotator cuff and tibialis posterior tendon, decorin was the most abundant proteoglycan in regions of tendon not under compression. Targeted deletion of decorin in a mouse model caused tendons to form which contained fibrils with very large diameters, sometimes reaching diameters of 660nm. In comparison, in corresponding wild type mice it was ~200 nm. It appeared that

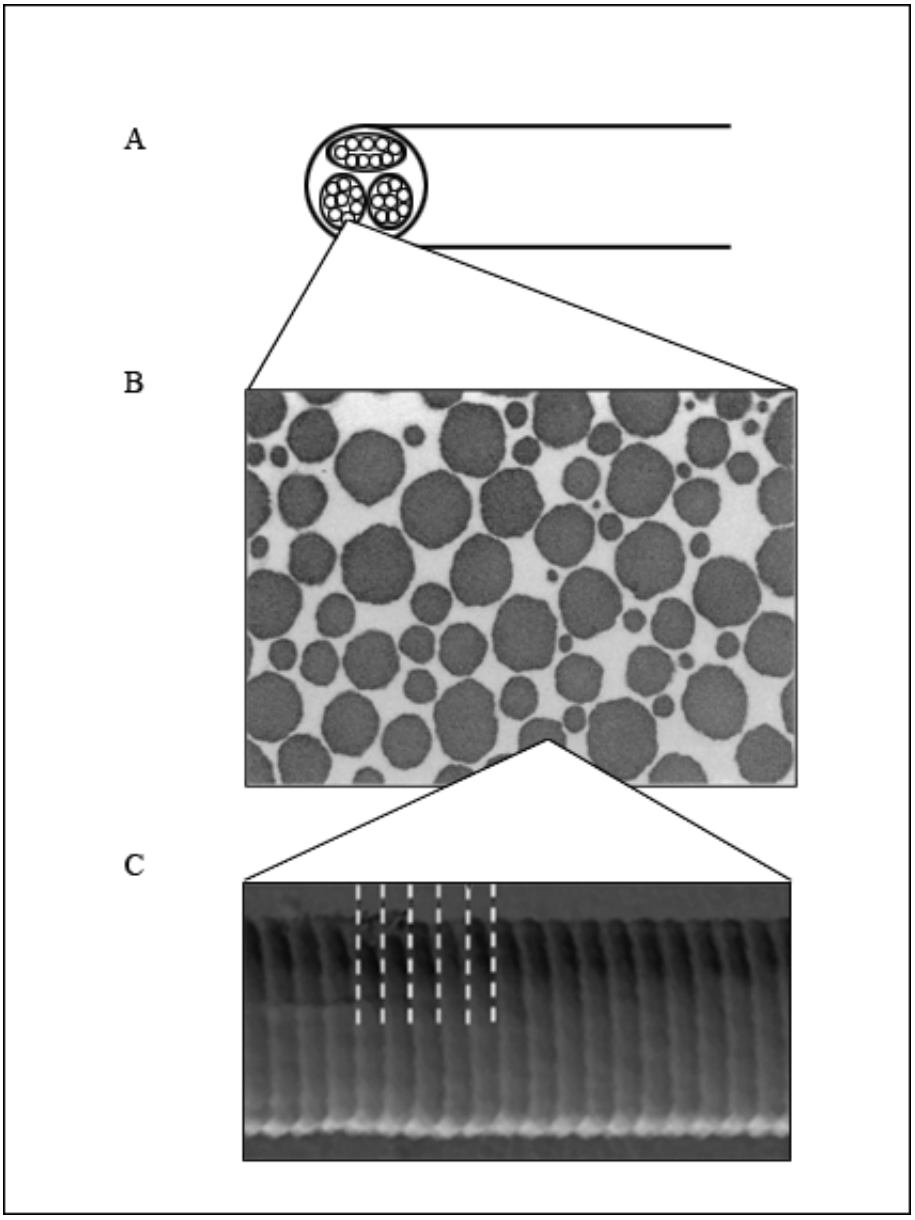

Figure 1.1: **Collagen Organization in Tendon** Collagen molecules in tendon are arranged end-to-end in staggered arrays, resulting in the appearance of 67nm repeating periods. These are demarcated by the white dashed lines in (C). The collagen fibrils combine to form fibers, shown in (B), which is a transmission electron microscopic cross-section of a rat tail tendon. The collagen fibers aggregate to form fascicles, shown in (A), a schematic of a cross section through a tendon. *Images B and C were reproduced from (Rowe 1985) and (Bozec et al. 2007), respectively.*

these abnormal fibrils were formed by lateral fusion of fibrils, indicating that decorin is likely to be important for limiting collagen fibril aggregation (Danielson et al. 1997). The influence of the absence of decorin in tendons was variable depending on the type of tendon. For instance, in the decorin knock-out mice, the patellar tendon has a larger elastic modulus than tendons from wild-type mice. However, this observation was not present in flexor digitorum longus tendons. This suggests that the mechanical influence of proteoglycans in tendons is dependent on the type of tendon (Robinson et al. 2005).

Elastic Fibers Elastic fibers confer elastic properties to the tendon, allowing the tendon to store and release elastic energy (Kannus 2000), which improves the efficiency of force transmission from muscle to the tendon (Scott 2003). Elastin molecules aggregate with proteins such as fibrillin-1, fibrillin-2 and microfibrillar-associated glycoproteins (MAPG) to form elastic fibers (Kielty et al. 2005). Mutations in the fibrillin-2 genes disrupt elastin fiber assembly resulting in congenital contractural arachnodactyly (CCA), which causes contractures of the hands. Consequently, it has been suggested that fibrillin-2 has a role in the function of flexor tendons. A study by Ritty et al. (2002), determined that in flexor digitorum profundus tendon, fibrillin-2, MAPG-1 and -2 staining was largely confined to the pericellular matrix, which surrounded clusters of 2-5 tendon fibroblasts. The MAPG staining extended from the pericellular matrix to the interfascicular space between collagen bundles. Ritty et al. (2003) also isolated the clusters of cells within their matrix from the rest of the tendon (Figure 1.2). Immunolabelling showed that the pericellular matrix contained fibrillin-2 and type VI collagen. The study also described a fibrillin-2 based macromolecular structure, which ran parallel to the cell arrays and had a 100-150nm diameter and 300-1000 μm length (Figure 1.2). Freeze fracture of the samples demonstrated that these macromolecular structures emerged from the cell bodies. This led the authors to propose that these fibrillin-2 based macromolecules may function as mechanical sensors or guiding tracks for cell migration into the interfascicular space after tendon injury. In addition to elas-

tic components, McNeilly et al. (1996) reported that the interfascicular space also contained cell-cell membrane connections. These cellular projections were not detectable by DiI, a stain used to identify the cell membrane, in the cell arrays isolated by Ritty et al. (2003). The study's authors speculated that the loss of the cellular projections may be attributed to these cellular extensions being labile, causing them to dissolve rapidly under stressful conditions.

1.2.2 Tendon Cells

Tendons are composed of a heterogenous population of cells which include: tendon internal fibroblasts or tenocytes (McNeilly et al. 1996), tendon surface cells (Richardson et al. 2010) and tendon progenitor stem cells (Bi et al. 2007).

Tendon Internal Fibroblasts (Tenocytes) The cells located in the central portion of the tendon are specialized fibroblasts also known as tenocytes. McNeilly et al. (1996) used the membrane dye DiI to stain freshly dissected tendons to observe the cellular distribution in rat FDP. Tenocytes were described as having an elongated shape in longitudinal sections. They were located in rows of 2-8 cells and were intimately associated with collagen fascicles. DiI staining also demonstrated that tenocytes had many cellular projections. 3-dimensional modelling of these cellular processes showed that these projections extended anteriorly, posteriorly and laterally to the cells, connecting rows of cells to each other. This resulted in the formation of a network of cells spanning the entire extracellular matrix of tendons (Figure 1.3). Immunostaining for the gap junction protein, connexin (Cx) 43 demonstrated that the protein was present between longitudinal and lateral cell processes. Staining for Cx32, another gap junction protein, was more prominent in the tendon periphery and was located at cell bodies rather than between cell processes.

Function During developement, intercellular junctions have been shown to be important in the tendon. Cadherin-11, an adherens junction found between tenocytes,

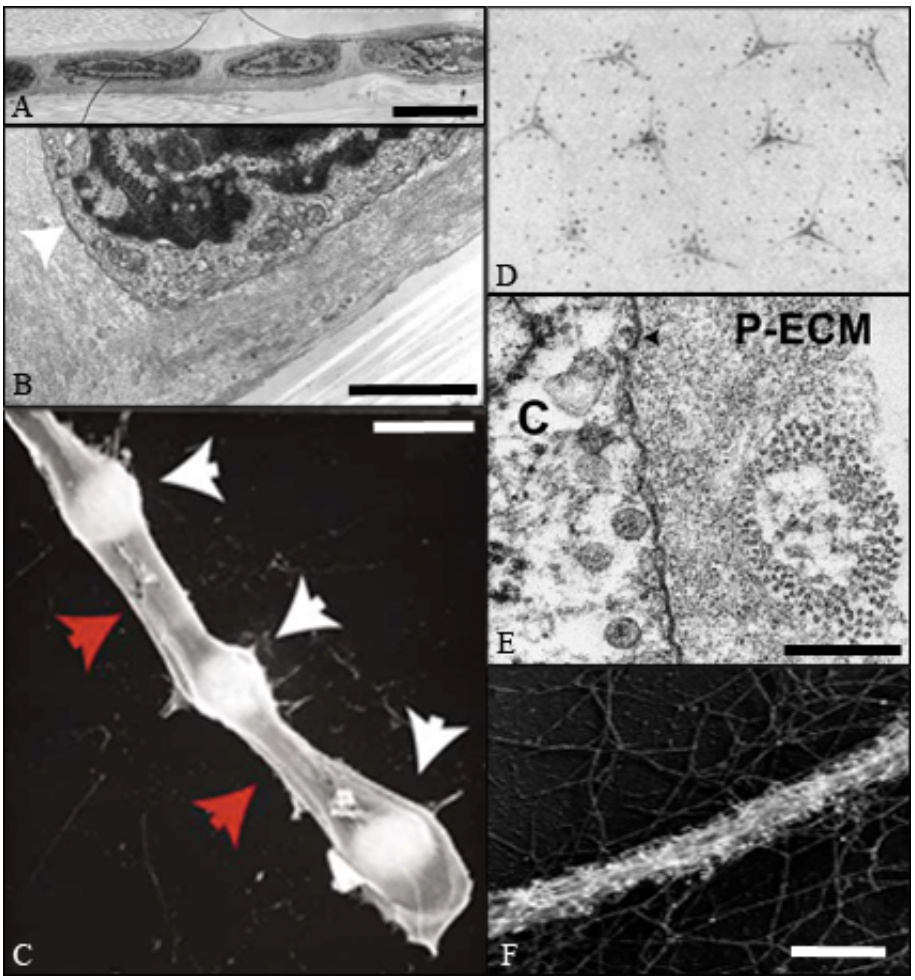

Figure 1.2: **The Pericellular Matrix and Elastic Fibers in Tendon** Ritty et al. (2003) described a pericellular matrix that is present around rows of cells in tendon, which is visible by transmission electron microscopy (TEM) (A) and (B), Bar = 7 μm (A), 1.7 μm (B). These rows of cells were isolated and imaged using scanning electron microscopy (SEM) seen in (C), Bar = 100 μm. They were shown to contain fibrillin-2, versican and collagen VI. In addition, elastic fibers were described which ran alongside cells, illustrated in (D), a gold-chloride formic-acid tendon preparation that stains elastic fibers black. A fibrillin-2 based macromolecular structure was identified and was seen in TEM (E) and SEM (F) images of tendon, Bar = 250 nm (E), 200 nm (F). *White Arrow=Cell, C=Cell, P-ECM=pericellular extracellular matrix. All the images except D were reproduced from (Ritty et al. 2003), D was obtained from (Gemmill 1906)*

has been shown to be important for extracellular matrix production and alignment in embryonic tendons (Richardson et al. 2007). This was demonstrated by knockdown of cadherin-11, which caused collagen fibrils to become misaligned, resulting in cell detachment and loss of plasma membrane channels. Other intercellular junction proteins have been shown to have an important function in tendons (Richardson et al. 2007). The presence of gap junctions proteins between tenocytes in tendons, suggests that tenocytes function as syncytium in response to stimuli (Wall and Banes 2005). Banes et al. (1999b) proposed that gap junctions facilitate intercellular communication, permitting the cells, as a network, to respond to generalized and localized mechanical stimuli. Waggett et al. (2006) showed that cells obtained from chicken deep digital flexor tendons increased collagen production in response to cyclic tensile loading. This response to loading was attenuated by administrating halothane, which blocks gap junctions. Banes et al. (1999a) showed that *ex vivo* chick flexor tendons demonstrated a similar response. Loading tendon explants also increased collagen production and it was possible to diminsh this effect using gap junction inhibitors. The increase in collagen production with loading, may explain why tendons increase in size if they are exercised more (Couppé et al. 2008). Hence, tenocytes and their intercellular connections, by modulating the tendon's response to mechanical stimuli, are likely to play an important part in maintaining optimal tendon function.

Other Cells in Tendon A layer of 2-3 flattened cells encircling the tendon periphery, has been described by McNeilly et al. (1996) . The cells in this layer are connected via the tight junctions, tight junction protein-1 and claudin-1 (Richardson et al. 2010). Richardson et al. (2010) provided evidence that suggests that these cells have an epithelial phenotype. These cells reside on a basement membrane and express markers such as keratin, which are characteristic of epithelial cells. Banes et al. (1988b,a) and Tsuzaki et al. (1993) discovered that the extracellular matrix that these tendon surface cells reside in contains fibronectin, lipid, proteoglycans, type I and type III collagen. Tendons also may have a resident tendon progenitor stem cell population. Bi et al.

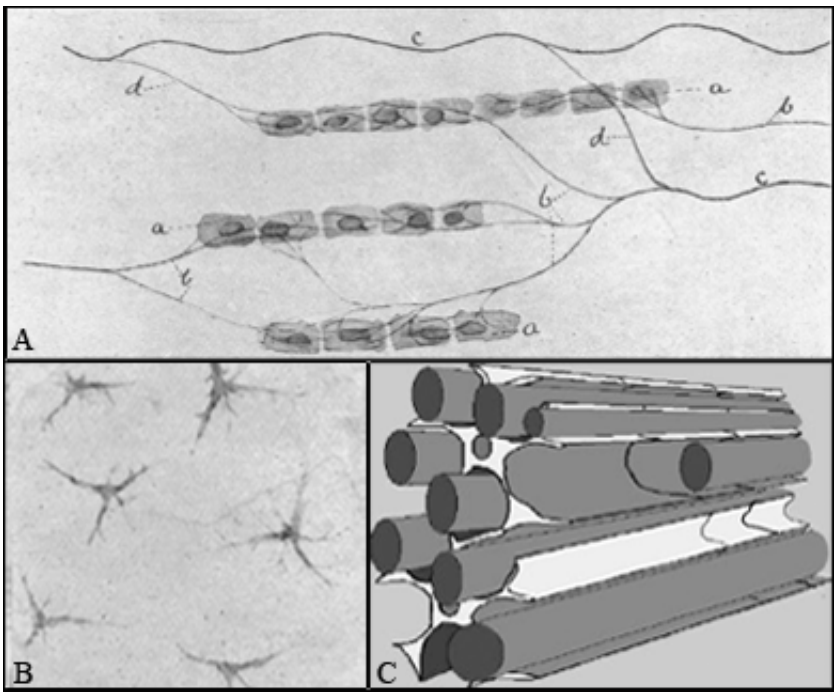

Figure 1.3: **Tenocytes** Tenocytes are located in rows of cells in tendons (A). These rows are connected longitudinally and laterally by cellular projections, which can be seen extending from the cells in (B). (C) is a 3-dimensional schematic depiction of the cellular projections, which also illustrates the close proximity of the cells to the collagen fibrils. *a-d=elastic fibers stained using a gold-chloride formic-acid preparation. A and B were reproduced from Gemmill (1906), C was reproduced from Ralphs (2002)*

(2007) isolated cells from tendons which show stem cell features. The isolated cells were pluripotent and were capable of inducing ectopic tendon formation. These cells were also described as residing in an extracellular matrix niche composed of biglycan and fibromodulin. However, these potential tendon progenitor stem cells have not been localized in the tendon.

1.3 Suturing

1.3.1 Current Tendon Repair Strategies

The only treatment available for significant tendon injury is surgery. Surgery usually involves suturing the tendon ends back together or grafting tendon tissue from donor sites for more extensive injuries. The use of sutures is required for both these types of surgery. Primary surgical repair of the flexor digital tendons was advocated by a group of pioneering surgeons who showed that primary tendon repairs improved patient outcome (Kleinert and Pickford 1997).

This approach to repair flexor digital tendons led to the emergence of multiple suturing techniques to repair tendons, which ranged from the simple interrupted suture to more intricate suture designs (Figure 1.4). The more complex suture designs were composed of three basic design elements: the knot, to tie the suture ends, the grasping components, to grip the tissue, and connecting components to unite the knot and grasping components. The grasping component describes a suture configuration, which encircles the tissue, gripping it (Figure 1.4). This is a common design feature of sutures used to repair tendons, as grasping components are thought to confer strength to the repair site by gripping the tissue (Hatanaka and Manske 2000). In surgical practice, the use of sutures with a greater number of grasping components has been advocated, as multi-stranded sutures have been described as being better at maintaining unity between the tendon ends (Winters et al. 1998).

However, some evidence has emerged which suggests that suturing itself may have

deleterious effects of tissue. In a study by Kraemer et al. (2009), capillary blood blow was shown to be reduced by 57% ten minutes after suturing rat tendons. There was also an increase in the venous filling pressure suggesting that venous stasis occurs. Oxygenation, on the other hand, remained the same. The influence of these changes has not been studied nor the long term impact these acute changes may have on tendon repair.

1.3.2 The Effects of Suturing on the Extracellular Matrix

Recent evidence has emerged which challenges the practice of using suture repair techniques with a greater number of grasping components. McDowell et al. (2002) provided evidence that suturing may invoke additional damage to the tendon it is used to repair. The site of the suture-tendon interface was investigated as it was hypothesized that it was compromising the outcome of the tendon repair by being the site of adverse changes to the extracellular matrix, The study found that during the first four weeks of healing, following repair by two different types of grasping sutures (Kessler and Savage repairs), there was a decrease in the ultimate tensile strength of chicken flexor tendons, which peaked 14 days after the repair. This weakness was associated with a concomitant increase in the activity of the MMP-1, MMP-2 and MMP-9. However, the tendons used in the experiment were unloaded and unloading of tendons has been shown to upregulate MMP expression (Leigh et al. 2008) . Hence, the observed increase in MMP expression may be secondary to unloading of the tendon, rather than the direct effect of suturing.

However, the hypothesis that suturing leads to weakening of the tendon via increased MMP expression was supported by Pasternak et al. (2007), in a study which examined suture the amount of force required to pull out a tendon before and after treatment with doxcycyline, which possesses broad-spectrum MMP inhibitory activity. Sutures that were coated with doxycycline were found to have improved suture holding capacity as illustrated by the greater energy and forces required to pull the

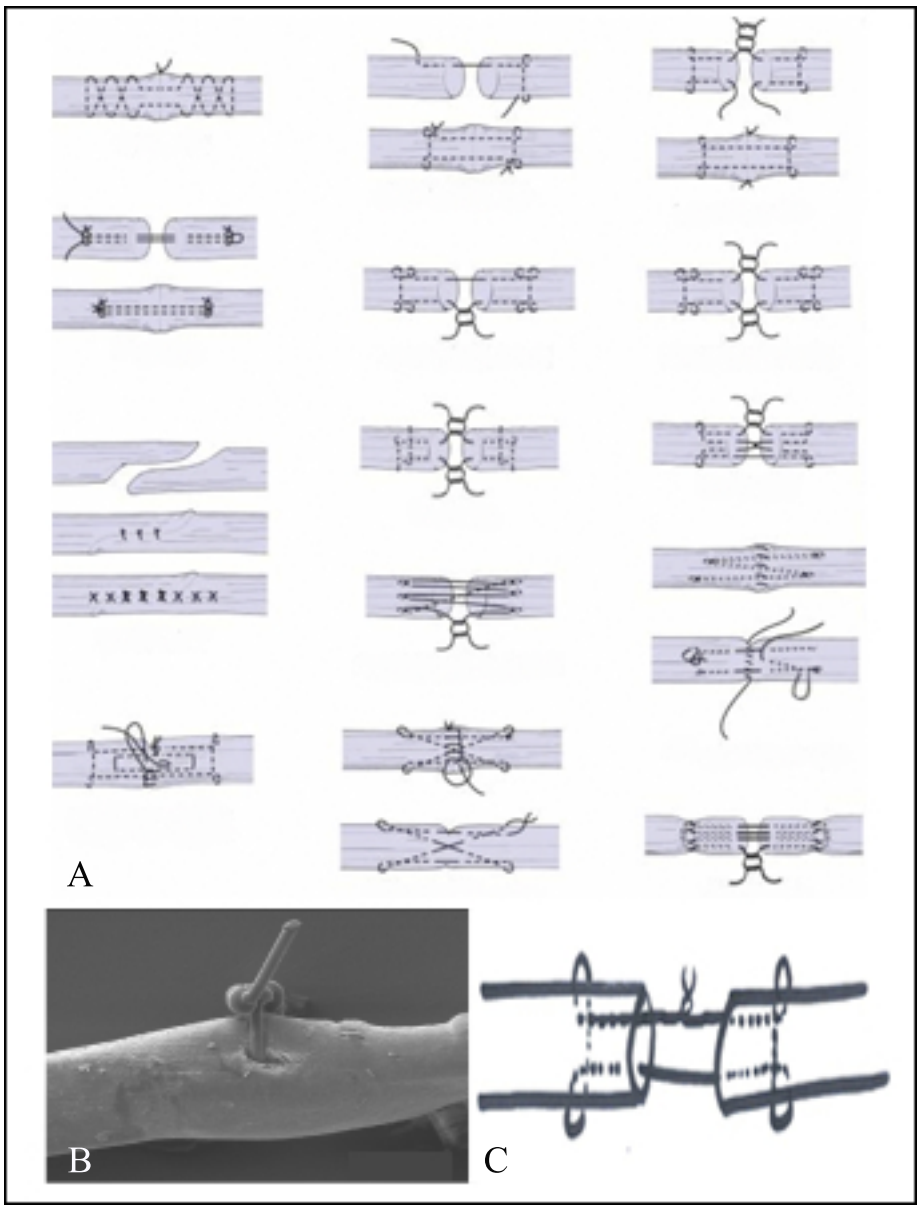

Figure 1.4: **Suture Configurations** (A) is an illustration demonstrating the wide variety of suture types used to repair tendons. (B) is an image of a single interrupted suture obtained using scanning electron microscopy. (C) is a diagram showing a modified Kessler suture. A knot can be seen connecting the sutures in either tendon end. The suture loops seen in the distal part of both tendon ends are the grasping components of the suture. *A and C were reproduced from (Zlowodzki 2010), B was reproduced from (Wong et al. 2006b)*

suture out during biomechanical testing. The main limitation of the study is that MMP expression was not measured before and after treatment with doxcycline so it cannot be determined with great certainty that the observed biomechanical improvement was due to the decreased MMP activity at the repair site. Despite evidence emerging that suturing is associated with damage to the tendon, the effects of suturing on the cells and extracellular matrix of tendon have not been extensively investigated.

1.3.3 The Effects of Suturing on Cells

The effect of suturing on cells in the tendon was investigated by Wong et al. (2006b), who identified acellular bell-shaped regions around simple interrupted sutures in tendons (Figure 1.5) in histological sections. Similar acellular regions were also described around suture sites in fetal tendons, cornea and cartilage (al Qattan et al. 1995; Matsuda et al. 1999; Hunziker and Stähli 2008). It is probable that localized loss of cells has a damaging effect on the tendon. This speculation is based on the reasoning that loss of cells disrupts the intercellular network between cells in the tendon, interrupting cell-cell communication (McNeilly et al. 1996) , which has been shown to be important for mechanotransduction in the tendon (Waggett et al. 2006). The loss of cell-cell connections was further highlighted by the lack of staining for the actin cytoskeletal marker TRITC-phalloidin in sutured regions of tendon (Wong et al. 2010) (Figure 1.5).

Yet, the effects and mechanisms of the formation of these acellular zones remain unknown.

1.3.3.1 Investigating the Mechanisms of Acellular Zone Formation

Wong et al. (2006b) carried out studies, which ruled out some mechanisms as being the instigators of acellular zone formation and also implicated certain factors as being likely contributors to the formation of acellular zones.

The hypothesis that acellular zone formation is secondary to localized ischemia in

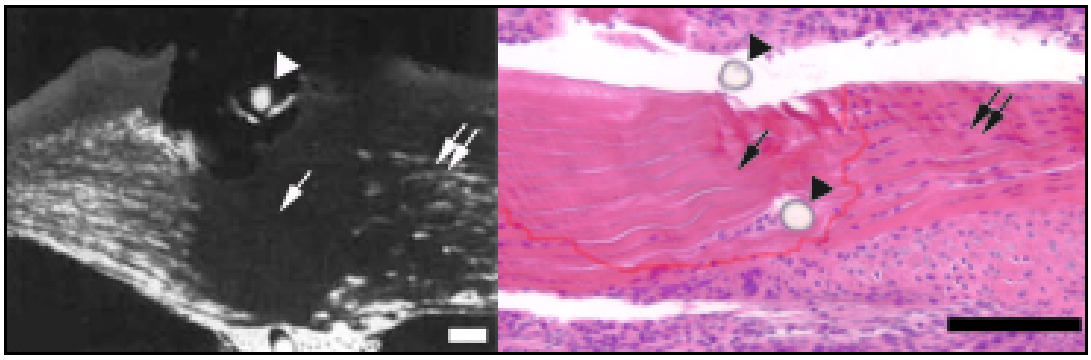

Figure 1.5: **The Acellular Zone** The image on the left is of an acellular zone that has developed after suturing cornea. The image on the right is of haematoxylin and eosin staining of a cross-section of a sutured tendon. In the middle of the image, an acellular zone can be seen. *Triangles=Suture, Single Arrow=Acellular Zone, White Double Arrows=Cornea, Black Double Arrows=Tendon, Bars = 50 µm (white), 100 µm (black). Left image was reproduced from (Matsuda et al. 1999), Right image was reproduced from (Wong et al. 2006b)*

the tissue caused by the suture was investigated. This hypothesis was questioned when Wong et al. (2006b) showed that the acellular zone was present in both the vascularized rat and rabbit tendons and in avascular regions of mouse flexor digitorum profundus tendons (Wong et al. 2006a).

Another potential explanation for acellular zone formation was that the suture caused cell death, as a result of toxic effects inherent in the suture material. To test this hypothesis Wong et al. (2006b) passed sutures through *in vivo* tendons but did not tie the suture ends, leaving the suture *in situ*. Unlike, tied sutures which caused acellular regions to form in tendons, untied sutures did not result in acellular zone formation. This experiment also suggests that the mechanical compressive effects extruded by the suture are important contributors for acellular zone development.

The importance of the mechanical effects of suturing was further highlighted by Wong et al. (2006b), who showed that the acellular zone did not appear in tendons *in vivo*, if one of the tendon ends was severed.

In a later study also by Wong et al. (2010), it was shown that immunohistochemical staining of inflammatory cell markers revealed that inflammatory cells were mostly

present in the tissue surrounding tendons but not in the tendon itself. Histologically, the acellular zone had an intact extracellular matrix with no evidence of any damage. This implied that a mechanism such as apoptosis, which does not usually invoke an inflammatory reaction or tissue damage, was responsible for the emergence of the acellular zone.

Surprisingly, immunostaining for the apoptotic markers Bcl-2, Bax, activated caspase 3 and cytochrome c was not evident at the suture repair site 6 hours after mouse FDP tendons were sutured *in vivo*. DNA integrity gel analysis, did not reveal the presence of the 180 bp laddering that is usually associated with apoptosis, nor was terminal deoxynucleotidyl transferase dUTP nick end labeling (TUNEL) staining present in the sutured regions. Although these findings imply that apoptosis is less likely to be the candidate responsible for acellular zone formation, it still cannot be excluded. Chiefly, because the screening for apoptotic markers was carried out 6 hours after the repair and the levels of the apoptotic proteins stained for could have diminished much earlier. In some cases, the apoptotic signaling pathway has been shown to take place within one hour (Green 2005). Furthermore, there are many other types of caspase independent cell death pathways that have been recognized, which could be contributing to acellular zone development; including, autophagy, necroptosis and programmed necrosis.

Cell migration is another potential means by which the acellular zone could evolve. Ruling out cell migration is difficult as it is technically challenging to image cells at a resolution high enough to track cells *in vivo*; an *ex vivo* model of acellular zone formation would facilitate this.

1.3.3.2 Potential Mechanisms of Acellular Zone Formation

Cell Death Cell death has traditionally been classified as either being apoptosis or necrosis. Recently, however, many other cell death mechanisms have been discerned, such as autophagy, necroptosis, paraptosis, pyroptosis, entosis and several others. Also, as much fewer studies of cell death are carried out *in vivo* than *in vitro*; it is possible that there are many other cell death types that occur *in vivo* exclusively, that

have not been defined yet (Degterev and Yuan 2008).

Cell death mechanisms can also overlap, complicating matters further. Different cell death mechanisms can get activated at the same time and cross-talk can occur between their signaling cascades. Some cell death pathways have been described as being apoptosis-like, as they show morphological features of apoptosis but operate independently of the caspase pathway that is considered integral to apoptosis (Danial and Korsmeyer 2004). Evidence has also emerged, which suggests that necrosis, often described as being a passive cell death modality, also shows programmed cell death characteristics (Hitomi et al. 2008). This 'programmed' necrosis has been given the name 'necroptosis'. The receptor-interacting proteins (RIP) have been shown to be critical for regulating necroptosis (Declercq et al. 2009)and inhibition of RIP1 by the inhibitor necrostatin-1 (Nec-1) has been shown to reduce cell necrosis *in vivo*, in a brain injury model (Degterev et al. 2005).

The wide range of cell death modalities, makes a systematic approach to studying cell death necessary. A Nomenclature Committee on Cell Death (NCCD) was established, in attempt to unify cell death criteria (Kroemer et al. 2009). Its guidelines recommend the use of more than one classification type to define cell death, as no clearly defined pathways exist to distinguish the divergent types of cell death. The NCCD also recommends exercising caution when defining necrosis, as it still described in negative terms, by the absence of apoptosis or autophagy.

The main classifications that are used to categorize cell death are classifications based on either morphological or biochemical features. Figure 1.6 summarizes the main morphological cell death features and the assays used to identify them, obtained from the NCCD recommendations. Morphological assessments of cell death are usually carried out by identifying features characteristic of apoptosis, autophagy or necrosis (the only cell death types distinguishable morphologically) on transmission electron microscopic (TEM) images. However, standalone morphological assessment is not sufficient, as it excludes the other types of cell death that cannot be categorized using TEM. It can also be argued that a morphological definition of cell death is less

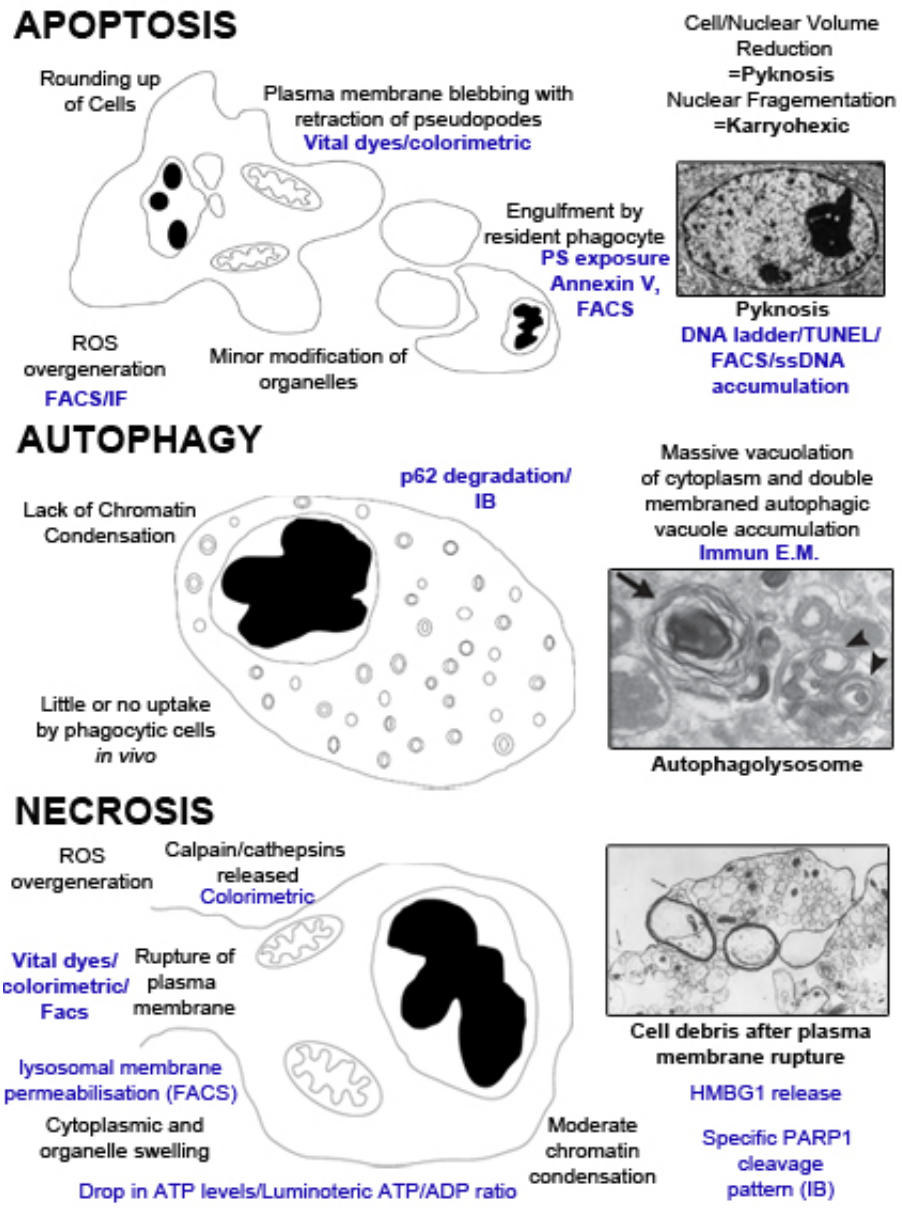

Figure 1.6: **Classifying Cell Death** There are two main methods for classifying cell death: by morphological features of the cells on transmission electron microscopy (TEM) or by examining the biochemical markers the cells express. The three main subtypes of cell death are apoptosis, autophagy and necrosis. The images on the left hand side are a schematic representation of the cell death features found in each cell death type. The figures on the right are of characteristic features that can be found on TEM. Black text provides a description of the features and blue text gives examples of methods that can be used to detect the aforementioned feature. *ROS=reactive oxygen species, FACS=fluorescence-activated cell sorting, PS=phosphodiester, IF=immunofluoresence, HMGB1=high-mobility group protein B1, PARP1=poly(ADP-ribose) polymerase, E.M.=electron microscopy, IB=immunoblotting. TEM images were reproduced from (Hotchkiss et al. 2009), description of cell death features was adapted from (Kroemer et al. 2009)*

useful than a biochemical definition. This is because, unlike biochemical signaling pathways, morphological features are not amenable to targeted therapies (Green and Kroemer 2005). As the acellular zone is potentially a clinical problem, identifying signaling pathways, which can be targeted would be of therapeutic benefit. Hence, the use of an approach, which uses both morphological and biochemical approaches to study the acellular zone is essential.

To facilitate investigation of the acellular zone, a clear definition of exactly when the acellular zone develops is important. This is to ensure that the time points studied correlate with ongoing cell death. Electron microscopic examination of the forming acellular zone would establish the cell death morphology. Next, a microarray analysis would provide an unbiased perspective of the cell signaling pathways that are activated in a developing acellular zone. A microarray would, ideally, be carried out in an *ex vivo* model of acellular zone development. This is because the acellular zone has been shown to trigger a significant inflammatory response in the tissue which surrounds the sutured tendons (in the skin and synovial sheath) but not in the tendon itself (Wong et al. 2010) . This inflammatory reaction is likely to activate various cell damage and cell death mediators, which would be difficult to separate from the cellular events occurring exclusively in the tendon. Even if a sham injury is used in attempt to control for this response; it is likely to be less effective in the tendon, which is sparsely populated by cells compared to its surrounding tissues. Thus, any signaling pathways that are stimulated are susceptible to being masked by the greater cellular response that would be expected from the tissues which surround tendon.

Cell Migration The pathways involved in cell migration are dynamic and extremely complicated (Schmidt and Friedl 2010). This is because cell migration is more of an emergent process rather than a distinct single molecular event and involves the integration of a multitude of factors. For cell migration to occur, certain elements must be present. Cell-migration adhesion complexes (CMAC) are a necessary component. CMACs are hubs that receive and co-ordinate signals between the extracellular ma-

trix and cells. They are composed of integrins, of which 24 distinct types have been identified and their associated adaptor proteins, which may include more than 100 different proteins. Several different types of inputs could trigger cell migration through CMACs, which can either be mechanical (such as tension or stiffness) or chemical (such as through activation of Rac) (Lock et al. 2008).

To summarize, cell migration can be triggered by physical or chemical factors (triggers) which, through CMACs can trigger molecular events. These molecular pathways (molecular) lead to changes in the extracellular matrix, cell polarity, the microfilament and microtubular system, vesicular trafficking and plasma membrane protrusions and dynamics (sub-system), which promote cell migration (system). See Figure 1.7 Hence, an approach, which investigates cell migration at each of these levels: the trigger, molecular level, subsystem level, system level; would provide a global picture that can be used to determine whether cell migration is a predominant mediator of acellular zone development.

- Trigger: the mechanical effects of the suturing are the most likely trigger for cell migration, if cell migration was involved in acellular zone development. The micromechanical effects of suturing are dealt with further in Aim 4.

- Molecular: a microarray analysis can be used to screen for molecules involved in cell migration such as FAK, GEFs, Src, p130cas, paxillin, vinculin, talin. The wide encompassing approach of a microarray is necessary, as there are few preceding studies in the field which have investigated the signaling events involved in forming the acellular zone. Once integral pathways have been identified, a more targeted approach can be employed in the future.

- Subsystem: again, a microarray array can be used to screen for molecules associated with cell migration such as microtubular/microfilamentous or vesicular trafficking proteins. The presence of plasma membrane features such as filopodia and podosomes can be investigated using TEM.

- System: Ultimately, direct visualization is the most accurate method of determining whether cell migration occurs or not in the acellular zone. As cell migration is difficult to track *in vivo* (Even-Ram and Yamada 2005), an *in vitro* model of acellular zone formation is required to determine if cell migration takes part in acellular zone development.

Hence, the use of the microarray analysis and TEM to investigate cell death in the acellular zone can be extended to include cell migration features as well as cell death. The development of an *ex vivo* model of acellular zone development is also imperative to achieve Aims 2 and 3, as well as the temporal and spatial characterization of acellular zone development outlined in Aim 1.

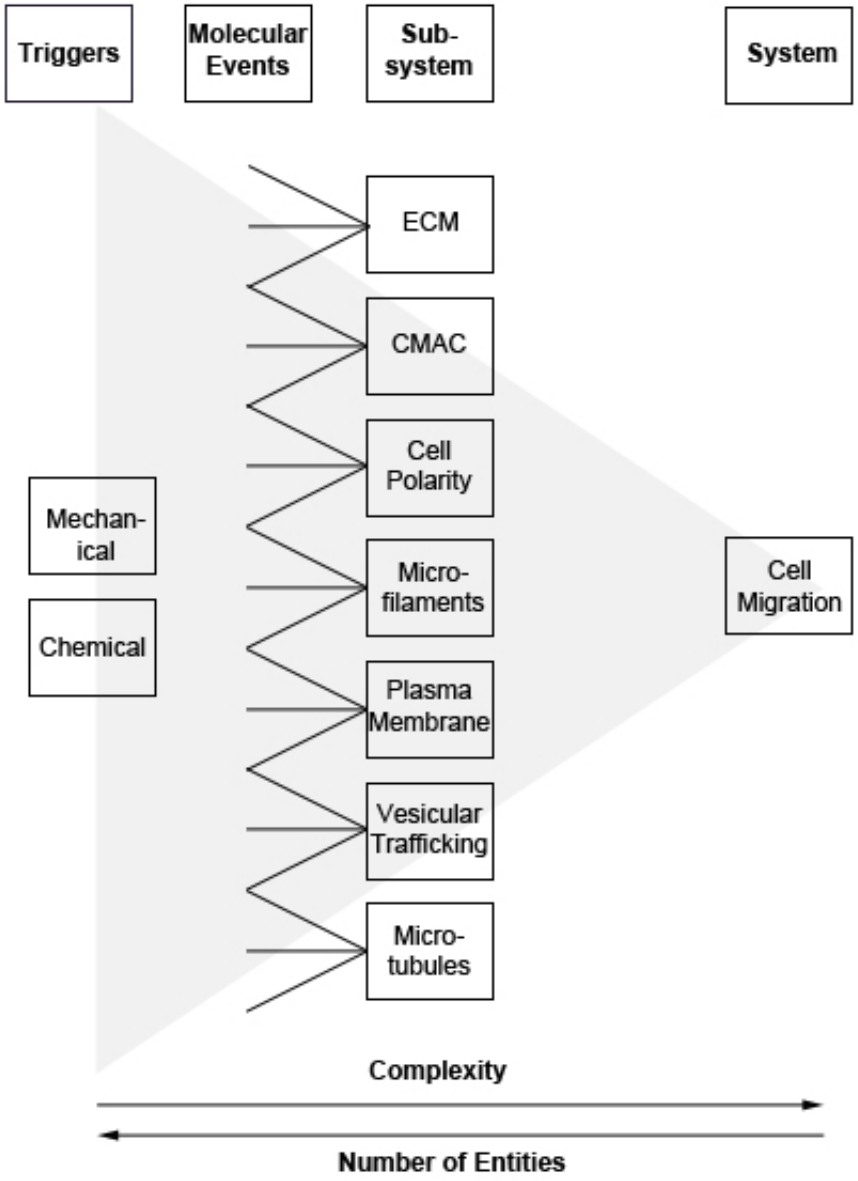

Figure 1.7: **Cell Migration as an Emergent Process** Cell migration can be triggered by chemical or mechanical factors, which through cell-migration adhesion complexes (CMAC) can trigger molecular events. These molecular events (molecular events) cause changes in the extracellular matrix (ECM), cell polarity, microfilaments, microtubules, vesicular trafficking and plasma membrane protrusions and dynamics (sub-system), resulting in cell migration (system). Hence, cell migration is a complex cellular response, which requires the integration of a large number of signaling molecule *Adapted from (Lock et al. 2008)*

1.4 Hypothesis and Aims

The following hypotheses were tested:

1.4.0.3 Hypotheses

- Non-apoptotic cell death and/or cell migration lead to acellular formation in sutured tendons.
- Suturing causes mechanical and morphological changes to the extracellular matrix, which contribute to the persistence of the acellular zone in sutured tendons.

1.4.0.4 Aims

Hence, the aims of this thesis are:

1. *Aim: confirm the association between the suture grasp and the acellular zone*

   If the shape of the suture conforms to the grasp of the suture, this would confirm that it is the forces that are exerted by the suture on the tissue that are responsible for acellular zone formation. This would provide further insight into the mechanisms of acellular zone formation. This information could also be used to design *in vitro* models of tendon injury, which would facilitate investigation of the acellular zone.

2. *Aim: establish the time course of acellular zone formation*

   Different injury mechanisms have different temporal characteristics (Gurtner et al. 2008). Establishing the time it takes to form the acellular zone would provide further insight into the potential mechanisms which cause it. Furthermore, determining whether the acellular zone is a chronic feature of suturing would indicate whether permanent changes in the tendon's architecture occur after this type of injury. Critically, knowing the time characteristics of acellular zone formation is essential for designing future experiments aimed at elucidating the mechanism of its development.

3. *Aim: elucidate whether the acellular zone forms predominantly via cell death or cell migration*

   Discerning whether the acellular zone forms via cell death or cell migration, is the first step towards identifying targets that can be modulated to prevent acellular zone development. The signaling pathways involved in these cellular processes must also be identified to achieve this.

4. *Aim: to confirm that the suture significantly alters the mechanical properties and the organization of the extracellular matrix of the tendon it grips*

   As the extracellular matrix hosts the cells, an understanding of how suturing affects it, may help explain the observed cellular effects of suturing. For example, the mechanical properties of the extracellular matrix and its organization can promote or inhibit cell migration (Hadjipanayi et al. 2009). As the acellular zone is a local effect, a correlation between the acellular zone and the mechanical effects within the corresponding area would further support the hypothesis that the mechanical forces exerted by the suture contribute to the cell loss. Obtaining readings of the mechanical properties of the sutured region can also be used as a baseline to compare to the mechanical effects after inhibition of the acellular zone.

Part II

Materials and Methods

CHAPTER 2

MATERIALS AND METHODS

2.1 Materials

All chemical were obtained from Sigma (Cambridge, UK), unless stated otherwise; cell culture material from Corning and Falcon (supplied by Appleton Woods, Birmingham, UK), unless otherwise stated; all surgical instruments were obtained from Fine Science Tools (Suffolk, UK). The operating was performed using a MZ7.5 operating stereomicroscope, on a flexiarm stand with a vertical halogen lamp illumination from Leica Microsystems Ltd (Germany).

2.2 Animal Husbandry

The C57/BL6 mouse background (Jackson Laboratories, 2008) was used, as many transgenic strains have been developed on it. All the mice that were used were male and eight weeks old. The animals were housed in the animal unit within the Incubator building at Manchester University. Groups of 12 mice were placed together and left to acclimatize for 1 week before the procedures were carried out. All housing conditions

were in accordance with Home Office Regulations of the 1986 Animals in Scientific Procedures Act. All mice were culled using CO_2 overdose inhalation, followed by cervical dislocation.

2.3 Home Office Regulations

All wounding procedures were conducted under section 19b of the Home Office Project License held by Professor Gus McGrouther and Home Office Personal License held by Sarah Al Youha and Jason Wong. Jason Wong performed the *in vivo* animal surgeries. Following animal wounding, the animals were housed separately. All animal procedure were approved the Local Ethical Committee at the University of Manchester and compiled with British Home Office regulations on the care and use of laboratory animals.

2.4 Anaesthesia and Preparation of Operating Field

Surgery was performed under general anaesthetic, using 4% isopentane (Abott Ltd) and 4 litres/minute oxygen driver to induce anaesthesia. General anaesthesia was maintained using 2% isopentane with 2 litres/minute oxygen drive and 1.5 litres/minute nitrous oxide. The areas of interest were shaved to remove any hair and cleaned using 70% ethanol. An elastic band was used as a tourniquet to reduce blood flow to the region to be operated on. The anaesthetized mouse was placed under the operating microscope and the limb was held in place using Blu-tack (Bostik Ltd). After the procedure, the mice were monitored to ensure adequate recovery after anaesthesia. The mice were then left to freely mobilize.

2.5 *In Vivo* Injury Models

2.5.1 Single Interrupted Suture

The operating field was cleaned using sterile wipes. A skin incision was made on the palmar aspect of the phalanx in the mouse hindlimb to expose the underlying flexor digitorum superficialis (FDS). A 10/0 polyamide suture (BBraun Medical, Inc) was inserted at approximately 50% of the depth of the tendon. Three throws were used to secure the suture in place. Saline (0.9%) was used regularly to wash the wound to avoid dehydration of the tendon. The skin wound was closed using a 10/0 polyamide suture.

2.5.2 Kessler Suture

A longitudinal skin incision was made along the dorsal aspect over the distal mouse tibia. The Achilles tendon was exposed and a 50% division of the tendon was performed using microscissors. A 10/0 polyamide suture was used to perform a modified Kessler repair (see Figure 1.4 for illustration). Saline (0.9%) was sprayed regularly to avoid drying of the tendon. The overlying skin was sutured using a 10/0 polyamide suture.

2.6 *In Vitro* Single Suture Explant Model

The mouse was put in a prone position and the hindlimb was fixed in place using Blu-tack. The skin was separated to reveal the underlying tendons. The tendon of interest was identified and the overlying structures were carefully dissected away to expose it. The pulleys holding the tendon in place were cut to free the tendon. Aclands clamps (Mercian Surgical Co Ltd) were used to grip the ends of the tendon. The distance between the Aclands clamps was adjusted to modify the tension exerted across the tendon. The ends of the tendons were cut using a single sharp excision. A 10/0

polyamide suture (BBraun Medical, Inc) was passed through at approximately 50% of the depth of the tendon. Three tight knots were made to secure the suture in place. The clamped tendons were placed in sterile 6-well cell culture plates. 5ml of media was added to each well and the plates were incubated (See Figure 2.1).

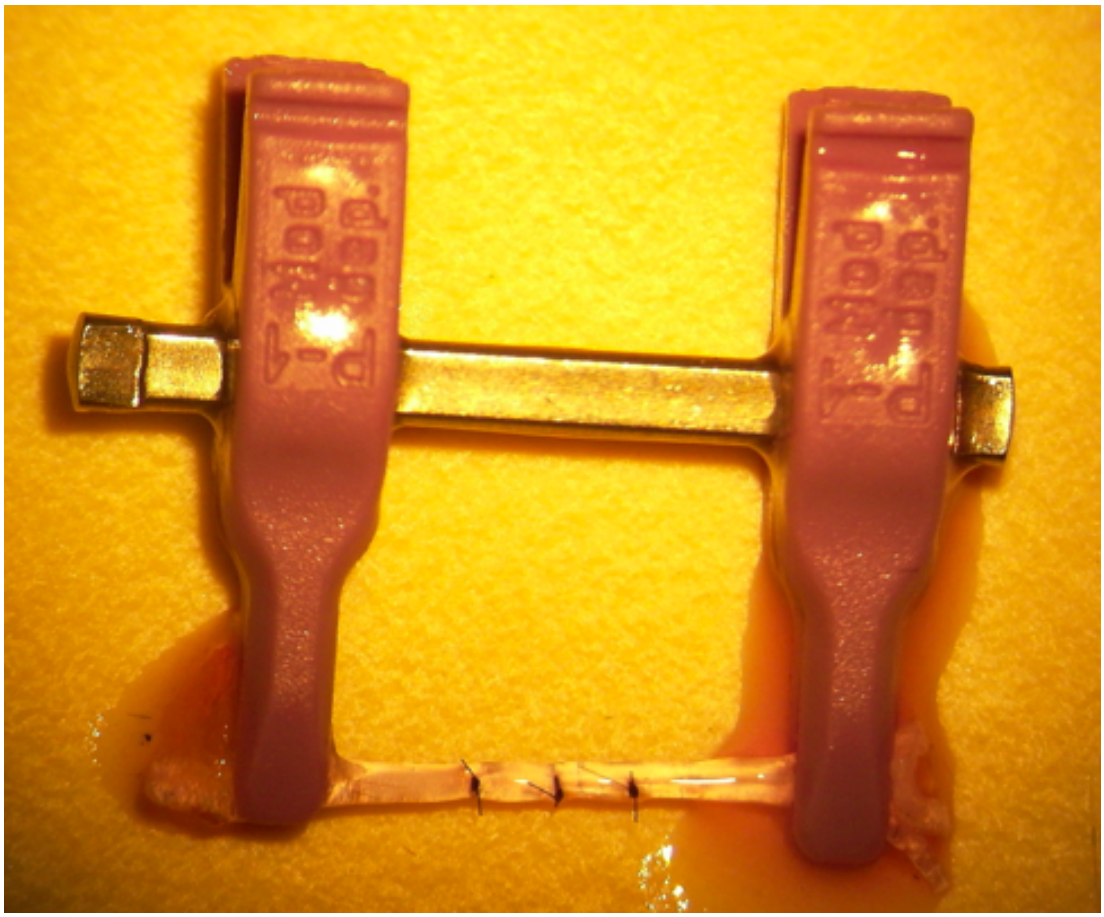

Figure 2.1: ***In Vitro* Model** The flexor digitorum profundus tendon was held under tension using Acland's clamps (Mercian Surgical Co Ltd) to grip the the tendon ends. A 10/0 polyamide suture (BBraun Medical, Inc) was used to make three single interrupted sutures, which can be seen in the middle of the tendon *(metal bar on double approximating Acland's microvessel clamp = 1.00 mm)*

2.7 Dissection of Flexor Digitorum Profundus (FDP)

An operating stereomicroscope (Leica MZ7 operating microscope, Leica Microsystems) and microsurgical instruments were used to dissect all the tendons. The hindlimb was fixed in position using Blu-tack (Bostik Ltd). The hairs on the area of interest were shaved and a coronal incision was made distal to the ankle joint on the dorsal aspect of the limb to expose the tendon below. A sagittal incision was made, which extended from the coronal incision to the midline of palm to make a T-shaped incision. The skin was separated using forceps to expose the underlying tendons. The overlying FDS tendon was dissected away to reveal the FDP. Cutting the pulley and making a sharp excision in the proximal and distal end freed the FDP.

2.8 Cell Culture

The media used for all the experiments, unless stated otherwise, contained Dulbeccos Modified Eagles Medium (DMEM), penicillin (100 U/mL), streptomycin (100 μg/mL), L-glutamine (2 mM) and 10% fetal calf serum. This was changed every 2 days. The samples were incubated at 37°C in 5% CO_2.

2.9 Tissue Collection and Fixation

2.9.1 Histology and Immunohistochemistry

A Schedule 1 procedure, in accordance with the Home Office Regulations was used to cull the mice. The required tissue was dissected and placed in cassettes. The samples were placed in zinc fixative (Beckstead 1994) for 48 hours before being transferred to 50% ethanol, in preparation for tissue processing.

2.9.2 Cryofixation

Fresh tendons were embedded in optimal cutting temperature (OCT) compound and orientated in the desired position. The samples were snap frozen in liquid isopentane (-160°C) cooled in liquid nitrogen. Samples were stored in -80°C until required.

2.10 Tissue Processing

2.10.1 Decalcification

After fixation, the whole digits to be decalcified were excised and tip of the nails were cut. The digits were place in buffered 20% ethylenediaminetetraacetic acid (EDTA) solution (Tennants Disribution Ltd), pH 7.4. This solution was changed every 5 days for 15 days. The digits were then placed in 50% ethanol, in preparation for wax processing.

2.10.2 Filleting of Tendon

Tendons that were not decalcified were filleted off the bone so decalcification was not necessary. An incision was made in the skin and microscissors were used to separate the tendon and skin from the bone.

2.10.3 Tissue Processing Setting

The samples were wax processed using an automatic TissueTek Vacuum Infiltration Processor (Bayer Diagnositcs Ltd) and the Shandon Citadel Processor 2000 (Thermo Scientific Fisher, Inc). Molten Paraplast Plus paraffin wax (Sherwood Medical Ltd) was used to embed the samples after they were orientated correctly. The details of the programme used to process the samples are shown in Table 2.1.

Table 2.1: Tissue Processing Settings

Solvent	Time (minutes)	Temperature (°C)
50% IMS	60	35
70% IMS	60	35
90% IMS	60	35
100% IMS	90	35
100% IMS	90	35
100% IMS	90	35
50% IMS/50% Toluene	30	35
100% Toluene	30	35
100% Toluene	30	35
100% Toluene	60	50
Wax	30	60
Wax	30	60
Wax	30	60
Wax	30	60

2.11 Histology

2.11.1 Tissue Sectioning

Sections (7 μm thick) were prepared from paraffin embedded blocks. Superfrost Excell slides (Thermo Fisher Scientific, Inc) were used to mount the sections. The slides were incubated at 37°C to dry.

2.11.2 Dewaxing

The paraffin embedded sections were placed in xylene (Genta Medical, York, UK) twice for 5 minutes. The slides were then run through a graded ethanol series to rehydrate the samples for 5-10 seconds (100% ethanol 100% ethanol, 90% ethanol, 70% ethanol, 50% ethanol).

2.11.3 Haematoxylin and Eosin (H&E) Staining

After dewaxing, the slides were immersed in filtered haematoxylin for 4 minutes. Running tap water was used to blue the sections for 5 minutes. Next, the slides were transferred to Eosin Y for 30 seconds and then rinsed in water for 10 seconds, ready for dehydration and mounting. In some instances an automated staining machine was used (Thermo Shandon Linistain GLX Stainer, Thermo Fisher Scientific, Inc).

2.11.4 Dehydrating and Mounting Slides

After staining, the slides were dehydrated by being immersed for 5-10 seconds in a graded alcohol series (50% ethanol, 70% ethanol, 90% ethanol, 100% ethanol, 100% ethanol). Next the slides were placed in xylene for 5 minutes twice. Pertex mounting media (Cell Path, plc) was used and 50 mm x 22 mm glass cover slips (Scientific Laboratory Supplies Ltd) were used to mount the slides. The slides were left to dry overnight before imaging. Slides that were stained using the automated staining machine were mounted using Histomount (Flowgen Bioscience Ltd) and were left to dry overnight before imaging.

2.12 Immunofluorescence

2.12.1 TRITC labelled Phalloidin

Tendons were fixed in a zinc based fixative (Beckstead 1994) at 4°C for 48 hours. Samples were subsequently placed in 0.1% Triton X in phosphate buffered saline (PBS) for 48 hours then rinsed in 100% PBS solution for 10 minutes prior to transferring them to a solution of PBS containing Hoechst 33258-bisbenzimidazole dye (Sigma Chemical Co) and TRITC labeled Phalloidin (Sigma, Aldrich) at the concentration of 1: 1000 and 1:500, respectively, overnight at 4°C respectively. Tendons were washed in PBS for 10 minutes, and then the samples were submerged in 50% glycerol (VWR Inter-

national Ltd, Poole, UK): 50% PBS for 24 hours at 4°C, then sequentially 75% and 100% glycerol stored at 4°C for 24 hours.

2.13 Assays

2.13.1 Live/Dead Assay

The tendons were incubated for an hour with media containing 2 μM of calcein AM (InVitrogen, Life Technologies) and 4 μM of propidium iodide (Sigma Aldrich). Calcein AM stains living cells green when activated by intracellular esterase activity (excitation 495 nm and emission 515 nm). Propidium iodide stains dead cells red. Dead cells usually have a damaged cell membrane, allowing the membrane impermeant propidium iodide to enter the cells and bind to DNA, which enhances its fluorescence (excitation 536 nm and emission 617 nm).

2.14 Electron Microscopy

Glutaraldehyde (2%) in 100 mM, pH 7.0 was used to fix the tendons for 30 minutes at room temperature. The areas of interest in the tendons were diced and fixed overnight at 4°C in fresh fixative. Next, tendons were placed in 1% glutaraldehyde and 1% OsO_4 in 50 mM phosphate buffer, pH 6.2, for 50 mins at 4°C. After a wash in distilled water the specimens were bloc stained using 1% aqueous uranyl acetate for 16 hours overnight. The tendons were dehydrated and embedded in Spurrs resin (Canty et al. 2004). Ultrathin sections (~60 nm) were collected using formvar-coated copper 1000 μm slot grids. Sections were stained with lead citrate and examined using the Tecnai 12 BioTwin transmission electron microscope. Images were recorded on 4489 film (Kodak) and scanned using an Imacon Flextight 848 scanner (Precision Camera and Video). A Tecnai 12 BioTwin transmission electron microscope operated at a 100-keV accelerating voltage was used to collect the images on film. Transmission electron

microscopy negatives were scanned using an Imacon Flextight 848 scanner and saved in TIFF format. Image J was used to process and analyze the images .

2.15 Image Capture

2.15.1 Brightfield Microscopy

2.15.1.1 Histology

Images were collected on an Axiovision (Carl Zeiss, Ltd) upright microscope using a 10x objective captured using an Axiovision colour CCD camera through Axiovision software.

2.15.1.2 Fluorescence

Images were collected on an Olympus BX51 upright microscope using a 10x/ 0.30 Plan Fln objective and captured using a Coolsnap ES camera (Photometrics) through MetaVue Software (Molecular Devices, plc). Specific band pass filter sets for (DAPI, FITC and Texas Red) were used to prevent bleed through from one channel to the next.

2.15.2 Confocal/Multiphoton Microscopy

Images were collected on a Leica TCS SP2 AOBS inverted confocal microscope using a 10x/ 0.30 Plan Fluotar objective and 3x confocal zoom. The confocal settings were as follows, pinhole 1 airy unit, scan speed 1000 Hz unidirectional, format 1024 x 1024. Images were collected using the following detection mirror settings; FITC 494-530 nm; Texas red 602-665 nm; Cy5 640-690 nm using the 488 nm (20%), 543 nm (100%) and 633 nm (100%) laser lines respectively. When it was not possible to eliminate cross-talk between channels, the images were collected sequentially. When acquiring 3D optical stacks the confocal software was used to determine the optimal number of Z sections. Only the maximum intensity projections of these 3D stacks are shown in

the results.

2.16 Time Lapse

2.16.1 Brightfield

Images were acquired on a AS MDW live cell imaging system (Leica, plc) using a 5x/ 1.30 Plan Apo glycerine objective, the (BGR) filter set (Chroma [61002]) and a (red (DS Red)). Precise LED fluorescent light source. Point visiting was used to allow multiple positions to be imaged within the same timecourse and cells were maintained at 37°C and 5% CO_2. The images were collected every 20 minutes using a Coolsnap HQ (Photometrics) camera.

2.16.2 Confocal/Multiphoton

Images were collected on a Leica TCS SP2 AOBS inverted confocal microscope using the same setting described above every 20 minutes. A customized chamber was used to maintain the temperature at 37°C and the CO_2 concentration at 5%. Images were also collected using a Swept Field confocal (Nikon) using a (60x/ 1.40 Plan Apo) objective on an inverted TE2000 inverted microscope equipped with the perfect focus system to eliminate focus drift. The settings were as follows, pinholes (30 μm), scan speed (1400 Hz or 100 f/s), format (512 x 512). Images GFP and Dsred were excited with the 488 nm and 543 nm laser lines respectively. Images were acquired on a Cascade 512B EM CCD camera (Photometrics) through the Elements Software (Nikon). Point visiting was used to allow multiple positions to be imaged within the same timecourse and cells were maintained at 37°C and 5% CO_2.

2.16.3 Atomic Force Microscopy (AFM)

Atomic force microscopy was used to gain an appreciation of the organization of the collagen fibrils in sutured and unsutured regions within the sam tendon. This technique was adapted from Hodson et al. (2009). Tissue sections (5 μm thick) were obtained. These were mounted on circular glass coverslips (13 mm diameter). The samples were left to air dry overnight before they were imaged by AFM.

Intermittent contact mode in air using a Multimode AFM with a Nanoscope IIIa controller and a 12 μm, 12 μm, 3.2 μm (X,Y,Z dimension) E scanner, was used to image the samples. The instrument was calibrated periodically using a grating with 180 nm deep, 10 μm x 10 μm depressions. Cantilever oscillation frequencies and drive amplitudes were determined by the Nanoscope software. Height, amplitude and phase images at scan sizes of 5 μm or 10 μm were captured at an initial scan rate of 1.97 Hz, integral and proportional gain settings of 0.3 and 0.5 respectively and a setpoint which was lower than that automatically determined on initial tip contact. Surface tracking (and hence image quality) was optimised by dynamically lowering the scan rate, increasing the gains and lowering the setpoint (or conversely increasing the drive amplitude). Given the inherent roughness of most tissue sections it may not be possible to resolve all areas within the same scan, although using alternative instruments and/or piezo scanners with larger X, Y and X ranges would help to alleviate this problem.

2.16.4 Polarized Light Microscopy

Polarized light microscopy was also used to study collagen fibril orientation. Cryosections (5 μm thick), were mounted using glycerol. The specimens were imaged using a Nikon AM2100 microscope, which had a photonic PL300 light source. The images were captured using a Nikon Coolpix 4500 camera, using a 10x objective. To visualize the fibrils, the slides were rotated between crossed polarized filters.

2.17 Image Processing

2.17.1 Brightfield/Confocal

Images were processed and analyzed using ImageJ (http://rsb.info.nih.gov/ij). Image J was also used to create time-lapse videos.

2.18 Ribonucleic Acid (RNA)

2.18.1 RNA isolation

The tendons were dissected using autoclaved surgical instruments and placed in 250 μl of TRIZol (Invitrogen Ltd), after rinsing them with PBS. They were immediately frozen in liquid nitrogen and stored at -80°C. All the surfaces and equipment was cleaned with RNaseZap (Ambion, Inc). The tissue was disrupted using a Mikro-Dismembrator (Sartorius) (twice at 2,000 rpm for 90 seconds) and added to a new tube to make 1 ml TRIZol. This was incubated for 5 minutes at room temperature. 175 μl of chloroform was added to the sample and shaken vigorously for 15 seconds. After incubating the sample at room temperature for 3 minutes it was centrifuged at 4°C for 10 minutes at 13,000 rotations per minutes (rpm). The aqueous, colourless phase on top was carefully transferred to a new tube. The RNA was precipitated by adding equal volumes of isopropanol to each sample and was incubated at -20°C overnight. The samples were centrifuged for 10 minutes at 13,000 rpm at 4°C the following day. The supernatant was gently removed without disturbing the pellet. The pellet was washed with 1ml 75% ethanol and centrifuged for 10 minutes at 10,000 rpm at 4°C. The supernatant was removed again without disturbing the pellet. The pellet was left to air dry until it became opaque at the edges. 50 μl of DEPC water (Ambion, Inc) was used to resuspend the pellet. The sample was incubated at 65°C for 5 minutes and then on ice for 1 hour. The RNA concentration was measuring on a Nanodrop (Thermo Fisher Scientific, Inc).

2.18.2 Checking RNA integrity

RNA integrity was checked by running a 1% agarose gel (electrophoresis grade from Lonza) in Tris/Borate/EDTA (TBE) buffer, loaded with 1 μl of the sample and 7 μl of running buffer.

2.19 Microarray

Microarray data were processed and analysed using Partek Genomics Solution (version 6.5, Copyright 2009, Partek Inc., St. Charles, MO, USA) with the following options: probesets of the core subset were quantile normalised and RMA background correction applied. Exons were summarised to genes by calculating the mean of the exons (log 2). Validation and gene enrichment strategies consisted of the following steps: to establish relationships and compare variability between replicate arrays and experimental conditions, principal components analysis (PCA) was used. PCA was chosen for its ability to reduce the effective dimensionality of complex gene-expression space without significant loss of information (Quackenbush 2001). Differential expression in response to treatments was calculated by t-test using Partek Genomics Solution (version 6.5, Copyright 2009, Partek Inc., St. Charles, MO, USA). Correction for false discovery rates was done using the method of QVALUE (Storey and Tibshirani 2003). Two-way comparisons made were: UnS_UnT_vs_UnS_T, S_T_vs_UnS_T, S_UnT_vs._S_T and S_UnT_vs._UnS_UnT (S=Sutured, T=Under Tension, UnS=Not Sutured, unT=Not under tension)

2.19.1 Clustering Analysis

A genelist of 1098 differentially expressed genes with significantly altered expression was created by filtering for a p value of 0.05 and fold change of 1.25 in any of the four 2-way comparisons mentioned above. Genes were clustered based on expression profile over our experimental conditions and functional categories or pathways of each

cluster were identified. For each condition, mean expression (log2) was determined for significant genes and then normalised prior to clustering by z-transformation (mean = 0, Standard deviation = 1 for each gene). Genes were segregated into 10 clusters using a K-means algorithm (Manhattan distance) followed by hierarchical clustering of each resulting K-means cluster using the maxdView software using the "Super Grouper" plugin (available from http://bioinf.man.ac.uk/microarray/maxd/).

2.19.2 Gene Ontology

Information was obtained for genes with a fold change greater than 1.5 and a p value less than 0.05, using the Online Mendelian Inheritance in Man (OMIM) database. Based on this information, genes were categorized into functional groups for each two-way comparison and cluster. Functional annotation of the genes list of genes contained within each cluster, was also performed using DAVID version 2. (http://david.niaid.nih.gov/-david/version2/index.htm) (Dennis et al. 2003) to analyse over-representation Gene Ontology categories.

2.19.3 qPCR validation

RNA (0.5 μg) was used to make complementary DNA. The primer sequences used were are shown in Table 2.2.

Table 2.2: Primer Sequences

Gene	**Sense (5'->3')**	**Anti-sense (5'->3')**
Hprt[1]	TGCTCGAGATGTCATGAAGG	TATGTCCCCCGTTGACTGAT
Fos	ATGGGCTCTCCTGTCAACAC	GACACGGTCTTCACCATTCC
Ikbke	AGCCCAGGAGAGTCTGAACA	AGTCGGTTGTTGTCCTGGAG
Jun	AAAACCTTGAAAGCGCAAAA	CGCAACCAGTCAAGTTCTCA
Nfkb2	TGACTGTGGAGCTGAAGTGG	GCCTTTAGAAGGAGGCGAGT
Rbm39	AACGGCCATGAAGAACGTAG	GGCCTCGGAATCTTCTATCC

[1] Housekeeping gene

Quantitive PCR (qPCR) was carried out using the SYBR®Green core kit (Euro-

gentec, UK) and an Opticon (MJ Research) qPCR thermal cycler. The fold change was calculated using the following method (Howe et al. 2004): the *Ct* value (threshold cycle) of the housekeeping gene was subtracted from the *Ct* value of the gene of interest, to obtain the ΔCt value. The $\Delta\Delta Ct$ value was calculated by subtracting the mean ΔCt value of the controls from the ΔCt of the sample of interest. The formula $2^{-\Delta\Delta Ct}$ was used to obtain the relative fold increase, which was subsequently converted to a percentage by multiplying the fold change by 100.

2.20 Micromechanical Measurements

2.20.1 Nanoindentation

Nanoindentation was used to compare the micromechanical properties of sutured regions of tendon to neighbouring unsutured regions of tendon. Crysections that were 30 μm thick were obtained. The experiment was carried out at room temperature in a controlled environment chamber. A Triboscope nanoindenter (Hysitron, Minnesota, USA), mounted on an AFM microscope (Explorer: Veeco, California, USA), was used in place of the AFM tip, which was controlled with a Veeco APEM-1000 Autoprobe Electronics Module. A 10 μm conospherical diamond tip was used to indent the samples.

To compare the mechanical properties of the sutured regions to the unsutured regions in the tendon, a series of indentations were set using a high precision X-Y stage with a 10 μm resolution (LINOS Photonics GmbH, Goettingen, Germany) to move the sample. Arrays of 100 indentations (four 5 by 5 grids) were set up, close and away from the suture. The drift rate was set to 0.15 nm/s and the loading rate to 200 μN/s.

To distinguish between the mechanical effects of the glass side and the tissue, the nanoindentation data were analyzed using FilmDoctor software. The mechanical properties of the glass slides were defined for single layer system of 30 μm thickness. The Poisson's ratio was assumed to be 0.5 for the samples. An effective spherical indenter

was fitted to the unloading curve using the equivalent half-space value for E, determined from the classical Oliver-Pharr method, as the initial value for the fitting procedure. A value for the radius of curvature of the effective sphere fitting the unloading curve was selected manually for each indent, until the best fit was achieved. E was subsequently determined from the upper portion of the unloading curve using this effective sphere radius. The measurements from each set of indents were averaged to provide a mean estimate of Young's modulus for the regions sampled. This method was adapted with help from Dr. Riaz Akhtar (Akhtar et al. 2009a).

2.20.2 Scanning Acoustic Microscopy (SAM)

Further mechanical information was deduced using scanning acoustic microscopy, which also provided information regarding the density of the tissue being studied. This enabled further comparisons to be made between sutured and unsutured regions of tendon. This was achieved by assistance from Dr. Mike Sherratt (Akhtar et al. 2009b). Cryosections (5 μm thick) were used, which were mounted on glass slides. Distilled water was added to the sections, as a coupling fluid and the samples were imaged at room temperature. The images were obtained using a SAM 2000 (KSI Gmbh, Heborn, Germany), using 1 GHz lens. For quantitive analysis, a frequency of 648 MHz was used. Analysis was carried out using the V*(f)* method.

2.20.2.1 V*(f)*-technique

This method takes advantage of the interference that is generated within thin tissue specimens mounted on glass slides. Imaging takes place near the focal plane (z = 0) so no incident P = waves are considered. P-waves are reflected by both the tissue-substrate and the tissue-coupling fluid. The amplitude of the returned signal is an interference of these reflected signals that is determined by the tissue thickness and the substrate and tissue properties. As the mechanical properties of the slides used, the substrate, are known, the unknown parameters which determine the amplitude of the

reflected wave are wave speed, tissue thickness, density and wave attenuation.

Thus, the estimated wave speeds can be calculated. The formula thickness /wavelength_in_water - thickness/wavelength_in_sample=phase/360 was used.

2.21 Statistical Analysis

Statistical analysis was carried out using IBM SPSS Statistics, version 18 (Illinois, USA). Graphs were produced using Delta Graph, Red Rock Software, Version 5 (Utah, USA). A p value of 0.05 or less, was considered significant, unless stated otherwise. All error bars used represent two standard deviations from the mean. Unless otherwise specified, at least three mice were used for each experimental condition. Approximately, 20 sections were obtained from electron microscopic samples and 60 sections from histological samples, of which 15-20 were used to count objects manually using Image J.

2.21.1 Measuring the Volume of the Acellular Zone

Measuring the area of every fourth section and multiplying it by 28 estimated the acellular zone volume for 4 sections (4 sections multiplied by the section thickness, 7 μm). 20 sections from the main body of the tendon were used and the volume of every 4 sections was added up to give the total volume. An association between suture depth and volume of acellularity was performed using Pearsons two-tailed bivariate correlation analysis.

2.22 3-Dimensional Reconstruction

A three dimensional representation of the histology of the tendon in relation to the suture and the acellular zone was obtained from 7 μm thick sections. The software Reconstruct (Fiala 2005)was used to accomplish this. Multiple images of the same tendon were montaged using Photoshop CS3 (Adobe, California) to obtain a single

image. Images of serial sections were uploaded to the programme in the correct order. The thickness between the different sections was entered and the images were calibrated. Next, the images were aligned to ensure that corresponding structures were overlying each other. The outlines of the structures of interest (the tendon, the acellular zone and the suture) were individually traced using a pen-like tool in the software. Also, spheres were used to mark cells. A 3-dimensional reconstruction was generated using this information by the software.

Part III

Results

CHAPTER 3

TEMPORAL AND SPATIAL CHARACTERIZATION OF THE ACELLULAR ZONE

3.1 Introduction

Wong et al. (2006b) first formally identified the acellular zone following a single interrupted suture repair in mouse, rat and rabbit tendon. It is important to define the temporal characteristics of the acellular zone, to determine which time points are critical to study in future studies aimed to elucidate the mechanisms of acellular zone formation. Also, by defining the timing of cellular events, insight can be gained into the potential mechanisms of acellular zone formation. The long term fate of the acellular zone is unknown; whether it remodels, repopulates, persists or increases in size. Also, the precise time at which the acellular zone form has not been determined.

In the study by Wong et al. (2006b) it was hypothesized that the grasping component of the suture was essential for the acellular zone to occur. This was concluded

based on the finding that the acellular zone did not develop when the suture was left *in situ* but not tied. Therefore, tying the suture was an important determinant of the acellular zone. The relationship between the grasping component of the suture and the acellular zone can be explored by investigating the relationship between suture depth and acellular zone volume. In addition, further insight can be gained by studying the relationship between the grasping component of the suture and the acellular zone form and volume in a Kessler repair. The Kessler suture is comprised of three main components: the knot, the connecting part and the grasping part. The knot contains the highest concentration of suture material so an acellular zone in its vicinity is likely to be secondary to a foreign body reaction to the suture material. The connecting part runs along the axis of the tendon and is not in the vicinity of the injury. The grasping component is designed to grip the tissue it enwraps to enable the repair to withstand the high tensile forces a tendon is expected to endure.

Therefore, the aims of this part of the study were:

- To monitor acellular zone formation from 6 hours to one year.
- To investigate the relationship between suture grasp depth and acellular zone volume.
- To establish if the acellular zone occurs in a Kessler suture and if so, to characterize the relationship between the different components of the suture and the acellular zone.

The expected outcome of this aim was a better understanding of the temporal events in the formation of the acellular zone and a glimpse into the molecular mechanism of acellular zone formation. Initial studies involved using a single suture model as it is the simplest model to use to measure acellular zone volume over time. However to gain an appreciation of the relationship of the suture design to the acellular zone a Kessler suture was employed. As the Kessler suture is relatively complex compared to the single suture, it was technically too difficult to perform a Kessler repair on an FDP tendon so the Achilles tendon was used, which is larger in size.

3.2 Single Suture Model

To determine the time it takes the acellular zone to form and to establish its long term fate, samples of sutured tendons were obtained after different time points. A single interrupted suture was inserted into 53 mouse FDP tendons (See Figure 1.5) . After 6 hours (n=3) and 1 (n=4), 3 (n=6), 5 (n=5), 7 (n=5), 14 (n=6), 21 (n=6), 28 (n=4), 56 (n=3), 84 (n=5), 168 (n=3), 365 (n=3) days, the tendons were dissected from the mice and chemically fixed. The tendons were then prepared for histological examination. The acellular zone's volume was estimated by multiplying the area of the acellular zone in every 4th section by 28 (as each section was 7 μm thick, so the thickness of 4 sections could be estimated by multiplying 4 by 7). Around 20 sections per sample were analyzed, and the estimated volume from the 20 sections was added up to give a total acellular zone volume. Although this method does not provide a precise volume for the acellular zone; its accuracy is strengthened by the fact that the acellular zone after a single suture always produces the same semi-elliptical shape. This calculation method would not be feasible if other suture configurations were used, as the acellular zone shape would not be as reproducible.

Histological analysis revealed that an acellular zone was present 6 hours after the tendons were repaired. The mean volume of the acellular zone at 6 hours was 2,101,885 μm^3 at 6 hours (+/- 2 SD = 1237378, SD = standard deviations). This was less than the acellular zone 24 hours after suturing, which was was 5,619,390 μm^3 (+/- 2 SD = 1334265). The difference between the acellular zone volume 6 hours and 24 hours after suturing was statistically significant (p = 0.0163). However, after 24 hours, the acellular zone volume appeared to fluctuate, as depicted in Figure 3.1. Although the acellular zone volume was larger one year after suture insertion (6,950,496 μm^3, +/- 2 SD = 230689), compared to one day after the repair, this difference was not statistically significant (p value = 0.4408). This suggests that the acellular zone is probably developing at 6 hours and is fully developed at 24 hours. Hence, future experiments aimed at elucidating the acellular zone's mechanism of formation should

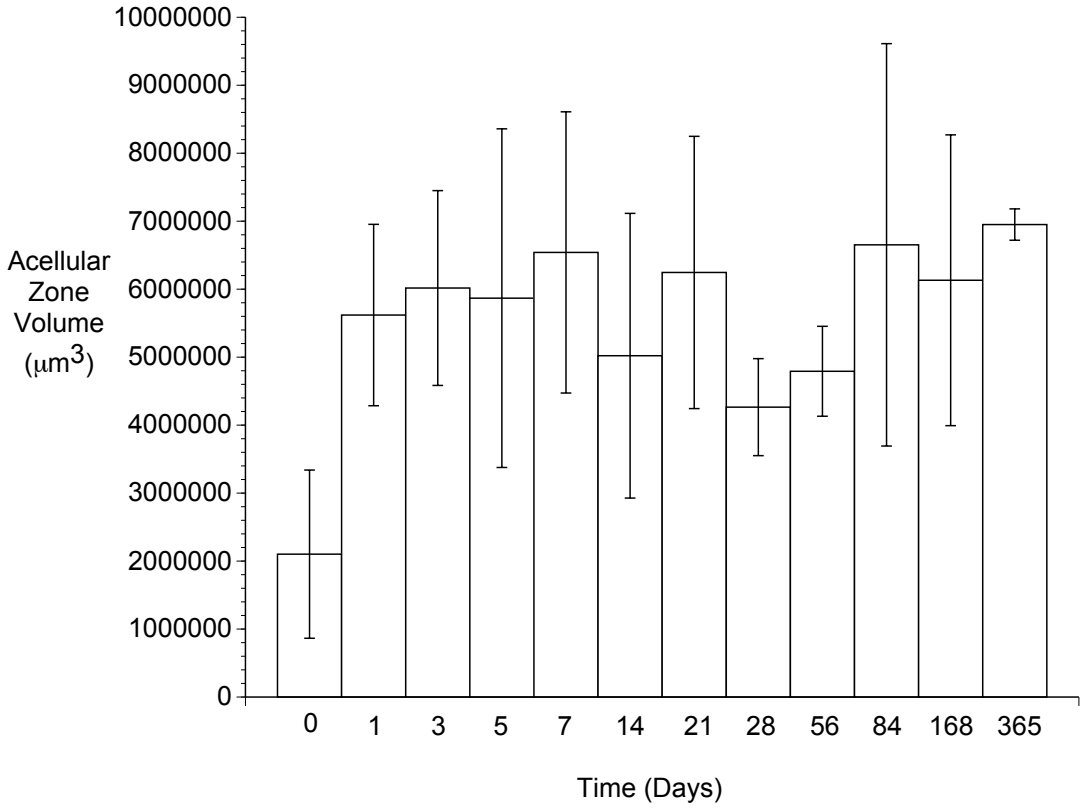

Figure 3.1: **The Acellular Zone After a Single Suture Over Time** Bar graph showing the acellular zone's volume from 6 hours (Day 0) after suturing and up to a year after a single suture repair in mouse flexor digitorum profunduns tendons. Between 3-6 injured mouse tendons were used for each time point. The acellular zone's volume does appear to increase from 6 hours to 24 hours after the which repair but does not change significantly after one day. Notably, cells do not appear to repopulate the acellular zone a year after the repair. Error bars = 2 standard deviations

study the acellular zone, as it develops, within the 24 hour time frame. These findings also indicate that the acellular zone is likely to remain permanently acellular once it has developed.

3.3 Kessler Suture Model

Determining whether the acellular zone is caused by the physical forces exerted by the suture grasp is very important, as it will facilitate the design of any future *in vitro* models of acellular zone formation. In addition, it would confirm that compressive forces are responsible for triggering the reaction that causes the acellular zone to form. To confirm the association between the suture's grasping component and the acellular zone, the acellular zone was examined in a Kessler repair, as it is a multi-stranded suture with multiple components that can be compared simultaneously. A fifty percent incision was made in the Achilles tendon of nine mice. This incision was repaired using a Kessler repair (See Figure 1.4C). Three mice were culled at each time point (3 days, 3 weeks and 3 months after the repair). The Kessler suture was observed at different time points to establish if the acellular zone after a Kessler repair was similar to an acellular zone after a single suture repair with no wound in it, in that it did not change in size after time. The Achilles tendons were dissected and histological sections (7 μm thick) were obtained. Sections were stained using H&E and TRITC-phalloidin, to detect any cell debris that may not be visible using H&E staining.

An acellular zone was present after a Kessler suture was used to repair a 50% incision in mouse Achilles tendon, 3 days, 3 weeks and 3 months after the repair (Figure 3.2). The acellular regions were restricted to the distal ends of the tendon, which coincided with the grasping components of the Kessler suture. In contrast, the mid-tendon, which is also the site of the 50% incision, appeared to be more cellularised. 3-dimensional reconstruction of the acellular zone, suture and tendon showed that the acellular zone was largest around the site of the grasping component of the Kessler suture. The site of the suture knot, in the mid-tendon, was more cellular. This con-

ferred a bow-tie configuration to the acellular zone, where the acellular zone around the grasping part of the suture became gradually smaller as it approached the knot. This gave the acellular zone the appearance of two round bottomed cones, where the tips of the cones meet at the site of the knot (See Figure 3.3). TRITC-phalloidin staining, which is a marker for the cellular actin cytoskeleton, and the nuclear stain Hoescht 33258 demonstrated that the acellular regions were devoid of nuclear and cytoskeletal staining (see Figure 3.2).

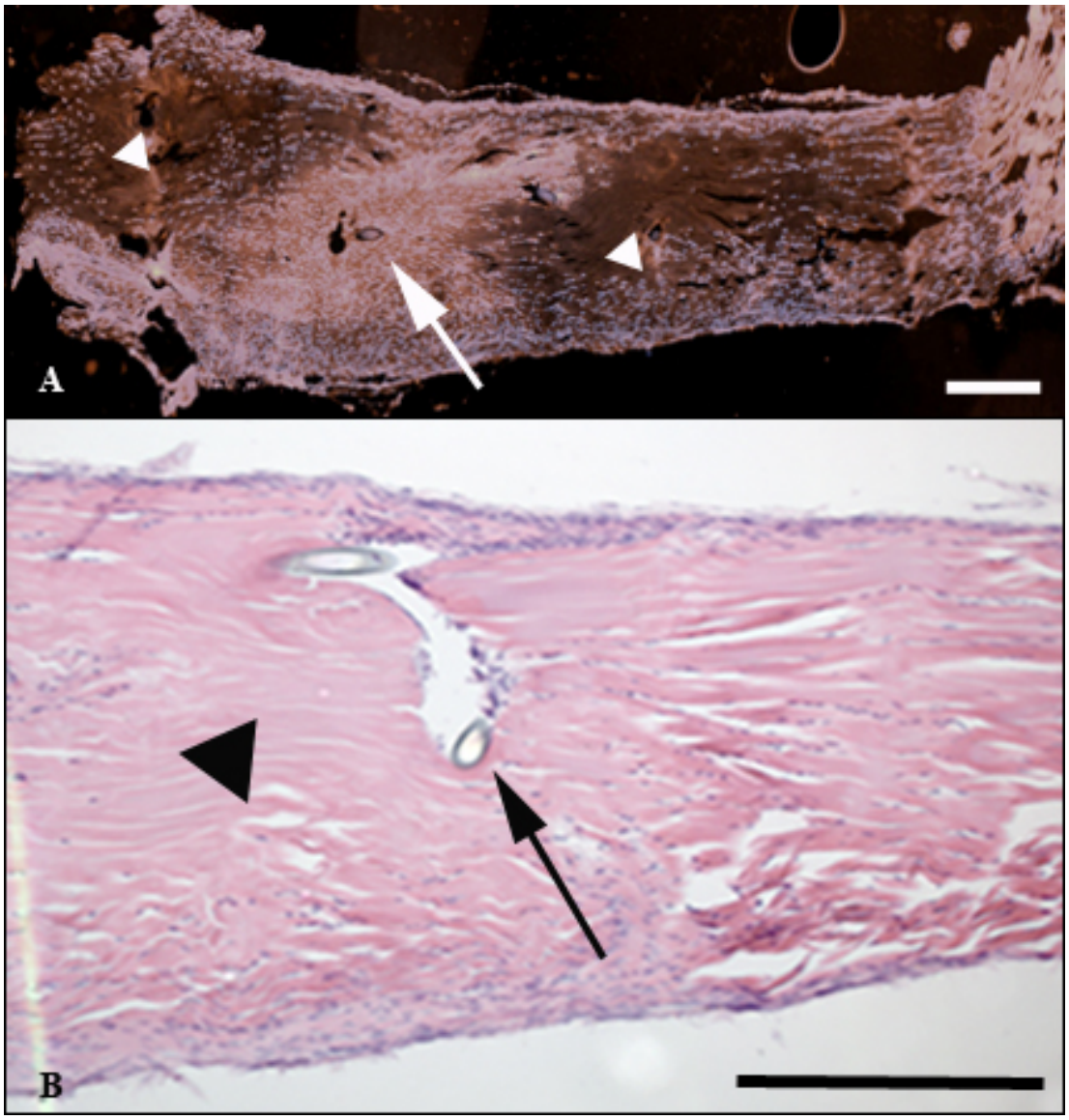

Figure 3.2: **The Shape of the Acellular Zone in a Kessler Suture** (A) A section from a mouse Achilles tendon, where an incision and knot was made in the tendon and repaired with a Kessler suture, then stained with TRITC-phalloidin and Hoescht 33258. The staining shows that the acellular regions were restricted to the distal ends of the tendon (white triangles). In contrast, the mid-tendon region (white arrow), also the site of the incision, appeared to be more cellularized. (B) Histological section from the same tendon showing the acellular region (black triangle) and the suture (black arrow) (scale bars = 100 μm).

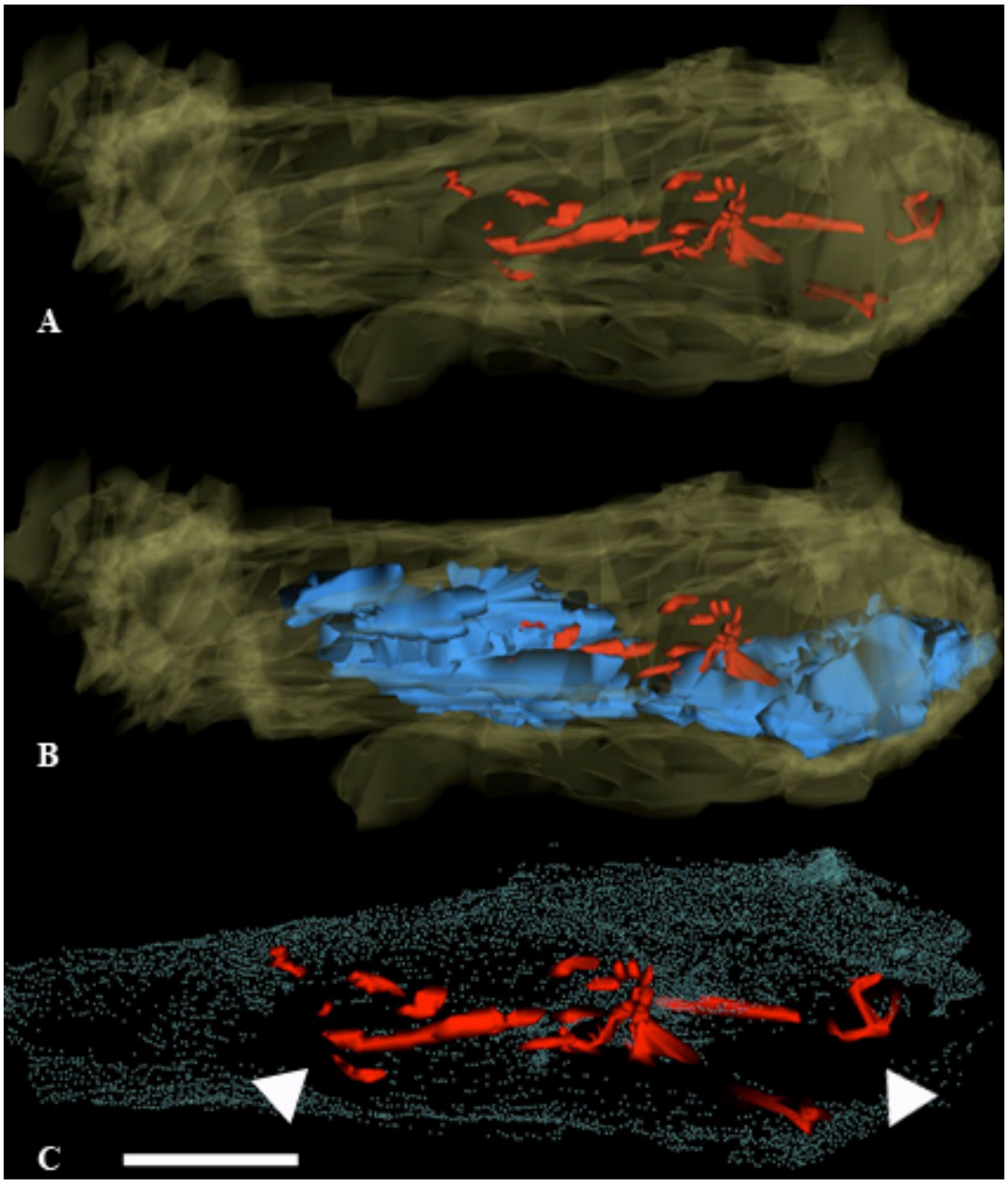

Figure 3.3: **3-dimensional Reconstruction of the Tendon, Suture and Acellular Zone** 3-dimensional reconstruction of (A) a Kessler suture repair and incision in a mouse Achilles tendon and (B) acellular zone. (C) Shows a Kessler suture in relation to the cells (grey-blue) in the Achilles tendon. The reconstruction shows the acellular zone is confined to the tendon's flanking regions and is more prominent around the suture's grasping components, conferring a bow-tie appearance to the acellular zone after a Kessler repair. In the mid-tendon region, which coincided with an incision, the tendon contained a large number of cells, compared to the rest of the tendon. *suture=red, tendon=yellow, acellular zone=light blue, cells=grey-blue* (scale bar = 100 μm)

The acellular zone did not appear to change in size with time, after a Kessler repair. As seen in Table **??**, the mean acellular area per section was 779,582 μm^2 after 3 days, 466, 552 μm^2 after 3 weeks and 648,603 after 3 months μm^2. The mean percentage of the total tendon area that the acellular zone occupied in histological sections was 10%. The change in acellular zone size was not statistically significant (p value = 0.069 between 3 days and 3 weeks, p value = 0.01788 between 3 weeks and 3 months and p value = 0.5621 between 3 days and 3 weeks, paired t-test). The proportion of the acellular zone occupied by the tendon was different (mean percentage of acellular area occupying total tendon area on sections = 13.9% after 3 days, 5.9% after 3 weeks and 9.2% after 3 weeks). This difference was statistically different between 3 days and 3 weeks (p value = 0.0022) and between 3 weeks and 3 months (p value = 0.0471) but not between 3 days and 3 weeks (p value = 0.1289). However, these differences could be accounted for by the difference in the mean tendon total area in the different time points (mean tendon area = 5,509,369 μm^2 at 3 days, 8,335,558 μm^2 at 3 weeks and 6,853,024 μm^2). The p values were 0.0001 between 3 days and 3 weeks, 0.0257 between 3 weeks and 3 months and 0.0255 between 3 days and 3 months (See Figure 3.5).

The relationship between the grasping component of the suture and the area occupied by the acellular region on histological sections, showed that a greater grasping suture length was correlated with a greater acellular region. (correlation coefficient = 0.781, p=0.0001). The acellular zone area near the muscular end of the tendon (mean = 299,243 μm^2) occupied a smaller volume than the acellular zone near the bone (mean = 441,452 μm^2, ±2SD = 399376) in the tendon but this difference was not statistically significant (p value = 0.116, unpaired t-test). There was no statistically significant difference between the grasp length of the suture in the muscular end of the tendon (mean 1062 μm^2, ±2SD = 205305) compared to the grasp length of the suture in the bony end of the tendon (717 μm^2), (p value = 0.06, unpaired t-test) (see Figure 3.4).

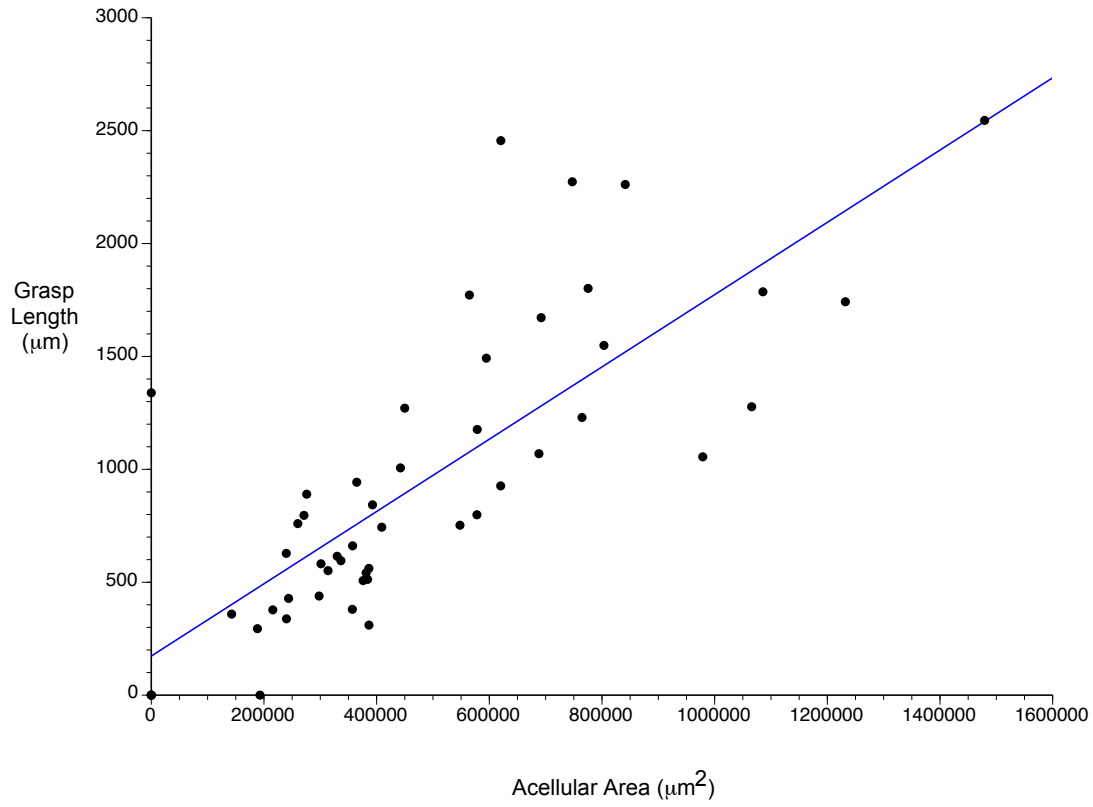

Figure 3.4: **The Relationship Between the Size of the Kessler's Grasp and the Acellular Zone** A scatter plot demonstrating the relationship between the acellular area and the length of the suture's grasp per section. The grasping part of the suture refers to a configuration of the suture, which grips the tendon.The was obtained from nine mouse Achilles tendons, which were repaired using a Kessler suture (tissue fixed 3 days (n=3), 3 weeks (n=3) and 3 months (n=3) after the repair). A best fit line is shown in blue and appears to be closely related to the distribution of the dots, suggesting that there is a relationship between the suture's grasp size and the acellular zone's size.

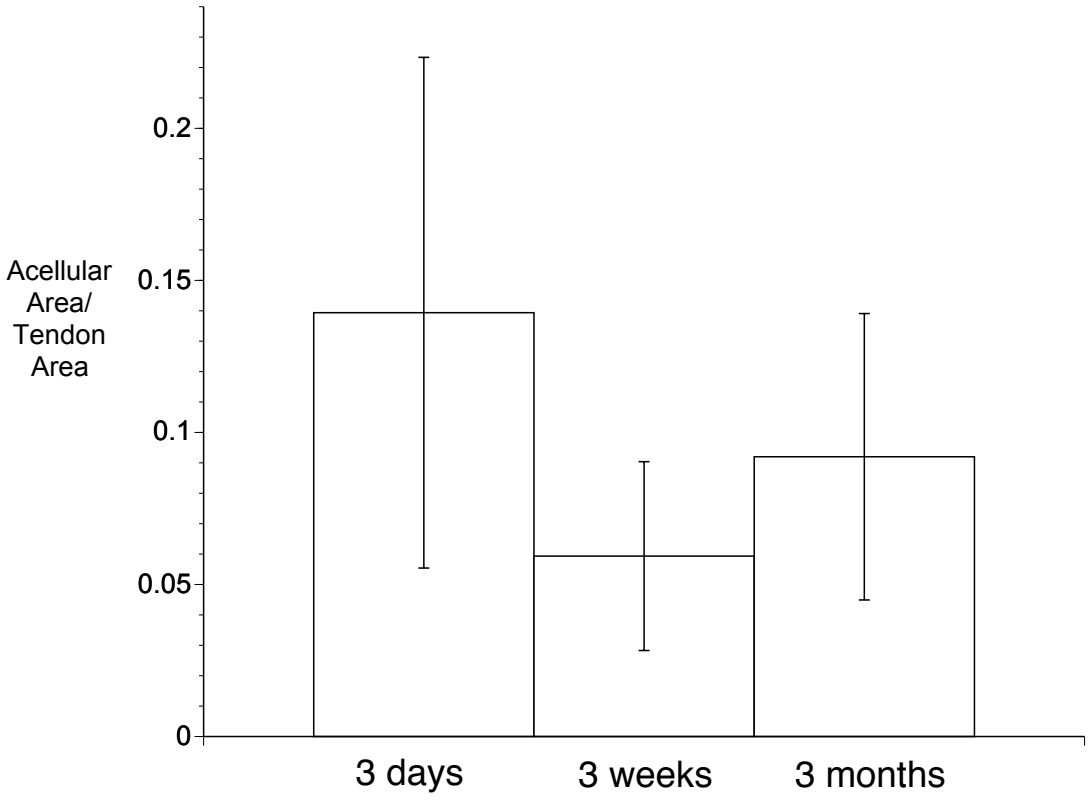

Figure 3.5: **The Acellular Zone in a Kessler Suture Over Time** Bar graph showing the proportion of the tendon occupied by the acellular zone (the sum of the areas that are acellular divided by the total tendon area in serial histological sections) in Achilles tendons repaired with a Kessler suture, over time. The time points observed were 3 days (n=3), 3 weeks (n=3) and 3 months (n=3). The Acellular zone appears to occupy a greater proportion of the tendons at 3 days. The acellular zone may have been occupying a larger proportion of the tendon at 3 days, as younger tendons are smaller in size. Error bars = ±2SD.

3.4 Discussion

This worked spanned the entire first of study and provided valuable information about the acellular zone that was used to design an *in vitro* model of acellular zone formation. The results demonstrated that an acellular zone is formed within 24 hours of suturing the tendon and did not change after that. In hindsight, the experiment could have ended after 1 day, however, we would have not learnt that the acellular zone appears to never re-populate with cells, which is an intriguing finding. Hence, it can be concluded that the results of this part of the study, suggest that there were at least two components to the formation of the acellular zone. An initial reaction of cells in the immediate vicinity of the injury and a permanent change to the tissue that was refractory to repair or re-cellularisation.

The 6 hour lag between the initial insult, the tying of the suture and the formation of the acellular zone, shows that a relatively slow signaling process occurs within cells. For example, necrosis occurs almost instantly after cells are damaged, whereas other cell death mechanisms such as anoikis, where the cells detach from the extracellular matrix, have been shown by Valentijn et al. (2003), to take several minutes to hours to initiate. The persistence of the acellular zone for at least a year after injury suggests that the extracellular matrix is damaged or altered so that it no longer supports cellular attachment or infiltration. Damage to the extracellular matrix by suturing has been demonstrated by McDowell et al. (2002) and Pasternak et al. (2007) who both showed an increased expression of certain MMPs at the suture site accompanied by biomechanical weakening. This biomechanical weakening was shown to be reversible by Pasternak et al. (2007) by coating the sutures with doxycycline, which can inhibit MMP activity. This may explain why, in clinical practice, *in vivo* studies conducted in animals, have shown that partial tendon lacerations left to heal on their own always healed better than lacerations that were sutured (Zobitz et al. 2000). This observation was also noted in humans, where a prospective randomized clinical trial, showed that Achilles tendon ruptures healed better using non-surgical treatment methods compared

to tendons repaired using a suture (Nistor 1981).

However, it is not always feasible in practice to leave injuries on their own and suturing is necessary. Hence, there is a need for optimizing surgical repairs using sutures, to reduce the tissue damage incurred by the suture. To achieve this, further characterizing the cellular and molecular mechanisms that are upregulated after suturing is necessary. This need is emphasized by the fact that suturing appears to trigger a tissue response that is dissimilar to the healing response after an incision. The difference in tissue response to suturing compared to an incision is highlighted by Kessler suture study. Histological analysis of incisions in mouse Achilles tendons repaired with a Kessler suture showed that the laceration becomes hypercellular and within the same tendon, the grasping regions of the Kessler suture become acellular. Although both injuries occur within the same tendon, the cellular responses are different. This suggests that an injury after a cut heals by a different mechanism to an injury after suturing. Hence, the need for further characterizing the cellular and molecular events after suturing, to identify targets, which can be used to optimize surgical repairs. Also, this dichotomous tissue response supports the claim that the mechanical compressive forces that are created within surrounding tissue by tying a suture are triggering acellular zone formation and not the suture material. Consequently, understanding the mechanisms of acellular zone formation may also provide insight into the pathways involved in mechanotransduction, which has implications for other mechanically stressed tissues such as blood vessels, muscle and cartilage (Jaalouk and Lammerding 2009).

In conclusion, this part of the study has shown that the acellular zone develops within 24 hours and thus future studies to elucidate the mechanisms of its formation should be set within that time frame. Also, the acellular does not repopulate a year after the repair and appears to heal via a different mechanism to lacerations. The other parts of this study will aim to characterize the cellular and molecular events that occur after suturing and to describe the mechanical and ultrastructural features of the sutured extracellular matrix to gain insight into why the acellular zone remains acellular.

CHAPTER 4

THE CELLULAR RESPONSE TO SUTURING

4.1 Introduction

The acellular zone is likely to form by either cell migration away from the suture or via cell death. Evidence of apoptosis was not detected by Wong et al. (2010), who demonstrated a lack of staining for apoptotic markers 6 hours after suturing. However, as described in the preceding literature review, there are many other types of programmed and non-programmed cell death that may be contributing to generation of the acellular zone. To rule out cell death definitively, electron microscopic examination of the developing acellular region around the suture was necessary. This would confirm the absence of cells and if cells are present, would allow morphological descriptions of the appearance of the cells and the extracellular matrix, which cannot be deduced from histological sections.

However, ruling out cell death is not a sufficient premise to conclude that the acellular zone is primarily due to cell migration. Cell migration would need to be confirmed

by carrying out a time lapse study of the acellular zone as it is forming and tracking cell movement as it occurs. To achieve this, an *in vitro* model of acellular zone development is required so that the optimal imaging methods to visualize individual cells in the tendons can be used. Establishing whether the acellular zone forms via cell migration or cell death is important as this information is pivotal to understanding its development.

4.2 Electron Microscopic Examination of Early Acellular Zone Formation

Electron microscopy was used to examine mouse FDP tendons that were repaired using a single suture. This was carried out to characterize the morphology of the cells in the developing acellular zone. This is a key step to determine if cell death occurs in the acellular zone. Also, if cell death occurs in the acellular zone, electron microscopy could give an indication of the morphology of the dying cells (refer to Section 1.3.3.2 for details using the features used to classify the morphology of cell death). As Chapter 3 established the the acellular zone was developing at 6 hours and fully developed at 24 hours, the following time points were selected: 30 minutes after the repair, to examine instant cellular changes, 3 hours after the repair, to assess early changes and 24 hours after the repair to examine late cellular changes (n = 3 for each time point).

4.2.1 Uninjured Tendon

As shown in Figure 4.1, uninjured tendon fibroblasts had an elongated spindle-like shape. The cells were located in clusters of 3-5 cells, which were aligned with the long axis of the tendon. Thin long projections protruded from the cells, connecting them longitudinally and transversely. The cells were closely apposed to the surrounding collagen fibrils and no inflammtory cells were observed. The nuclei of the cells compromised a large portion of the cell body and it contained darkly staining patches, probably of dense chromatin. The cell membrane of the cells could be seen and was continuous around the cells. Mitochondria, endoplasmic reticulum and ribosomes could be seen. The cytoplasm of the cells appeared to be devoid of lysosomes and the organelles did not appear swollen.

4.2.2 30 minutes post-repair

After 30 minutes post-suture, the cells adopted a more rounded shape compared to uninjured tendon (see Figure 4.1). The cellular processes connecting the cells were also lost. No apoptotic bodies were found. The pericellular extracellular matrix contained irregular, small diameter fibrils (see Figure 4.10), with visible banding. Cell fragments could also be seen interspersed between the collagen fibrils. No inflammatory cells could be detected.

The nucleus appeared large and was not condensed or degraded. A cell membrane was present around the cells. The mitochondria and endoplasmic reticulum appeared to be larger than in uninjured tendon, in relation to the size of the nucleus, indicating that they could be swollen (Figure 4.2).

4.2.3 3 hours post-repair

At 3 hours after the repair, the cells remained round with no visible cellular processes. No apoptotic bodies were detected. Single cells were seen between fibrils, instead of 3-5 cells observed in uninjured tendons. The extracellular matrix was full of cell fragments and narrow diameter fibrils could be seen around the cells. Inflammatory cells were not present.

Occasionally, uneven clumps of chromatin were seen but did not have the characteristic appearance of the condensed, disintegrated nuclei seen during apoptosis. The endoplasmic reticulum appeared dilated and some mitochondria lost their cristae. The cytoplasm appeared to be more vacuolated than it did at 30 minutes after repair and in uninjured tendon. Cytoplasmic contents were detected in the extracellular space. Most cells had an absent cell membrane or a partially degraded one (Figure 4.3).

4.2.4 24 hours post-repair

The cells at 24 hours after the repair, displayed similar features to earlier time points. Namely, cell rounding, loss of cytoplasmic processes and presence of narrow diameter

fibrils around the cells. Generally, there were less cells, especially ones with an intact nucleus. Most regions contained cell remnants scattered in between collagen fibrils. Less of the narrow diameter fibrils could be seen around the cells and no inflammatory cells were found in the main tendon body. The collagen fibrils that were present, had visible banding, appeared organized but there was more space between the fibrils, which may be due the space occupied by the cells being vacated.

Few cells were intact and the space formerly inhabited by cells, contained spilt cytoplasmic contents with no encasing cell membrane. Ribosomes, lysosomes and cell fragments could be found in former cell spaces and between collagen fibrils (Figure 4.4).

In summary the cells within the acellular regions display features of cell necrosis and lack features of apoptosis or autophagy. Cells appeared rounder, lacked cellular processes and a matrix composed of narrow diameter fibrils surrounded the cells.

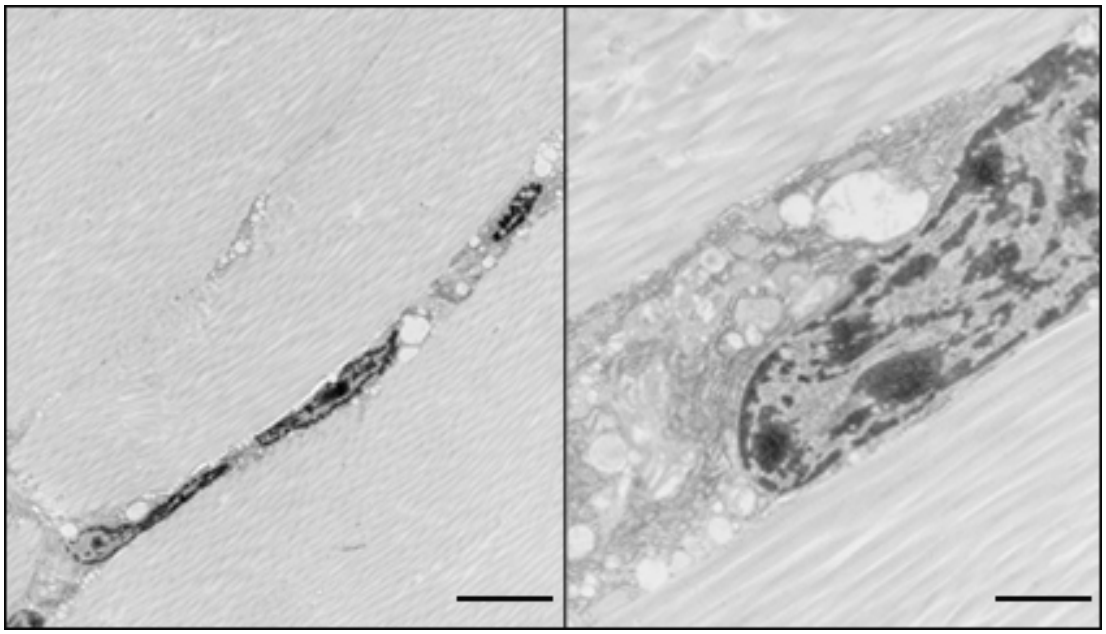

Figure 4.1: **Electron Microscopy of Cells in Uninjured Tendons** Electron microscopic images of tendon fibroblasts in mouse flexor digitorum superficialis tendons. (Left) The cells were located in rows containing 3-5 cells, aligned along the long axis of the tendon. The cells were elongated and cytoplasmic projections extended from the cells' bodies. (Right) The cells were closely opposed to the collagen fibrils. The nuclei of the cells were large and the cell membranes were intact. *scale bar: left = 5 μm, right = 1.7 μm*

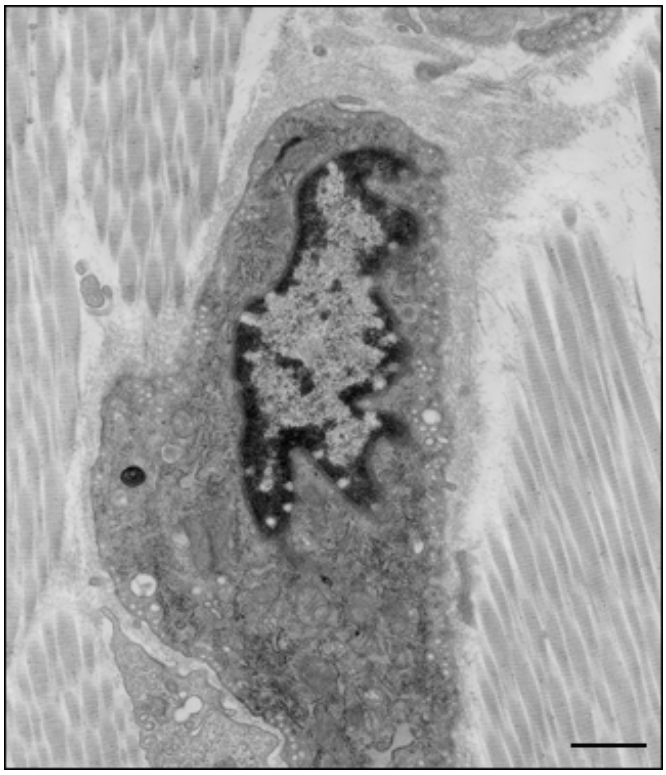

Figure 4.2: **Electron Microscopy of Cells 30 minutes after Suturing** The electron microscopic image is of a tendon fibroblast, from a mouse flexor digitorum superficialis tendon, 30 minutes after the tendon has been sutured. the cell appears more rounded, compared to cells in uninjured tendons. The cellular processes which connect the cells in uninjured tendons were no longer seen. A pericellular matrix was more prominent around the cells and was composed of narrow diameter irregular fibers. The cell nucleus was large and the cell membrane of the cells was intact. *scale bar: 8 μm*

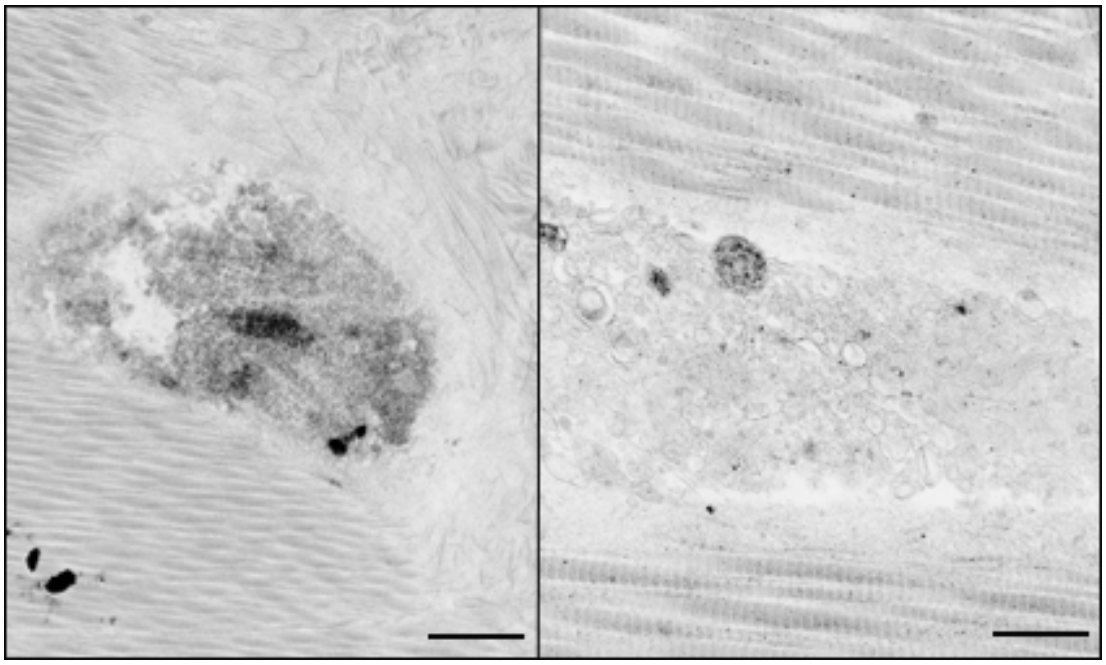

Figure 4.3: **Electron Microscopy of Cells 3 hours after Suturing** Electron microscopic images of mouse flexor digitorum superficialis tendons, 3 hours after a repair with a single interrupted suture. (Left and Right) The cells do not appear to have an intact cellular membrane. The cytoplasmic contents appear degraded and vacuolated. Cellular fragments could be seen in the extracellular matrix, intermingled with narrow diameter fibrils. The cell nucleus, in some cells, contained uneven clumps. No cytoplasmic projections could be seen, connecting the cells.*scale bar: left = 1.7 μm, right = 6 μm*

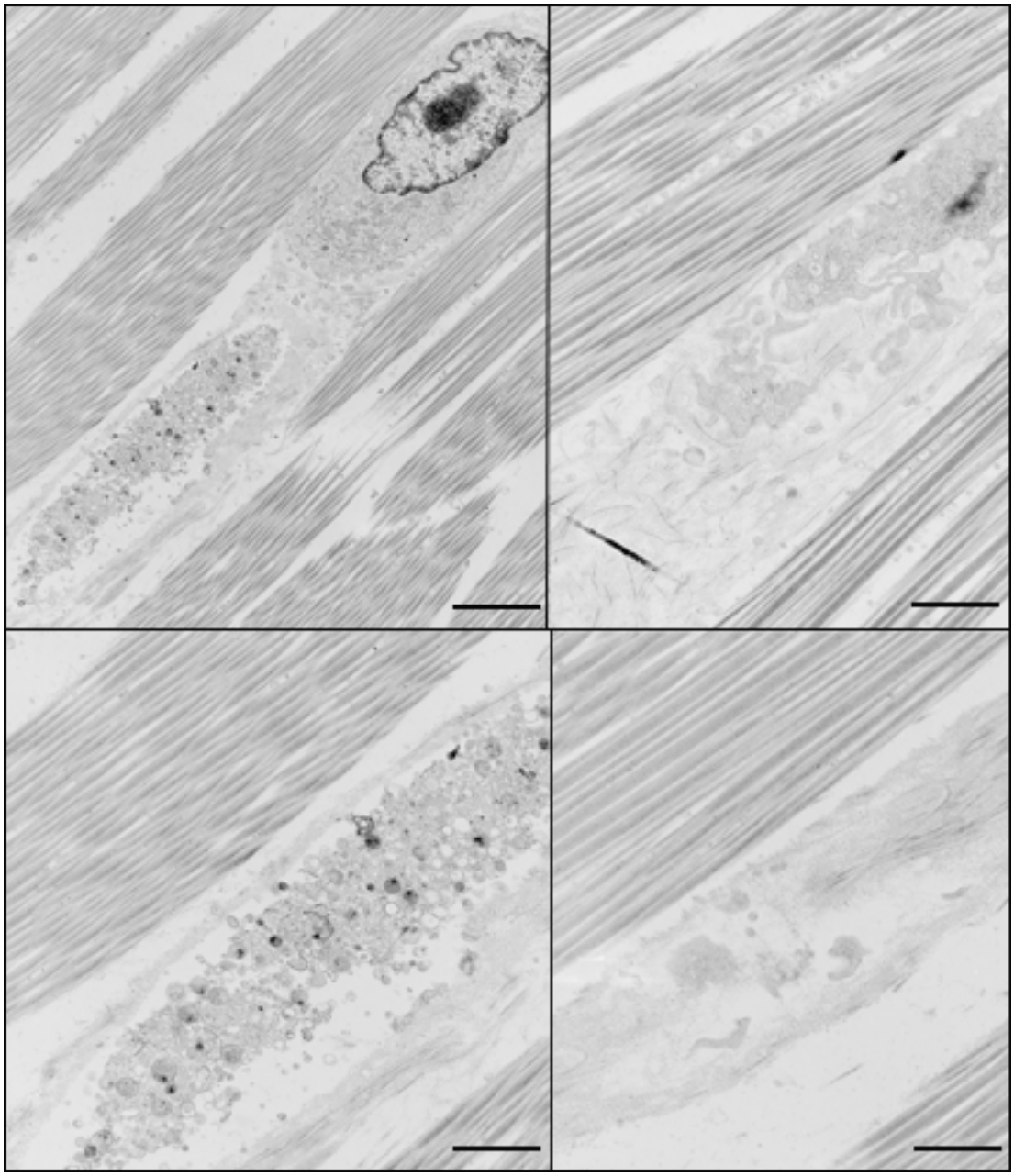

Figure 4.4: **Electron Microscopy of Cells 24 hours after Suturing** Electron microscopic images of mouse flexor digitorum superficialis tendons, 24 hours after they have been sutured. The cells were more rounded, had no cytoplasmic connections and were surrounded by narrow diameter fibrils. The collagen fibrils were not closely apposed to the cells. Cell fragments could be seen interspersed between collagen fibrils.*scale bar: top left = 5 μm, top right = 6 μm, bottom left = 2.3 μm, bottom right = 8 μm*

4.3 *Ex Vivo* Model of Acellular Zone Formation in Sutured Tendon

Exciting results showed that the acellular zone is in fact a death zone. However, to exclude the involvement of factors such as inflammation, animal-to-animal variation (i.e. males vs female hormonal influences, sedentary vs active mice, differences in feeding regime); it was necessary to develop an *ex vivo* model for tendon wounding that was aimed to be a robust method for studying tendon injury. A desirable feature of this model would be that it could be used to conduct live cell imaging and could be used to compare the effects of adjusting variables such as tension across the tendon. Also, a larger sample size could be used, whilst the number of animals used for *in vivo* could be reduced, in accordance with the guidelines of 'The National Centre for the Replacement, Refinement and Reduction of Animals in Research' (NC3Rs), established by the UK Government.

Different methods were used in an attempt to induce the acellular zone *in vitro*. After several trials, using different conditions; it emerged that tension was necessary for acellular zone formation. Acland clamps were used to exert consistent amounts of tension across the tendon. The amount of tension across the tendons could also be varied by sliding the clamps along a bar, which changed the distance between the clamps (see Figure 4.5). Tendons that were clamped and dissected, to maintain the tendons under tension were compared to tendons that were dissected but the clamps were brought close together were compared. The tendon explants that were held between clamps that were brought close together were referred to as 'untensioned' tendons, as the tension across these tendon explants was low compared to tendons that were stretched using the clamps.

An acellular zone was evident in flexor digitorum profundus tendons that were placed under tension during suturing (see Figure 4.5). The acellular zone observed had a bell-shape, although it appeared smaller than the acellular zone found in tendons sutured *in vivo*. The extracellular matrix appeared aligned and the fibrils did not display

evidence of damage histologically. Tendons that were not placed under tension and sutured, did not have an acellular zone on histological examination (see Figure 4.5). Histologically, the fibrils looked disorganized, running in multiple orientations and broken fibril ends could be seen.

4.3.1 Electron Microscopic Examination of *Ex Vivo* Model

Although, histologically the acellular zone was evident *in vitro*, electron microscopic examination of acellular zone formation *in vitro* was required to verify that the mechanism of acellular zone development was similar to its formation *in vivo*. The morphology of the cells could be compared in tendons sutured *in vivo* and *in vitro*. As histological findings showed that tension across the tendons must be maintained for acellular zone development *in vitro*; its influence on cell morphology must be determined to distinguish the effects of tension on cell morphology from the effects of suturing. Hence, electron microscopic examination of sutured and unsutured tendons and under and not under tension was carried out. FDP tendons were carefully dissected from wild type mice and either sutured and placed under tension, sutured and not placed under tension (see Figure 4.5), not sutured and not placed under tension or sutured and not placed under tension (n = 3 for each experimental group). The tendons were then prepared for electron microscopic examination, 24 hours after the tendons were left in culture.

4.3.1.1 Unsutured Tensioned Tendon

The cells were elongated in unsutured tendons under tension and had long processes connecting the cells, as seen in uninjured tendons *in vivo* (see Figure 4.1). The cells had a large nucleus, that occupied about half the cellular body on longitudinal sections. The extracellular matrix contained organized collagen fibrils, with clear banding. The cells were closely apposed to the cell matrix. Mitochondria with visible cristae could be seen in the cytoplasm. An intact cell membrane surrounded the cells (see Figure 4.6). These observations show that uninjured tendons placed under tension *in vitro* had

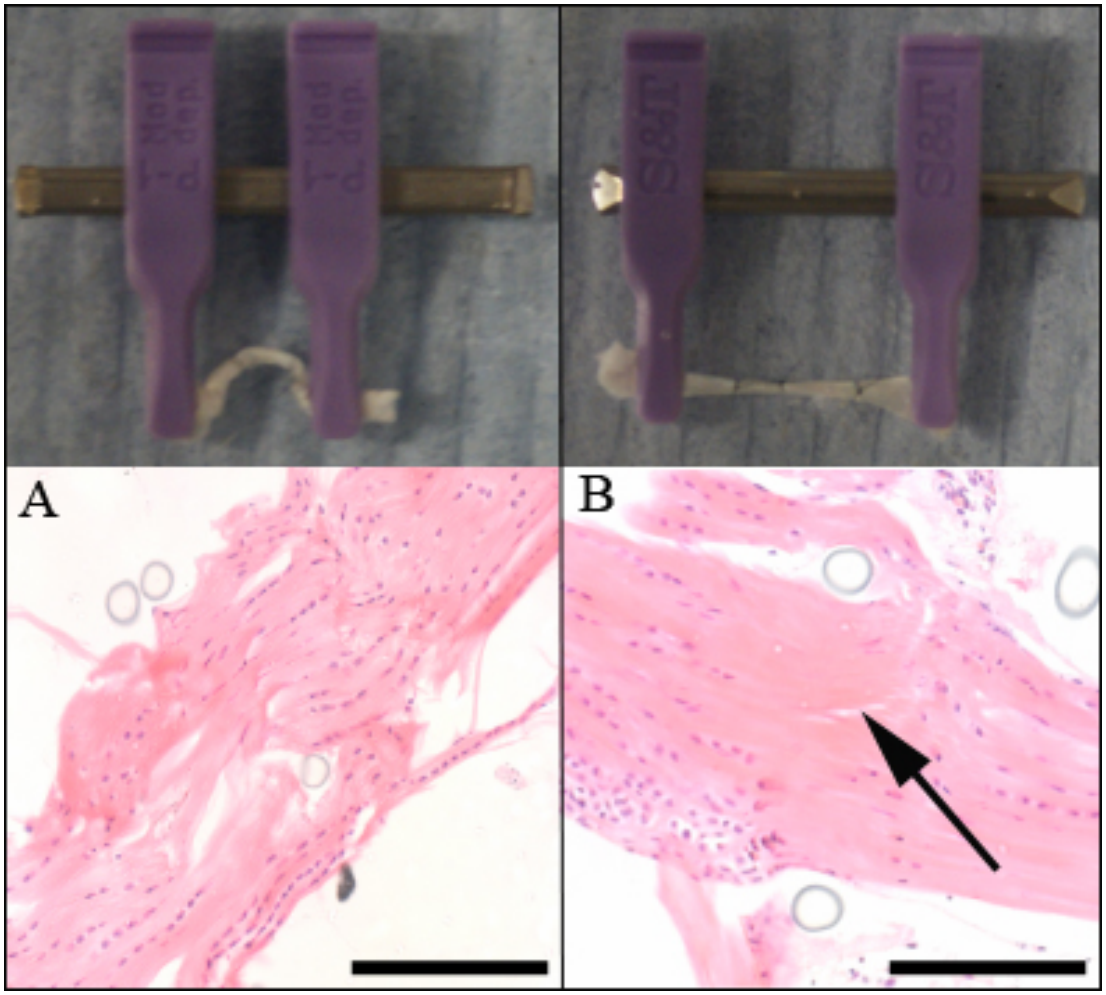

Figure 4.5: **Histology of *Ex Vivo* model** Mouse flexor digitorum profundus tendons were dissected. Acland clamps (metal bar = 1.00 mm) were used to grip the tendons ends, to modify the amount of tension across the tendon. The tendons were either not placed stretched (top left), or stretched so that the tendons were under greater longitudinal stress (top right). The tendons were sutured and medium containing DMEM, fetal calf serum, L-glutamine and penicillin-streptomycin was added. They were placed in an incubator (37°C, 5% CO_2) for 3 hours. After 3 hours, the tendons were fixed and histologically examined. In the tendons not placed under tension the extracellular matrix appeared disorganized and no acellular zone was present (bottom left). In the tendons placed under tendon, an acellular zone (black arrow) was seen between the two sutures (bottom right). Scale bar = 100μm.

similar morphological features to uninjured tendons *in vivo* and no evidence of damage to the cells or extracellular matrix could be detected.

4.3.1.2 Sutured Tensioned Tendon

The cells in the sutured tendon explant under tension were more rounded and did not posses cytoplasmic processes. Occasionally, cytoplasmic contents could be detected outside the cells, in the surrounding extracellular matrix, scattered between collagen fibrils. The pericellular matrix consisted of narrow diameter fibrils, with visible banding. The cells appeared to be detached from the extracellular matrix. The nucleui appeared intact and there were no visible nuclear condensations or observable nuclear fragmentation. Several lysosomes could be seen in the cytoplasm. Endoplasmic reticulum and mitochondria could still be seen in some cells (See Figure 4.7). The features observed in sutured tendon explants under tension were comparable to those in suture tendons *in vivo* (see Figure 4.4). In both conditions, the cells displayed evidence of cell necrosis, the cells were detached from the extracellular matrix and a pericellular matrix consisting of narrow diameter fibrils was observed.

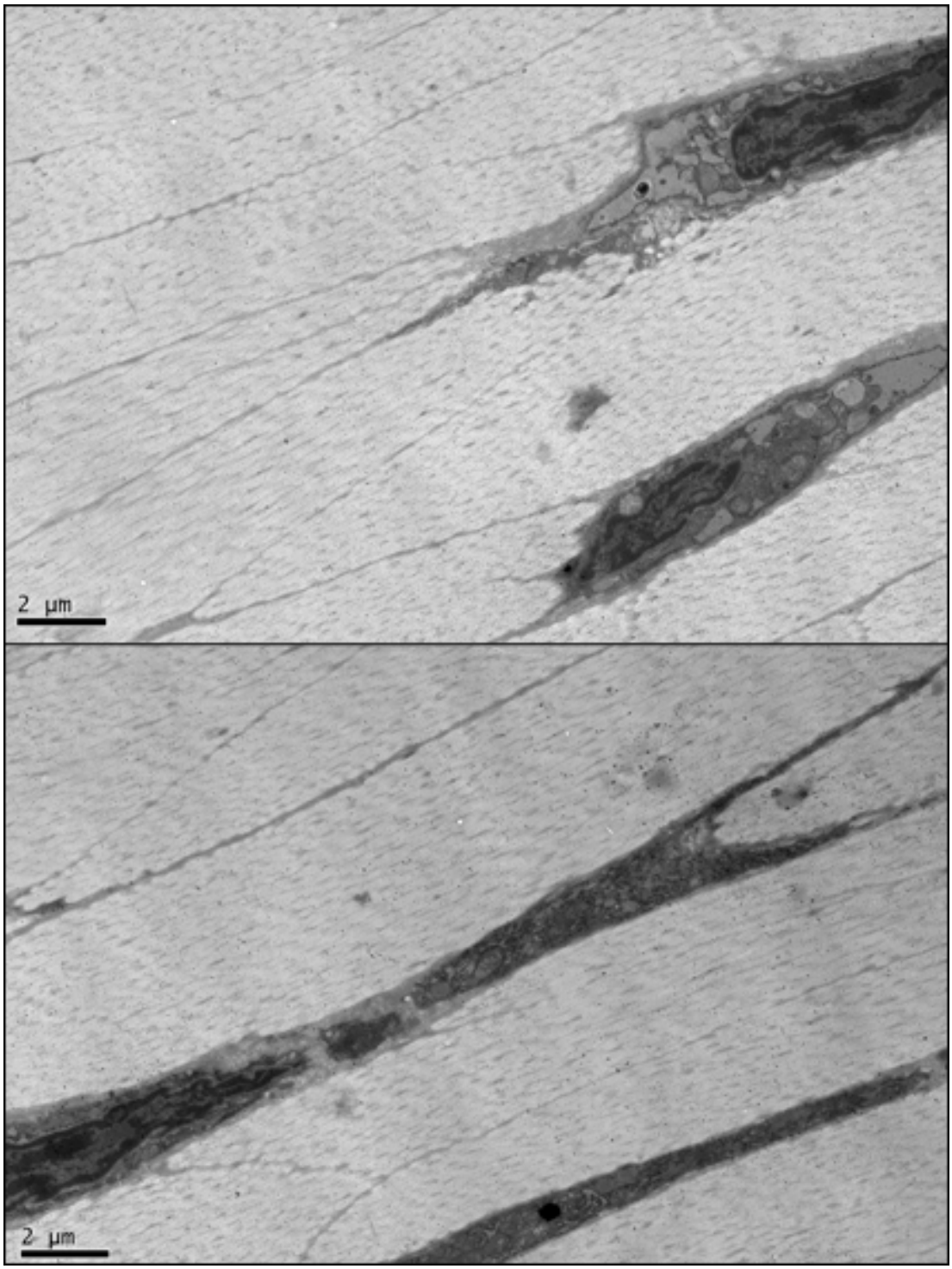

Figure 4.6: **Tendon Explants Unsutured and Under Tension** Electron microscopic images of mouse flexor digitoorum profundus tendon explants, which were stretched using Acland clamps. The tendons were placed in culture conditions (37°C, 5% CO_2) for 24 hours and then prepared for electron microscopy. The images show that the cells are elongated, with long processes connecting the cells. The cells had a large nucleus and the cell membranes were intact. The cells were also closely apposed the extracellular matrix. *scale bar: 2 µm*

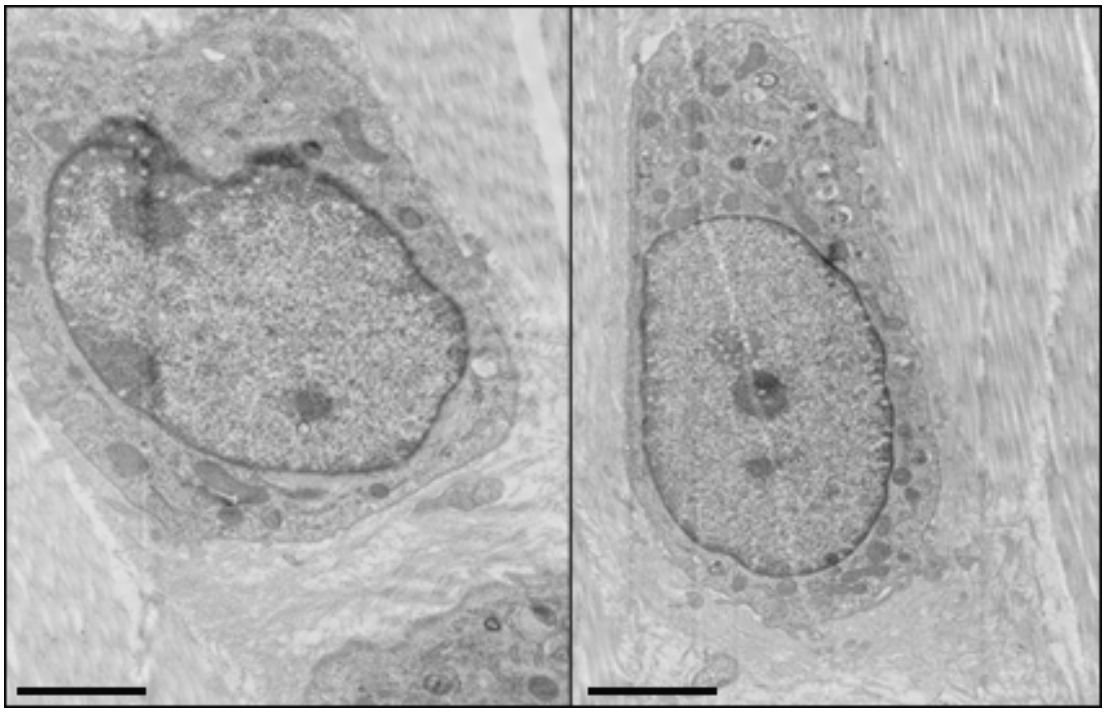

Figure 4.7: **Tendon Explants Sutured and Under Tension** Electron microscopic images of mouse flexor digitorum profundus tendon explants, which were stretched using Acland clamps and sutured. The tendons were placed in culture conditions (37°C, 5% CO_2) for 24 hours and then prepared for electron microscopy. The images show that that the cells were more rounded than in unsutured explants under tension and lacked the cytoplasmic processes also seen in unsutured explants. The pericellular matrix contained narrow diameter fibrils and the cells appeared to be more separated from the extracellular matrix, compared to unsutured explants. The nuclei appeared intact and lysosomes were present diffusely in the cytoplasm. Some cellular contents could be seen dispersed between the collagen fibrils. *scale bar: left = 1 μm, right = 1 μm*

4.3.1.3 Unsutured Tendon Not Under Tension

In tendons that were not sutured and not placed under tension, the cells appeared round with no interconnecting cellular projections. The pericellular matrix contained narrow diameter fibrils. The cells were not closely apposed to the collagen fibrils, which appeared organized with clear banding. The nuclei were large, appeared intact and had a visible nuclear envelope. The endoplasmic reticulum and mitochondrial cristae could be seen. The cell membranes were preserved in some cells (see Figure 4.8). These finding showed that the loss of tension across tendons induced some cell damage and shared some features with sutured tendons, including the loss of cellular connections, rounding of the cells and the appearance of a pericellular matrix which contained narrow diameter fibrils (see Figure 4.4 and Figure 4.7).

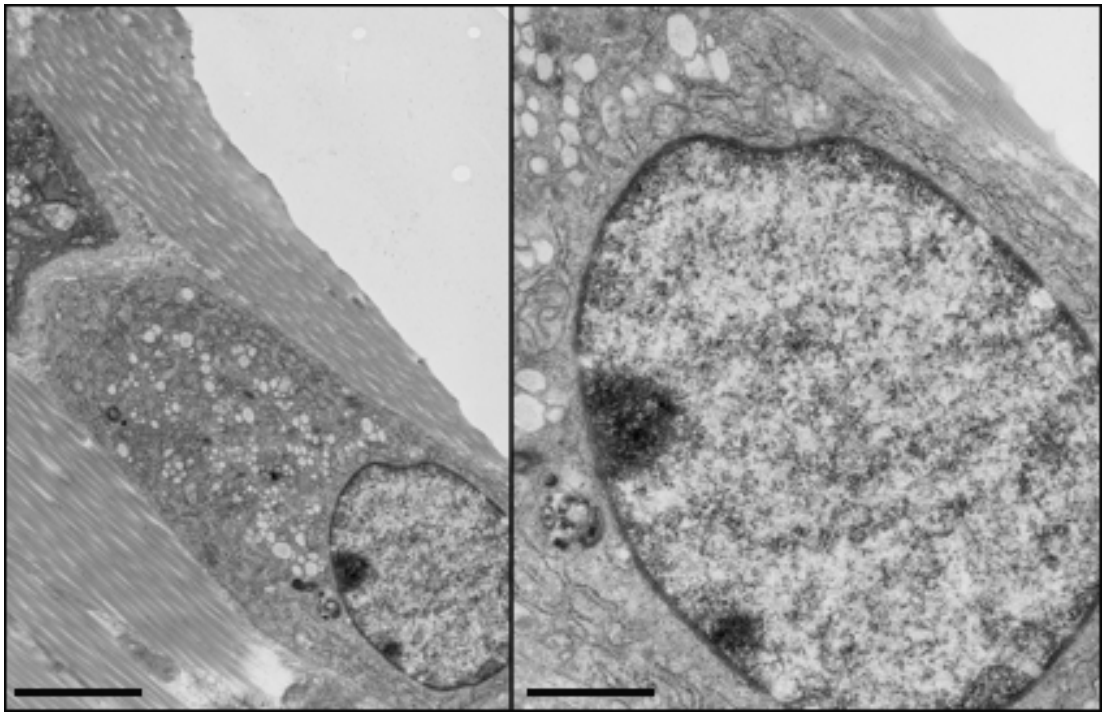

Figure 4.8: **Tendon Explants Not Sutured and Not Under Tension** Electron microscopic images of mouse flexor digitorum profundus tendon explants, which were gripped using Acland clamps but not stretched. The tendons were placed in culture conditions (37°C, 5% CO_2) for 24 hours and then prepared for electron microscopy. The images show that that the cells were round with no interconnecting cellular projections. The pericellular matrix contained narrow diameter fibrils and the cells were not closely apposed to the collagen fibrils. The nuclei and the cell membranes appeared intact. The cytoplasm of the cells appeared to contain a large number lysosomes. *scale bar: left = 0.5 μm, right = 2 μm*

4.3.1.4 Sutured Tendon Not Under Tension

The extracellular matrix around the cells contained a large amount of cell remnants in sutured tendons not under tension. The surrounding collagen fibrils were disorganized, emanating from multiple directions. Narrow diameter fibrils were present that had banding and the cells looked detached from the matrix. The nuclei were large with a preserved nuclear envelope. The chromatin had regions that were lightly and darkly stained, with no detectable fragmentation or condensation. A cell membrane was present around the cells, which had numerous lysosomes at its border with the cytoplasm. The cytoplasm was saturated with lysosomes of varying sizes that appeared to encase cellular contents. Occasionally, double-membraned phagolysosomes could be seen. Some mitochondria were darkly stained. Cytoplasmic regions not occupied by lysosomes contained very thin, short fibrillar structures that were randomly orientated (See Figure 4.9). Evidence of cell damage was present in sutured tendons not under tension. This shows that suturing causes damage to tendon whether it is under tension or not.

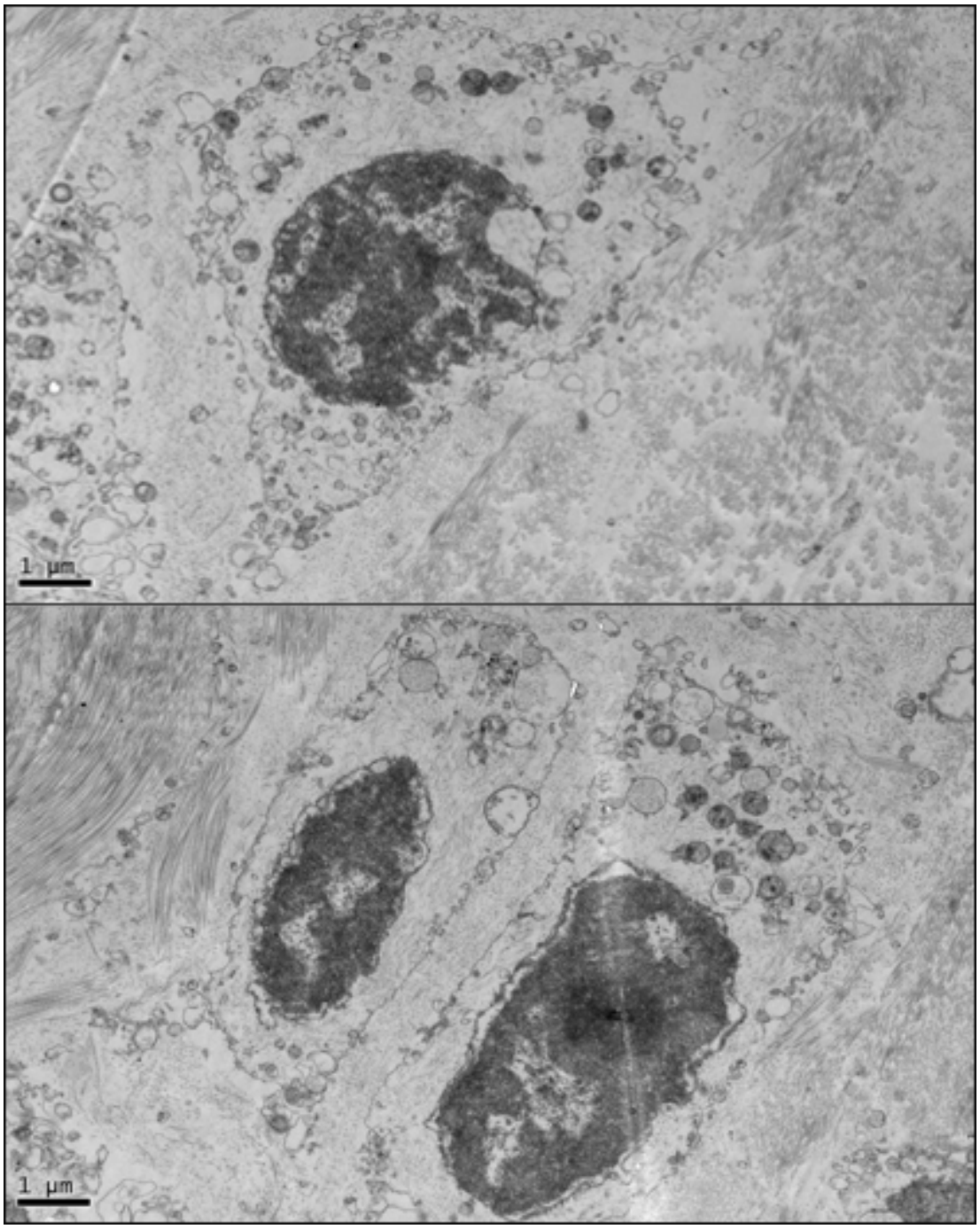

Figure 4.9: **Tendon Explants Sutured and Not Under Tension** Electron microscopic images of mouse flexor digitorum profundus tendon explants, which were gripped using Acland clamps but not stretched and sutured. The tendons were placed in culture conditions (37°C, 5% CO_2) for 24 hours and then prepared for electron microscopy. The images show that the extracellular matrix around the cells contained a large number of cell remnants, was disorganized and narrow diameter fibrils were seen around the cells. The cells were rounded, had no cytoplasmic connections between the cells and appeared detached from the extracellular matrix. the nuclei were preserved but the cell membranes could not been seen surrounding the cells. Numerous lysosomes and some phagolysosomes were evident in the cytoplasm. The cytoplasm of the cells also contained disorganized short, narrow fibers. *scale bar: 1 µm*

4.3.2 Measurements of Cell Shape in Uninjured Tendons, Sutured Tendons and Tendon Explants

It was observed that the cells appeared more rounded in sutured tendons and tendon explants than uninjured tendons *in vivo*. To confirm this observation, measurements were obtained of the tendon fibroblasts' length, width and area occupied in electron microscopic sections (n=3, 30 sections, see Table 4.1 for means and standard deviations). To obtain the measurements three tendons were used for each conditions. For each conditions tendon 20 sections were obtained. Of those five sections, five images were taken per tendon. Each parameter (length, width and area) was measure in fifty different fibroblasts in each image. The tendon fibroblasts from uninjured tendons (mean = 35.5 μm) had a greater length than the cells in sutured tendons (mean = 10.0 μm) and tendon explants (mean = 10.9 μm). The difference in tendon fibroblast length in electron microscopic sections was statistically significant between cells from uninjured tendon and explants (p value = 0.0001) and cells from uninjured tendons and sutured tendons (p value = 0.0001) but not between cells from explants and sutured tendons (p value = 0.5434). The cells from uninjured tendons also had a smaller width (3.7 μm) than cell from explants (6.2 μm) and sutured tendons (5.1 μm). This difference was statistically significant between cells from uninjured tendons and explants (p value = 0.0005) and cells from uninjured tendons and sutured tendons (p value = 0.007) but not between cells from explants and sutured tendons (p value = 0.1982). The area occupied by the cells in the uninjured tendons (64.5 μm^2) appeared larger than the area occupied by the cells from the explants (48.2 μm^2) and the sutured tendons (35.5 μm^2). The difference in area size does not appear to be significantly different between the uninjured tendon and the tendon explants (p value = 0.128) or the tendon explant and the sutured tendon (p value = 0.1966) but does appear to be significant between the sutured tendons and the uninjured tendons (p value = 0.03).

Table 4.1: The Effect of Injury on Cell Shape

	Cell Length (μm) (SD)	**Cell Width (μm) (SD)**	**Cell Area (μm^2) (SD)**
Uninjured Tendon	35.5 (10.0)	3.7 (0.92)	64.5 (28.3)
Explant	10.0 (2.8)	6.2 (2.0)	48.2 (20.7)
Sutured Tendon	10.9 (2.8)	5.1(0.8)	35.5 (13.4)

4.3.3 Diameter of Narrow Fibrils Observed in Sutured Tendons and Tendon Explants

Sections 4.2 and 4.3.1 describe the emergence of a matrix, which surrounded the cells, composed of disorganized narrow diameter fibrils. These narrow diameter fibrils were observed in sutured tendons and tendon explants but not in uninjured tendons. These fibrils had a mean diameter of 38.1 nm in tendon explants and 38.1 nm in sutured tendons. This diameter was significantly smaller than that of the adjacent collagen fibrils (214.5 nm), (p value = 0.0001) (See Figure 4.10).

4.4 Visualization of Acellular Zone Formation in Sutured Tendon Explants

In unsutured tendons not under tension, propidium iodide (red, marker for cell death) staining could be seen immediately on the tendon surface. The rest of the tendon stained green for calcein AM (marker for cell viability). At the beginning of the experiment 92% of the cells were stained red. After 5 hours, the staining was not visible, probably secondary to photobleaching. No cell migration could be detected using particle tracking on Image J (NIH, USA). In sutured tendons under tension, propidum iodide staining (red, dead cells) was evident around the suture at the start of the experiment. Some staining was also present at the tendon surface. The rest of the tendon

stained greed for calcein AM (viable cells). At the beginning of the experiment, 9% of the cells stained red and the rest were green. After 1 hour 21% of the cells around the suture stained red. One hundred percent of cells around the cells around the suture stained red after 3 hours. This increase in propidium iodide staining of cells progressed outwardly, away from the suture, towards the distal tendon ends. After 5 hours, staining was difficult to see as the dyes are likely to have bleached (See Figures 4.11 and 4.12). It was not possible to detect any significant cell migration.

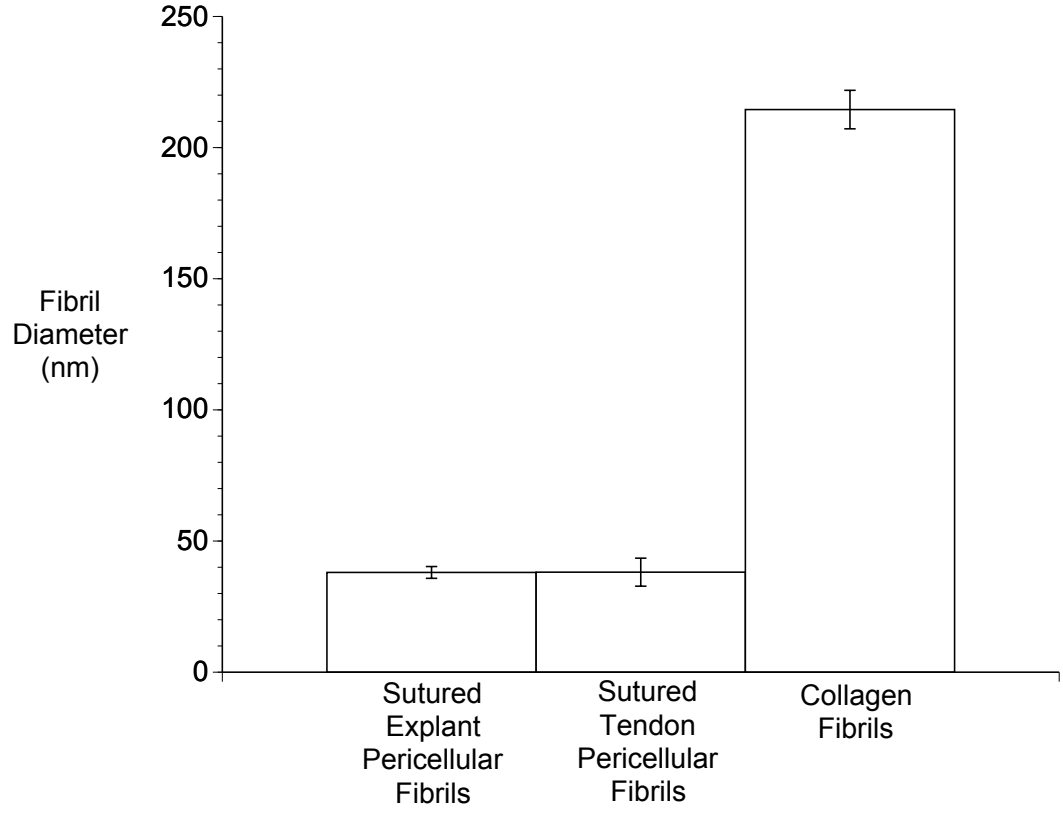

Figure 4.10: **The Diameter of Fibrils in the Pericellular Matrix** Bar graph of the diameter of different fibrils in sutured tendon explants and sutured tendons. Mouse flexor digitorum profundus tendons and explants (placed under tension using Acland clamps) were sutured and fixed for electron microscopic examination, 24 hour later. A newly formed pericellular matrix was observed around cells in sutured regions of tendon and tendon explants which contained narrow diameter fibrils. The narrow diameter fibrils had a mean diameter of 38.1 nm in sutured tendon explants and 38.1 nm in sutured tendons. This was statistically significant (p = 0.0001, *t-test*) compared to the diameter of collagen fibrils, which was 214.5 nm. Error bars = standard deviation

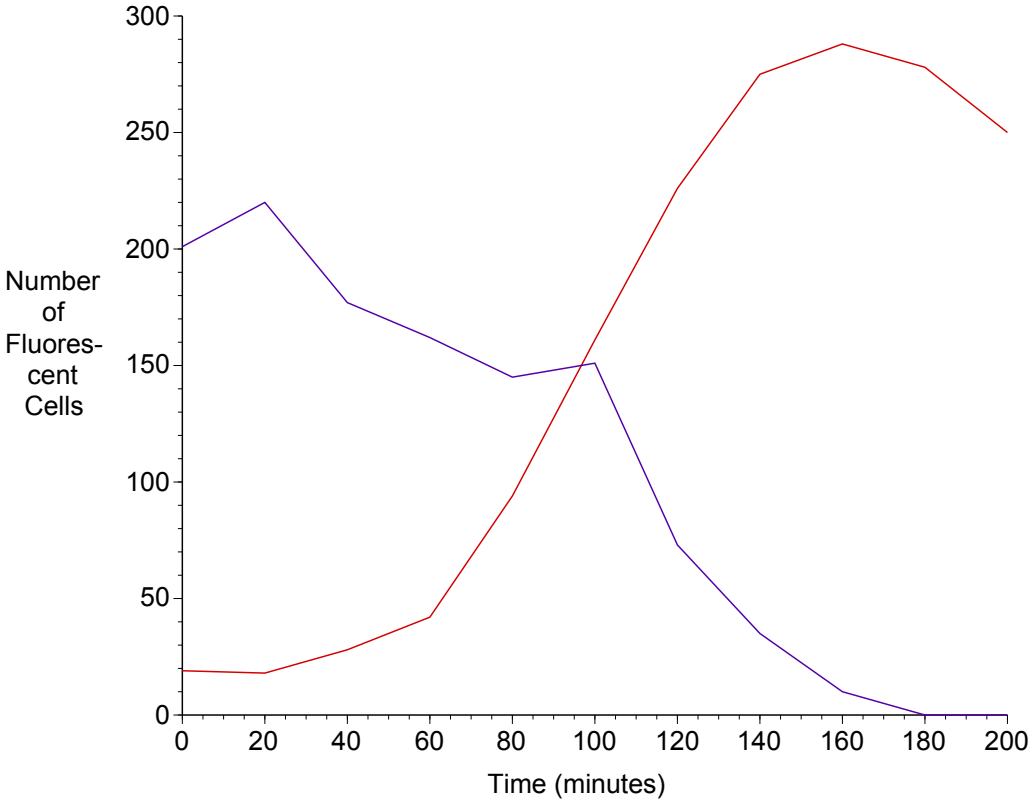

Figure 4.11: **Time Lapse Study of the Developing Acellular Zone** Line graph, illustrating the number of cells stained with propidium iodide (red) and calcein AM (purple) in a sutured tendon (mouse flexor digitorum profundus), placed under tension using Acland clamps, over 24 hours. The tendon explants were placed in a chamber, which maintained the temperature at 37°C and the carbon dioxide concentration at 5%. After 20 minutes, the number of cells with calcein AM staining (which stains viable cells), begins to decrease and no cells stained with calcein AM can be detected after 180 minutes. Cells with propidium iodide staining gradually increase in number, peaking between 160-180 minutes.

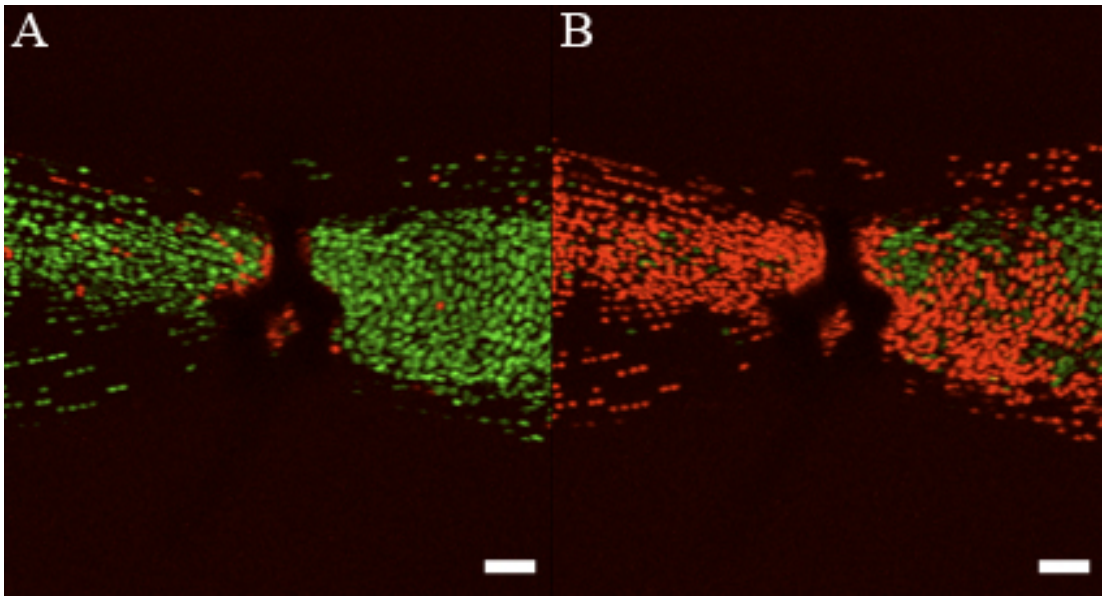

Figure 4.12: **The Spread of Cell Death in the Developing Acellular Zone** Propidium iodide staining (red, stains dead cells) can be seen around the suture at the start of the experiment (left). The rest of the tendon stained green for calcein AM (green, stains viable cells). After 180 minutes the tendon contained a much large number of cells, which stained for propidium iodide and few cells that stained for calcein AM. Scale bar = 100 μm.

4.5 Discussion

The aims if this chapter were to determine the mechanisms involved in acellular zone formation. The findings in this chapter suggest that cell death is the principal mode of acellular zone formation. Morphological evidence of cell death was obtained from electron microscopic images of the developing acellular zone. As features of apoptosis and autophagy were not detected in the region around the suture , necrosis was deemed to be the most likely mode of cell death in the acellular zone, by exclusion of the former two. However, this is a negative definition of cell death and biochemical evidence to confirm the cell death modality is required. As there are no specific markers for cell necrosis, this has to be achieved by excluding the presence of biochemical markers for apoptosis and autophagy (Kroemer et al. 2009). The exclusion of apoptosis as the predominant mode of cell death in the evolving acellular zone was supported by Wong et al. (2010), who found that the acellular zone did not express apoptotic immunohistochemical markers (Bax, Bcl-2, activated cleaved caspase 3 and cytochrome C) in the extracellular matrix of a region of sutured tendon, six hours after the tendons were sutured.

Electron microscopy of the evolving acellular zone also showed that the tendon fibroblasts become more rounded after suturing and that they were surrounded by a matrix composed of fibrils that had a diameter ~38 nm. This matrix also developed around tendon fibroblasts in tendon explants. The rounding of the cells and the loss of cellular projections in sutured tendons may determinately affect cell function, as the cells lose their cell-to-cell contacts. The development of an *in vitro* model of acellular zone formation provides insight into how the acellular zone develops, in additions to its use a tool to investigate acellular zone formation. The fact that the acellular zone can form *in vitro* suggests that inflammatory cells, other extratendinous cells and ischemia are improbable contributors to the evolvement of the acelullar zone and supports the notion that the acellular zone is secondary to changes within the tendon. This reinforces the findings in Chapter 3, which showed a correlation between the size of the

suture grasp and the size of the acellular zone. The importance of tension was also highlighted in the formation of the acellular zone. Electron microscopy showed that the cells in tendon explants that were not under tension, the cells were more rounded . A similar finding in tendon explants, was shown by Arnoczky et al. (2008), who demonstrated via transmission electron microscopy studies, a loss of the intimate contacts between the tendon cells and pericellular matrix in stress deprived tendons. In addition, Egerbacher et al. (2008) showed that in these stress deprived explant cells underwent apoptosis, 24 hours later and expressed MMPs (Arnoczky et al. 2007). These findings emphasized the importance of controlling for tension in the microarray that was carried out. Hence the use of sutured and unsutured explants under and not under tension in the microarray.

The visualization of acellular zone evolvement *in vitro* showed that cell death occurs in the acellular zone, as observed by electron microscopy and that cell migration was not likely to be involved in the process of forming the acellular zone. The time lapse study also demonstrated that the acellular zone propagated from the suture site in a bell shaped wave. This suggests either that signals are transmitted from cells closest to the injury to cells deep within the tendon, or that cells respond differently to the injury depending on the distance away from the injury site. Thus cell death appears to occur in a bell shaped wave away from the suture site to form a distinct acellular or death zone, 24 hours after suturing. Chapter 3 showed that this acellular zone persists for up to a year. The next aim would be to elucidate the molecules involved in acellular zone formation, which can be targeted to prevent acellular zone formation.

CHAPTER 5

GENE EXPRESSION IN SUTURED TENDON EXPLANTS

5.1 Introduction

The previous chapter concluded that cell death was the major mechanism for the generation of the acellular zone. This new chapter contains an exploratory study, which aimed to gain a novel insight into the mechanisms of cell death.

A microarray approach was used to characterize molecules involved in acellular zone formation to confirm the findings from the previous chapter by comparing the genes detected in the microarray analysis to the morphological features observed in electron microscopy studies and to identify potential therapeutic targets. Conducting a proteonomic analysis was considered to identify genome wide changes in proteins, and, using a candidate approach to identify proteins that might indicate the mode of cell death. However, performing a microarray study was considered to be a good starting point for those studies. Also, within the time frame of the thesis, the excellent microarray facilities in the University of Manchester's Faculty of Life Sciences could

be used. Proteonomics would have taken considerably longer and would have not been feasible within the time scale of this PhD. In addition, there are several different approaches in proteonomics and without a gene analysis first, it would have been high risk to attempt to do a proteonomic analysis of the acellular zone.

The microarray analysis utilized tendon explants, as it permitted the study of the effects of suturing in isolation of confounding factors, such as the inflammatory response in skin. It also permitted certain parameters, such as tension to be used. Three sutures were used instead of one as this maximized the tendon's biological response to the suture, so more tissue could be used for the microarray, whilst minimizing the number of mice that needed to be used significantly.

5.2 Microarray Analysis of Sutured Tendon Explants

Microarray analysis was carried out using tendon explants. Mouse FDP tendons were dissected and treated in four different ways. Tendons were either sutured and placed under tension using Acland clamps, sutured and not placed under tension, not sutured and placed under tension using Acland clamps and not sutured and not placed under tension (n = 4 for each experimental group). Explants were studied under and not under tension to distinguish between differences in gene expression due to tension and changes in expression due to suturing, as the previous chapter revealed that varying tension induced a cellular response. Also, the effects of the treatments on gene expression could be compared to their electron microscopic appearance, which was also described in the previous chapter.

The explants were left in culture for 3 hours before RNA was isolated and processed for microarray analysis. The 3 hour time point was used as it corresponds to the developing acellular zone, which was elucidated in Chapter 3. The parts of the tendon that were gripped by the clamp were removed by a sharp incision, just before RNA isolation, to minimize the effects of the grip of the clamps on gene expression. An *in vitro* of acellular zone formation was used because of the advantages of using an *in vitro* model mentioned in the introduction of Chapter 4 to study the acellular zone. The main advantage is that the use of tendon explants ensures that the differences in gene expression were solely due to the tendon cells and not due to the surrounding tissues.

5.2.1 One Way Comparisons

The mean expression across the probe set was calculated to be 82.45. Changes in gene expression in response to treatment was calculated using the t-test. Changes were considered to be significant if the following criteria were met: the fold change in gene expression was greater than 1.5, had a p value less than 0.05 and the difference in the raw value of mean expression greater than 50 between the groups. Information was

obtained about the genes that met the aforementioned criteria using OMIM. Based on the information obtained from OMIM about a particular gene, the genes were categorized into functional groups. The frequency of genes in each functional groups was calculated to gain an idea about the cellular processes influenced by the different treatments.

5.2.1.1 Unsutured Untensioned vs Unsutured Tensioned Tendons

Fifteen genes were considered to be significantly different when tension was varied in uninjured explants. Moxd1 had the lowest p value, which was 0.005 and Gbp2 had the highest fold change, which was -3.07. A third of the genes in this set were related to the inflammatory cascade (Ubl5, Lipocalin, Clec4e, Cfbb). Other genes encoded for extracellular matrix proteins, Wnt signaling molecules, cytoskeletal proteins, oxygen stress response mediators, glutamate signaling proteins and mediators of cell senescence (See Figure 5.1).

5.2.1.2 Sutured Tensioned vs Unsutured Tensioned Tendons

Significant changes in gene expression were observed in 38 genes between sutured tendons under tension and unsutured tendons not under tension. Txnip had the lowest p value, which was 0.000265 and Hspa1a had the greatest fold change, which was 2.65. Inflammatory mediators represented the largest family of genes, accounting for 32% of the total number of genes. Three other gene families had a large number of genes. These were genes linked to programmed cell death pathways (n=5, 13%), the Fos/Jun Ap-1 transcription complex and pathway (n=4, 11%), and metabolic pathways (n=4, 11%). The remaining genes encoded extracellular matrix proteins, oxidative stress mediators, components of the NfκB pathway, growth factors, cell cycle determinants and transcription factors (See Figure 5.2).

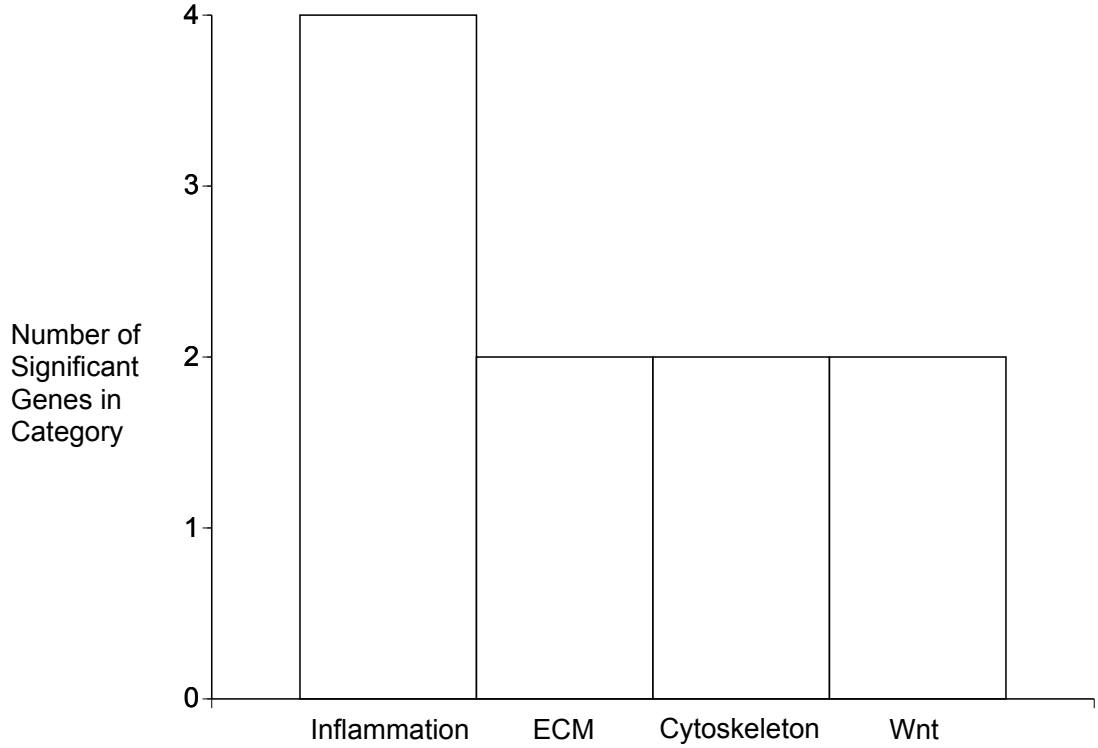

Figure 5.1: **Unsutured Untensioned vs Unsutured Tensioned Tendons** A cDNA microarray was used to compare gene expression in unsutured mouse tendon explants, not under tension to gene expression in unsutured mouse tendon explants, under tension, after 3 hours in culture. The bar graph illustrates the number of genes associated with each of the following: inflammation, extracellular matrix (ECM), cell's cytoskeleton, Wnt signaling and others. It shows that genes associated with inflammation are the most highly upregulated when tendons are under less tension.

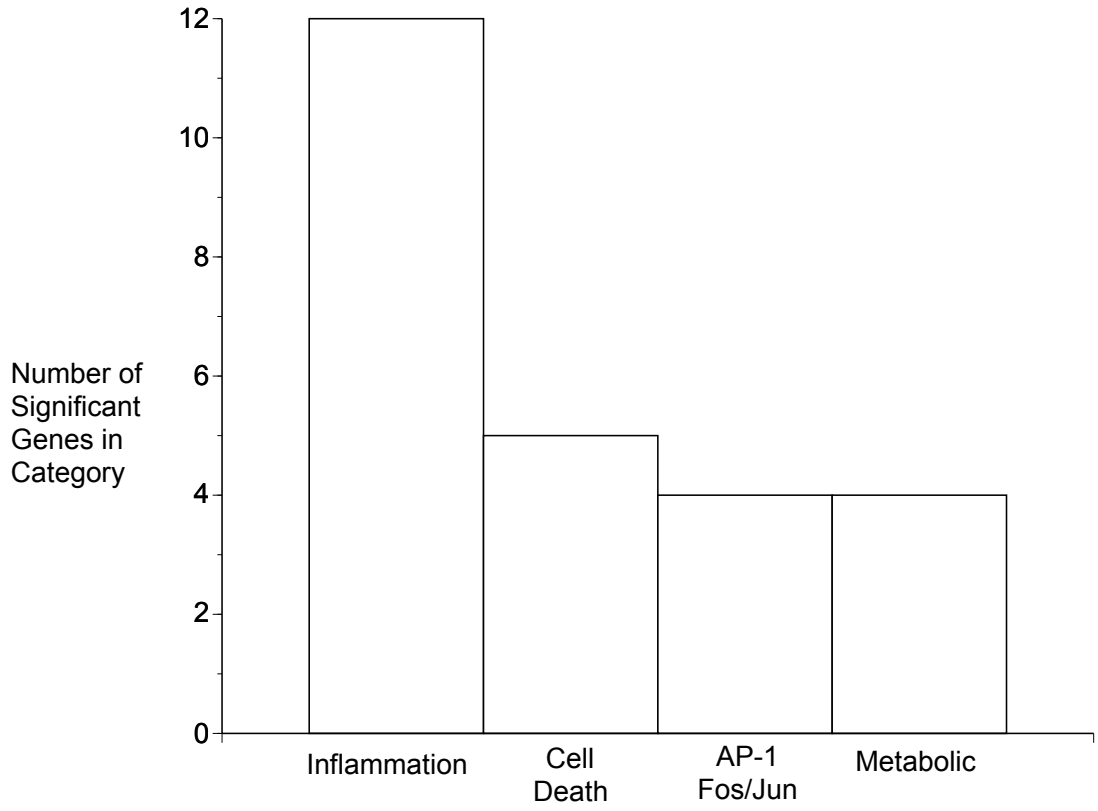

Figure 5.2: **Sutured Tensioned vs Unsutured Tensioned Tendons** A cDNA microarray was used to compare gene expression in sutured mouse tendon explants, under tension to gene expression in unsutured mouse tendon explants, under tension, after 3 hours in culture. The bar graph illustrates the number of genes associated with each of the following: inflammation, cell death, AP-1 Fos/Jun, metabolism and others. It shows that genes associated with inflammation are the most highly upregulated when tendons are sutured. Also, genes associated with cell death, the transcription factors Fos/Jun and metabolism are upregulated.

5.2.1.3 Sutured Untensioned vs Sutured Tensioned Tendons

Around half of the genes, of the 28 in this group, were reported to be associated with inflammation in the literature (n=15, 54%). Cd74 had the lowest p value, which was 0.006 and also demonstrated the greatest fold gene, which was 3.02. The second largest gene families were one which encoded for extracellular matrix proteins (n=3, 11%) and cell adhesion molecules (n=3, 11%). The rest of the genes were related to apoptosis, NfκB pathway, cell signaling, growth factors, cell cycle, metabolism and transcription (See Figure 5.3).

5.2.1.4 Sutured Untensioned vs Unsutured Untensioned Tendons

Suturing untensioned explants, resulted in the greatest number of genes (96), which had a significant change in gene expression. The gene with the lowest p value was Jun, which was 0.00039 and Nos2 had the largest fold change, which was 5.36. Consistent with the other findings, comparing the different experimental conditions, inflammatory mediators made up the largest subset of genes (n=26, 27%). This proportion was similar to the ones found in the other experimental groups. A third of those inflammation related genes encoded for either chemokines or members of the clotting cascade. The second largest gene family was comprised of genes linked to programmed cell death (n=11, 11%). Other notable gene families include genes related to extracelular matrix (n=8, 8%), Fos/Jun AP-1 transcription complex (n=6, 6%), growth factor (n=6, 6%), transcription factors (n=6, 6%), NfκB pathway (n=5, 5%) and the cellular cytoskeleton (n=4, 4%). The remaining groups contained genes which are thought to play a role in glutamate signaling, GTPases, MAPK signaling, oxidative stress response, cell senescence, cell cycle and metabolism (See Figure 5.4).

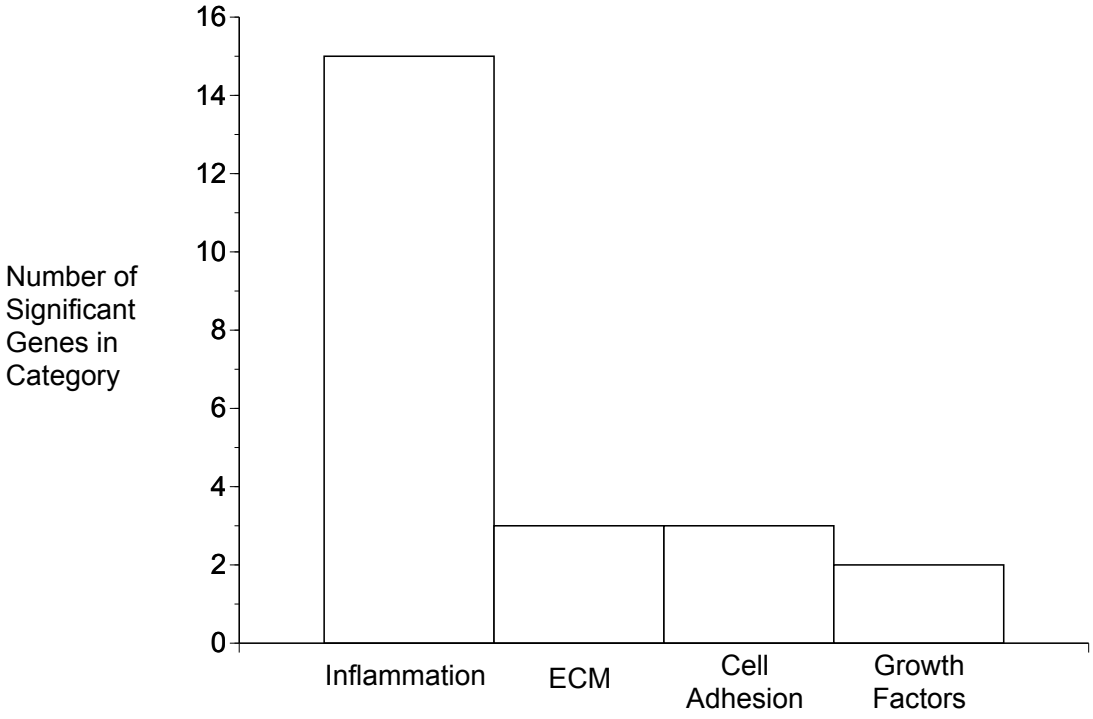

Figure 5.3: **Sutured Untensioned vs Sutured Tensioned Tendons** A cDNA microarray was used to compare gene expression in sutured mouse tendon explants, not under tension to gene expression in sutured mouse tendon explants, under tension, after 3 hours in culture. The bar graph illustrates the number of genes associated with each of the following: inflammation, extracellular matrix (ECM), cell adhesion molecules, growth factors and others. It shows that genes associated with inflammation are the most highly upregulated when tendons are sutured and under tension. Genes related to the extracellular matrix, cell adhesion molecular and growth factors were also upregulated.

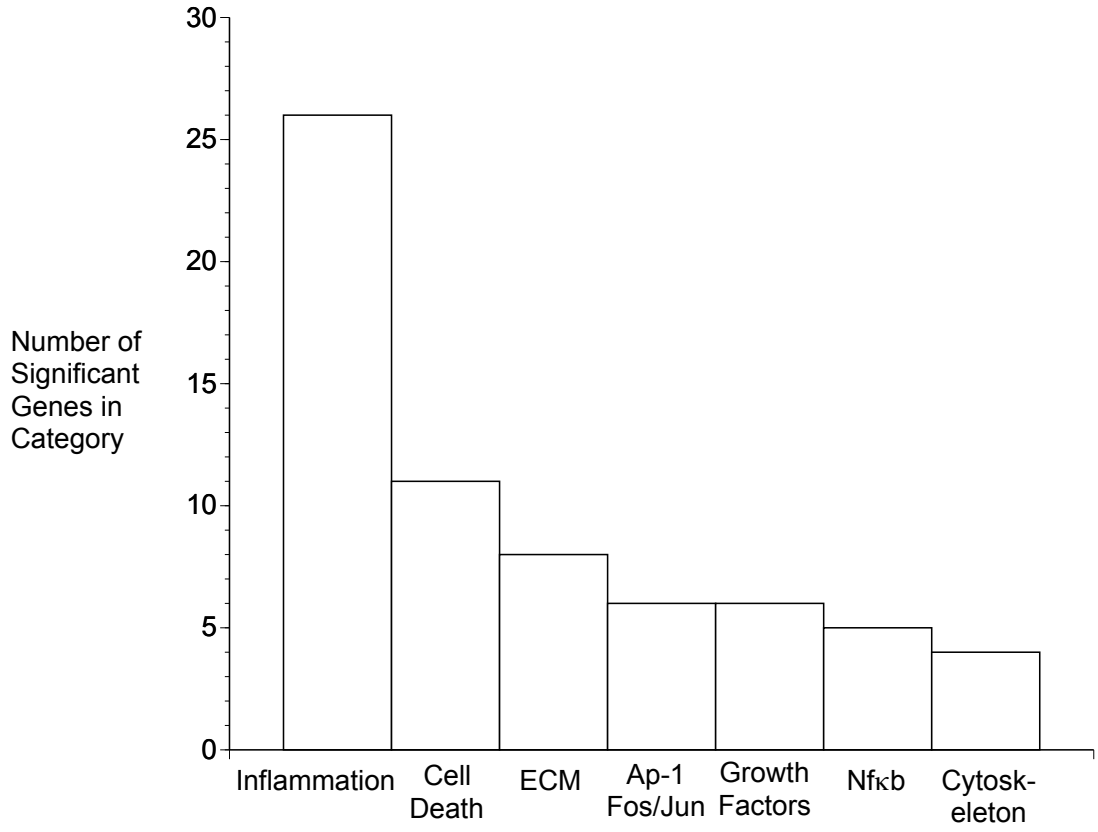

Figure 5.4: **Sutured Untensioned vs Unsutured Untensioned Tendons** A cDNA microarray was used to compare gene expression in sutured mouse tendon explants, not under tension to gene expression in unsutured mouse tendon explants, not under tension, after 3 hours in culture. The bar graph illustrates the number of genes associated with each of the following: inflammation, cell death, the extracellular matrix (ECM), Ap-1 Fos/Jun transcription complex, growth factors, Nfκb pathway, the cell's cytoskeleton and others. It shows that genes associated with inflammation are the most highly upregulated when tendons are sutured. Genes related to cell death, the extracellular matrix, the Ap-1 Fos/Jun transcription complex, growth factors, Nfκb and the actin cytoskeleton are also upregulated.

5.2.2 Sources of Variation

Suturing had a statistically significant influence on causing a change in gene expression between experimental groups (mean F ratio = 1.51, above 1.0 was considered significant). Tension had an F ratio of 1.02, which was not considered significant. This outcome is supported by the findings from the one way comparisons, where experimental groups that compared whether a sample had a suture or not, contained a larger number of significant genes (n=38, n=96) that when the condition that was compared related to tension (n=15, n=28). When suturing and tensioning were combined the mean F ratio was 1.62. This was slightly higher than the F ratio of suturing alone (1.51) (See Figure 5.5).

Factorial analysis of variance (ANOVA) showed that there were 1227 genes that were influenced by suturing that had a p value below 0.05, 573 gene that were affected by tension and 1270 genes that were altered by a combination of suturing and changing the amount of tension across the sample. Jun oncogene was the gene with the lowest p value, which was 0.0002. See Table 5.1 for the 20 genes with the lowest p value, after ANOVA factorial anlaysis (factors = suturing and tension)

5.2.3 KEGG (Kyoto Encyclopedia of Genes and Genomes) Pathways Analysis

The KEGG pathways database, contains records of networks of molecular interactions within cells. The type of pathways included in the KEGG database include: 1. metabolic pathways (such as carbohydrate metabolism e.g. glycolysis), 2. genetic information processing pathways (like RNA polymerase), 3. signaling pathways (such as MAPK signaling pathway), 4. cellular processes (like cell motility, lysosomes e.g. apoptosis), 5. organismal systems (such as pathways specific to the immune system e.g. NOD-like receptor signaling pathway), 6. human diseases (for example, cancer) and 7. drugs (such as penicillins). In the case of the acellular zone, significant cell signaling pathways and cellular processes would be most interesting groups to observe.

Table 5.1: Genes with the Lowest p, After An ANOVA Factorial Analysis (Factors = Suturing and Tension)

Rank	**Gene Symbol**	**Gene Name**	***p-value***	**Pathway**
1	Jun	Jun oncogene	0.00020	Ap-1 Fos/Jun
2	Ccrn4l	CCR4 carbon catabolite repression 4-like	0.00100	Circadian Rhythm
3	Spata2	spermatogenesis associated 2	0.00100	Necroptosis
4	Ccnl1	cyclin L1	0.00100	Splicing
5	Ip6k2	inositol hexaphosphate kinase 2	0.00100	IPK/Apoptosis
6	Plekhm1	pleckstrin homology domain containing, family M	0.00100	Vesicular Transport
7	Ttll4	tubulin tyrosine ligase-like family, member 4	0.00100	Microtubule
8	Snap29	synaptosomal-associated protein 29	0.00100	Membrane Trafficking
9	Tmem108	transmembrane protein 108	0.00100	Unknown
10	Nr4a1	nuclear receptor subfamily 4, group A, member 1	0.00100	Apoptosis/Liver Regeneration
11	Txnip	thioredoxin interacting protein	0.00100	Oxidative Stress Mediator
12	Fgf9	fibroblast growth factor 9	0.00100	Growth Factor
13	Hif1a	hypoxia inducible factor 1, alpha subunit	0.00100	Hypoxia
14	Errfi1	ERBB receptor feedback inhibitor 1	0.00200	Cell Growth
15	Gem	GTP binding protein	0.00200	NfκB
16	Atf3	activating transcription factor 3	0.00200	Transcription
17	Tyms-ps	thymidylate synthase, pseudogene	0.00200	Unknown
18	AI646023	expressed sequence AI646023	0.00200	Unknown
19	Zfp369	Nzinc finger protein 369	0.00200	Unknown
20	Eif3b	eukaryotic translation initiation factor 3, subunit B	0.00200	Protein Synthesis

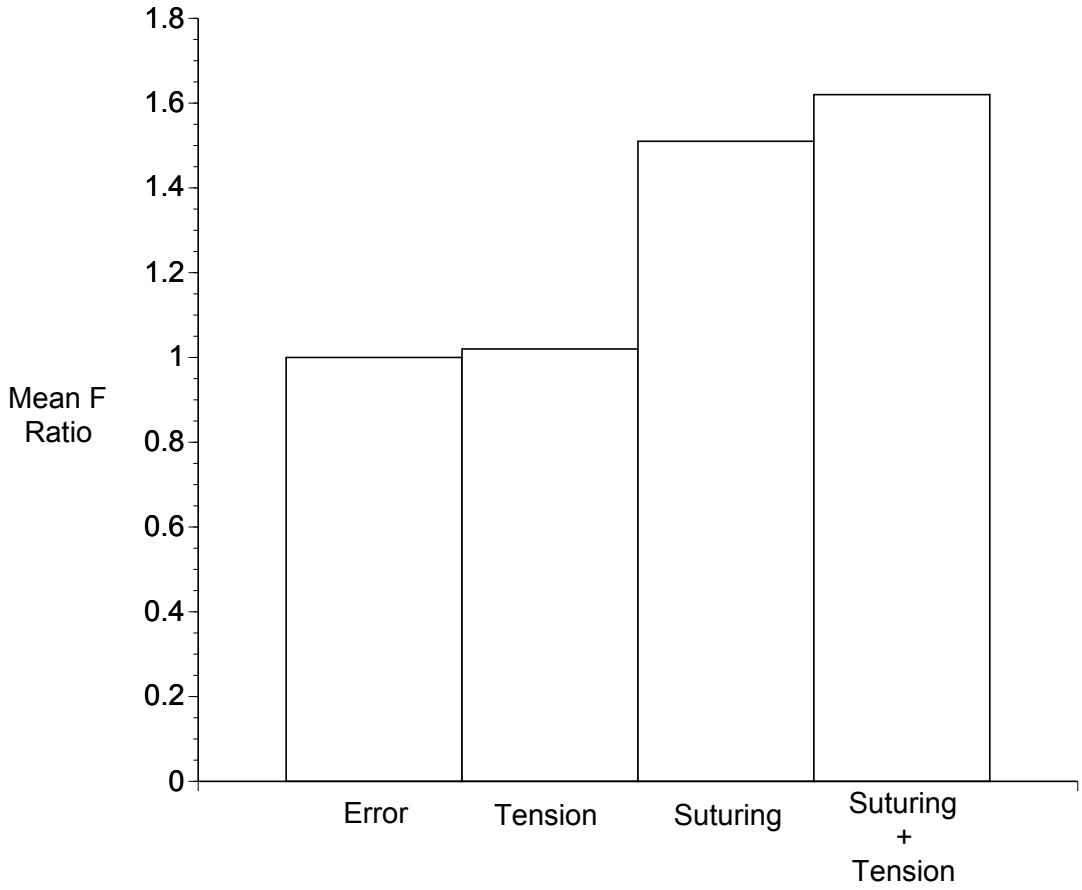

Figure 5.5: **Sources of Variation** Mouse tendon explants were either sutured and placed under tension (n=4), unsutured and placed under tension (n=4), sutured and not placed under tension (n=4) or unsutured and not placed under tension(n=4). The tendons were cultured for 3 hours, and then samples were obtained for a cDNA microarray. The microarray showed that suturing had a more significant influence than tension on gene expression. The bar graph shows that the mean F ratio for tension was 1.02, which is close to 1.0 (the error) and thus not considered significant. Suturing had a mean F ratio of 1.51 and suturing plus tension ha d a mean F ratio of 1.62, both of which are greater than 1.0 and thus are considered significant.

In the analysis conducted using DAVID (NIH, USA), all the genes tested in the microarray (16,756 genes, background group) were compared to genes that had a p value less than 0.05 and were influenced by both suturing and tension in the Factorial ANOVA analysis (1270 genes, experimental group). The pathways analysis compares genes that are components of known pathways in the background genes group and the

experimental gene group. Pathways that were considered statistically significant, are pathways in which its member genes are present at a higher frequency in the experimental group compared to the background group and had a p value less than 0.05. Also a Benjamini value was assigned to the pathway, which is a measure of the probability of a false discovery rate (i.e. the likelihood of a discovery being due to chance, which might occur due to the large sample size of 16,756 genes). A Benjamini value less than 0.05 indicates that the pathway detected in the experimental group is unlikely to have been detected due to chance.

Pathways that had the lowest p values related to inflammation (Nod-like Receptor signaling, Toll-like receptor signaling), MAPK signaling, cell death (apoptosis) and neural growth factor (neurotrophin signaling) and cancer (see Table 5.2). Three pathways had both a significant p value and a significant Benjamini value; the Nod-like receptor signaling pathway, the MAPK signaling pathway, and the pathways in cancer. The MAPK pathway is of greatest interest as the pathways in cancer relate to a disease and the Nod-like receptor pathway is related to inflammation, which is has not been observed in the acellular zone. Thirty two genes out of the 1270 genes in the experimental group were part of the MAPK pathway, representing 2.5% of the total gene number. This frequency was considered to be statistically significant (p value = 0.00026, Benjamini value = 0.02).

Table 5.2: KEGG (Kyoto Encyclopedia of Genes and Genomes) Pathways

Pathway	**Gene Count**	**%**	***P*-value**	**Benjamini**
Nod-like Receptor Signaling	15	1.2	0.00001	0.0022
MAPK	32	2.6	0.00026	0.0200
Pathways in Cancer	33	2.6	0.00026	0.0200
Apoptosis	13	1	0.00570	0.2000
Toll-like Receptor Signaling	14	1.1	0.00630	0.1800
Neurotrophin Signaling	16	1.3	0.01100	0.2600

5.2.4 Cluster Analysis of Microarray Data

Clustering analysis yielded 9 clusters which contained 67-169 genes each (see Figure 5.6). All the clusters had a large proportion of genes related to inflammation, cell signaling and metabolic functions. As noted in previous findings, suturing appeared to exert a greater influence than tension, accounting for 6 of the clusters.

Genes that were only upregulated when tendons were sutured and placed under tension accounted for a cluster of 115 genes, which were associated with growth factors, extracellular matrix, ubiquitin proteosome pathway and GTPases. Interestingly, the Lox12 gene was present in this cluster, which encodes for lysyl oxidase, an amine oxidase that catalyses the formation of cross links in collagens and elastins. Another gene which may be of interest, is Prkcd, which was present in one of the clusters that contained genes that were upregulated in sutured tensioned tendon and down regulated in unsutured tensioned tendons. Prkcd encodes protein kinase S, delta , an enzyme that is activated by calcium and apoptosis and is associated with acellular capillaries.

Genes that had increased expression in untensioned sutured explants and decreased expression in untensioned unsutured explants formed the second largest cluster. As with all cluster, a large proportion of the genes were linked to inflammation and metabolic functions. The Jak/Stat IL-6 receptor signaling family-related genes were present in this cluster (Il6, Jak2, Stat3, Lif). Growth factor associated genes could also be found (Fgf7, Gdf10, Ltbp2, Ltbp4, Ogfr). There were seven different extracellular matrix genes in the cluster, of which, two were fibulins (fbln1, fbln2). The GTPase related Rhoj, Rock1, Rock2, Myo1b and Arhgap18 were part of the cluster as well.

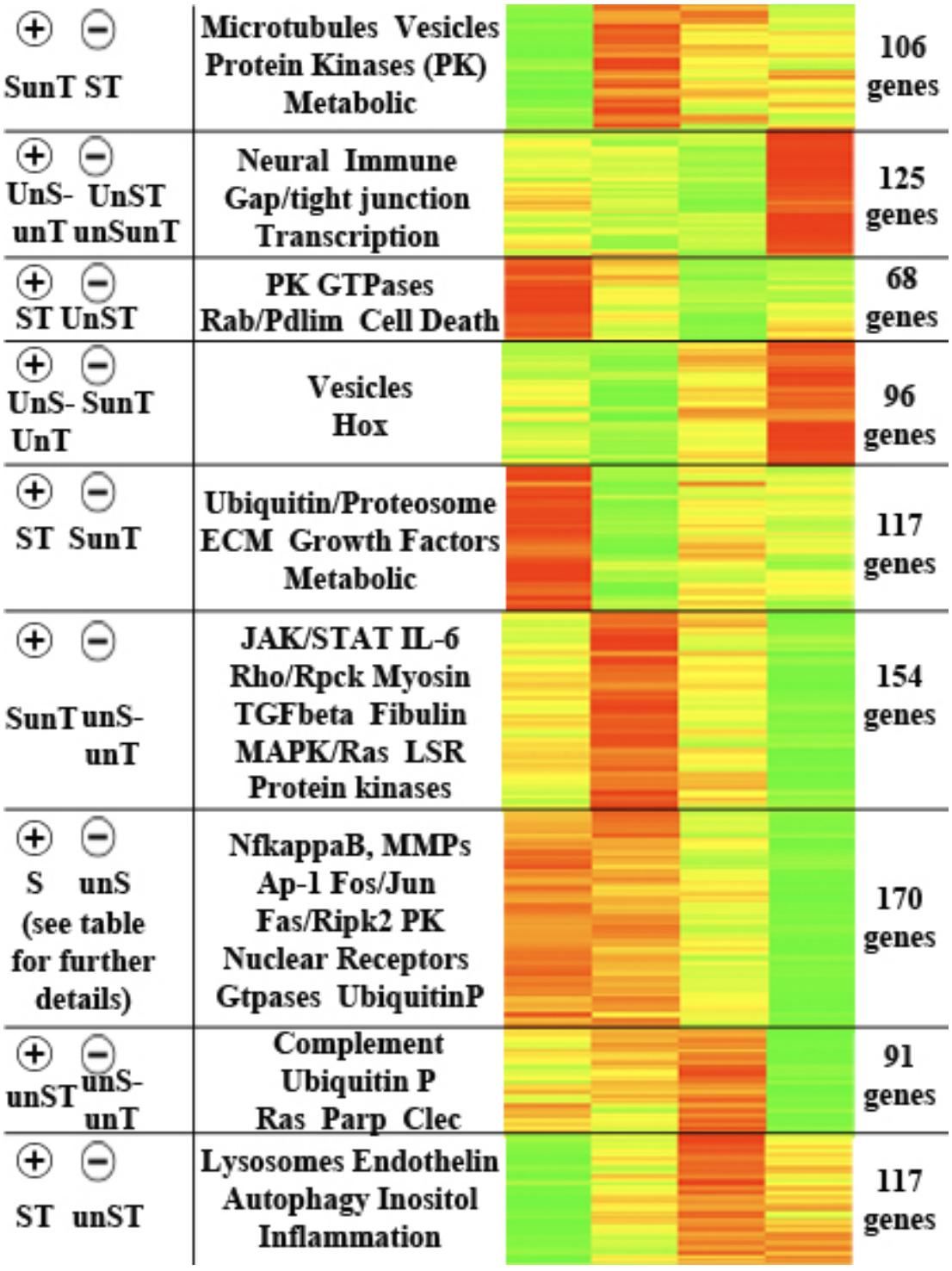

Figure 5.6: **Cluster Analysis** Mouse tendon explants were either sutured and placed under tension (n=4), unsutured and placed under tension (n=4), sutured and not placed under tension (n=4) or unsutured and not placed under tension(n=4). The tendons were cultured for 3 hours, and then samples were obtained for a cDNA microarray. Cluster analysis yielded 9 clusters, which contained 67-169 genes each.. The pathways which account for the largest number of genes in a cluster are listed alongside the cluster. The heatmap adjacent to the list of pathways shows whether the gene expression in the cluster was generally on (red), off (green) or unchanged (yellow). *ST = sutured tensioned, UnST= unsutured tensioned, SunT = sutured untensioned, unSunT = unsutured untensioned*

The largest cluster consists of genes that had increased expression after suturing, regardless of whether the sample was under tension or not. This is consistent with previous findings, which implicate suturing as having a larger influence than tension in changing gene expression. Certain pathways can be discerned in this cluster (see Table 5.3). Almost all the genes necessary to encode proteins involved in Nfκb signaling can be found in this cluster (Nfkb2, Nfkb1, Nfbia, Nfkbiz, Nfbib, Rel, Myd88, Tnip1, Taf9, Irak2, Hivep1, Tnfaip3). Fos and the all the different types of the Jun oncogene (c-Jun, JunD, JunB) are also present. Other cell death and fate determining genes made up this cluster. A group of GTPase related genes were included in the cluster (Rnd3, Rhou, Rnd1, Dlc1, Arhgef3). Many proteases could be noted, such as Mmp3, Mmp12, Mmp13 and numerous members of the ubiquitin proteosome pathway. In addition, there was a large number of nuclear receptors in the cluster, one of which is known to be associated with the Nfκb pathway.

5.3 qPCR validation

qPCR was carried out on a select number of changes to ensure that the changes in gene expression detected in the microarray analysis, were also evident by qPCR analysis. Genes from the Ap-1 Fos/Jun pathway (Fos, Jun, Rbm39) and the Nfκb pathway (Nfkb2, Ikbke) that were significant in the microarray were tested. Those pathways were chosen as they were hypothesized to be central to acellular zone formation based on analysis of the microarray data. RNA was isolated from 9 sutured tendons under tension and 9 unsutured tendons under tension, 3 hours after the tendons were left in culture. After suturing, Fos's expression was 83% more than controls' (p value = 0.1035), Ikbke's expression was 105% more than controls' (p value = 0.0261), Jun's expression was 205% more than controls' ((p value = 0.007), Nfkb2's expression was 67% more than controls' ((p value = 0.2105) and Rbm39's expression was 60% more than controls (p value = 0.0311) (see Figure 5.7). The changes in gene expression were similar to those detected in the microarray analysis.

Table 5.3: Cluster Analysis (Sutured Vs. Unsutured)

Pathway	Genes	Gene Count	%
NfκB	Nfkbiz Nfkb2 Nfkb1 Tnip1 Nfkbia Taf9 Myd88 Irak2 Rel Nfbib Atf3	11	6.5
Gtpases	Dlc1 Rnd1 Rnd3 Rhou Arghef3 Gem	6	3.5
Growth Factors	Fgf9 Ereg Igf1r Cyr61 Nov Ehd1	6	3.5
Ubiquitin/Proteosome	Smurf1 Spsb1 Znrf1 Ube2q2	4	2.4
Ap-1 Fos/Jun	Fos Jun JunB JunD	4	2.4
Cell Death	Spata2 Ripk2 Fas	3	1.8
Nuclear Receptors	Nr4a1 Nr4a2 Nr4a3	3	1.8
Mmp	Mmp3 Mmp12 Mmp13	3	1.8

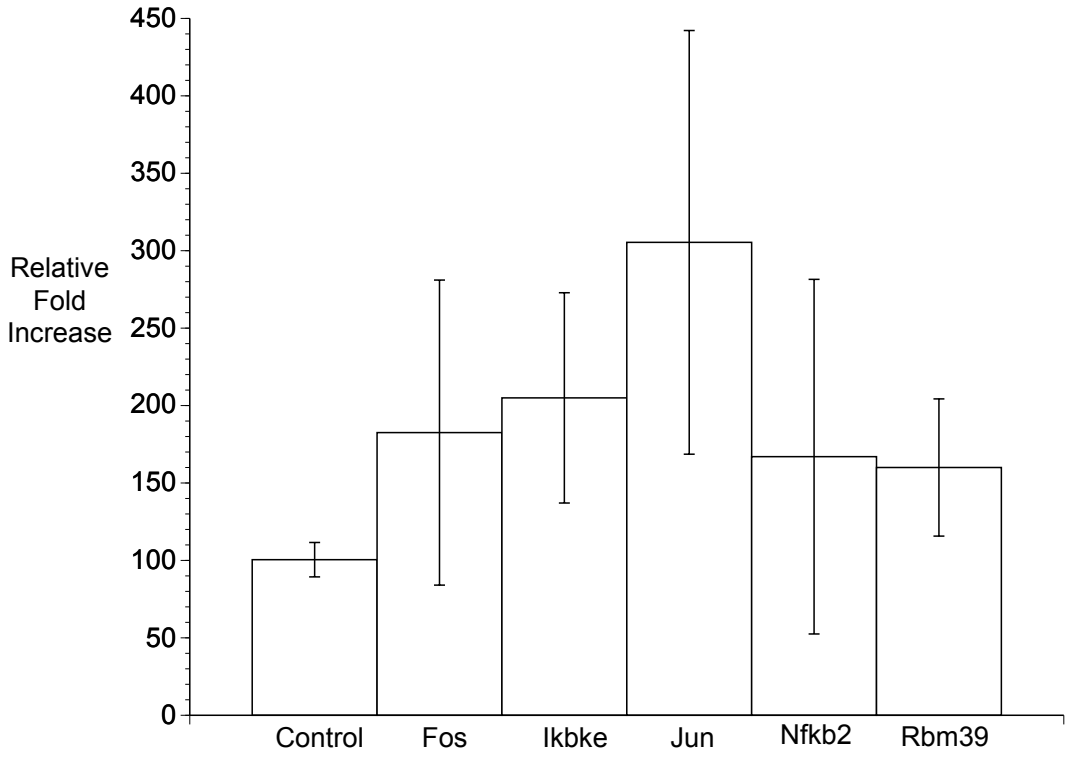

Figure 5.7: **qPCR validation** Mouse tendon explants were either sutured and placed under tension (n = 9) or unsutured and placed under tension(n = 9). The tendons were cultured for 3 hours and then RNA was isolated and qPCR was performed. qPCR showed that suturing caused the genes Fos, Ikbke, Jun, Nfkb2 and Rbm39 to become upregulated. The upregulation of Jun, Ikbke and Rbm39 were all statistically significant.

5.4 Preliminary Results Using Necrostatin-1

Preliminary work was carried out to determine if necroptosis is a potential mediator of acellular zone development. Necrostatin-1 (Sigma, UK) which was shown by Degterev et al. (2008) to be a potent inhibitor of Ripk1, reduced cell death in tendon explants (See Figure 5.8). Future work could confirm the efficacy of Necrostatin-1 in reducing the size of the acellular zone and elucidating if that improves tendon repair. Other types of injuries secondary to surgery, such as ischemia-reperfusion injuries, where necrosis also occurs, could benefit from a similar approach.

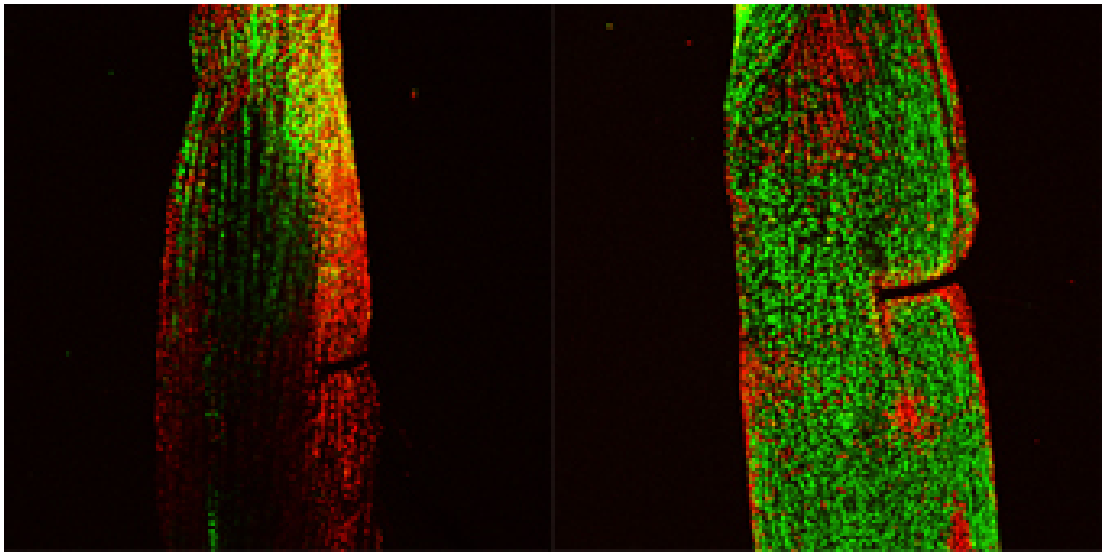

Figure 5.8: **Necrostatin-1** A mouse tendon explant was preincubated in either DMSO (left) or 100 μM Necrostatin-1 supplemented media (right) (media contained Dulbeccos Modified Eagles Medium (DMEM), penicillin (100 U/mL), streptomycin (100μg/mL), L-glutamine (2 mM) and 10% fetal calf serum), for 30 minutues. The tendons were sutured and incubated at 37°C and 5% CO_2 for 24 hours. The sutured explant, which was incubated with Necrostatin-1 appeared to exhibit less death (less red staining) than tendons incubated with DMSO. *green staining = calcein AM (stains viable cells), red staining = propidium iodide (stains dead cells)*

5.5 Discussion

Analysis of genes expressed in sutured tendons suggests that necrosis and necroptosis are the modes of cell death that lead to development of the acellular zone. Gene expression analysis also suggests that the MAPK pathway, Ap-1 Fos/Jun complex and the Nfκb pathway are involved in the cellular response to suturing. The cDNA microarray analysis of sutured tendons demonstrated some evidence of programmed cell death. Ripk 1, Ripk2, Spata2 and Fas, which are genes that have been associated with programmed necrosis (necroptosis) (Hitomi et al. 2008) were significantly upregulated after suturing. Hitomi et al. (2008) also showed that these genes were not specific for necroptosis and can overlap with apoptosis. However, based on the lack of morphological features of apoptosis in the tendons cells taken from the same time point, it is improbable that apoptosis occurs

A limitation of this *in vitro* model is that the tendons used have been dissected and clamped, which introduces an additional injury to the tendon. This was counteracted by using unsutured controls and cutting the clamped ends just before samples were prepared for RNA isolation. Despite accounting for these shortcomings, the mechanisms of acellular zone formation *in vitro* and *in vivo* may differ. Also, tendon fibroblasts are normally under cyclic tension, exerted by the muscle it connects to, whereas the clamps used to keep the tendons are tension only provide static tension. However, it took the acellular zone 24 hours to develop in culture and the RNA samples for microarray analysis were obtained 3 hours after the tendons had been sutured. As the development of the acellular zone is what is of interest, by studying the region surrounding the suture at 3 hours that requirement is met. Also, the introduction of cyclic tension, would introduce an additional variable that would need to be controlled for, making the experiments' results difficult to interpret. Using cyclic tension would be more suited for studies studying the long-term effects of suturing in culture.

The microarray study supports the hypothesis that the acellular zone share a similar signaling pathway *in vitro* and *in vivo*. Genes associated with the MAPK pathway, the

Ap-1 Fos/Jun transcription complex and Nfκb pathway, as well genes related to oxidative stress and MMPs were shown to be upregulated after suturing by the microarray. Some of these pathways have also been shown to be upregulated after suturing tendons *in vivo*. Chicken flexor digitorum profundus tendons *in vivo*, were repaired using a Kessler suture (Tang et al. 2004). Genes involved in the Nfκb were shown to be upregulated 2, 4 and 8 weeks after the repair. McDowell et al. (2002) demonstrated that suturing tendons induced the upregulation of MMPs at the suture repair site. The microarray analysis also revealed potential genes of interest such as Prkdc, which was upregulated after suturing. In diabetic mouse retinas, increased Prkdc activity was linked with an increase in the number of acellular capillaries (Behl et al. 2008). However, all these genes, although linked to suturing, have not been localized to the acellular zone. Immunohistochemistry, western blots and in situ hybridization are required to confidently ascertain that these genes are associated with the acellular zone. However, as changes to the extracellular matrix and cell death, have been shown to be localized to the acellular zone around the suture; it is likely to also be the site of upregulation of those genes by the suture. Also, the necrostatin-1 experiment needs to be expanded to a large number of explants. In addition, the death genes hypothesized to be central to acellular zone formation should be studied in a knock out mouse model, in which Scleraxis-Cre is the driver and where the tendons are then injured.

One of the most intriguing findings from the microarray study is that inflammatory mediators are highly expressed in sutured tendons. Despite the occurrence of cell necrosis and the expression of genes related to inflammation, invasion of inflammatory cells into the suture site does not ensue. The lack of inflammatory cell infiltration is unexpected, as it almost always occurs after other injuries, such as lacerations (Gurtner et al. 2008). However, two fundamental differences between an incision and a suture repair may account for this differing cellular response. The single suture repair model causes less damage to the epithelial surface tendon layer than an incision, a layer which was shown by Richardson et al. (2010) to be important for preventing cellular migration across the epithelial barrier. Secondly, a suture causes compression of the

extracellular matrix within its grasp and an incision releases tension in the extracellular matrix it transects. The barrier hypothesis is weakened by the observation that an acellular zone forms in a Kessler suture, despite the presence of an incision adjacent to the acellular zone. The hypothesis that the compression forces exerted by the suture on the tissue were responsible for the formation of the acellular zone was supported by Wong et al. (2006b) who demonstrated that an untied suture did not cause an acellular zone to form and that tight knot is a necessary prequisite for the acellular zone to form. Potential reasons why the acellular zone persists a year after it has been repaired and why inflammatory cell infiltration does not occur at the acellular zone are explored in Chapter 6.

CHAPTER 6

THE EFFECTS OF SUTURING ON THE EXTRACELLULAR MATRIX

6.1 Introduction

The previous results chapters proposes that cell death is the main effector that leads to acellular zone formation. Yet, this does not explain the findings in Chapter 3, which demonstrate that acellular zone does not get repopulated with cells a year after the tendon was sutured. Although, cell death would be expected after injury, cellular infiltration by inflammatory and non-inflammatory cells would be expected (Chen et al. 2007), to remodel and repair the area. This does not happen if a suture is the sole perpetrator of the injury. This chapter will aim to explain why the acellular zone appears to be refractory to re-cellularization.

The difference in the sequence of cellular events following the two types of injury (incision v.s. suture), could be explained by the differences in mechanical properties exerted on the tissue between incisions and sutures. Incisions lead to severing of taut fibrils, relieving the injured region of tension and exposing the core of the tendon. On

the other hand, sutures, which enwrap a region of the tendon, tendon to compress the fibrils within it and leave the surface of the tendon relatively intact.

Work by Richardson et al. (2010) has explored the role the surface tendon cells in tendon injury, showing that preservation of the architecture of the surface of the tendon is mandatory for its role as a barrier. However, the mechanical effects of the suture on the cells has not been studied. Suturing may prevent repopulation of the acellular zone by compressing the fibrils within its grasp. This could reduce the pore size between the fibrils, making it too dense for cells to migrate into the region (Friedl and Wolf 2010). A similar effect can be observed in dense scar tissue or fibrosis, where overproduction of collagen fibrils leads to a relatively acellular extracellular matrix (Sun and Weber 2000).

This chapter will explore the hypothesis that the acellular zone persists after suturing due to the suture compressing the fibrils within it, making the extracellular matrix it enwraps too dense for cellular migration by inflammatory and non-inflammatory cells to occur. To achieve this, the stiffness of the extracellular matrix within the suture grasp will be compared to the adjacent, uninjured matrix, using biomechanical methods. Next the spacing between the fibrils will be observed and measured using electron microscopy and atomic force microscopy. Finally, the biomechanical properties of the extracellular matrix of sutured tendons were measured to compare them to the mechanical properties of the unsutured region of tendons. This was carried out to establish if cell migration into the acellular zone does not occur due to altered mechanical properties of the sutured matrix. Hence, the aims of the studies in this chapter are to determine if the extracellular matrix enwrapped by the suture has different mechanical properties to the uninjured matrix in the adjacent regions and to establish if the spacing between fibrillar bundles is reduced in sutured matrix compared to unsutured matrix surrounding it.

6.2 The Morphology of the Extracellular Matrix of Sutured Tendons

The extracellular matrix of mouse FDP tendons sutured *in vivo* and chemically fixed 24 hours later, was imaged using polarized light, scanning acoustic, atomic force and electron microscopy. Polarized light and scanning acoustic microscopy was used to observe the extracellular matrix at a lower magnification than the magnification that can be obtained using atomic force and electron microscopy. Atomic force and electron microscopy were used to measure the spacing between fibrils, to asses the organization of the fibrils and the ultrastructural appearance of the extracellular matrix. These imaging modalities were used to determine if the fibrils in the sutured extracellular matrix were packed closer together compared to fibrils in the adjacent extracellular matrix, as differences in collagen fibril density could account for the lack of cellular infiltration into the sutured extracellular matrix.

6.2.1 The Spacing Between Collagen Fibrils in Sutured and Unsutured Regions of Tendons

The organization of the collagen fibrils were observed in longitudinal sections of tendons that were sutured *in vivo*. Polarized light microscopy and scanning acoustic microscopy were used, as they could be used to image the collagen fibrils.

Polarized light microscopy of 5 μm thick cryosections of tendons cryofixed 6 hours after suturing show collagen fibrils that appear to be more closely packed in the sutured region compared to the unsutured region. The orientation of the fibrils also appears to change direction as it passes through the sutured area. In the non-sutured fibrils the fibrils were organized into parallel arrays (see Figure 6.1).

Scanning acoustic microscopy imaging of 5 μm thick cryosections of tendon, cryofixed 6 hours after suturing, revealed that in the unsutured regions of tendon, fibrils were parallel and orientated along the long axis of the tendon. Conversely, in the su-

tured region of the same tendon, fibrils appeared to be more closely packed. At lower magnifications, this made the sutured region appear darker than the unsutured region. The fibrils also appeared to change orientation as they passed through the sutured area (See Figure 6.1).

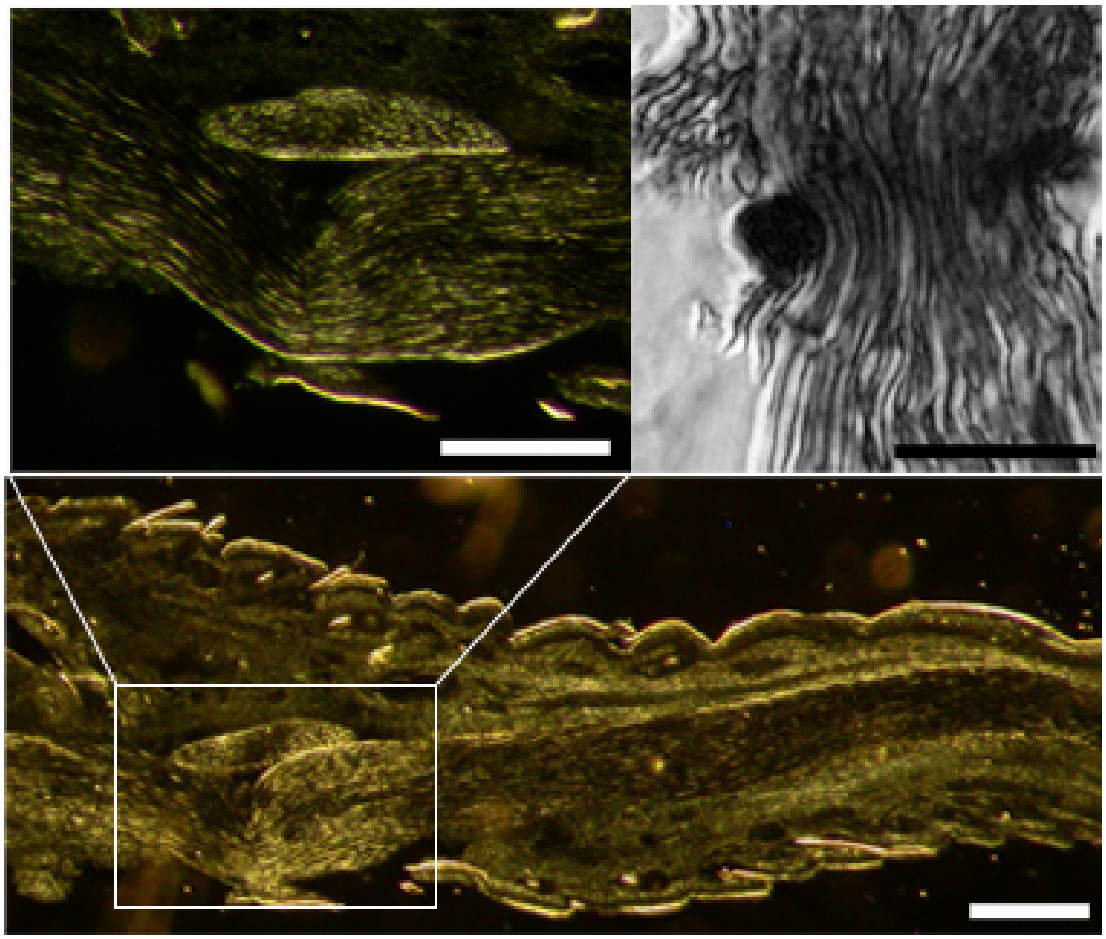

Figure 6.1: **Polarized Light Microscopy** Flexor digitorum profundus mouse tendons were cryofixed 6 hours after they had been sutured *in vivo*. Sections (5μm thick) were obtained and were imaged using polarized light microscopy (top left, bottom) and scanning acoustic microscopy (top right). The images show that the fibrils appear to be more closely packed in the sutured region compared to the unsutured regions. Also the orientation of the fibrils in the sutured regions appears to change, unlike the fibrils in the unsutured regions which are organized in parallel arrays. Scale bar = 100 μm

6.2.2 Measuring the Spacing between Collagen Fibrils and Collagen Bundles

The spacing between the collagen fibrils and collagen bundles was measured using the distance between fibrils and bundles in sections of mouse tendons that were sutured *in vivo* and imaged 24 hours later. Atomic force microscopy was used to measure the interfascicular distance in longitudinal sections and electron microscopy of transversely orientated tendons was used to measure the distance between collagen bundles. These measurements were needed to confirm if suturing caused the collagen fibrils to be packed closer together, preventing cellular infiltration into the sutured region.

6.2.2.1 Measurements of the Spacing Between Collagen Bundles in Sutured and Unsutured Regions of Tendon

Measurements were obtained from the TEM images of sutured and unsutured regions of tendon, as well as from uninjured tendon (n = 3 each). 25 sections were obtained from each tendon. Of those, five sections were imaged. Five images were obtained from each of the sections. In each image, 50 measurements were taken. This measurements were obtained by measuring the distance between collagen bundles. The mean distance between collagen bundles was 101 nm for uninjured tendons, 358 nm for unsutured regions of sutured tendons, and 379 nm for the sutured regions of tendon. The difference in interfascicular length was statistically significant between the uninjured tendon and both unsutured and sutured regions of sutured tendons (p value = 0.0001 for both). The difference in interfascicular length between the sutured and unsutured regions in sutured tendons was not statistically significant p value = 0.4263) (see Figure 6.2).

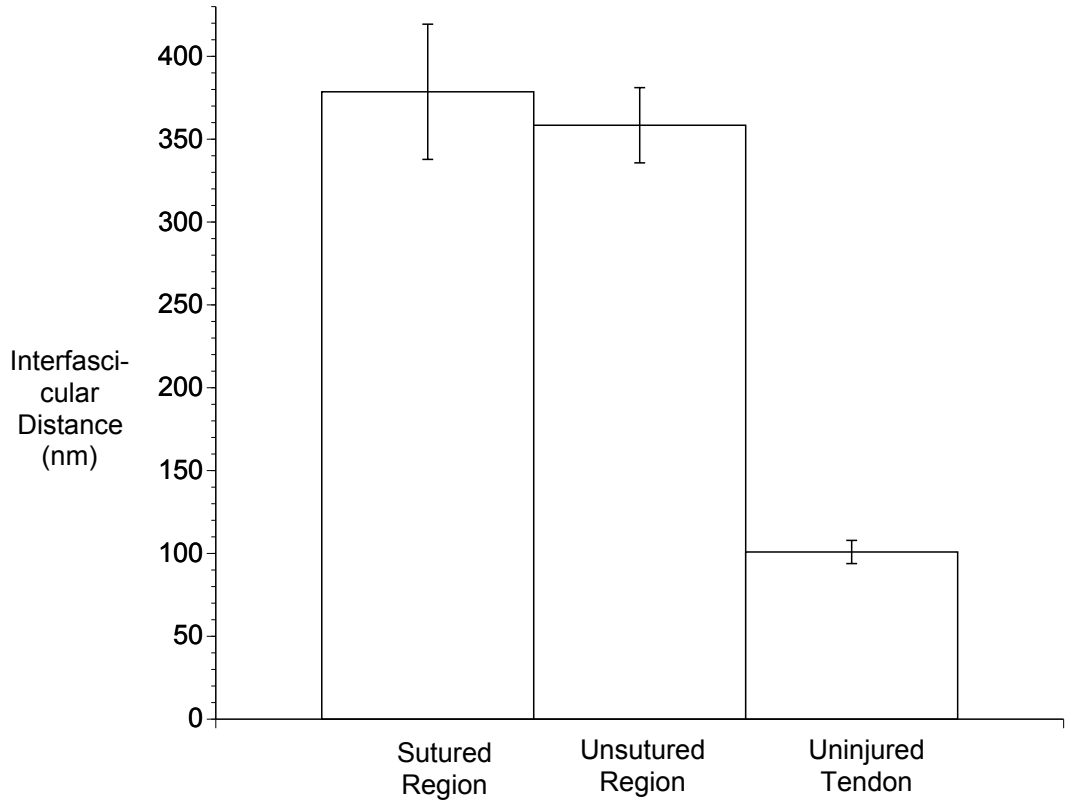

Figure 6.2: **Interfascicular Distance** Flexor digitorum profundus mouse tendons were prepared for electron microscopy 24 hours after they had been sutured *in vivo*.Transverse transmission electron microscopy (TEM) were obtained from sutured and unsutured regions of tendon. Images were also obtained from uninjured mouse tendons. The mean distance between collagen bundles was 379 nm for the sutured regions of tendons, 358 nm for unsutured regions of sutured tendons and 101 nm for uninjured tendons. The difference in interfascicular distance was significant between uninjured and sutured tendons but not between the sutured and unsutured regions of sutured tendons (n=3, error bars = 2 standard deviations).

6.2.2.2 Measurements of the Spacing Between Collagen Fibrils in Sutured and Unsutured Regions of Sutured Tendon

Flexor digitorum profundus mouse tendons were cryofixed 6 hours after they had been sutured *in vivo*. Sections (5μm thick) were obtained and were imaged using atomic force microscopy (n=3 for each experimental group).

In unsutured regions of sutured tendons, individual fibrils could easily be distinguished and spaces could be seen between the fibrils (see Figure 6.2.2.2). The banding on the fibrils was clear and when measured was around 67nm, consistent with that of collagen fibrils. The mean interfibrillar distance was 158 nm (See Figure 6.4).

The fibrils in the sutured areas of sutured tendons appeared closely packed. It was very difficult to distinguish between the individual fibrils, as the fibrils look almost fused together. The banding pattern on the fibrils could not easily seen and when it could, the banding on the different fibrils did not align, as it does with in the unsutured regions (see Figure 6.2.2.2). The mean interfibrillar distance was 142 nm (See Figure 6.4). The difference between the interfibrillar distance in the unsutured regions of tendon and the sutured regions of tendon was statistically significant (p value = 0.0009) (See Figure 6.4).

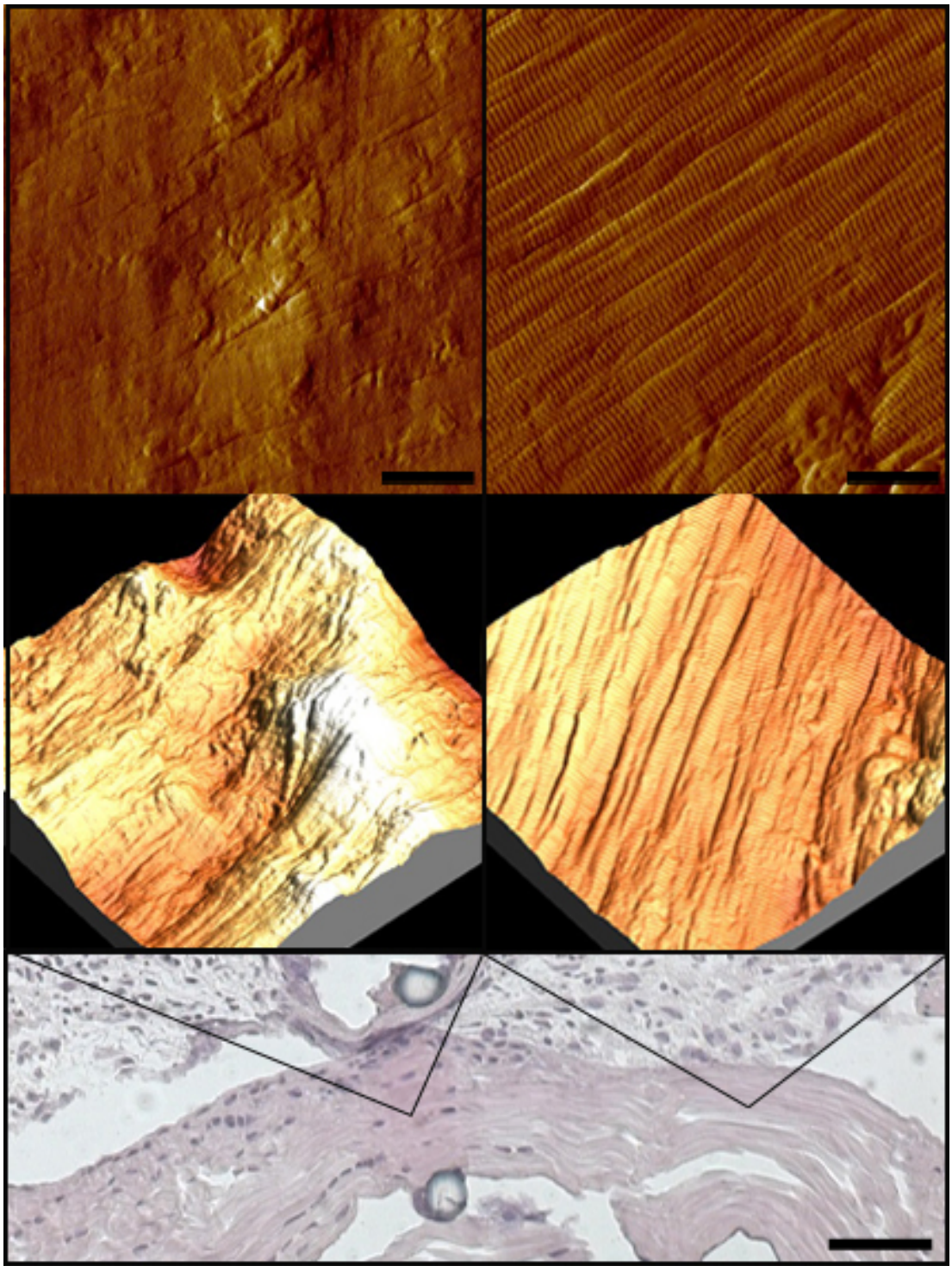

Figure 6.3: **Atomic Force Microscopy** Flexor digitorum profundus mouse tendons were cryofixed 6 hours after they had been sutured *in vivo*. Sections (5μm thick) were obtained and were imaged using atomic force microscopy. Alternate sections were also stained using haematoxylin and eosin (see bottom). The fibrils in the sutured region (left top and middle images) appeared closely packed and it was difficult to distinguish between the individual fibrils, as if the fibrils were fused. The banding on the different fibrils was not aligned and the fibrils appeared disorganized. The unsutured regions (right top and middle images) had parallel aligned fibrils. *top images: atomic microscopy phase images, bottom images: 3-dimensional representation of combined height atomic force microscopy images*. Scale bars = 1 μm (top), 100 μm (bottom)

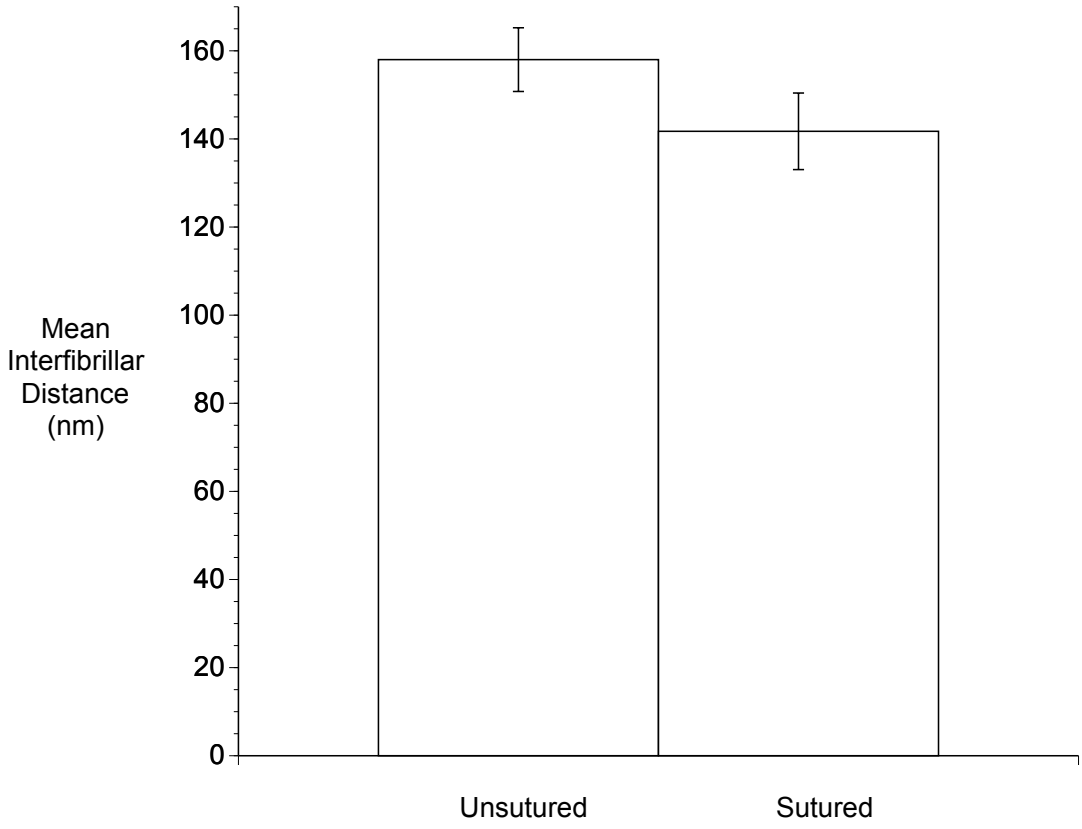

Figure 6.4: **The Effects of Suturing on the Distance Between Fibrils** Flexor digitorum profundus mouse tendons were cryofixed 6 hours after they had been sutured *in vivo*. Sections (5μm thick) were obtained and were imaged using atomic force microscopy. Phase atomic force microscopy images were analyzed using the WSxM software (Nanotec, Spain). Measurements of the distance between fibrils was obtained. The bar growth shows that the mean fibrillar distance in the unsutured region of tendons was 158 nm. The mean distance between sutured tendons was less (142 nm), (n=3, error bars = 2 standard deviations).

6.2.3 Orientation of Fibrils

The orientation of fibrils in sutured and unsutured regions of sutured tendons could be evaluated by obtaining a fourier transform of the atomic force microscopic images and using the ImageJ plugin, Orientation J (NIH, USA). This was necessary to determine if the differences in spacing between the collagen bundles and fibrils were due to the disorganization of collagen fibrils in sutured tendons. Also, loss of the organized arrangement of collagen fibrils in the sutured region of tendons may account for the lack of cellular infiltration into the sutured extracellular matrix.

The fibrils in the unsutured region had parallel fibrils that were orientated along the long axis of the tendon (see Figure 6.2.2.2). Phase atomic microscopy images of the unsutured region of tendon were processed using OrientationJ an ImageJ (NIH, USA) plugin. The plugin produces a histogram of the orientation of regular structures in the image. The unsutured region showed two peaks, which were likely to be the result of the regular 67 nm banding on collagen fibrils and the regular spacing between collagen fibrils (See Figure 6.5). This supports the observation that the collagen fibrils in the unsutured region of tendon are arranged in an organized manner. Further, a fourier transformation of the same region shows that the unsutured region of tendon produces a transformation with 3 relatively straight peaks in the fourier space. These peaks are likely to correspond to the repeating 67 nm bands on the collagen fibrils and the regular spacing between collagen fibrils as well (See Figure 6.7).

The fibrils appeared less organized than in the unsutured regions, with some fibrils not orientated in the usual parallel arrangement (see Figure 6.2.2.2). The unsutured region only exhibited a single peak (-80°), which is most likely to correspond to the 67 nm repeating bands on collagen fibrils (See Figure 6.6). A fourier transformation of the same region confirmed this observation. The fourier space of the sutured region of tendon had one curved faint peak, which is most likely produced by the 67 nm repeating bands on collagen fibrils (See Figure 6.7). The lack of other peaks, suggests that the fibrils are too irregularly organized to produce a peak on fourier transformation.

These findings support the notion that the fibrils in the sutured region are disorganized.

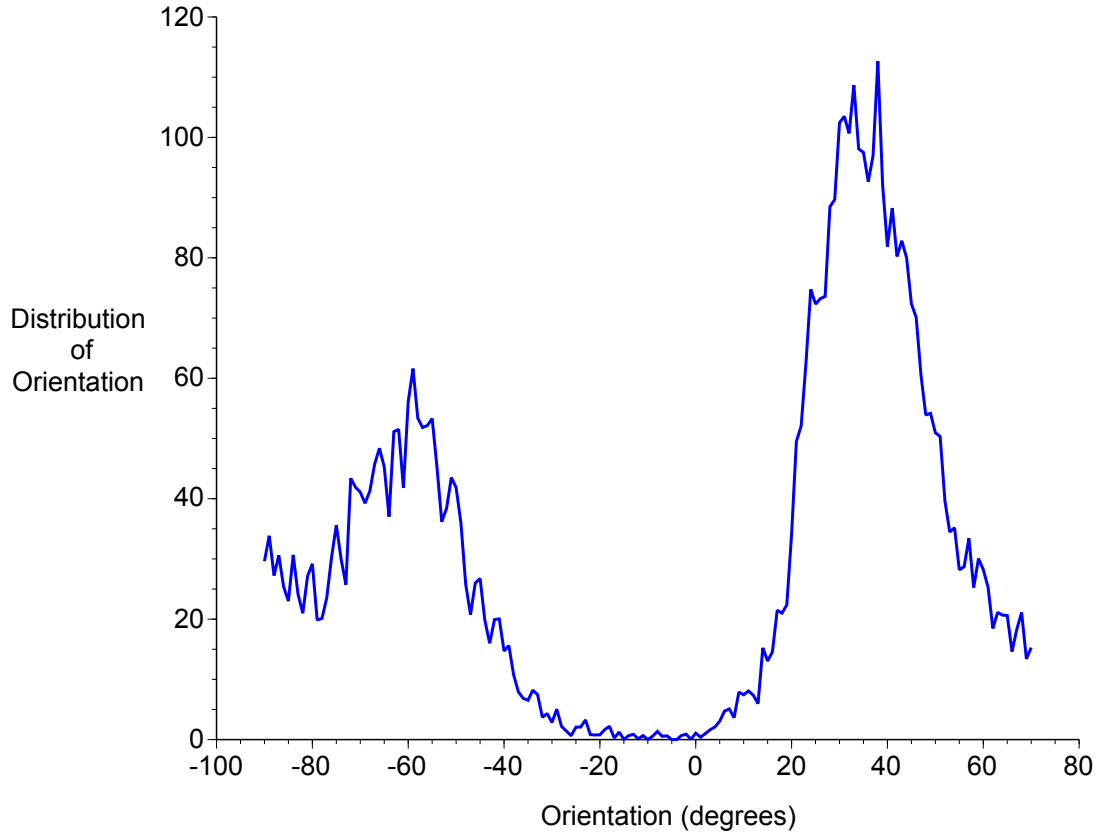

Figure 6.5: **Orientation of Fibrils in an Unsutured Region** Flexor digitorum profundus mouse tendons were cryofixed 6 hours after they had been sutured *in vivo*. Sections (5μm thick) were obtained and were imaged using atomic force microscopy. Phase atomic microscopy images were processed using OrientationJ, an ImageJ plugin (NIH, USA), which calculates the orientation of components in an image. A histogram of the orientation of components detected by the software is shown. The unsutured region shows two peaks (-60° and 50°) which are most likely to be the product of the 67 nm repeating bands on collagen fibrils and the regular spacing between collagen fibrils.

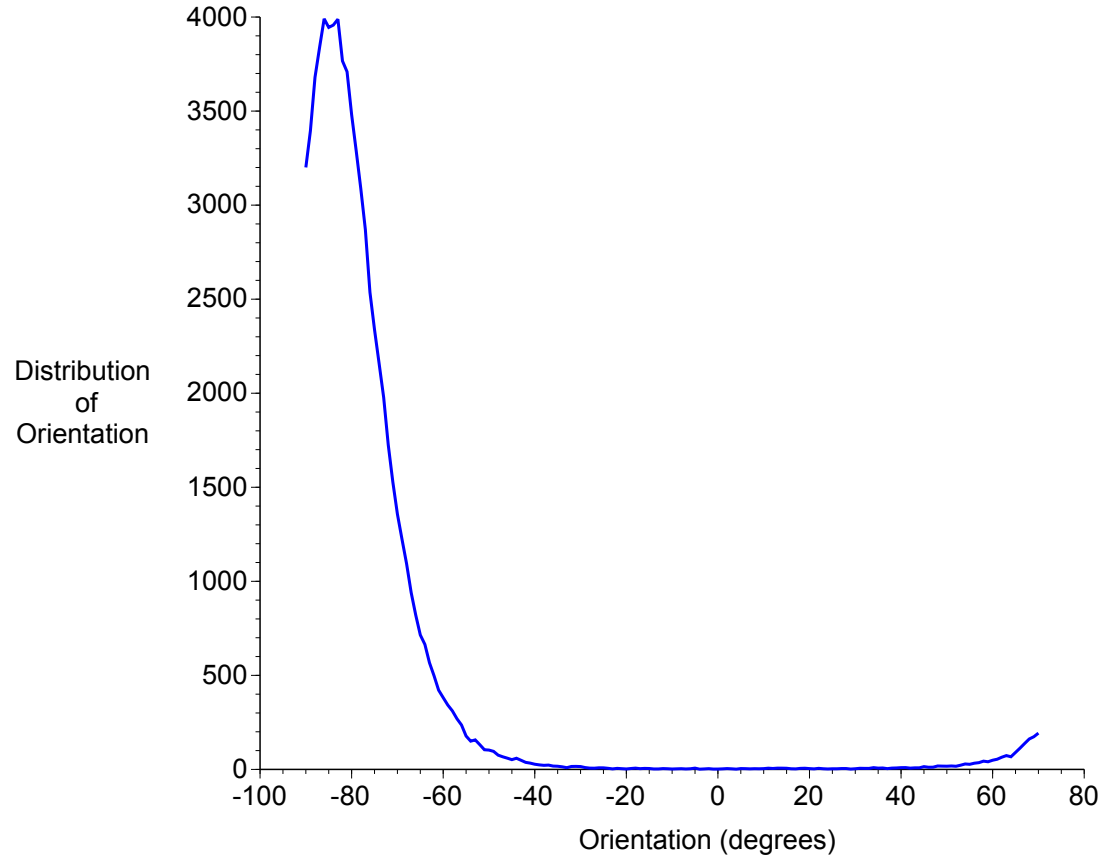

Figure 6.6: **Orientation of Fibrils in a Sutured Region** Flexor digitorum profundus mouse tendons were cryofixed 6 hours after they had been sutured *in vivo*. Sections (5μm thick) were obtained and were imaged using atomic force microscopy. Phase atomic microscopy images were processed using OrientationJ, an ImageJ plugin (NIH, USA), which calculates the orientation of components in an image. A histogram of the orientation of components detected by the software is shown. The sutured region shows one peak (-80°) which is most likely to be the product of the 67 nm repeating bands on collagen fibrils.

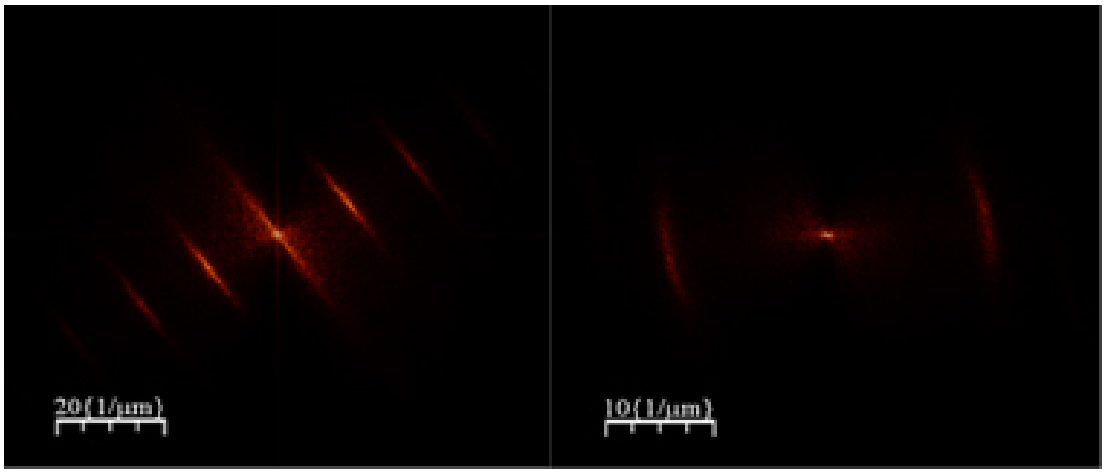

Figure 6.7: **Fourier Transform** Flexor digitorum profundus mouse tendons were cryofixed 6 hours after they had been sutured *in vivo*. Sections (5μm thick) were obtained and were imaged using atomic force microscopy. Fourier transformations were obtained from atomic microscopy phase images. The unsutured region of the tendon (left) produces a fourier space with 3 straight peaks, which probably correspond to the 67 nm repeating bands and the longitudinal repeating spaces between the fibrils. The fourier space of the sutured region of the tendon (right) has one curved faint peak, which is likely to correspond to the repeating 67 nm bands on collagen fibrils. The lack of other peaks suggests that the fibrils are disorganized.

6.2.4 Ultrastructural Morphology of Uninjured and Sutured and Unsutured Regions of Sutured Tendons

The ultrastructural appearance of the extracellular matrix of uninjured and sutured and unsutured regions of sutured tendons was evaluated by electron microscopy. Mouse FDP tendons were sutured *in vivo* and processed for electron microscopy 24 hours later. Transverse sections of tendon were obtained. The organization of the collagen fibrils and the appearance of the extracellular matrix, including its relationship with the cells were noted. This was carried out to determine if the extracellular matrix of the sutured regions of tendons showed evidence of damage and disorganization, which may explain the lack of cellular infiltration into the sutured regions. Uninjured tendons were also imaged to to compare their extracellular matrix to that of sutured tendons, to establish if suturing caused generalized extracellular matrix alterations that extended into the unsutured regions of tendon.

6.2.4.1 Uninjured Tendon

In the uninjured tendon, the cells appeared star shaped, as they had thin, protruding cellular projections (see Figure 6.8). The cells were nested in a darkly stained fibrous matrix that consisted of very narrow diameter fibers. This fibrous, dark matrix surrounding the cells extended between collagen fibrils, forming a conduit between the cells and delineating the collagen bundles. The cells were in close contact with the collagen fibrils and no obvious white spaces were visible in the sections. There were large and narrower diameter collagen fibrils present, which were arranged in parallel. Scattered between the collagen fibers were elastic fibers and bundles, which stained as darkly as the dark matrix that surrounded the cells and ran between the collagen bundles (see Figure 6.9).

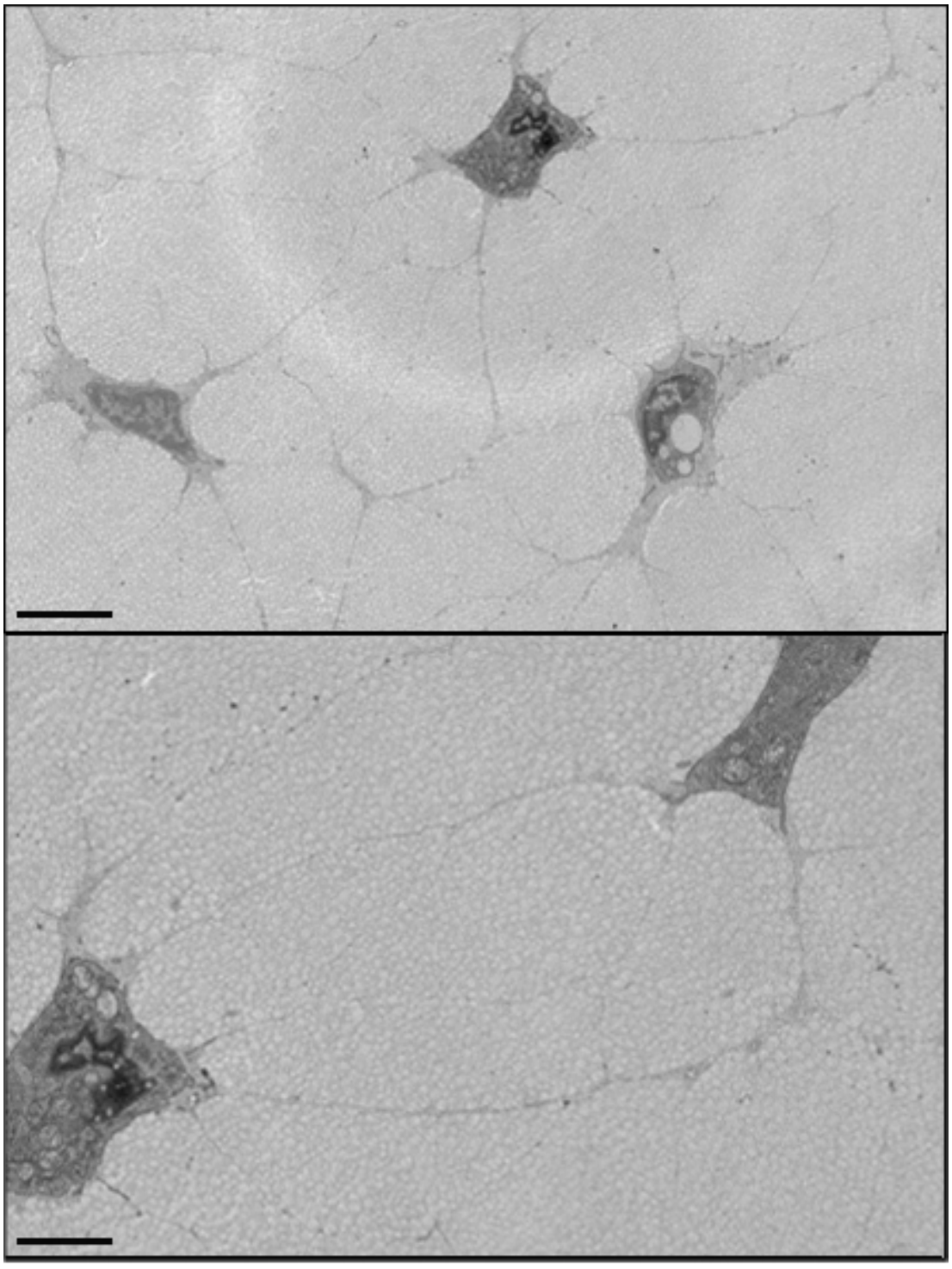

Figure 6.8: **Transverse Electron Microscopy of Uninjured Tendon** Flexor digitorum profundus mouse tendons were prepared for electron microscopy. Transverse transmission electron microscopy (TEM) were obtained. The cells appear to be closely apposed to the extracellular matrix. The cells were surrounded by a darkly staining fibrous matrix. The matrix appeared to extend to the space between the collagen bundles *scale: top = 5 μm, bottom = 2 μm*

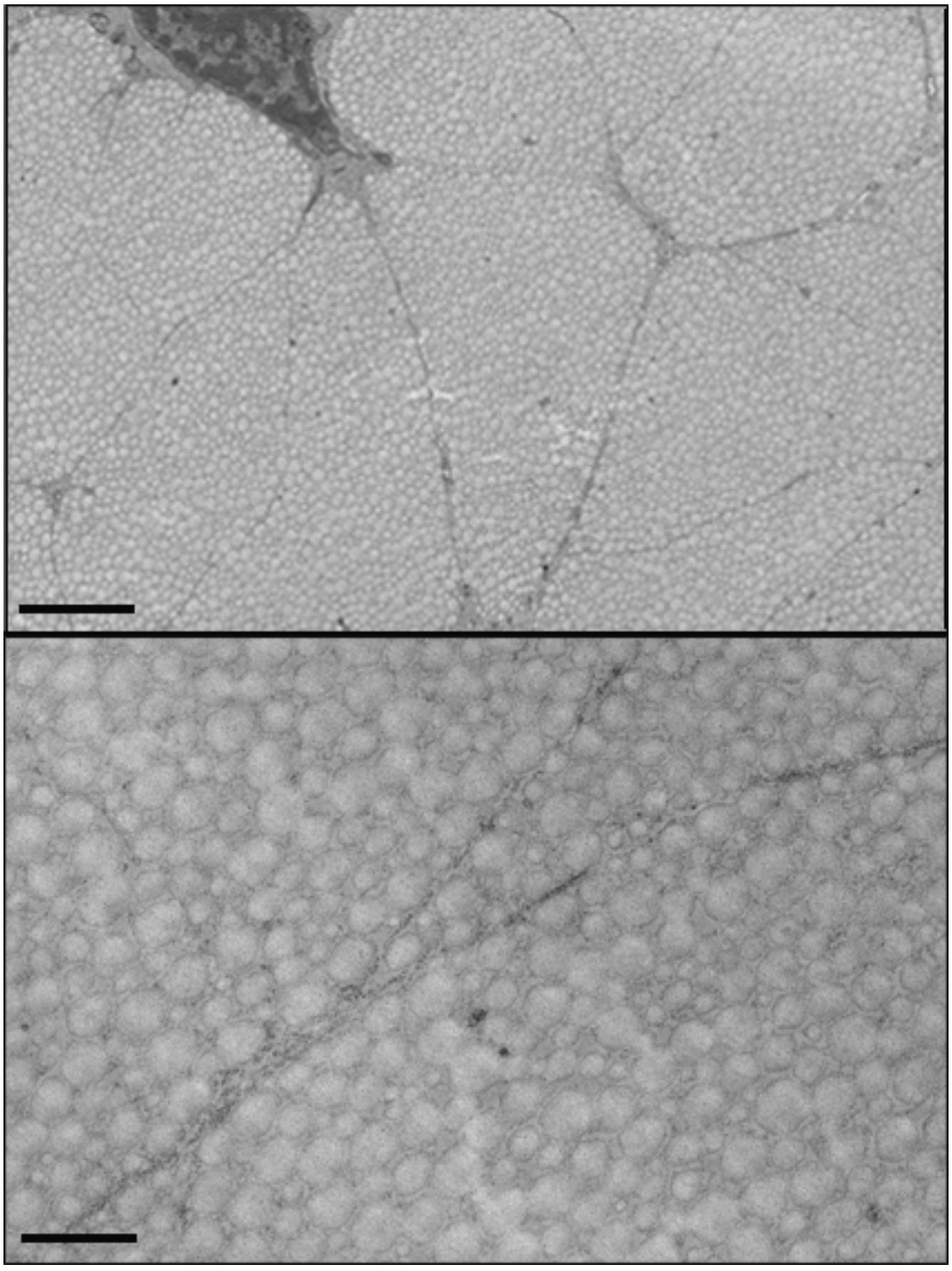

Figure 6.9: **Transverse Electron Microscopy of Uninjured Tendon 2** Flexor digitorum profundus mouse tendons were prepared for electron microscopy. Transverse transmission electron microscopy (TEM) were obtained. The cells appear to be closely apposed to the extracellular matrix. A dark fibrous matrix can been between the collagen bundles. The space between the bundles appears narrow. *scale bar: top = 2 μm, bottom = 0.5 μm*

6.2.4.2 Sutured tendon, Unsutured Region

This region was approximately 1mm from the suture. The cells, as described in Chapter 4, appeared rounded than in uninjured tendon, having lost their spiky cellular projections. The surrounding dark matrix was still present around the cells but the space between the collagen bundles was largely void of the the darkly staining fibrous matrix present in uninjured tendons. This made the bundles easier to distinguish (see Figure 6.10). Some elastic bundles could be seen between collagen fibrils. The collagen bundles were made up of large and narrower diameter fibrils, orientated parallel to the long axis of the tendon. In some areas, the collagen fibrils within the bundles appeared disorganized and unevenly spaced (see Figure 6.11).

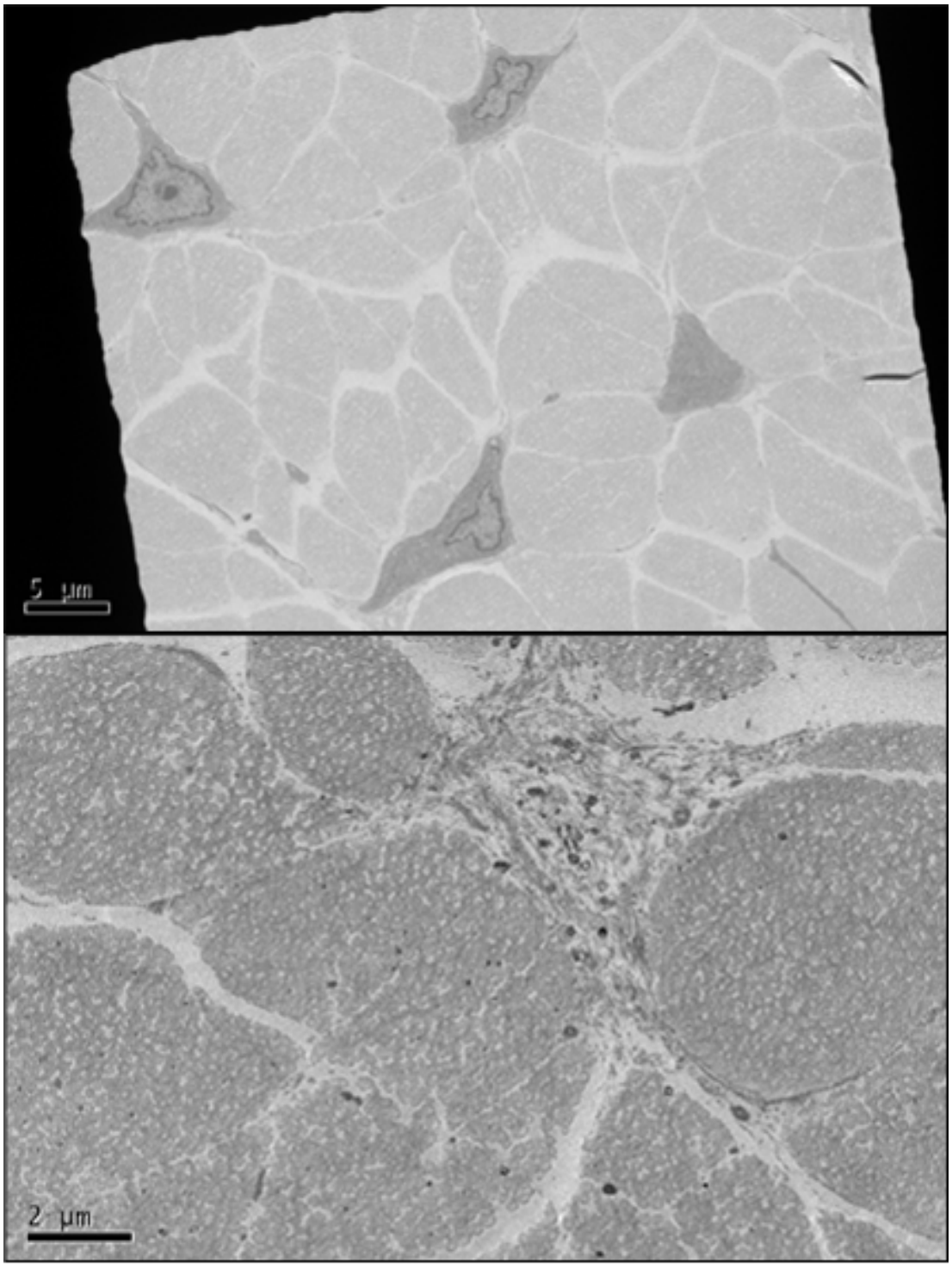

Figure 6.10: **Transverse Electron Microscopy of an Unsutured Region of Tendon** Flexor digitorum profundus mouse tendons were prepared for electron microscopy 24 hours after they had been sutured *in vivo*. Transverse transmission electron microscopy (TEM) were obtained from unsutured regions of the tendon (~1 mm away from the suture). The collagen bundles had space between them, unlike the the dark matrix seen in the uninjured tendons. The space between the collagen bundles also appeared larger. *scale bar: top = 5 µm, bottom = 2 µm*

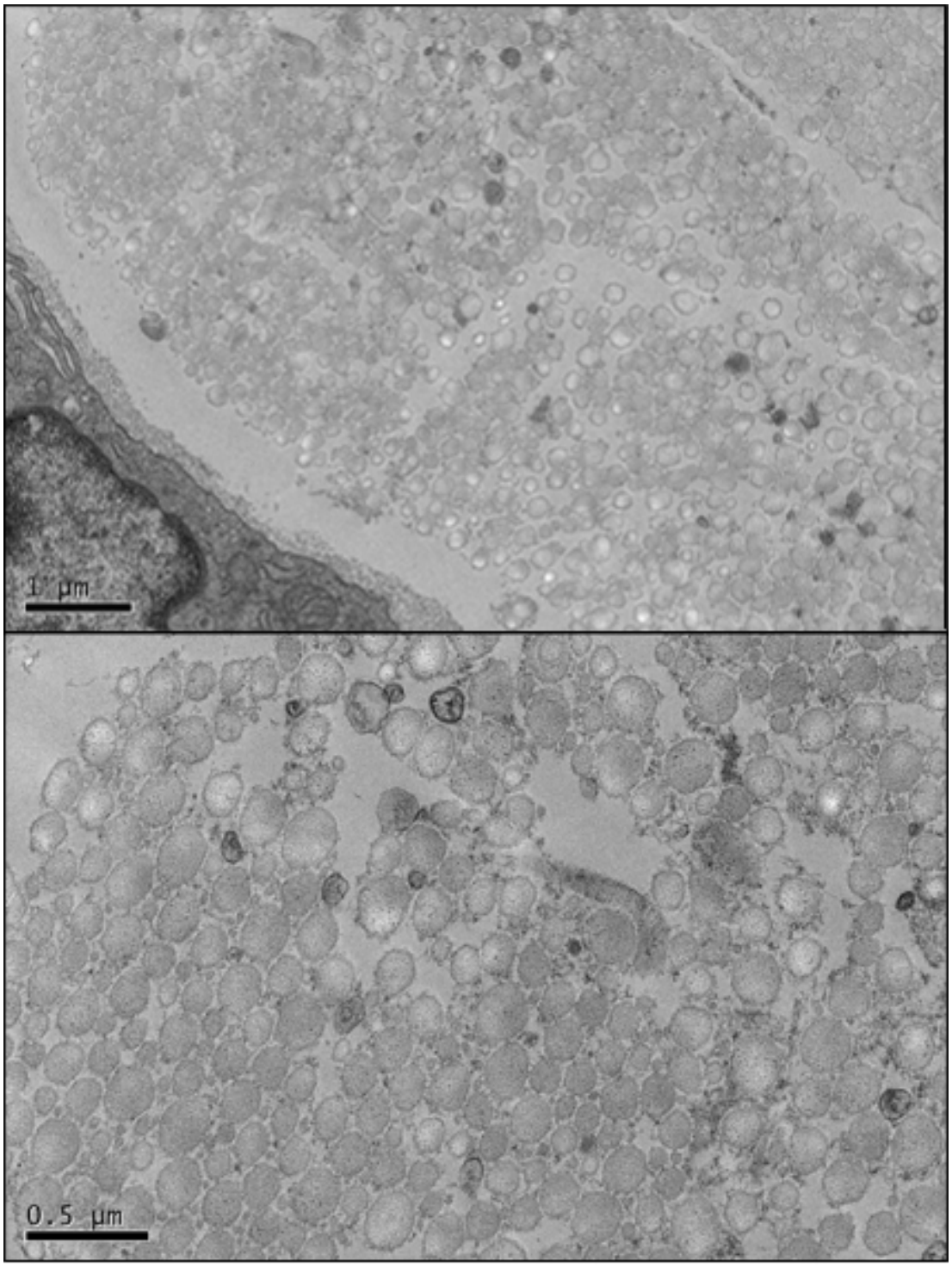

Figure 6.11: **Transverse Electron Microscopy of an Unsutured Region of Tendon 2** Flexor digitorum profundus mouse tendons were prepared for electron microscopy 24 hours after they had been sutured *in vivo*. Transverse transmission electron microscopy (TEM) were obtained from unsutured regions of the tendon (~1 mm away from the suture). The collagen fibrils within the bundles appeared disorganized, with uneven spaces between the fibrils. *scale bar: top = 1 µm, bottom = 0.5 µm*

6.2.4.3 Sutured Region

Immediately adjacent to the suture, there were no cells detectable. The extracellular matrix was very disorganized and had cell remnants intermixed within it. No large diameter collagen fibrils could be seen. Fibrils of narrower diameter with banding could be seen but they emanated from multiple directions, making them appear randomly orientated. These randomly orientated fibrils were densely packed (See Figure 6.13). Further away from the suture, bundles were easier to distinguish as white space was present between them (See Figure 6.12). The dark fibrous matrix alluded to in the uninjured tendon was not seen between the bundles but occasionally cell debris could be seen in its place. Within the bundles, disorganized collagen fibrils were present that gradually became more organized the greater the distance between it and the suture became. More cells were also evident, further from the suture and space between the bundles increased in length.

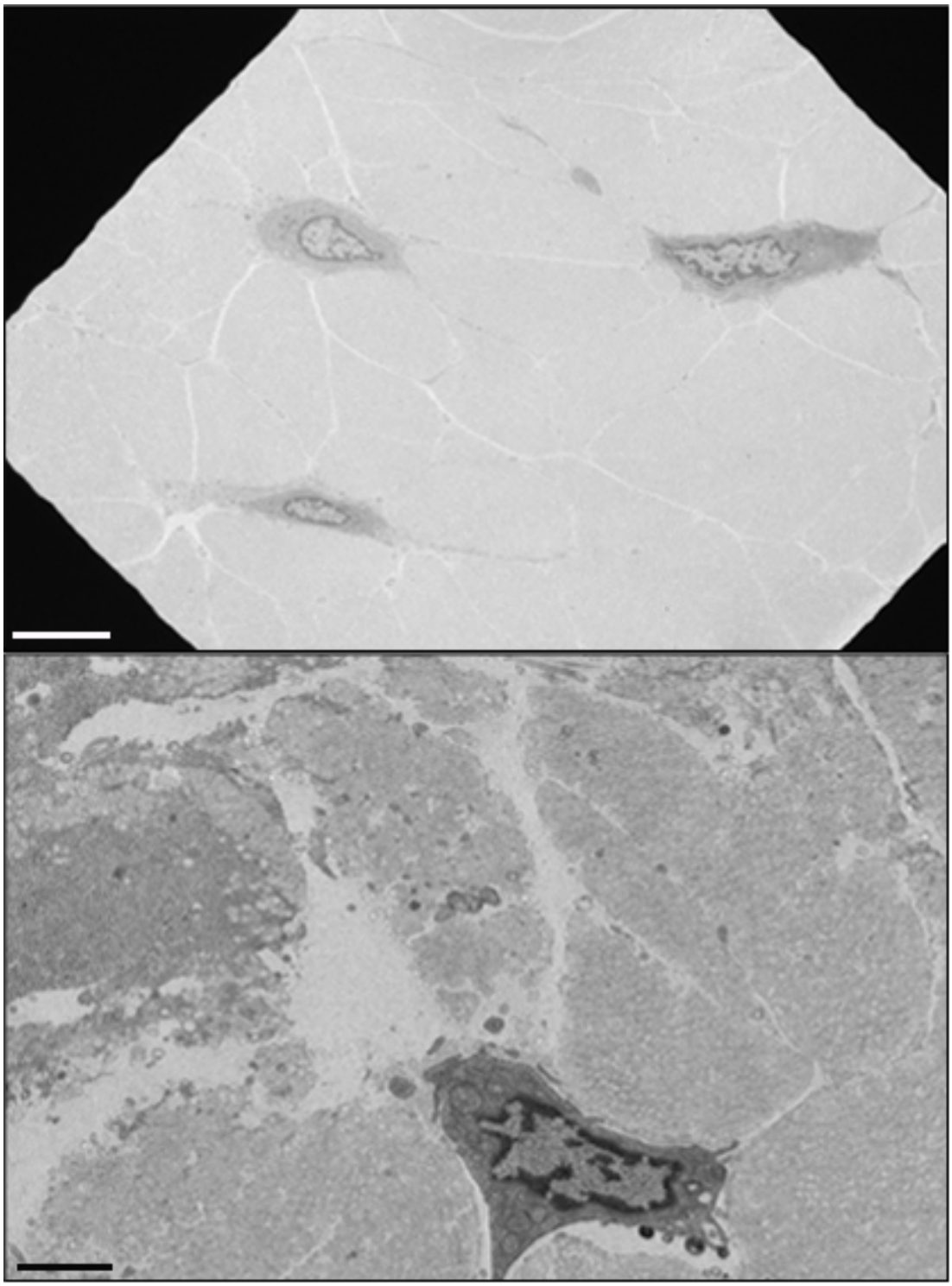

Figure 6.12: **Transverse Electron Microscopy of a Sutured Region Tendon** Flexor digitorum profundus mouse tendons were prepared for electron microscopy 24 hours after they had been sutured *in vivo*. Transverse transmission electron microscopy (TEM) were obtained from a sutured region of the tendon. The space between the bundles was white, unlike that of the uninjured tendon which contained a dark matrix. The bundles in some regions appeared disorganized (bottom) *scale bar: top = 5 μm, bottom = 2 μm*

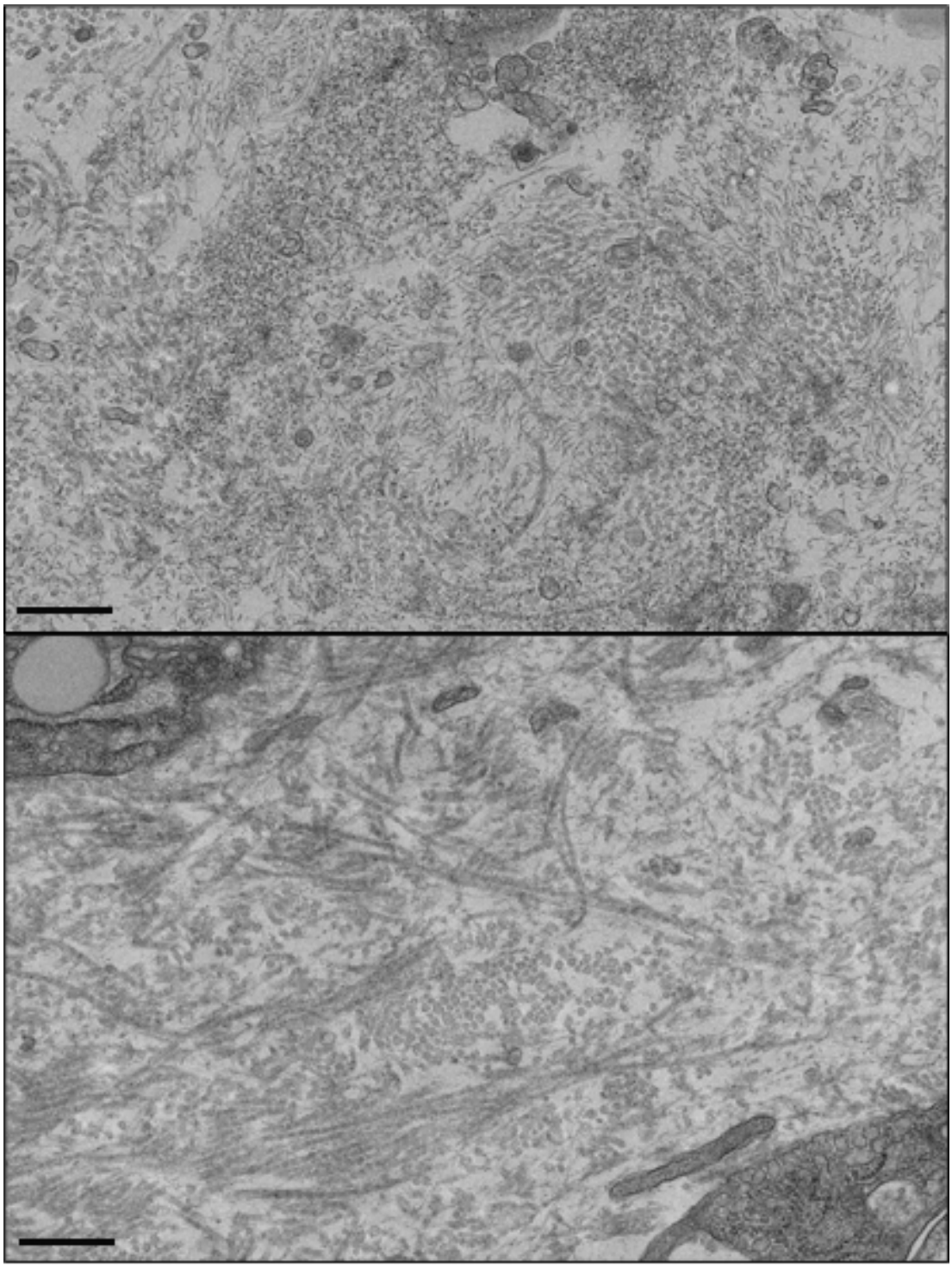

Figure 6.13: **Transverse Electron Microscopy of a Sutured Region of Tendon 2** Flexor digitorum profundus mouse tendons were prepared for electron microscopy 24 hours after they had been sutured *in vivo*.Transverse transmission electron microscopy (TEM) were obtained from a sutured region of the tendon. The extracellular matrix was very disorganized and cell remnants were present dispersed between the fibrils. These randomly orientated fibrils were densely packed. *scale bar: 0.5 μm*

6.2.5 The Mechanical Properties of the Sutured Extracellular Matrix

The density of the collagen fibrils was compared in sutured and unsutured regions of the same tendon using scanning acoustic microscopy. The Young's modulus in sutured regions of tendons was compared to the modulus in unsutured regions of the same tendon using nanoindentation. The density of the collagen fibrils and the Young's modulus, which measures the stiffness of tissue, were both measured, as both have been shown to affect cell migration.

6.2.5.1 Reflected Wavespeeds During Scanning Acoustic Microscopy

Scanning acoustic microscopy was used to image 5 μm thick cryosections of mouse tendons that were cryofixed 6 hours after they have been sutured *in vivo*. A series of images was obtained from different depths of the cryosection, which contained information on sound speed. These images were used to create a corrected phase image of the sutured region of tendon. In the sutured region, the tendon appeared redder than it did in the unsutured adjacent region, which appeared blue. The redder an image, the greater the reflected sound speeds and the bluer the image, the less the reflected sound speeds in that region (See Figure 6.14).

Calculations were obtained of the estimated wavespeeds of the reflected sound waves. The unsutured regions, flanking the suture had wavespeeds of 2183 m/s. The sutured region had calculated wavespeeds of 2700 m/s, which was much higher than the value in the unsutured regions.

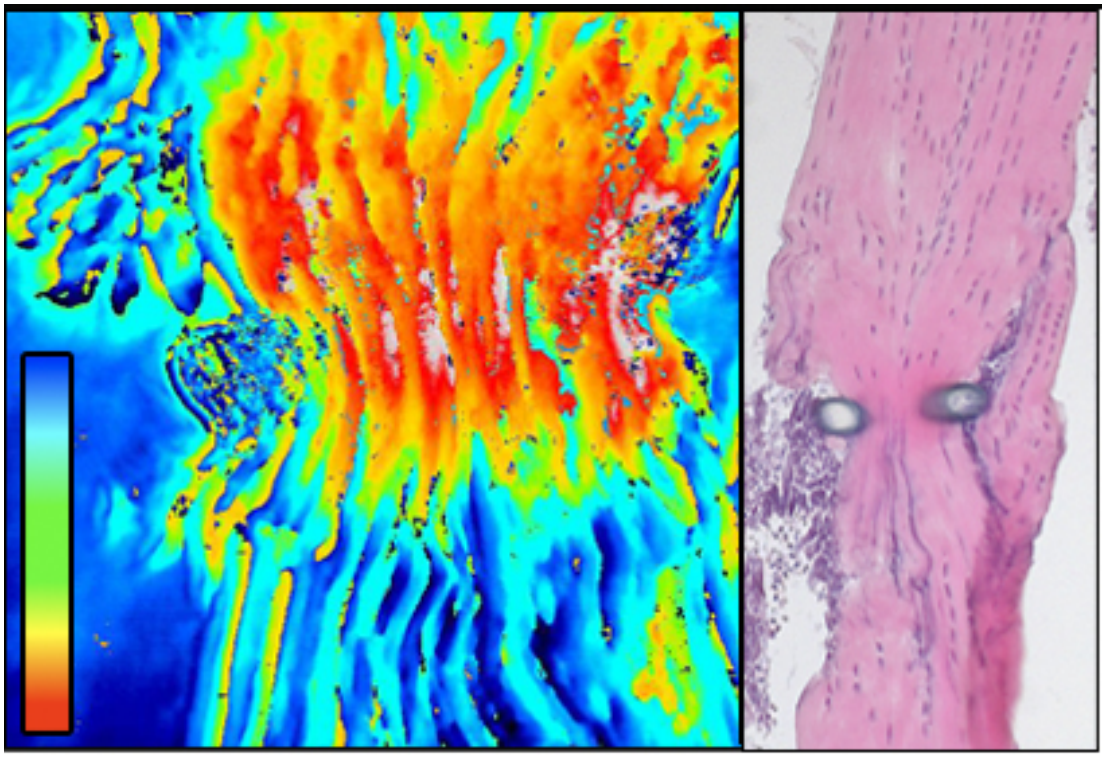

Figure 6.14: **Scanning Acoustic Microscopy** Flexor digitorum profundus mouse tendons were cryofixed 6 hours after they had been sutured *in vivo*. Sections (5μm thick) were obtained and were imaged using scanning acoustic microscopy. Alternate sections were stained using hematoxylin and eosin (right). A corrected phase image was obtained from a series of images taken at a different depth, which contained information on sound speed (left). The redder the image the higher the sound speed and the blue the image the less the sound speed (see gradient in bottom left corner). The sutured part appears to have a higher sound speed.

6.2.5.2 Nanoindentation

Nanoindentation was performed on flexor digitorum profundus mouse tendons, which were cryofixed 6 hours after they had been sutured *in vivo*. Sections (30μm thick) were used to perform the nanoindentation in two samples. 100 indents were obtained in the sutured regions and 100 indents in the unsutured regions. The mean Young's modulus was measured and it was deemed to be 112 MPa in the sutured region and 123 MPa in the unsutured region in one sample. In another sample, the mean Young's modulus was 123 MPa in the sutured region and 158 MPa in the unsutured region. Both samples show that the sutured region of tendon has a lower Young's modulus than the unsutured region of sutured tendons (See Figure 6.15).

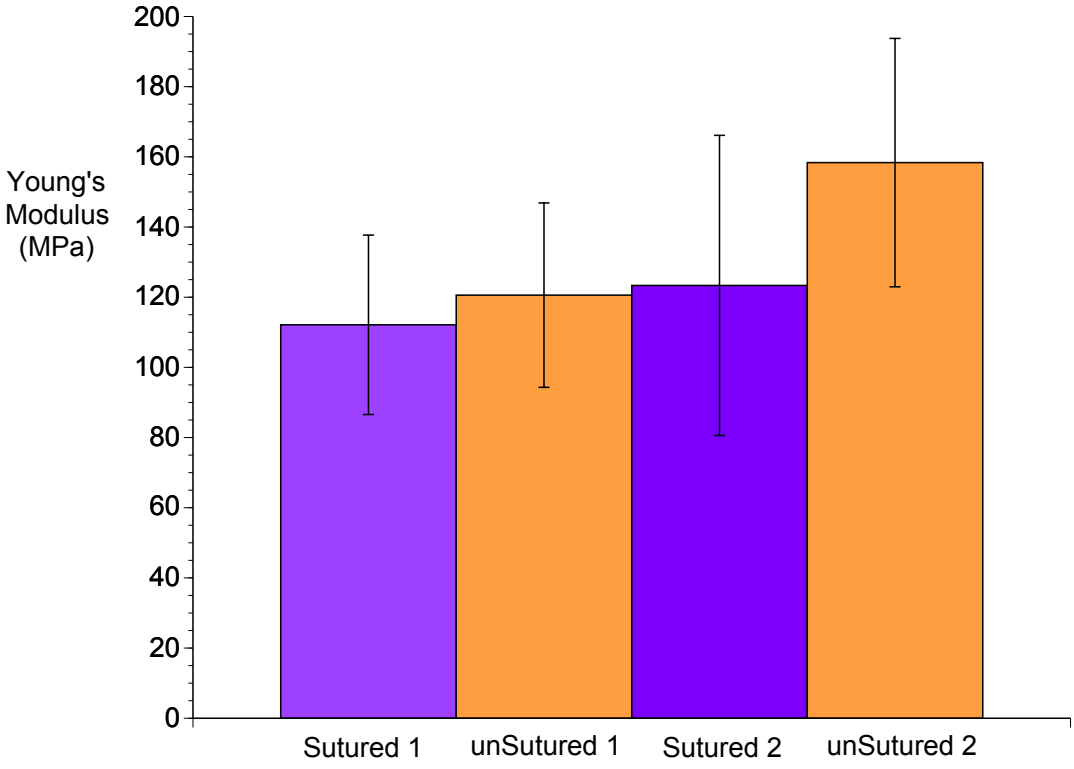

Figure 6.15: **Nanoindentation** Flexor digitorum profundus mouse tendons were cryofixed 6 hours after they had been sutured *in vivo*. Sections (30μm thick) were obtained. Nanoindentation was performed on 2 samples. 100 indents were obtained in the sutured regions and 100 indents in the unsutured regions. The bar graph shows that the mean Young's modulus was calculated to be 112 MPa and 121 MPa in the sutured regions and 123 MPa and 158 MPa in the unsutured regions.

6.3 Discussion

The aims of this chapter were to examine the arrangement and biomechanical properties of sutured regions of tendon compared to unsutured regions of tendon.

The fascicular arrangement of collagen was examined using transverse transmission electron microscopy at a low magnification. This showed that the interfascicular space was wider in sutured tendons compared to uninjured tendons. Within the same tendon, there was no difference in the mean distance between collagen fascicles in the uninjured regions of sutured tendons (~1 mm away from the suture) and sutured regions of tendon. The wider spacing between fascicles in sutured tendons compared to uninjured tendons may have been occupied by a substance which has dissolved during processing for electron microscopy. Electron microscopy images also showed that the dark fibrous material observed between fascicles in uninjured tendon and described by Ritty et al. (2002), was no longer present in sutured tendons. The loss of this matrix may be another explanation for the lack of cell migration into the acellular zone, as Ritty et al. (2002) speculated that the distribution of the interfascicular matrix suggests that it functioned as guiding track for cell migration.

Scanning acoustic, polarized light and atomic force microscopy of sutured tendon sections suggest that the fibrils were more closely packed in the sutured regions, compared to the unsutured regions. Measurements of the interfibrillar length confirmed that the fibrils were more packed than the fibrils in the adjacent unsutured regions.

Fourier transform and analysis using OrientationJ of atomic microscopy images, provided evidence that the fibrils in the sutured regions of tendon were more disorganized that fibrils in the unsutured parts. However, atomic microscopy was performed on dehydrated cryosections. The dehydration of the tissue prior to image is a limitation, as the sutured tendons might dry differently to the unsutured regions. However, transverse transmission electron microscopy confirmed that the sutured region of the tendon contained fibrils that were more disorganized. These disorganized dense fibrils may explain the persistence of the acellular zone a year after they have been repaired.

Disorganized, dense fibrils are also a feature of scar tissue (Gurtner et al. 2008). The sutured tissue may be too dense for the diffusion of MMPs or cellular infiltration, as a result of the suture causing compaction of the underlying matrix, causing an 'internal scar'. These findings highlight the importance of targeting the pathways identified in Chapter 4 early, as attempting to prevent the formation of the dense disorganized tissue is easier that attempting to degrade it.

The mechanical implications of this disorganized sutured ECM were investigated using scanning acoustic microscopy and nanoindentation. As both approaches can measure biomechanical properties within a small region of tissue, the mechanical properties of sutured ECM can be compared to unsutured ECM, which is more difficult to accomplish using gross mechanical measures.

Nanoindentation, which was used to measure the biomechanical properties of the constituent fibrils, showed that the sutured ECM had a lower Young's modulus compare to the unsutured ECM. Other studies have also localized mechanical weakness to the suture grasp of a tendon repair (McDowell et al. 2002). The scanning acoustic microscopy illustrated the sutured region exhibited greater reflected wavespeeds, compared to unsutured regions of tendon. The greater wavespeeds in sutured regions of tendon compared to the unsutured regions, could be due to the greater packing density in the sutured region or secondary to the paucity of cells in the sutured areas compared to the unsutured areas of tendon. The difference in biomechanical properties of tendon may also explain the lack of cell infiltration into the sutured regions, as Hadjipanayi et al. (2009) showed that fibroblasts tended to migrate towards stiffer materials.

Part IV

Conclusions

CHAPTER 7

CONCLUSIONS

The aims of this thesis were to determine the mechanisms involved in acellular zone formation in tendons. The findings of this thesis suggest that the compressive forces of the suture, in combination with longitudinal stress across the tendon, result in cell death via necrosis and necroptosis, causing acellular regions to form. The MAPK, Ap-1 Fos/Jun and Nfκb are likely to be involved in mediating this response. These pathways also mediate the expression of genes involved in inflammation, oxidative stress and MMPs. The compressive physical forces exerted by the suture on the tissue it grips also cause the matrix to become dense and disorganized. As a result, inflammatory cells are unable to invade the suture site to repair and remodel it. This disorganized compact sutured ECM also appears to be weaker than the uninjured organized fibrils in the adjacent unsutured regions. This is similar to scar tissue, which is usually weaker than the native uninjured tissue (See Figure 7 for an illustrative depiction of the pathways that this thesis proposes are involved in acellular zone development). As scar tissue persists for a long time in tissue and rarely becomes repopulated with cels, this may explain why the acellular zone persists a year after the tendon has been repaired.

The notion that suturing, which is the main tool used by surgeons to treat injuries,

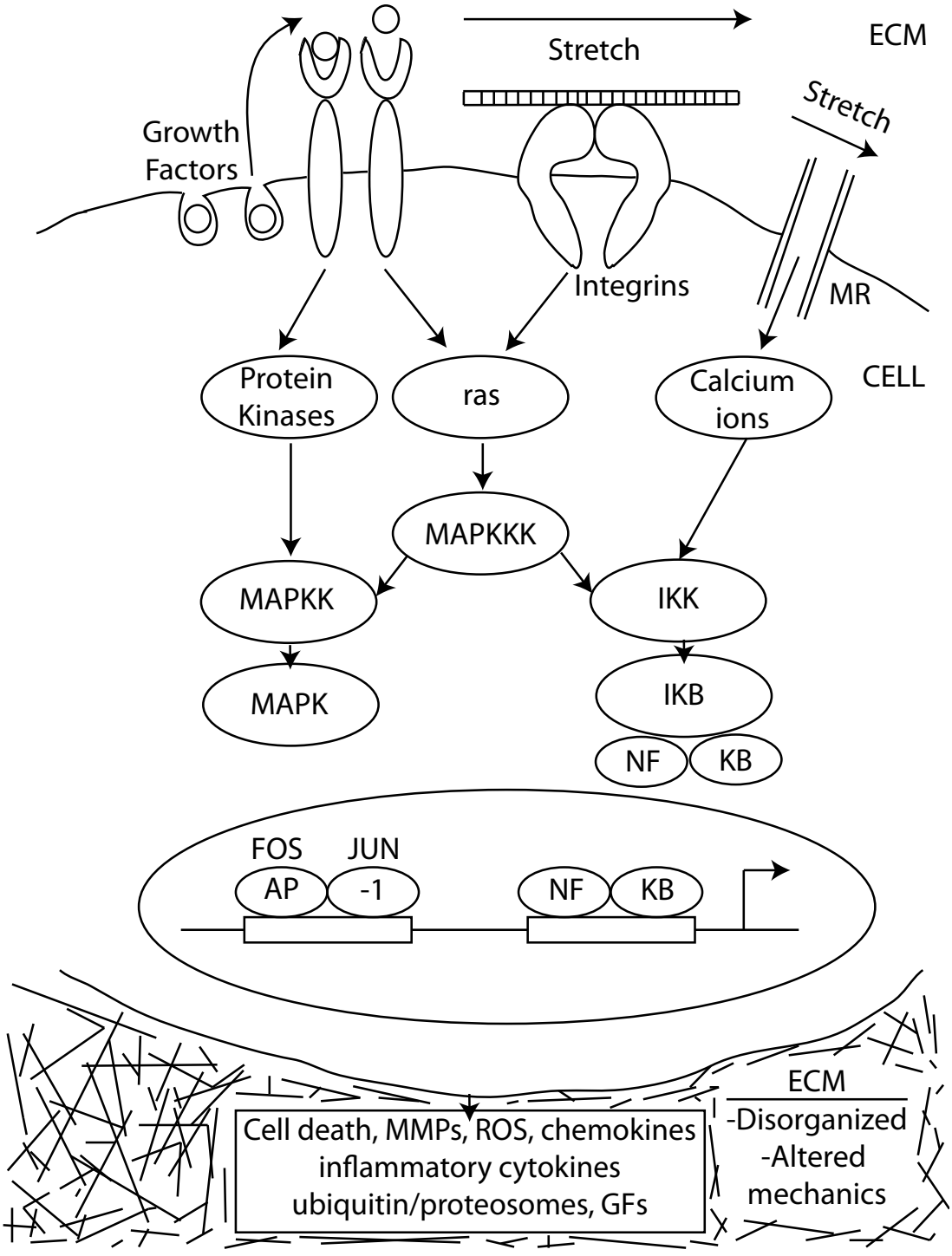

Figure 7.1: **Potential Pathways Involved in Acellular Zone Formation and Persistence** The findings of this thesis suggest that the compressive forces of the suture, result in cell death, causing the acellular zone to form. The MAPK, Ap-1 Fos/Jun and Nfκb are likely to be involved in mediating this response and expression of genes involved in inflammation, oxidative stress and MMPs. The compressive physical forces exerted by the suture on the tissue it grips also cause the matrix to become dense and disorganized, which appears to be weaker than the uninjured organized fibrils in the adjacent unsutured regions. These properties of the sutured ECM may explain the inability of inflammatory cells to invade it (*MR = mechanoreceptor). Image modified from (Chiquet et al. 2003)*

is invoking secondary damage to tissue, has also been proposed by McDowell et al. (2002), Pasternak et al. (2007) and Wong et al. (2006b). These findings emphasize the importance of developing alternative treatment strategies for injury, such as cell-based therapies, gene therapy and tissue engineering. In addition, suture can be coated with molecules, which could improve their function or minimize damage caused by them. For example, sutures have been shown to have improved mechanical properties after they have been coated with growth differentiation factor - 5 (Dines et al. 2007), pluripotent cells (Yao et al. 2008) and MMP inhibitors (Pasternak et al. 2007). Sutures coated with Necrostatin-1 or another inhibitor of the pathways proposed in Chapter 4 may yield similar therapeutic benefits. Another advantage of coating sutures is that the treatment used would be delivered instantly to the tissues, as it has been shown in Chapter 6 that after 24 hours, the acellular zone would be harder to treat, as a dense irregular matrix forms. Another method to improve the outcome after suturing, is to use multistranded sutures, which have a smaller grasp size. These principles can be used to improve treatment in other tissue which develop an acellular zone such as cornea and cartilage and to minimize damage caused by suturing in other tissues, such as gastrointestinal anastomoses, which are prone to ruptures that can be fatal (Pasternak et al. 2008).

Besides having implications for surgical treatment of tissue, the *in vitro* model of acellular zone formation can potentially be used as a model to study scar tissue formation and mechanotransduction. Fibrosis and scar tissue formation cause significant morbidity and mortality and feature in many diseases such as idiopathic pulmonary fibrosis, liver cirrhosis, as well as secondary to other diseases, such as infection, rheumatological diseases and heart failure. These diseases are difficult to treat and are difficult to investigate due to the lack of *in vitro* models. The acellular zone model in tendon might be a good model to use as tendons are simple tissues, which have an organized matrix and disorganized regions are easier to identify.

This thesis also raises questions that can be explored further in the future. The use of inhibitors such as Necrostatin-1 and inhibitors of the Nfκb are interesting targets

that can be tested, to determine if they can improve the outcome after tendon repair. The involvement of the pathways proposed would need to be confirmed *in vivo* first. Moreover, the long term micromechanical properties and morphological features on electron microscopy could be explored to establish if the acellular zone plateaus or remodels with time. Lastly, although the acellular zone has been described in mouse, rat, rabbit and lamb; its existence has not been confirmed in humans. It would be interesting to see if the acellular zone is present in humans and if its size is correlated with tendon ruptures, although it would be difficult to obtain that information. Perhaps, high resolution *in vivo* imaging be used to investigate the acellular zone in humans.

This thesis has investigated the acellular zone in tendons and proposed a number of mechanisms, which could be targeted to improve outcome after surgical repair. Original approaches were used such as the use of scanning acoustic microscopy, nanoindentation and *in vitro* models of tendon injury, which could be used to study the influence of other types of injuries.

REFERENCES

Akhtar, R., Schwarzer, N., Sherratt, M.J., Watson, R.E.B., Graham, H.K., Trafford, A.W., Mummery, P.M., Derby, B., 2009a. Nanoindentation of histological specimens: Mapping the elastic properties of soft tissues. J Mater Res 24, 638–646.

Akhtar, R., Sherratt, M.J., Watson, R.E.B., Kundu, T., Derby, B., 2009b. Mapping the micromechanical properties of cryo-sectioned aortic tissue with scanning acoustic microscopy. Mater Res Soc Symp Proc 1132E.

Ananthanarayanan, S., Veis, A., 1972. The molecular parameters of monomeric and acid-soluble collagens. low shear gradient viscosity and electric birefringence. Biopolymers 11, 1365–77.

Arnoczky, S.P., Lavagnino, M., Egerbacher, M., Caballero, O., Gardner, K., 2007. Matrix metalloproteinase inhibitors prevent a decrease in the mechanical properties of stress-deprived tendons: an in vitro experimental study. Am J Sports Med 35, 763–9.

Arnoczky, S.P., Lavagnino, M., Egerbacher, M., Caballero, O., Gardner, K., Shender, M.A., 2008. Loss of homeostatic strain alters mechanostat "set point" of tendon cells in vitro. Clin Orthop Relat Res 466, 1583–91.

Bailey, A.J., Robins, S.P., Balian, G., 1974. Biological significance of the intermolecular crosslinks of collagen. Nature 251, 105–9.

Banes, A.J., Donlon, K., Link, G.W., Gillespie, Y., Bevin, A.G., Peterson, H.D., Bynum, D., Watts, S., Dahners, L., 1988a. Cell populations of tendon: a simplified method for isolation of synovial cells and internal fibroblasts: confirmation of

origin and biologic properties. J Orthop Res 6, 83–94.

Banes, A.J., Horesovsky, G., Larson, C., Tsuzaki, M., Judex, S., Archambault, J., Zernicke, R., Herzog, W., Kelley, S., Miller, L., 1999a. Mechanical load stimulates expression of novel genes in vivo and in vitro in avian flexor tendon cells. Osteoarthritis Cartilage 7, 141–53.

Banes, A.J., Link, G.W., Bevin, A.G., Peterson, H.D., Gillespie, Y., Bynum, D., Watts, S., Dahners, L., 1988b. Tendon synovial cells secrete fibronectin in vivo and in vitro. J Orthop Res 6, 73–82.

Banes, A.J., Weinhold, P., Yang, X., Tsuzaki, M., Bynum, D., Bottlang, M., Brown, T., 1999b. Gap junctions regulate responses of tendon cells ex vivo to mechanical loading. Clin Orthop Relat Res , S356–70.

Beckstead, J.H., 1994. A simple technique for preservation of fixation-sensitive antigens in paraffin-embedded tissues. J Histochem Cytochem 42, 1127–34.

Behl, Y., Krothapalli, P., Desta, T., DiPiazza, A., Roy, S., Graves, D.T., 2008. Diabetes-enhanced tumor necrosis factor-alpha production promotes apoptosis and the loss of retinal microvascular cells in type 1 and type 2 models of diabetic retinopathy. Am J Pathol 172, 1411–8.

Benjamin, M., Kaiser, E., Milz, S., 2008. Structure-function relationships in tendons: a review. J Anat 212, 211–28.

Berenson, M.C., Blevins, F.T., Plaas, A.H., Vogel, K.G., 1996. Proteoglycans of human rotator cuff tendons. J Orthop Res 14, 518–25.

Bi, Y., Ehirchiou, D., Kilts, T.M., Inkson, C.A., Embree, M.C., Sonoyama, W., Li, L., Leet, A.I., Seo, B.M., Zhang, L., Shi, S., Young, M.F., 2007. Identification of tendon stem/progenitor cells and the role of the extracellular matrix in their niche. Nat Med 13, 1219–27.

Birk, D.E., Trelstad, R.L., 1986. Extracellular compartments in tendon morphogenesis: collagen fibril, bundle, and macroaggregate formation. J Cell Biol 103, 231–40.

Bozec, L., van der Heijden, G., Horton, M., 2007. Collagen fibrils: nanoscale ropes. Biophys J 92, 70–5.

Canty, E.G., Kadler, K.E., 2002. Collagen fibril biosynthesis in tendon: a review and recent insights. Comp Biochem Physiol A Mol Integr Physiol 133, 979–85.

Canty, E.G., Lu, Y., Meadows, R.S., Shaw, M.K., Holmes, D.F., Kadler, K.E., 2004. Coalignment of plasma membrane channels and protrusions (fibripositors) specifies

the parallelism of tendon. J Cell Biol 165, 553–63.

Capaldi, M.J., Chapman, J.A., 1982. The c-terminal extrahelical peptide of type i collagen and its role in fibrillogenesis in vitro. Biopolymers 21, 2291–313.

Carlson, M.A., 1997. Acute wound failure. Surg Clin North Am 77, 607–36.

Chan, T.K., Ho, C.O., Lee, W.K., Fung, Y.K., Law, Y.F., Tsang, C.Y., 2006. Functional outcome of the hand following flexor tendon repair at the 'no man's land'. J Orthop Surg (Hong Kong) 14, 178–83.

Chen, C.J., Kono, H., Golenbock, D., Reed, G., Akira, S., Rock, K.L., 2007. Identification of a key pathway required for the sterile inflammatory response triggered by dying cells. Nat Med 13, 851–6.

Chiquet, M., Renedo, A.S., Huber, F., Flück, M., 2003. How do fibroblasts translate mechanical signals into changes in extracellular matrix production? Matrix Biol 22, 73–80.

Couppé, C., Kongsgaard, M., Aagaard, P., Hansen, P., Bojsen-Moller, J., Kjaer, M., Magnusson, S.P., 2008. Habitual loading results in tendon hypertrophy and increased stiffness of the human patellar tendon. J Appl Physiol 105, 805–10.

Danial, N.N., Korsmeyer, S.J., 2004. Cell death: critical control points. Cell 116, 205–19.

Danielson, K.G., Baribault, H., Holmes, D.F., Graham, H., Kadler, K.E., Iozzo, R.V., 1997. Targeted disruption of decorin leads to abnormal collagen fibril morphology and skin fragility. J Cell Biol 136, 729–43.

Declercq, W., Vanden Berghe, T., Vandenabeele, P., 2009. Rip kinases at the crossroads of cell death and survival. Cell 138, 229–32.

Degterev, A., Hitomi, J., Germscheid, M., Ch'en, I.L., Korkina, O., Teng, X., Abbott, D., Cuny, G.D., Yuan, C., Wagner, G., Hedrick, S.M., Gerber, S.A., Lugovskoy, A., Yuan, J., 2008. Identification of rip1 kinase as a specific cellular target of necrostatins. Nat Chem Biol 4, 313–21.

Degterev, A., Huang, Z., Boyce, M., Li, Y., Jagtap, P., Mizushima, N., Cuny, G.D., Mitchison, T.J., Moskowitz, M.A., Yuan, J., 2005. Chemical inhibitor of nonapoptotic cell death with therapeutic potential for ischemic brain injury. Nat Chem Biol 1, 112–9.

Degterev, A., Yuan, J., 2008. Expansion and evolution of cell death programmes. Nat Rev Mol Cell Biol 9, 378–90.

Dennis, Jr, G., Sherman, B.T., Hosack, D.A., Yang, J., Gao, W., Lane, H.C., Lempicki, R.A., 2003. David: Database for annotation, visualization, and integrated discovery. Genome Biol 4, P3.

Dines, J.S., Weber, L., Razzano, P., Prajapati, R., Timmer, M., Bowman, S., Bonasser, L., Dines, D.M., Grande, D.P., 2007. The effect of growth differentiation factor-5-coated sutures on tendon repair in a rat model. J Shoulder Elbow Surg 16, S215–21.

Doyle, B.B., Hukins, D.W., Hulmes, D.J., Miller, A., Rattew, C.J., Woodhead-Galloway, J., 1974. Origins and implications of the d stagger in collagen. Biochem Biophys Res Commun 60, 858–64.

Dubay, D.A., Franz, M.G., 2003. Acute wound healing: the biology of acute wound failure. Surg Clin North Am 83, 463–81.

Egerbacher, M., Arnoczky, S.P., Caballero, O., Lavagnino, M., Gardner, K.L., 2008. Loss of homeostatic tension induces apoptosis in tendon cells: an in vitro study. Clin Orthop Relat Res 466, 1562–8.

Engel, J., Prockop, D.J., 1991. The zipper-like folding of collagen triple helices and the effects of mutations that disrupt the zipper. Annu Rev Biophys Biophys Chem 20, 137–52.

Even-Ram, S., Yamada, K.M., 2005. Cell migration in 3d matrix. Curr Opin Cell Biol 17, 524–32.

Fiala, J.C., 2005. Reconstruct: a free editor for serial section microscopy. J Microsc 218, 52–61.

Friedl, P., Wolf, K., 2010. Plasticity of cell migration: a multiscale tuning model. J Cell Biol 188, 11–9.

Gemmill, J.F., 1906. Notes on (a) the origin of elastic fibres in tendon; (b) branching of young tendon cells. J Anat Physiol 40, 396–9.

Green, D.R., 2005. Apoptotic pathways: ten minutes to dead. Cell 121, 671–4.

Green, D.R., Kroemer, G., 2005. Pharmacological manipulation of cell death: clinical applications in sight? J Clin Invest 115, 2610–7.

Gurtner, G.C., Werner, S., Barrandon, Y., Longaker, M.T., 2008. Wound repair and regeneration. Nature 453, 314–21.

Hadjipanayi, E., Mudera, V., Brown, R.A., 2009. Guiding cell migration in 3d: a collagen matrix with graded directional stiffness. Cell Motil Cytoskeleton 66, 121–8.

Hatanaka, H., Manske, P.R., 2000. Effect of suture size on locking and grasping flexor tendon repair techniques. Clin Orthop Relat Res , 267–74.

Hitomi, J., Christofferson, D.E., Ng, A., Yao, J., Degterev, A., Xavier, R.J., Yuan, J., 2008. Identification of a molecular signaling network that regulates a cellular necrotic cell death pathway. Cell 135, 1311–23.

Hodson, N.W., Kielty, C.M., Sherratt, M.J., 2009. Ecm macromolecules: height-mapping and nano-mechanics using atomic force microscopy. Methods Mol Biol 522, 123–41.

Hotchkiss, R.S., Strasser, A., McDunn, J.E., Swanson, P.E., 2009. Cell death. N Engl J Med 361, 1570–83.

Howe, J.G., Crouch, J., Cooper, D., Smith, B.R., 2004. Real-time quantitative reverse transcription-pcr for cyclin d1 mrna in blood, marrow, and tissue specimens for diagnosis of mantle cell lymphoma. Clin Chem 50, 80–7.

Hulmes, D.J.S., 2002. Building collagen molecules, fibrils, and suprafibrillar structures. J Struct Biol 137, 2–10.

Hunziker, E.B., Stähli, A., 2008. Surgical suturing of articular cartilage induces osteoarthritis-like changes. Osteoarthritis Cartilage 16, 1067–73.

Jaalouk, D.E., Lammerding, J., 2009. Mechanotransduction gone awry. Nat Rev Mol Cell Biol 10, 63–73.

Kadler, K., 1995. Extracellular matrix 1: Fibril-forming collagens. Protein Profile 2, 491–619.

Kadler, K.E., Hojima, Y., Prockop, D.J., 1987. Assembly of collagen fibrils de novo by cleavage of the type i pc-collagen with procollagen c-proteinase. assay of critical concentration demonstrates that collagen self-assembly is a classical example of an entropy-driven process. J Biol Chem 262, 15696–701.

Kadler, K.E., Holmes, D.F., Trotter, J.A., Chapman, J.A., 1996. Collagen fibril formation. Biochem J 316 (Pt 1), 1–11.

Kannus, P., 2000. Structure of the tendon connective tissue. Scand J Med Sci Sports 10, 312–20.

Kielty, C.M., Sherratt, M.J., Marson, A., Baldock, C., 2005. Fibrillin microfibrils. Adv Protein Chem 70, 405–36.

Kjaer, M., Magnusson, P., Krogsgaard, M., Boysen Møller, J., Olesen, J., Heinemeier, K., Hansen, M., Haraldsson, B., Koskinen, S., Esmarck, B., Langberg, H., 2006.

Extracellular matrix adaptation of tendon and skeletal muscle to exercise. J Anat 208, 445–50.

Kleinert, H.E., Pickford, M.A., 1997. David r. boyd lecture in trauma care and emergency medical systems: upper extremity injuries–past, present, and future. J Emerg Med 15, 709–19.

Kraemer, R., Lorenzen, J., Rotter, R., Vogt, P.M., Knobloch, K., 2009. Achilles tendon suture deteriorates tendon capillary blood flow with sustained tissue oxygen saturation - an animal study. J Orthop Surg Res 4, 32.

Kroemer, G., Galluzzi, L., Vandenabeele, P., Abrams, J., Alnemri, E.S., Baehrecke, E.H., Blagosklonny, M.V., El-Deiry, W.S., Golstein, P., Green, D.R., Hengartner, M., Knight, R.A., Kumar, S., Lipton, S.A., Malorni, W., Nuñez, G., Peter, M.E., Tschopp, J., Yuan, J., Piacentini, M., Zhivotovsky, B., Melino, G., 2009. Classification of cell death: recommendations of the nomenclature committee on cell death 2009. Cell Death Differ 16, 3–11.

Leigh, D.R., Abreu, E.L., Derwin, K.A., 2008. Changes in gene expression of individual matrix metalloproteinases differ in response to mechanical unloading of tendon fascicles in explant culture. J Orthop Res 26, 1306–12.

Lock, J.G., Wehrle-Haller, B., Strömblad, S., 2008. Cell-matrix adhesion complexes: master control machinery of cell migration. Semin Cancer Biol 18, 65–76.

Matsuda, A., Yoshiki, A., Tagawa, Y., Matsuda, H., Kusakabe, M., 1999. Corneal wound healing in tenascin knockout mouse. Invest Ophthalmol Vis Sci 40, 1071–80.

McDowell, C.L., Marqueen, T.J., Yager, D., Owen, J., Wayne, J.S., 2002. Characterization of the tensile properties and histologic/biochemical changes in normal chicken tendon at the site of suture insertion. J Hand Surg Am 27, 605–14.

McNeilly, C.M., Banes, A.J., Benjamin, M., Ralphs, J.R., 1996. Tendon cells in vivo form a three dimensional network of cell processes linked by gap junctions. J Anat 189 (Pt 3), 593–600.

Miterová, L., Stokrová, J., Hulejová, H., Adam, H., 1989. Comparison of two methods for evaluation of the length of collagen molecules. Folia Morphol (Praha) 37, 228–35.

Nistor, L., 1981. Surgical and non-surgical treatment of achilles tendon rupture. a prospective randomized study. J Bone Joint Surg Am 63, 394–9.

Parry, D.A., Barnes, G.R., Craig, A.S., 1978. A comparison of the size distribution of collagen fibrils in connective tissues as a function of age and a possible relation between fibril size distribution and mechanical properties. Proc R Soc Lond B Biol Sci 203, 305–21.

Pasternak, B., Missios, A., Askendal, A., Tengvall, P., Aspenberg, P., 2007. Doxycycline-coated sutures improve the suture-holding capacity of the rat achilles tendon. Acta Orthop 78, 680–6.

Pasternak, B., Rehn, M., Andersen, L., Agren, M.S., Heegaard, A.M., Tengvall, P., Aspenberg, P., 2008. Doxycycline-coated sutures improve mechanical strength of intestinal anastomoses. Int J Colorectal Dis 23, 271–6.

Prockop, D.J., Kivirikko, K.I., 1995. Collagens: molecular biology, diseases, and potentials for therapy. Annu Rev Biochem 64, 403–34.

al Qattan, M.M., Posnick, J.C., Lin, K.Y., 1995. The in vivo response of foetal tendons to sutures. J Hand Surg Br 20, 314–8.

Quackenbush, J., 2001. Computational analysis of microarray data. Nat Rev Genet 2, 418–27.

Ralphs, J.R., 2002. Cell biology of tendons. European Cells and Materials 4, 39–40.

Richardson, S., Alyouha, S., Van Agtmael, T., Yeung, C., Zeef, L., Lu, Y., Ormston, V., Wong, J., McGrouther, D., Kadler, K., 2010. Epithelial layer may have a protective role in tendon.

Richardson, S.H., Starborg, T., Lu, Y., Humphries, S.M., Meadows, R.S., Kadler, K.E., 2007. Tendon development requires regulation of cell condensation and cell shape via cadherin-11-mediated cell-cell junctions. Mol Cell Biol 27, 6218–28.

Riley, G., 2004. The pathogenesis of tendinopathy. a molecular perspective. Rheumatology (Oxford) 43, 131–42.

Ritty, T.M., Ditsios, K., Starcher, B.C., 2002. Distribution of the elastic fiber and associated proteins in flexor tendon reflects function. Anat Rec 268, 430–40.

Ritty, T.M., Roth, R., Heuser, J.E., 2003. Tendon cell array isolation reveals a previously unknown fibrillin-2-containing macromolecular assembly. Structure 11, 1179–88.

Robinson, P.S., Huang, T.F., Kazam, E., Iozzo, R.V., Birk, D.E., Soslowsky, L.J., 2005. Influence of decorin and biglycan on mechanical properties of multiple tendons in knockout mice. J Biomech Eng 127, 181–5.

Rowe, R.W., 1985. The structure of rat tail tendon. Connect Tissue Res 14, 9–20.

Schmidt, S., Friedl, P., 2010. Interstitial cell migration: integrin-dependent and alternative adhesion mechanisms. Cell Tissue Res 339, 83–92.

Scott, J.E., 2003. Elasticity in extracellular matrix 'shape modules' of tendon, cartilage, etc. a sliding proteoglycan-filament model. J Physiol 553, 335–43.

Storey, J.D., Tibshirani, R., 2003. Statistical significance for genomewide studies. Proc Natl Acad Sci U S A 100, 9440–5.

Sun, Y., Weber, K.T., 2000. Infarct scar: a dynamic tissue. Cardiovasc Res 46, 250–6.

Tang, J.B., Xu, Y., Ding, F., Wang, X.T., 2004. Expression of genes for collagen production and nf-kappab gene activation of in vivo healing flexor tendons. J Hand Surg Am 29, 564–70.

Tsuzaki, M., Yamauchi, M., Banes, A.J., 1993. Tendon collagens: extracellular matrix composition in shear stress and tensile components of flexor tendons. Connect Tissue Res 29, 141–52.

Valentijn, A.J., Metcalfe, A.D., Kott, J., Streuli, C.H., Gilmore, A.P., 2003. Spatial and temporal changes in bax subcellular localization during anoikis. J Cell Biol 162, 599–612.

Vogel, K.G., Ordög, A., Pogány, G., Oláh, J., 1993. Proteoglycans in the compressed region of human tibialis posterior tendon and in ligaments. J Orthop Res 11, 68–77.

Waggett, A.D., Benjamin, M., Ralphs, J.R., 2006. Connexin 32 and 43 gap junctions differentially modulate tenocyte response to cyclic mechanical load. Eur J Cell Biol 85, 1145–54.

Wall, M.E., Banes, A.J., 2005. Early responses to mechanical load in tendon: role for calcium signaling, gap junctions and intercellular communication. J Musculoskelet Neuronal Interact 5, 70–84.

Winters, S.C., Gelberman, R.H., Woo, S.L., Chan, S.S., Grewal, R., Seiler, 3rd, J.G., 1998. The effects of multiple-strand suture methods on the strength and excursion of repaired intrasynovial flexor tendons: a biomechanical study in dogs. J Hand Surg Am 23, 97–104.

Wong, J., Bennett, W., Ferguson, M.W.J., McGrouther, D.A., 2006a. Microscopic and histological examination of the mouse hindpaw digit and flexor tendon arrangement with 3d reconstruction. J Anat 209, 533–45.

Wong, J.K.F., Alyouha, S., Kadler, K.E., Ferguson, M.W.J., McGrouther, D.A., 2010.

The cell biology of suturing tendons. Matrix Biol .

Wong, J.K.F., Cerovac, S., Ferguson, M.W.J., McGrouther, D.A., 2006b. The cellular effect of a single interrupted suture on tendon. J Hand Surg Br 31, 358–67.

Wynn, T.A., 2007. Common and unique mechanisms regulate fibrosis in various fibroproliferative diseases. J Clin Invest 117, 524–9.

Wynn, T.A., 2008. Cellular and molecular mechanisms of fibrosis. J Pathol 214, 199–210.

Yao, J., Korotkova, T., Riboh, J., Chong, A., Chang, J., Smith, R.L., 2008. Bioactive sutures for tendon repair: assessment of a method of delivering pluripotential embryonic cells. J Hand Surg Am 33, 1558–64.

Zlowodzki, M., 2010. Flexor tendon injuries. Presentation.

Zobitz, M.E., Zhao, C., Amadio, P.C., An, K.N., 2000. Comparison of mechanical properties of various suture repair techniques in a partially lacerated tendon. J Biomech Eng 122, 604–7.

Appendices

Matrix Biology xxx (2010) xxx–xxx

Contents lists available at ScienceDirect

Matrix Biology

journal homepage: www.elsevier.com/locate/matbio

The cell biology of suturing tendons

J.K.F. Wong [a,*], S. Alyouha [a], K.E. Kadler [b], M.W.J. Ferguson [c], D.A. McGrouther [d]

[a] Plastic Surgery Research, University of Manchester, Stopford Building, Oxford Road, Manchester, M13 9PT, United Kingdom
[b] Wellcome Trust Centre for Cell-Matrix Research, Faculty of Life Sciences, Michael Smith Building, University of Manchester, Oxford Road, Manchester, M13 9PT, United Kingdom
[c] Faculty of Life Sciences, University of Manchester, Stopford Building, Oxford Road, Manchester, M13 9PT and Renovo Plc. The Manchester Incubator Building, 48 Grafton Street, Manchester, M13 9XX, United Kingdom
[d] Plastic Surgery Research, University of Manchester, Stopford Building, Oxford Road, Manchester, M13 9PT, United Kingdom

ARTICLE INFO

Article history:
Received 5 April 2010
Received in revised form 14 June 2010
Accepted 15 June 2010
Available online xxxx

Keywords:
Tendon
Mouse
Trauma
Suture
Inflammation
Necrosis

ABSTRACT

Trauma by suturing tendon form areas devoid of cells termed “acellular zones” in the matrix. This study aimed to characterise the cellular insult of suturing and acellular zone formation in mouse tendon. Acellular zone formation was evaluated using single grasping sutures placed using flexor tendons with time lapse cell viability imaging for a period of 12 h. Both tension and injury were required to induce cell death and cell movement in the formation of the acellular zone. DNA fragmentation studies and transmission electron microscopy indicated that cells necrosed.

Parallel *in vivo* studies showed that cell-to-cell contacts were disrupted following grasping by the suture in tensioned tendon. Without tension, cell death was lessened and cell-to-cell contacts remained intact. Quantitative immunohistochemistry and 3D cellular profile mapping of wound healing markers over a one year time course showed that acellular zones arise rapidly and showed no evidence of healing whilst the wound healing response occurred in the surrounding tissues. The acellular zones were also evident in a standard modified “Kessler” clinical repair. In conclusion, the suture repair of injured tendons produces acellular zones, which may potentially cause early tendon failure.

1. Introduction

Suturing of organised tissues plays a day-to-day role in repairing damaged structures in a surgeon's armamentarium. However the cellular trauma of suturing has never really been investigated. Suturing involves a number of mechanical insults on tissues and their cells. Suturing is initiated through the insertion of the sharp needle end that can be either a cutting or piercing injury. The cellular insult following this is small resulting in localised injury where the needle and suture pass through the tissue. The second insult is from the tying of the suture and applying a compressive force to the matrix and cells. This insult we have shown in the past to form an “acellular zone” (Wong et al., 2006). Finally the third insult arises from the persistence of a suture as a foreign material and how the systemic processes *in vivo* react to the retained material. Tendon lends itself well to the investigation of suture biology as it is a relatively homogeneous tissue with few specialised cell populations, hence local and systemic cellular responses can be observed with relative ease (Kajikawa et al., 2007). Furthermore it is a tissue with limited vasculature and hence less prone to ischemia and also has a well organised cellular network that allows cells to interact with each other via gap junctions (Ralphs, Waggett et al., 2002). Most importantly it is a tissue that is prone to traumatic insult either through lacerations e.g. in hand trauma (Elliot, 2002), or through rupture from sporting injuries (Ljungqvist, Schwellnus et al., 2008) with considerable financial implications to both healthcare provision and the manual workforce. With either of these major clinical problems the mainstay of treatment is surgical suture repair. In the process of searching for the ideal suture repair technique numerous novel methods have been devised to unite cut tendon ends. These techniques have often been developed on cadaveric human or animal models and assessed via biomechanical means such as testing load to failure, gliding excursion and gap formation (reviewed by Strickland, 2000). In the last decade there has been a trend to increase the number of core strands (Savage, 1985; Strickland, 2000), and the calibre of the suture used in repair (Taras, Raphael et al., 2001). Locking sutures as opposed to grasping methods have been incorporated into the core suture (Hotokezaka and Manske, 1997; Pennington, 1979) and supplemental epitendinous suture with interlocking properties have also been favoured in *ex vivo* studies (Dona, Turner et al., 2003). All of these repairs have the primary emphasis of adding tensile strength (Thurman, Trumble et al., 1998) and minimising gap formation (Gelberman, Boyer et al., 1999) in the repair but lead to increasing amounts of suture material being placed

Abbreviations: ST, Subcutaneous tissue.

* Corresponding author. Room 3.60 Stopford Building, Plastic Surgery Research, University of Manchester, Oxford Road, Manchester, UK. Tel.: +44 161 275 5076; fax: +44 161 275 1591.
E-mail address: jason.k.wong@manchester.ac.uk (J.K.F. Wong).

0945-053X/$ – see front matter © 2010 Elsevier B.V. All rights reserved.
doi:10.1016/j.matbio.2010.06.002

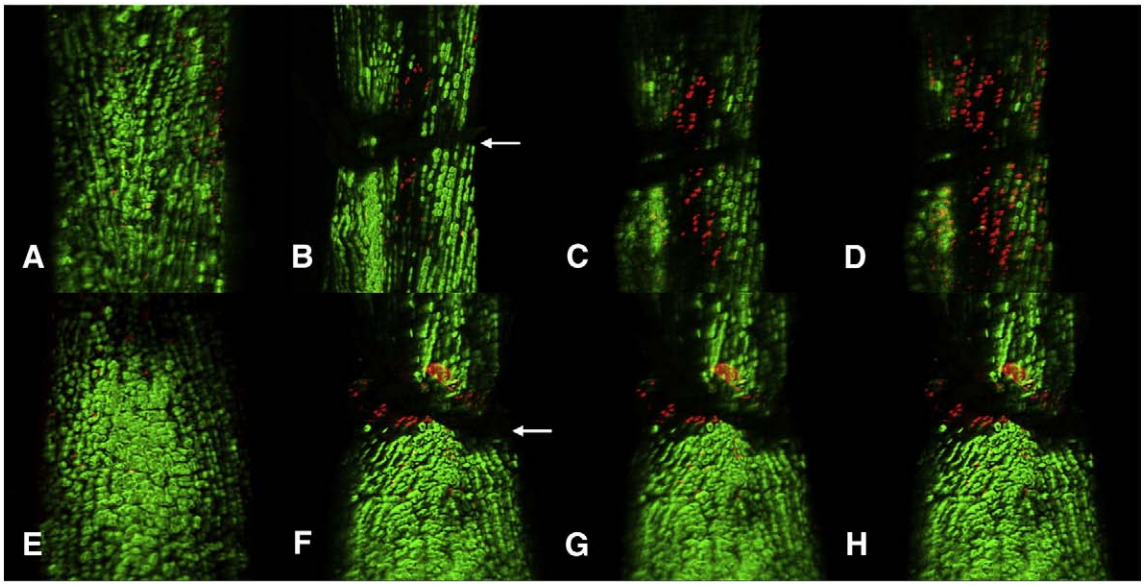

Fig. 1. Live/dead assay time lapse confocal microscopy of sutured tendon. Tendon is placed under tension (A, B, C and D) or without tension (E, F, G and H). Imaging of tendon before suturing (A and E). Images taken 30 min after suture (B and F), 6 h following injury (C and G), and 12 h following injury (D and H). Note formation of an acellular zone within 30 min of suturing tendon under tension and propagation of cell death over time compared to un-tensioned sutured tendon.

in the tendon substance. The cellular reaction to these multi-stranded techniques is not clear.

Importantly, scientific evidence to demonstrate the damage a surgeon can inflict from even the most trivial surgical procedures, such as a single suture, must be clarified. The possibility that our practice is negatively impacting on tissue biology has fundamental implications to all surgical procedures involving the suturing of tissue. The present study aims to investigate the formation of the acellular zone and the role of cell death in its formation. To understand the mechanisms of acellular formation, we used a combination of surgical manipulation in an explant live/dead time lapse culture system, transmission electron microscopy, *in vivo* immunohistochemical staining, and DNA fragmentation gel analysis. A time course study was performed over one year in a murine model to elucidate the fate of the acellular zone. Furthermore a modified Kessler repair was performed in mouse Achilles tendon to assess the distribution of acellular zones in a clinically relevant repair.

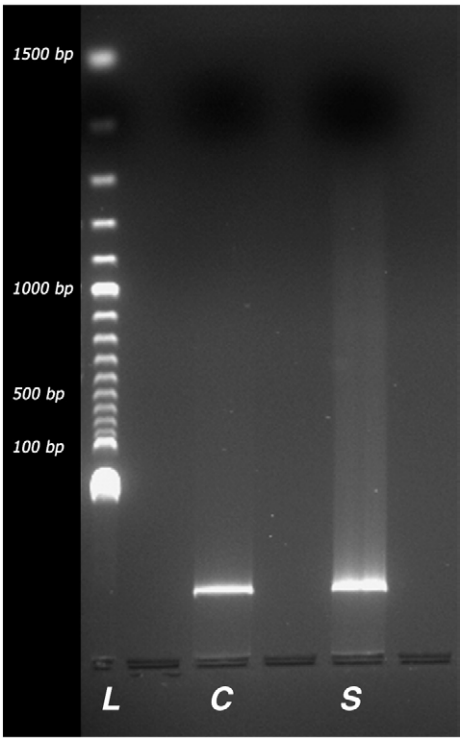

Fig. 2. DNA integrity gel analysis. L. DNA ladder at 100 bp intervals. C. Control unwounded tendon (n = 6). S. Suture wounded tendon (n = 6). Note; gel shows a nuclear smear and no evidence of 180 bp laddering associated with apoptosis.

2. Results

2.1. Role of tension in acellular zone formation

Control tendons placed in live/dead solution containing ethidium homodimer and calcien AM without tension were found to maintain a predominantly green cell fluorescence indicating these cells remained viable for the 12 h duration (data not shown). Unwounded tendon placed under tension showed some cell death at the anchored ends of the tendon but in the centre of the tendon explants, the cells remained

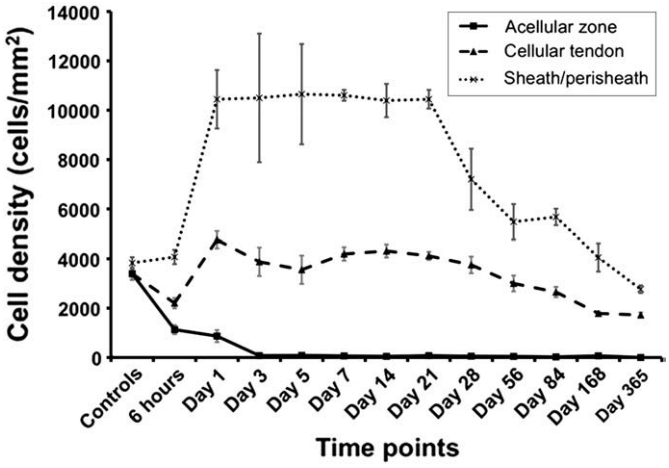

Fig. 3. Temporal cellular density changes following suture insertion. Cells were quantified in the acellular zone, cellular tendon, and sheath/perisheath (a.k.a. subcutaneous tissue) in order to calculate the mean number of cells per mm^2 at different time points. Within 6 h of suture there were significant changes in the cellularity of the sheath and the tendon that persisted for 1 year ($p = 0.039$) indicated by an asterisk. Error bars denote standard error of mean.

Please cite this article as: Wong, J.K.F., et al., The cell biology of suturing tendons, Matrix Biology (2010), doi:10.1016/j.matbio.2010.06.002

green for the duration of the time lapse capture. Tendons sutured with a 50% grasping suture with applied tension demonstrated an area of acellularity (Fig. 1) and there was an area of progressive cell death immediately around the suture. Tendons sutured with a 50% grasping suture, not under tension, showed some dead cells around the suture grasp but no formation of an acellular zone. Cell death was significantly greater in tendon sutured under tension ($p<0.05$). DNA integrity analysis showed a typical DNA smear suggesting that there had been cell necrosis, whereas laddering associated with the process of apoptosis was absent (Fig. 2).

2.2. In vivo cell biology of the fate of the acellular zone

2.2.1. Formation and persistence of the acellular zone

Following suturing tendon, the acellular zone formed rapidly and persisted for one year with no evidence of cellular repopulation of the matrix. Six hours after suturing of tendon, cells were present within the area of the tendon grasped by suture. Evidence of an acellular zone formation could be seen at 6 h but the acellular zone was not fully defined until 24 h following injury. The surrounding tissues became increasingly cellular and with peak cellularity at 24 h and persisted for 21 days. Tendon cellularity initially dropped at 6 h following suture insertion, and then the cellularity of the tendon remained elevated for up to 84 days (Fig. 3).

2.2.2. Ultrastructural changes of the cells in the acellular zone following suture

Cell morphology in unsutured tendon showed long thin elongated nuclei that have long cytoplasmic processes, which allowed contact with neighboring cells (Fig. 4-A). Following insertion of the suture, the cells became swollen and rounder in morphology (Fig. 4-B). Clumps of chromatin could be seen in the nuclei and the cells separated as the cytoplasm swelled (Fig. 4-C). After 24 h there was loss of plasma membrane integrity and nuclear fragmentation as the cells necrosed.

2.2.3. Apoptosis of surrounding cells

Evidence of apoptotic markers, Bax, Bcl-2, caspase 3, and cytochrome C was not observed in the tendon 6 h following suture or at a subsequent

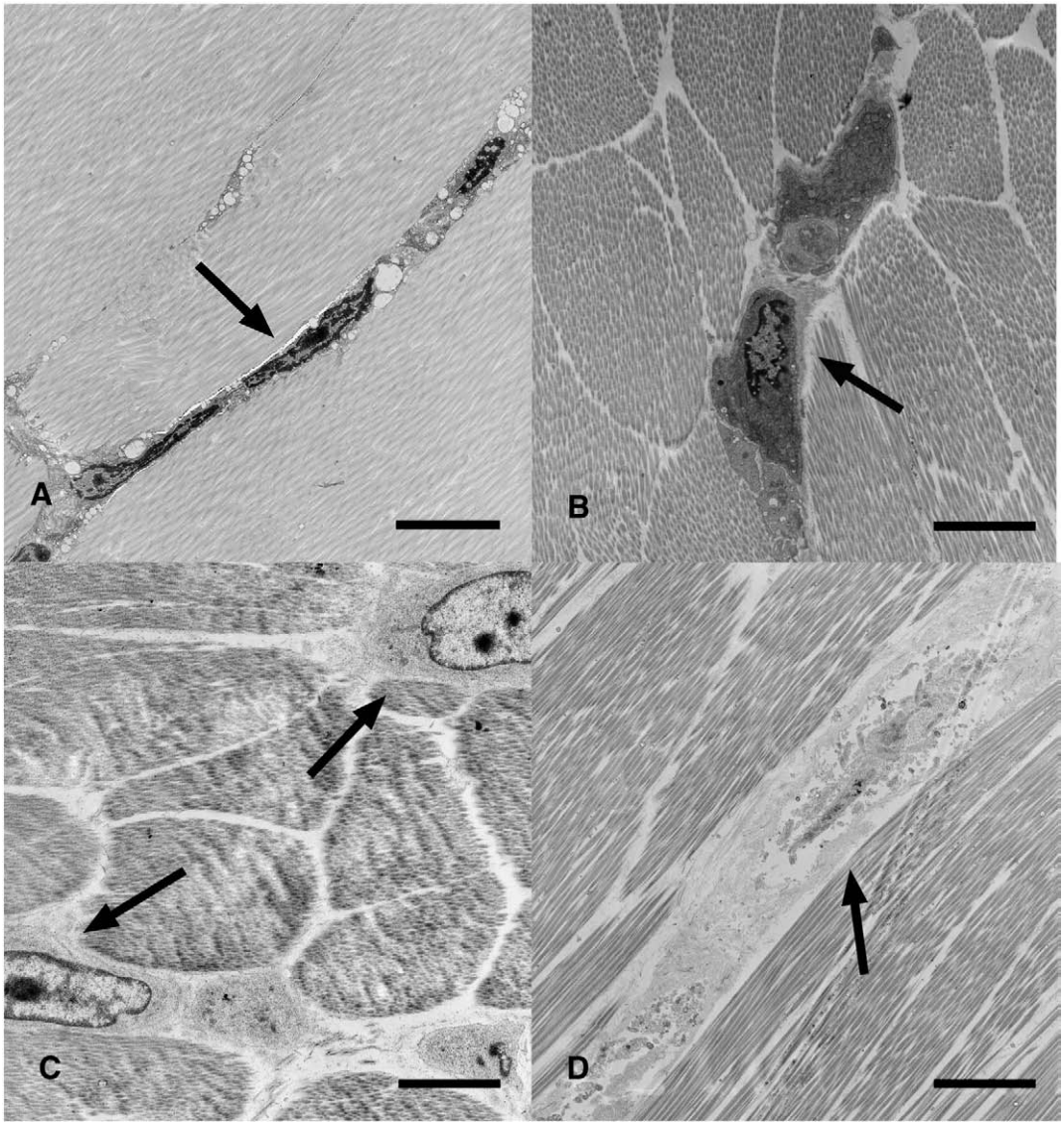

Fig. 4. Electron micrographs of tenocytes in situ A. Tenocytes in unwounded flexor tendon show thin elongated nuclei and cytoplasmic membranes in contact with (arrow) neighbouring cells. B. Tenocytes fixed immediately following grasping by suture. Cells are rounder in cross-section (arrow) than those in unwounded tendon and cell contacts less obvious. C. tenocytes 3 h following grasping suture. Cell processes are lost between cells and chromatin condensation can be seen in nucleus (arrows). D. Tenocytes 24 h after suture grasp. Fragmentation of nuclei, breakdown of cells and absence of plasma membrane (arrow) is most evident. Scale bar represents 5 μm.

Please cite this article as: Wong, J.K.F., et al., The cell biology of suturing tendons, Matrix Biology (2010), doi:10.1016/j.matbio.2010.06.002

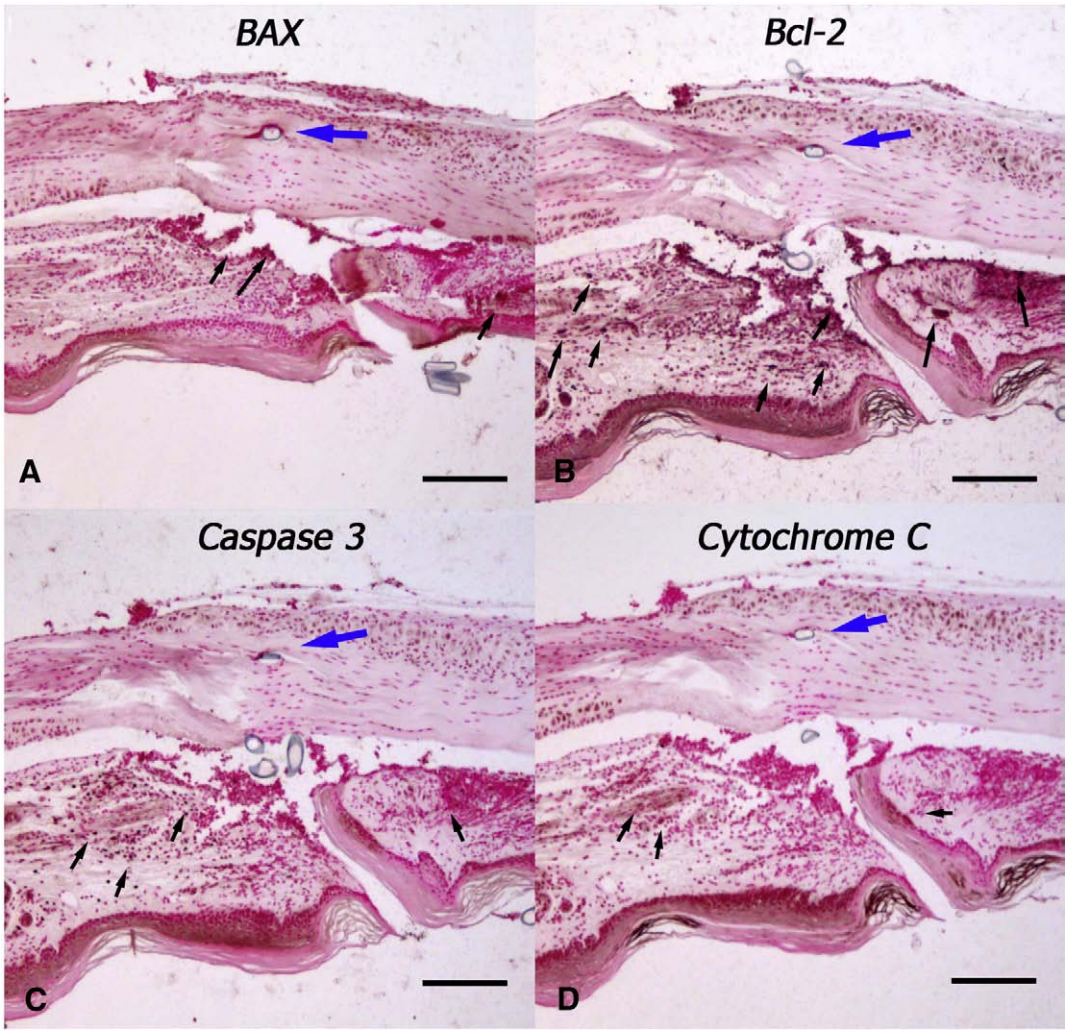

Fig. 5. Cellular staining for apoptotic markers in sutured tendon harvested at 6 h post injury. A. Bax, B. Bcl 2, C. Caspase 3, D. Cytochrome C. Suture is indicated by the blue arrow. Small black arrows indicate areas of antibody expression. Scale bar represents 200 μm.

seven day and six month time points, however expression of these markers was evident in the subcutaneous tissues (ST) (Fig. 5).

2.2.4. Disruption of cytoskeleton with cells under tensional load

TRITC-Phalloidin staining for F actin was not evident in the acellular zone at any of the time points, indicating that disruption of the actin cytoskeleton network had occurred in the tendon cells that had been sutured under tension (Fig. 6-C). The abolition of tension through proximal tenotomy prevented the acellular zone from forming and cells appeared to maintain close proximity in rows (Fig. 6-D).

2.2.5. Persistence of inflammation following suture

In the early phases of healing, CD45 and Ly6G were typically elevated in response to tissue injury (Fig. 7) but few inflammatory cells were seen to infiltrate the tendon tissue. The inflammatory cell reaction persisted for 14 days at a significantly elevated level compared with controls ($p<0.05$). Staining for markers of proliferation, synthesis, myofibroblast/pericytes, apoptosis and inflammation showed that most of the cellular activity occurred around the suture in the surrounding subcutaneous tissue (ST) (Fig. 8). 3D cellular mapping demonstrated that the vast majority of CD45 expressing cells co-expressed for neutrophil marker, Ly6G, at the early time points. CD45 expression persisted diffusely in the ST whereas Ly6G expression appeared to be localised around the suture forming a cuff of cells (Fig. 9). Mast cells stained with toludine blue were present in the dermis at 6 h post wounding but were then reduced in number for 28 days. Expression of F4/80 was generally low with peak expression occurring at day 3 and confined to the ST. Hsp 47 and BrdU staining also increased at day 3 in fibroblasts around the zone of injury. This expression was mainly confined to the ST (Fig. 10) and around the tissues situated dorsally and apposed to bone i.e. the vinculum. Peak levels of Hsp47 and BrdU labeling occurred between days 7 and 14. The epidermis was a notable site for BrdU staining and TUNEL staining. Peak staining of TUNEL was seen at day 7 mainly confined to the subcutaneous tissues and some areas of the tendon. There was a gradual decline in BrdU and TUNEL staining after 21 days and HSP 47 activity in the tissues dropped to baseline levels after 28 days. The expression of α-SMA declined slightly after cutting the subcutaneous tissues but then showed increasing expression by days 7 to 14 that slowly reduced to baseline levels over the course of the year (Fig. 8C).

2.3. Kessler repair model

Acellular zones could be seen to form in the grasping regions of the modified Kessler repair. Three dimensional reconstructions of this shows the acellularity was more extensive forming at all four grasping corners of the Kessler repair and along the axis of the core sutures (Fig. 7). Notably the area of tendon under greatest strain was outwith the suture repair, distally and proximally, highlighted by the acellularity

Please cite this article as: Wong, J.K.F., et al., The cell biology of suturing tendons, Matrix Biology (2010), doi:10.1016/j.matbio.2010.06.002

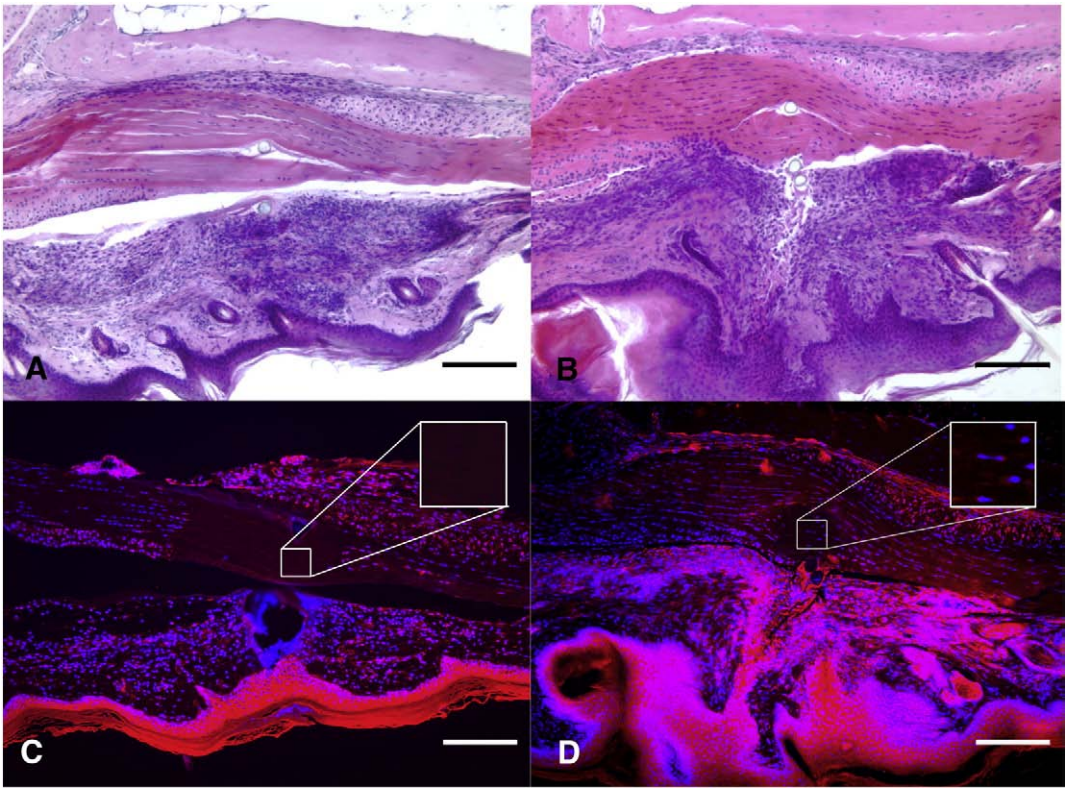

Fig. 6. Representative images of tendon 24 h after suture *in vivo*. Haematoxylin and Eosin staining (A and B) and Hoescht (Blue) and TRITC phalloidin (red) (C and D). A. Mouse FDP tendon sutured under standard physiological tension with acellular zone formation. B. Tendon sutured with tension abolished by proximal tenotomy with no acellular zone formation. C. Loss of actin staining in the acellular zone following grasping suture under tension. D. Actin staining and no acellular zone formation in tendon with tension abolished through proximal tenotomy. Scale bar represents 200 μm. (For interpretation of the references to colour in this figure legend, the reader is referred to the web of this article.)

of the matrix, whereas the tendon within the boundaries of the repair were more cellular and presumably under less strain.

3. Discussion

The primary suture repair of tendon can be dated back to Galen who later condemned the practice in his scriptures, *Ars Parva* (Manske, 2004). Subsequent surgery on tendon was revived by the work of Arab surgeons Rhazes, Avicenna and Abulcasis in tenth century A.D. (Kleinert, Spokevicius et al. 1995). Today, the primary repair of divided tendon ends in the acute clinical setting is common practice but it is unclear what effects suturing has on the cell biology of tendon. Our study showed that the grasping component of the suture forms acellular zones in flexor and Achilles tendons, whether this relates to a simple grasping suture or modified Kessler repair. This is a phenomenon that occurs in both intrasynovial and extrasynovial tendon hence is likely to arise in many clinical situations. Modifications of the Kessler repair are currently the most utilised repair method in the Western world (Tang, 2006) and performed on both hand flexor tendon lacerations and Achilles tendon ruptures. The validation of many tendon repair surgical techniques currently used in clinical practice is performed in cadaveric tissue but some studies have suggested tendon weakens after suture repair in living tissue (McDowell, Marqueen et al., 2002). Silva et al. had shown in canine flexor tendon insertion site injuries that the suturing of tendon resulted in significant softening of the tendon ends, resulting in a 45% drop in tensile strength at 10 days and 21 days following suture (Silva, Boyer et al., 2002). This highlights the importance of conducting studies on suture methodology on *in vivo* models, whereby the effect of inflammation and local cell damage can be considered.

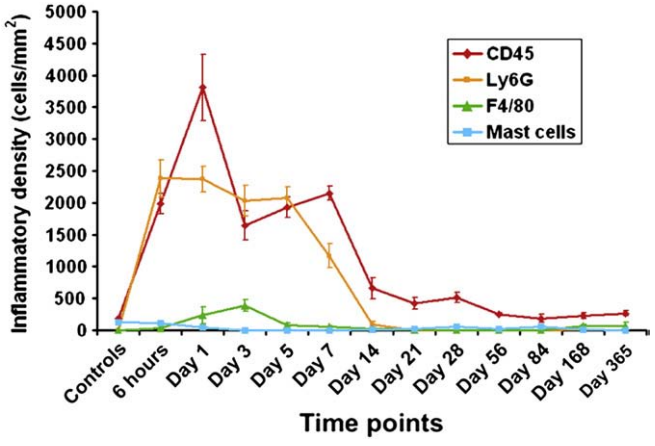

Fig. 7. Temporal inflammatory cell activity changes following suture insertion. Cell labeling of CD45, ly6G, F4/80 and mast cells was performed. There is an increase in CD45 and Ly6G+ve cells in the subcutaneous tissues that persist for 14 days. Error bars denote standard error of mean.

The present study has shown that a zone of acellularity begins to form within hours of suturing the tendon and that tension through the tendon is required for its formation. Furthermore due to mechanical traction, the tenocytes move out of the zone of grasp as their intercellular cytoplasmic contacts appeared to be disrupted. Studies have shown that tenocytes slide in rows, between tendon fascicles (Screen, Lee et al. 2003). The loss of cell-to-cell contacts through mechanical forces suggests cells are retracted away from the zone of injury, as opposed to migrating. Cell retraction is associated with rapid F actin reorganization, mediated by Rho kinase (Groeger and Nobes, 2007), and dephosphorylation of focal adhesion proteins (O'Brien, Kinch et al. 1997). The rapid cell retraction of tendon fibroblasts

Please cite this article as: Wong, J.K.F., et al., The cell biology of suturing tendons, Matrix Biology (2010), doi:10.1016/j.matbio.2010.06.002

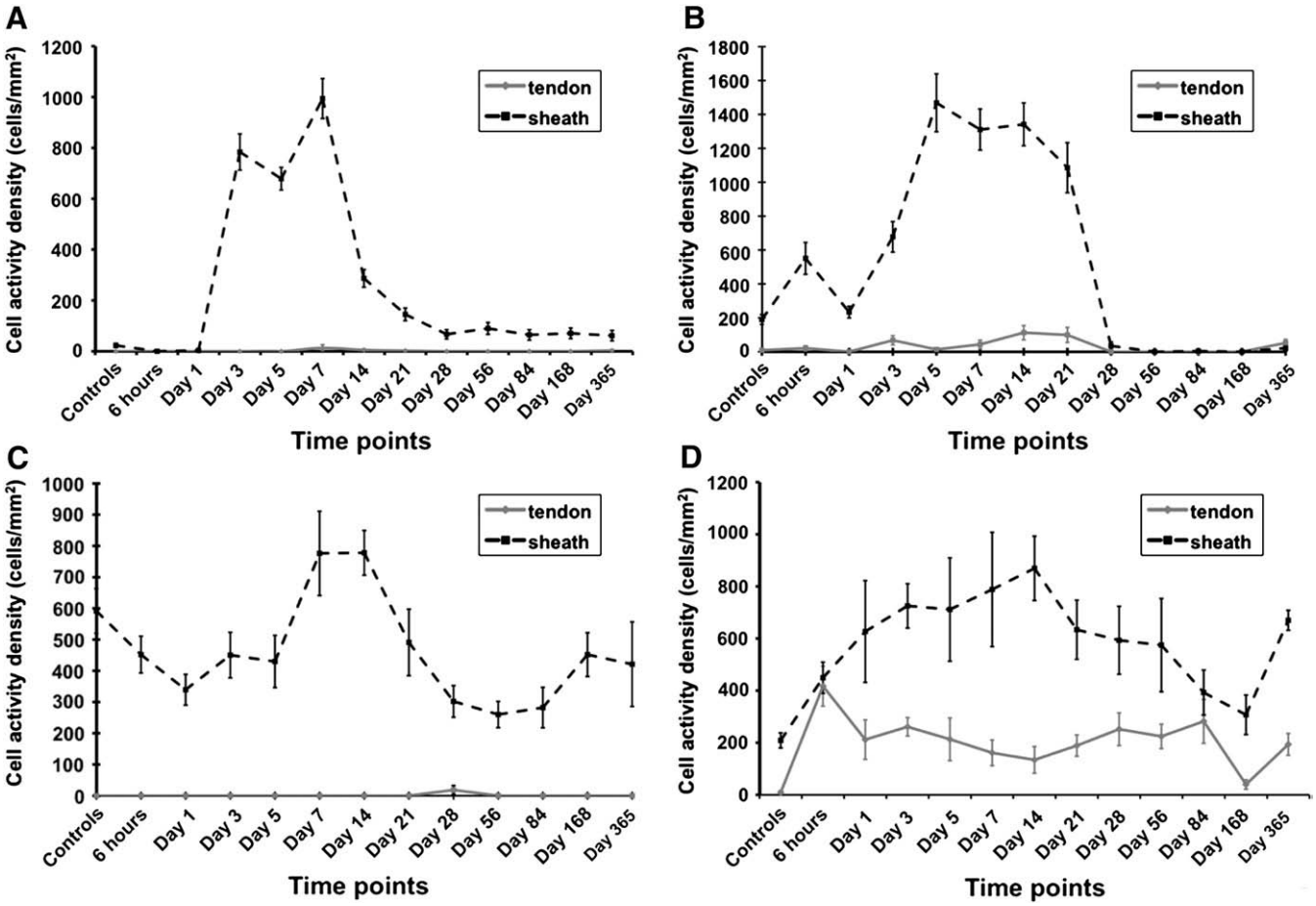

Fig. 8. Temporal cellular activity changes following suture insertion. The grey lined graph represents changes in the tendon and the dotted lined graph represents changes in subcutaneous tissues (ST). A. Cell proliferation (BrdU). B. Type 1 collagen synthesis (Hsp 47). C. Vascularisation and myofibroblast expression (α-SMA). D. Apoptosis/necrosis (TUNEL). Changes in activity of BrdU, Hsp 47 and α-SMA occur mainly in the ST, whereas apoptosis occurs in both the tendon and ST. Error bars denote standard error of mean.

following suture may limit the degree of damage to the neighboring cells. McNeilly et al. previously had shown that the cells connect through 3D cellular networks linked together by gap junctions that were likely to communicate mechanical loads and stresses to neighboring cells (McNeilly, Banes et al. 1996). Preservation of these cell-to-cell contacts would seem important for normal tendon homeostasis. Numerous studies have shown that connexin 43 and gap junctions have an important role in cell signaling between cells in the tendon matrix (McNeilly et al., 1996; Ralphs et al., 2002). In rat glioma cell populations these hemichannels in conjunction with their gap junction counterparts have been shown to propagate cyto c mediated cell death to neighboring cells (Decrock, De Vuyst et al. 2009). There is notable cell death associated with suturing a tendon but there was little to suggest that this was due to recognized apoptotic pathways such as those related to Bax, Caspase 3 and Cytochrome C. Our results indicate that the local cell death was characteristic of necrosis in the absence of the classic laddering associated with apoptosis (Tilly and Hsueh, 1993). Previously we have shown that this segment of the tendon in the mouse is avascular (Wong, Bennett et al. 2006) which would tend to indicate that ischemia appears unlikely to contribute to acellular zone formation.

The ultrastructural changes including loss of cell-to-cell contacts, cytoplasmic swelling, chromatin condensation in the nuclei, followed by loss of plasma membrane integrity and nuclear disruption, occurred rapidly and are hallmarks of cellular necrosis (Krysko, Vanden Berghe et al. 2008). The rate at which the acellular zone forms in time lapse and *in vivo* studies in conjunction with tension suggests the cells move out of the zone of injury through cell retraction, in addition to cellular necrosis. Through the loss of cell-to-cell contacts immediately in the acellular zone, cells lose their tension. Loss of tension to tenocytes can have dramatic effects on the surrounding matrix. The unloading of tendon fascicles leads to a greater than 400 fold increase in gene expression of interstitial collagenase (MMP 13) and stromelysin (MMP 3) within 8 h which have a role in matrix degradation (Leigh, Abreu et al. 2008). This may lead to a microenvironment favorable for cell movement. Disruption to the cellular actin cytoskeleton may provide one mechanism for this to occur. Lavagnino et al. (2005) showed that *in vitro* disruption of tendon fibroblast actin cytoskeleton by cytochalasin D, resulted in increased catabolic interstitial collagenase activity and inhibition of α1(I) collagen mRNA expression. The same effect was accomplished by alleviating mechanical tension in tendon fibroblast gels which exhibited collagenase activity within 24 h until a new homeostatic level of tension was acquired at around 14 days (Lavagnino and Arnoczky, 2005). Once the tendon fibroblasts reestablished tension *in vitro* they began to express α1(I) collagen mRNA and stopped expressing interstitial collagenase. The observed mechanical tuning of cells to their microenvironment is supported by McDowell's (2002) observations that the mechanical strength of suture repaired tendons is markedly diminished for two weeks after repair (McDowell et al., 2002). These results suggest that the cells take around two weeks to establish an internal cytoskeleton tension through interactions with the local extracellular environment. Our studies demonstrated a persistence of the acellular zones up to a year following injury which gives rise to some concern over the clinical impact of leaving sutures *in situ*.

The inflammatory insult from the single suture is present for 14 days and then gradually decreases however cells do not appear to

Please cite this article as: Wong, J.K.F., et al., The cell biology of suturing tendons, Matrix Biology (2010), doi:10.1016/j.matbio.2010.06.002

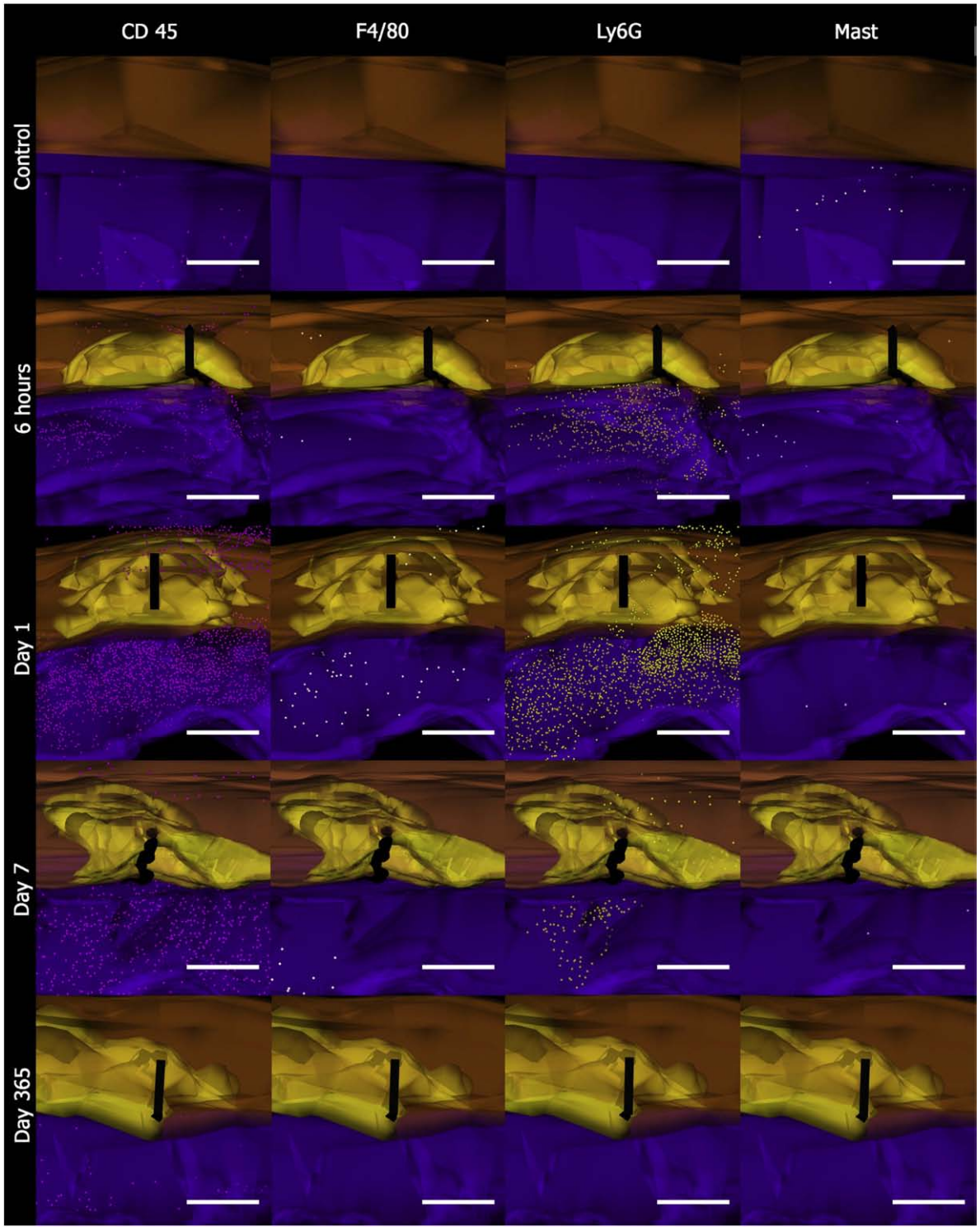

Fig. 9. 3D cellular mapping of inflammatory cell activity. Images of controls, 6 h, Day 1, Day 7, and Day 365 after suture. CD45+ve cells (pink), F480+ve cells (white), Ly6G+ve cells (yellow), Toludine blue+ve mast cells (silver). Tendon is represented in orange and subcutaneous tissue (ST) is represented in purple. The grasping suture is represented in black, and the acellular zone represented in yellow. Scale bar represents 200 μm. (For interpretation of the references to colour in this figure legend, the reader is referred to the web of this article.)

infiltrate the tendon substance. Little evidence of proliferation, synthesis, inflammation or apoptosis occurred in the tendon substance. These activities are far more evident in the surrounding sheath and ST, which followed a recognized pattern of wound healing. Using inflammatory markers we have shown that there was an early drop in the number of mast cells, which was due to injury induced degranulation seen at 6 h followed by a peak of CD45+ve and Ly6G +ve cells at 24 h following injury. This was followed by a peak in F4/80 expressing macrophages and elevated CD45 labeled cells at 3 days and persisting elevation in CD45 count but not F4/80+ve cells at day 7 in the ST. It is evident that inflammatory cell activity around the tendon persists to 14 days due to the presence of neutrophils. Archambault et al. (2002) have demonstrated in the flexicell system that rabbit fibroblasts in conjunction with inflammatory cytokine Il-1β significantly increased expression of MMP1 and MMP3 which was further increased by applying cyclical stretch forces (Archambault, Tsuzaki

Please cite this article as: Wong, J.K.F., et al., The cell biology of suturing tendons, Matrix Biology (2010), doi:10.1016/j.matbio.2010.06.002

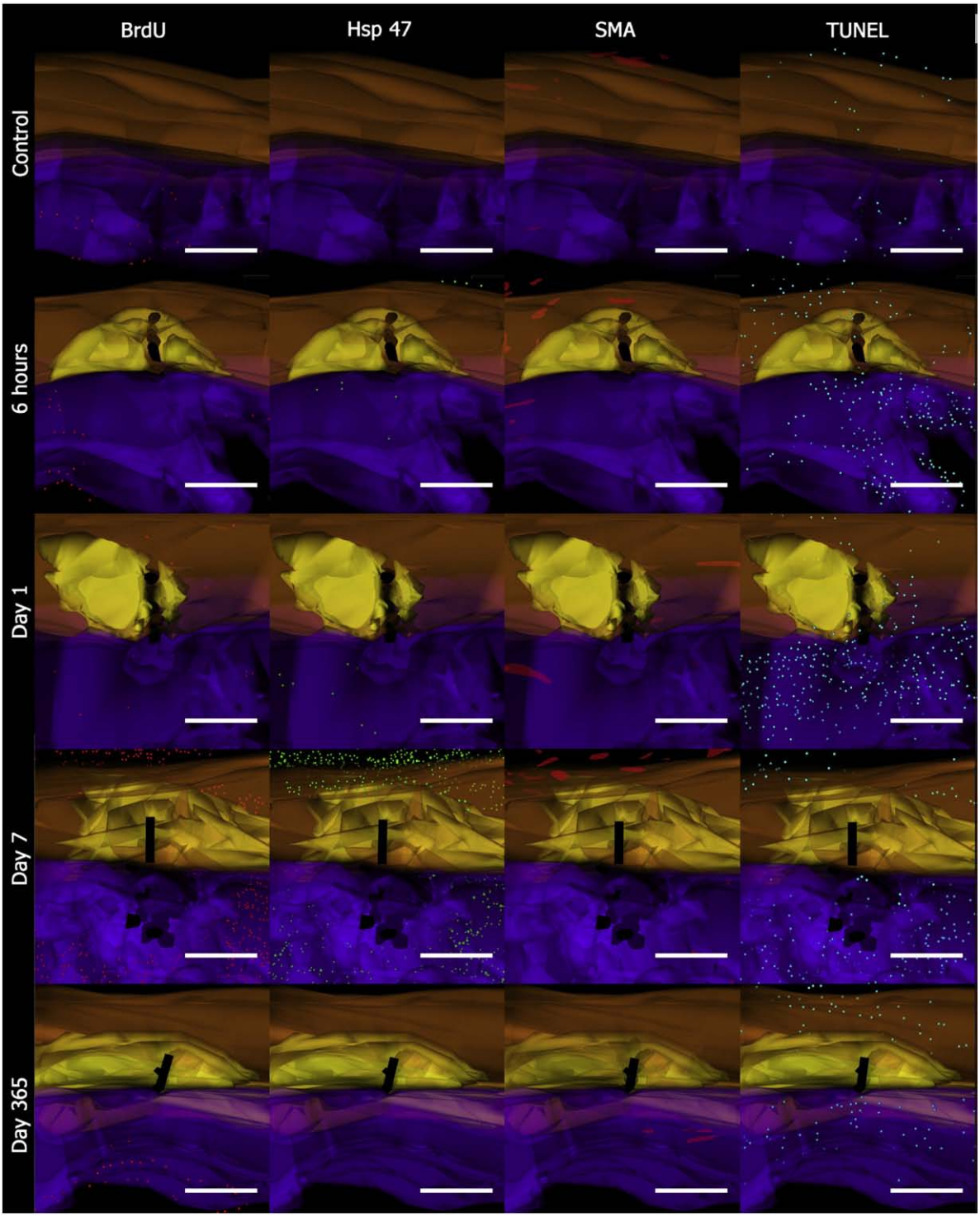

Fig. 10. 3D cellular mapping of cell activity**.** Image of controls, 6 h, Day 1, Day 7, and Day 365 after suture. BrdU+ve cells (red), Hsp 47+ve cells (green), α-SMA+vessels (red), TUNEL+ve cells (blue). Tendon is represented in orange and subcutaneous tissue (ST) is represented in purple. The grasping suture is represented in black, and the acellular zone represented in yellow. Scale bar represents 200 μm. (For interpretation of the references to colour in this figure legend, the reader is referred to the web of this article.)

et al. 2002). The environment we have created *in vivo* by the application of a suture and mobilization equates to a prolonged inflammatory environment with tendon fibroblasts under cyclical strain. Although MMP expression was not investigated in this particular study, it would appear that the acellular zone represents a physical manifestation of this degenerative response. This prolonged inflammatory activity may contribute to weakening of the tendon over this time period. Evidence from studies in rheumatoid tenosynovitis has shown that inflammation of the tendon sheath produces raised levels of proinflammatory cytokines and proteolytic enzymes such as MMP 1, 2 and 13 that can cause tendons to weaken and spontaneously rupture (Jain, Nanchahal et al. 2001). Zymography studies have demonstrated that MMP1 is the predominant matrix enzyme in spontaneously ruptured supraspinatous tendon (Riley, Curry et al. 2002). The relationship between matrix metalloproteinases, inflammation and acellular zone formation merits investigation.

The prolonged inflammatory activity surrounding the suture is mitigated by apoptotic activity in the surrounding tissues. Previously

Please cite this article as: Wong, J.K.F., et al., The cell biology of suturing tendons, Matrix Biology (2010), doi:10.1016/j.matbio.2010.06.002

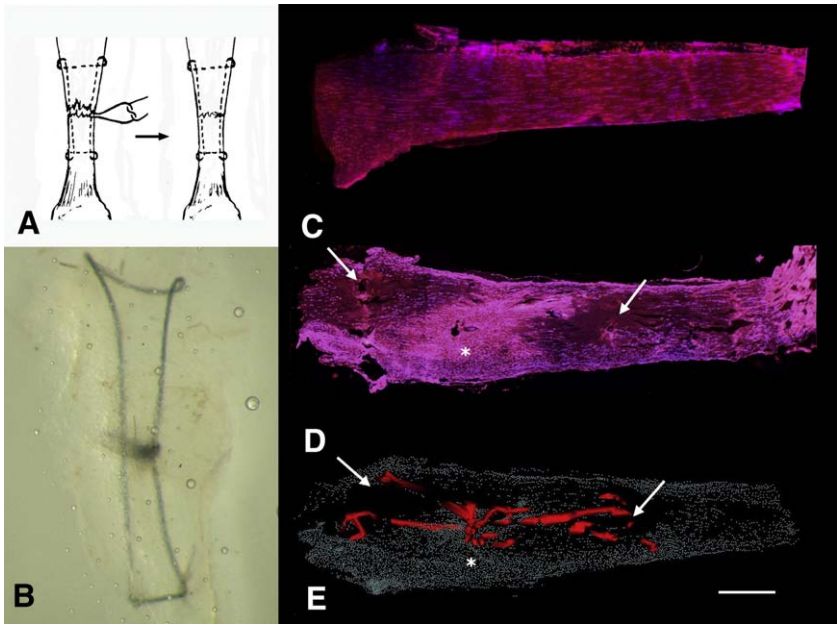

Fig. 11. Distribution of acellular zones following a modified Kessler Repair in Achilles tendon (stained with Hoechst 33258 and TRITC Phalloidin). (A) Schematic of modified Kessler repair being performed (B) Modified Kessler repair performed in mouse Achilles tendon cleared in glycerol (C) Normal unwounded mouse Achilles tendon demonstrating well defined linear rows of cells. (D) Kessler sutured mouse Achilles tendon at 3 weeks post wounding demonstrating hypercellularity at point of partial laceration and suture knot (asterisk) and large areas of acellularity related to the grasping components of the Kessler (white arrows). (E) 3D reconstruction of Kessler suture (red) in Achilles tendon three weeks following wounding. Note large acellular zones in high strain areas of the grasping components of the Kessler suture (white arrow). Scale bar = 500 μm. (For interpretation of the references to colour in this figure legend, the reader is referred to the web of this article.)

we found a similar inverse relationship between inflammation and apoptosis during the tendon adhesion formation process although more protracted (Wong, Lui et al. 2009) and a number of studies have shown that the process of cell death forms and important part of inflammatory cell clearance in wound healing (Chowdhury, Tharakan et al. 2006; Poon, Hulett et al. 2009).

Although the small animal numbers may be perceived as a limitation of the study, the experimentation was powered accordingly, based on our previous data that showed the *in vivo* suture model to be highly reproducible with low inter-animal variability. Our move towards using a combination of *ex vivo* and *in vivo* techniques were aimed to isolate and image the effect of suture and tension on tendon with and without the systemic influences of inflammation. We have shown that cell death plays a role at numerous points in the surgical suture of tissue and suturing of tendon has been shown in a number studies to induce biomechanical weakening of the tendon (Reynolds, Wray, Jr. et al. 1976; Bishop, Cooney, III et al. 1986; McDowell et al., 2002; Zobitz, Zhao et al. 2000) when performed in living tendon. The mechanism by which acellular zones form seem crucial to the loss in mechanical integrity as inducing acellular tendon using chemical treatments such as high concentration of cellular detergents have been shown not to impair the mechanical integrity of rat tendons (Cartmell and Dunn, 2000). Indeed acellular tissue reconstructions have been shown to be of benefit in reconstructing tendon injuries in clinical practice (Lee, 2007). The biochemical combination of necrosis, acellular zone formation and prolonged inflammation following suture may all contribute to tendon softening and each of these will be examined independently for their contribution in future studies. Numerous tissues exhibit evidence of the detrimental effect of suturing, like corneal tissue, which becomes hazy and can clearly be seen to have acellular zones following suture (Matsuda, Yoshiki et al. 1999), meniscal repair with sutures form acellular zones, which over time lead to joint degeneration and arthritic changes (Hunziker and Stahli, 2008). Cumulatively there is evidence to suggest that suturing unwounded tendon induces catabolic changes in the tendon. Importantly the study highlights the importance of tendon mechanobiology in maintaining normal tissue homeostasis and how simple surgical procedures can disrupt this biology significantly.

4. Methods

4.1. Live/dead tendon imaging

Nine middle digits, flexor digitorum profundus (FDP) tendons were harvested from freshly euthanized 10–12 week old C57/BLJ mice. Using an operating microscope (Leica MZ7.5, Germany) at 10–40 times magnification, the FDP tendon was dissected free. This was performed by making a longitudinal cut down the palmar surface of the digit from the tip of the digit to the palm. The pulleys and flexor digitorum superficialis (FDS) were sharply divided and FDP was divided at the level of the palm and at the distal insertion. Tendons harvested measured approximately 1 cm in length. Harvested tendons were immediately placed in sterile CO_2 independent media (Gibco, Ayrshire, UK) and Live/Dead assay kit solution (Molecular Probes, Oregon, USA) which contained 2 μM calcein AM and 4 μM EthD-1. Tendons bathed in this solution were incubated at 37 °C, 5% CO_2 for 1 h prior to inspection by confocal microscopy.

Calcein AM dye enters living cells and ethidium homodimer (EthD-1) is taken up by dead cells. Calcein AM fluoresces green when activated by intracellular esterase activity in living cells (excitation 495 nm and emission 515 nm). EthD-1 enters damaged cell membranes and fluoresces red on binding to nucleic acids (excitation 495 nm and emission 635 nm) but is excluded by living cell membranes.

Three experimental groups were performed in triplicate; control uninjured tensioned tendon, sutured tensioned tendon, and sutured untensioned tendon. Experiments were performed on 35 mm cover glass bottom sterile culture dishes (Fluorodish, World Precision Instruments Inc, CA, U.S.A.) with a thin layer of Sylgard (184 silicone Elastomer, Dow chemical, MI, U.S.A.) placed along the outer rim of the well. Sylgard lined culture dishes were incubated overnight at 55 °C to induce polymerization. Fixed position posts were anchored into the Sylgard rim in each dish using 0.1 mm diameter insect pins (Fine Science Tools GMbd, Germany).

Control tensioned tendons were sutured at both ends with 10/0 polyamide sutures (BBraun Medical, Sheffield, U.K.). The sutures at the ends of the tendon were tensioned around the insect pins anchored into

Please cite this article as: Wong, J.K.F., et al., The cell biology of suturing tendons, Matrix Biology (2010), doi:10.1016/j.matbio.2010.06.002

the Sylgard until the tendon was taught. The ends of the tendon were at least 3 mm away from the area to be imaged. The procedure was repeated for the sutured tensioned tendon. This was kept taught as above but a further 10/0 single grasping suture, grasping approximately 50% of the tendon fibres (Wong, Cerovac, Ferguson and McGrouther, 2006), was placed in the middle of the tendon in the region of image capture.

Sutured untensioned tendon was sutured as above in the middle of the tendon with a 10/0 single grasping suture. After placement of the single grasping suture, tension was immediately released from the tendon by removing the insect pins. Subsequently the samples were bathed in Live Dead solution and images were captured using a Biorad MRC 1024 Multiphoton confocal microscope (Biorad, CA, U.S.A.) with Spectra Physics Tsunami Infrared Laser (750 nm) (Newport Solutions, CA, U.S.A). Images were captured at two hourly intervals at 20× magnification and 2 μm thickness z stack slices for 12 h.

4.2. Analysis of DNA integrity

Six mice were used to analyse DNA integrity following suture using the standardised single suture injury model. The mouse tendon was harvested 24 h post injury and snap frozen in liquid nitrogen. Uninjured tendon was harvested from the contralateral limb of each mouse and acted as the controls. Six biological replicates were completed and pooled into wounded and unwounded sample groups for comparison. The DNA extraction protocol was adapted from that described by Tilly and Hsueh (1993). Pooled tendon was homogenised by pestle and mortar in liquid nitrogen. Further homogenisation was obtained by placing samples in 100 mM NaCl, 10 mM EDTA, 300 mM Tris HCl with a pH of 8.0; 200 mM sucrose, and 0.65% SDS before incubation for 30 min at 60 °C. The sample was then incubated for 1 h at 55 °C after Proteinase K was added at 500 μg/ml. Following the addition of Potassium acetate at 500 μg/ml, the sample was placed on ice for 30 min. Following centrifugation at 4500 rpm for 15 min at 4 °C, the supernatant was extracted once with phenol:chloroform:isoamylalcohol (25:24:1, by vol.). This mixture was further processed by the addition of chloroform: isoamylalcohol (24:1, v/v), and the DNA was precipitated with absolute ethanol. The DNA was dissolved in 200 μl TE, pH 8.0, and incubated with 2.5 μg DNase–free RNase (Sigma-Aldrich, USA) for 60 min at 37 °C. Following further phenol extraction and phenol precipitation, equal amounts of DNA were resolved on 2% agarose gels.

4.3. Transmission electron microscopy

Samples were prepared for electron microscopy as described previously (Canty, Lu et al. 2004). Briefly, mouse digital flexor tendons were sutured *in vivo* and harvested immediately, at 3 h post suture and at 24 h post suture, and were immediately fixed in 2% glutaraldehyde in 100 mM phosphate buffer, pH 7.0, for 30 min at room temperature. Control mouse digital flexor tendons were also harvested in an identical fashion from unwounded mice. Samples were then post fixed for 2 h at 4 °C in fresh fixative. After washing in 200 mM phosphate buffer, the samples were fixed in 1% glutaraldehyde and 1% OsO_4 in 50 mM phosphate buffer, pH 6.2, for 40 min at 4 °C. After being rinsed in distilled water the samples were stained en bloc with 1% aqueous uranyl acetate for 16 h at 4 °C, dehydrated and embedded in Spurrs' resin. Ultra-thin sections, ~60 nm thick, were cut for normal transmission electron microscopy and were collected on uncoated copper 200 grids. Serial sections were taken and placed on formvar-coated copper 1000 μm slot grids, stabilized with carbon film. All sections were subsequently stained with uranyl acetate lead citrate, and examined using a Philips BioTwin transmission electron microscope (Phillips Electron Optics, The Netherlands). Images were recorded on 4489 film (Kodak, UK) and scanned using an Imacon Flextight 848 scanner (Hasselblad, USA).

4.4. In vivo studies

All animal procedures were approved by the Local Ethical Committee at the University of Manchester and complied with British Home Office regulations on the care and use of laboratory animals. Our limitations in sample size per time point were justified from our previous studies where we were able to show that the variability between sutured animals, taking into account suture technique and reproducibility was small. Appropriate power calculations were used to calculate sample size.

39 mice were used for immunohistochemical studies and 3D reconstruction with cellular mapping. Our previously described model was used: this involved a standardised procedure; which used a single interrupted suture of a digital flexor tendon (Wong et al., 2006).

The *in vivo* study used the hind paw deep digital flexor of male C57/BL6 mice aged between 10 and 12 weeks (25–30 g). Surgery was performed under a standard mouse general anaesthetic protocol (Induction using 4% isofluorane (Abbott, UK) and 4 l/min oxygen driver, maintenance 2% isofluorane with 2 l/min oxygen driver and 1.5 l/min nitrous oxide). The left hindlimb was cleaned with 70% ethanol and blood flow to the operative field was reduced through application of a tourniquet using dressing elastic to the popliteal fossa. The anaesthetised mouse was positioned under a Leica MZ7 operating microscope (Leica Microsystems, Germany) and operated upon at 10 to 40 times magnification.

Second, third and fourth digits were suture wounded to study stress fibre architecture, cellular function markers and inflammatory markers respectively. Six control, unsutured tendons were taken from several corresponding digits on the contralateral paw in the corresponding area of injury.

A skin incision was made at the midpoint of the middle phalanx of each digit of the left hind paw to expose the tendon. The wound was regularly irrigated with 0.9% saline to avoid tendon dehydration.

A single 10-0 polyamide suture (BBraun Medical, UK) was inserted transversely through approximately 50% of the deep digital flexor tendon diameter and tied.

Following the application of the tendon suture, skin wounds were closed with a single 10-0 polyamide suture, the tourniquet removed and pressure applied to the wound to ensure haemostasis. The hind paws were cleaned with 0.9% saline and the wounds were left exposed to dry. The mice were allowed to mobilise freely and three mice were euthanized at 6 h, then at 1, 3, 5, 7, 14, 21, 28, 56 and 84, 168 and 365 days. Three mice had a slight variation in the operative protocol and underwent the same exposure and tendon wounding but had a further wound made at the level of the tarsal bones to allow for a proximal tenotomy of the deep digital flexor tendon. Hind paws were flexed and extended to ensure that normal tenodesis was obliterated hence removing traction forces from the sutured tendon site. This group of mice were euthanized 24 h following suturing and their tendons collected.

Four hours prior to mice euthanasia each mouse was injected with Bromodeoxyuridine (5-bromo-2-deoxyuridine, BrdU) injected into the peritoneal cavity at a dose of 10 μl/g of mouse.

The hind limbs were immersed in zinc fixative (Beckstead, 1994) for 48 h at 4 °C. The third digit of each sample was excised and decalcified in 20% EDTA for 15 days, with solution changes every 5 days, and then embedded in paraffin wax. The fourth digit soft tissue was filleted off the bone and stored in 70% ethanol until they were ready to be embedded in paraffin wax. Serial sections, 7 μm thick, were cut from paraffin embedded blocks. Four sections were mounted onto 4% APES and 1% Poly-L-lysine coated slides, and were dried at 37 °C for 24 h.

The central slide was identified from the sections by staining alternate slides for Harris haematoxylin (Raymond A Lamb, U.K.) and eosin (Raymond A Lamb, U.K.) or Hoechst 33258 bisbenzimidazole dye (Sigma Chemical Co., St Louis, USA) and TRITC labeled Phalloidin (Sigma-Aldrich, St Louis, USA) at the concentration of 1: 1000 and

Please cite this article as: Wong, J.K.F., et al., The cell biology of suturing tendons, Matrix Biology (2010), doi:10.1016/j.matbio.2010.06.002

1:500 overnight at 4 °C respectively. For the third digit, three sections from selected from around the central slide were antibody labelled (Supplement 1) for BrdU (marker for proliferation), Heat shock protein 47 (Hsp 47 or "collingin", marker for type 1 collagen synthesis), alpha smooth muscle actin, (α-SMA, marker for pericytes and myofibroblasts) and TUNEL (marker for DNA fragmentation/apoptosis). The fourth digit was serially sectioned and antibody stained with CD45 (pan leucocyte marker), Ly6G (neutrophil marker), F4/80 (activated macrophage marker), and toludine blue (mast cell stain) in triplicate per mouse digit. Labeling for apoptotic markers Bax (apoptotic marker), Bcl-2 (anti-apoptotic marker), Caspase 3 (apoptotic marker) and Cytochrome C (apoptotic marker) were performed at time points 6 h, 7 days and 6 months to look for evidence of apoptotic cells. Immunoperoxidase techniques were standardised following initial dilution studies to establish optimal dilutions and conditions for all primary antibodies. For mouse monoclonal antibodies a specific mouse on mouse (MOM) kit (Vector Laboratories) was used. For rat monoclonal antibodies, a standard rabbit anti rat biotinylated secondary antibody was used and amplified using the elite ABC kit (Vector laboratories). For rabbit polyclonal antibodies the rabbit ImmPRESS biotinylated kit was used. These kits were used as recommended in the manufacturer's guidelines. The TUNEL kit (Roche) was used with peroxidase conversion which allowed for assessment by 3,3′ diaminobenzidine (DAB) substrate staining. Antibody labeling of samples was undertaken using the protocol described below (Table 1). Samples were washed twice for 5 min using 0.1% tween (v/v) in phosphate buffered solution (PBS) between each step of the protocol.

Images of all stained sections of tendon with suture were obtained using a Leica DMRB Microscope (Leica Microsystems, Germany) and a Spot camera (Diagnostic Instruments Inc, USA) onto a silicon graphics PC (SGI, UK) and saved using Spot advanced software (Diagnostic instruments inc, U.S.A.) as .tiff files.

4.5. Calculating cellular changes in tendon, sheath and skin

Acellular zone variables were acquired as described from previous work on three sections that were 28 μm apart (Wong et al., 2006). Cells were counted in the acellular zone, the cellular tendon, and the sheath/subcutaneous tissues (ST) in specified sampling areas. The cell densities for any given area could therefore be calculated as cells/mm^2. Briefly, from the selected sections the acellular zone outline was defined by joining the peripheral nuclei at its margins. The area was measured by image analysis software (Image Pro Plus version 4.5, Media Cybernetics, USA).

The tissue sample area consisted of the area of tendon with the suture in the centre of the image captured. To calculate the cellularity of samples, Image Pro Plus software was calibrated to colour match the nuclei on the slides and individual nuclei were counted within defined fields of view (Supplement 2). Six fields of view were selected for calculating cellularity and cellular expression of antibodies. Cell counts were performed on three fields of view for the tendon (Supplement 2-A, B, and C) and three fields of view for the sheath and subcutaneous tissues (ST) on three different sections (Supplement 2-D, E, and F). The total number of fields analysed per digit was 18 fields (nine tendon and nine sheath/subcutaneous tissue fields). Each field measured 50 μm by 200 μm except the acellular zone field that was measured according to the area of acellularity formed (Supplement 2-A). Cells were counted using the Image Pro Plus software. The mean cell density was calculated from the three fields in their respective tissues (tendon and sheath/subcutaneous tissues). This sampling method was also used for quantification of immunohistochemical markers. For the inflammatory profile where inflammatory cells were not seen in the tendon substance, a mean cell density of expression was taken from three fields of view surrounding the sheath, proximal, adjacent and distal to the area of injury.

4.6. Three dimensional reconstruction and cellular mapping

Three dimensional reconstruction of electron microscopic topography using Reconstruct (Fiala, 2005) has previously been described. We have applied the same methodology to serial sectioned and aligned immunohistochemically labeled samples. Briefly, serial sectioned histology and immunohistochemical image files were calibrated and imported as .tiff files into the Reconstruct program. Wire maps were produced by tracing individual structures such as tendon, blood vessels and the subcutaneous tissues. The acellular zone was also mapped by tracing around the zone for ease of identification on the reconstructed images. Distances between each image were calibrated and individual cells were mapped according to their stereological position and reproduced using the program's sphere option. Boissonnat surface shading and colour selection and transparency features were introduced after processing of the three dimensional reconstruction. Tendon was highlighted in orange, the acellular zone was yellow, the subcutaneous tissue was purple, and the suture was black. CD45 positive (+ve) cells were labeled in pink, F4/80+ve cells in white, Ly6G+ve cells in yellow, and mast cells in silver. BrdU expression was mapped in red, Hsp47+ve cells were mapped in green, α-SMA+ve vessels were mapped in red, and TUNEL expression was mapped in blue.

4.7. Kessler repair model

Six C57 BL6 mice had modified Kessler repairs performed on their left Achilles tendon. Briefly, under standard anaesthetic protocol, hair bearing areas over the Achilles tendon were shaved, a tourniquet was

Table 1
Antibodies, pretreatments, reagents, and controls used for labeling samples. Incubation performed at room temp (RT) or 37 °C. ABC represents avidin–biotin complex.

Antibody	Pretreatment	Blocking solution	Primary incubation	Secondary incubation	ABC	Substrate	Control tissue
BrdU (Abcam)	10 min in 4 M HCL, 5 min in borate buffer	1% rabbit serum for 1 h at room temp (RT)	1:200 for 1 h 37 °C	1:200 rabbit anti-rat biotinylated IgG for 15 min RT	Yes	DAB	Spleen
Hsp-47 (Stressgen)	None	MOM block for 1 h RT	1:200 for 1 h 37 °C	MOM kit 2 IgG for 10 min RT	Yes	DAB	Skin wounds
α-SMA (Abcam)	None	2.5% goat serum for 1 h RT	1:200 for 1 h 37 °C	ImmPRESS kit for 30 min RT	No	DAB	Spleen
TUNEL (Roche)	30 min in Tris HCL +	None	2:3 for 1 h 37 °C	1:2:1 Sheep serum:PBS: POD kit for 30 min RT	No	DAB	Large intestine
CD45 (BD pharmingen)	None	1% rabbit serum for 1 h RT	1:100 for 1 h 37 °C	1:200 rabbit anti-rat biotinylated IgG for 30 min RT	Yes	DAB	Spleen
F4/80 (Serotec)	None	1% rabbit serum for 1 h RT	1:200 for 1 h 37 °C	1:200 rabbit anti-rat biotinylated IgG for 30 min RT	Yes	DAB	Spleen
Ly6G (BD pharmingen)	None	1% rabbit serum for 1 h RT	1:200 for 1 h 37 °C	1:200 rabbit anti-rat biotinylated IgG for 30 min RT	Yes	DAB	Skin wounds
Bcl-2 (BD pharmingen)	None	2.5% goat serum for 1 h RT	1:400 for 1 h 37 °C	ImmPRESS kit for 30 min RT	No	DAB	Skin and intestine
Bax (BD pharmingen)	None	2.5% goat serum for 1 h RT	1:400 for 1 h 37 °C	ImmPRESS kit for 30 min RT	No	DAB	Skin and intestine
Caspase 3 (R & D System)	None	2.5% goat serum for 1 h RT	1:200 for 1 h 37 °C	ImmPRESS kit for 30 min RT	No	DAB	Skin and intestine
Cytochrome C (Abcam)	None	2.5% goat serum for 1 h RT	1:200 for 1 h 37 °C	ImmPRESS kit for 30 min RT	No	DAB	Brain

Please cite this article as: Wong, J.K.F., et al., The cell biology of suturing tendons, Matrix Biology (2010), doi:10.1016/j.matbio.2010.06.002

applied to the mouse left hindpaw lower limb, and a longitudinal skin was made along the dorsal aspect over the distal mouse tibia. The Achilles tendon was exposed and a 50% division of the tendon was performed using microscissors. Using a 10/0 polyamide suture, a modified Kessler repair was performed (Kessler and Nissim, 1969). Mice were allowed to mobilise freely and were harvested 3 weeks following injury. Unwounded Achilles tendons were also harvested as controls. The tendons were carefully dissected from the hindlimbs and fixed in zinc fixative for 48 h at 4 °C. Tendon was processed and paraffin wax embedded for serial sectioning as above. Sections were cut at 7 μm thickness, then mounted on onto 4% APES and 1% Poly-L-lysine coated slides, dried for 24 h at 37 °C prior to staining with Hoechst 33258 and TRITC Phalloidin staining for 3D reconstruction. Images were captured with a standard fluorescent microscope (Leica DM RB light microscope, Switzerland).

4.8. Statistics

Data were analysed for normal distribution by plotting data on a histogram using SPSS 15.0 (SPSS Inc, Chicago, USA). Mean values were calculated using SPSS and expressed with the standard error of mean in brackets. The changes in cellularity seen at different time points were tested for significance using one way ANOVA and further analysed using a post hoc Tukey test. In all cases, the P value was considered significant if below 0.05.

Acknowledgements

The authors thank Renovo Plc (to JW), the Royal College of Surgeons of Edinburgh (to JW), The Academy of Medical Sciences (to JW), the Kuwait Ministry of Higher Education (to SA), and the Wellcome Trust (to KEK and JW) for generous grant support. Special thanks go to Miss Samantha Forbes for electron microscopy assistance.

Appendix A. Supplementary data

Supplementary data associated with this article can be found, in the online version, at doi:10.1016/j.matbio.2010.06.002.

References

Archambault, J., Tsuzaki, M., Herzog, W., Banes, A.J., 2002. Stretch and interleukin-1beta induce matrix metalloproteinases in rabbit tendon cells in vitro. J. Orthop. Res. 20, 36–39.
Beckstead, J.H., 1994. A simple technique for preservation of fixation-sensitive antigens in paraffin-embedded tissues. J. Histochem. Cytochem. 42, 1127–1134.
Bishop, A.T., Cooney III, W.P., Wood, M.B., 1986. Treatment of partial flexor tendon lacerations: the effect of tenorrhaphy and early protected mobilization. J. Trauma 26, 301–312.
Canty, E.G., Lu, Y., Meadows, R.S., Shaw, M.K., Holmes, D.F., Kadler, K.E., 2004. Coalignment of plasma membrane channels and protrusions (fibripositors) specifies the parallelism of tendon. J. Cell Biol. 165, 553–563.
Cartmell, J.S., Dunn, M.G., 2000. Effect of chemical treatments on tendon cellularity and mechanical properties. J. Biomed. Mater. Res. 49, 134–140.
Chowdhury, I., Tharakan, B., Bhat, G.K., 2006. Current concepts in apoptosis: the physiological suicide program revisited. Cell. Mol. Biol. Lett. 11, 506–525.
Decrock, E., De Vuyst, E., Vinken, M., Van Moorhem, M., Vranckx, K., Wang, N., Van Laeken, L., De Bock, M., D'Herde, K., Lai, C.P., Rogiers, V., Evans, W.H., Naus, C.C., Leybaert, L., 2009. Connexin 43 hemichannels contribute to the propagation of apoptotic cell death in a rat C6 glioma cell model. Cell Death Differ. 16, 151–163.
Dona, E., Turner, A.W., Gianoutsos, M.P., Walsh, W.R., 2003. Biomechanical properties of four circumferential flexor tendon suture techniques. J. Hand Surg. Am. 28, 824–831.
Elliot, D., 2002. Primary flexor tendon repair—operative repair, pulley management and rehabilitation. J. Hand Surg. Br. 27, 507–513.
Fiala, J.C., 2005. Reconstruct: a free editor for serial section microscopy. J. Microsc. 218, 52–61.
Gelberman, R.H., Boyer, M.I., Brodt, M.D., Winters, S.C., Silva, M.J., 1999. The effect of gap formation at the repair site on the strength and excursion of intrasynovial flexor tendons. An experimental study on the early stages of tendon-healing in dogs. J. Bone Joint Surg. Am. 81, 975–982.
Groeger, G., Nobes, C.D., 2007. Co-operative Cdc42 and Rho signalling mediates ephrinB-triggered endothelial cell retraction. Biochem. J. 404, 23–29.
Hotokezaka, S., Manske, P.R., 1997. Differences between locking loops and grasping loops: effects on 2-strand core suture. J. Hand Surg. Am. 22, 995–1003.
Hunziker, E.B., Stahli, A., 2008. Surgical suturing of articular cartilage induces osteoarthritis-like changes. Osteoarthritis Cartilage 16, 1067–1073.
Jain, A., Nanchahal, J., Troeberg, L., Green, P., Brennan, F., 2001. Production of cytokines, vascular endothelial growth factor, matrix metalloproteinases, and tissue inhibitor of metalloproteinases 1 by tenosynovium demonstrates its potential for tendon destruction in rheumatoid arthritis. Arthritis Rheum. 44, 1754–1760.
Kajikawa, Y., Morihara, T., Watanabe, N., Sakamoto, H., Matsuda, K., Kobayashi, M., Oshima, Y., Yoshida, A., Kawata, M., Kubo, T., 2007. GFP chimeric models exhibited a biphasic pattern of mesenchymal cell invasion in tendon healing. J. Cell. Physiol. 210, 684–691.
Kessler, I., Nissim, F., 1969. Primary repair without immobilisation of flexor tendon division within the digital sheath. Acta Orth Scand. 40, 587–601.
Kleinert, H.E., Spokevicius, S., Papas, N.H., 1995. History of flexor tendon repair. J. Hand Surg. Am. 20, S46–S52.
Krysko, D.V., Vanden Berghe, T., D'Herde, K., Vandenabeele, P., 2008. Apoptosis and necrosis: detection, discrimination and phagocytosis. Methods 44, 205–221.
Lavagnino, M., Arnoczky, S.P., 2005. In vitro alterations in cytoskeletal tensional homeostasis control gene expression in tendon cells. J. Orthop. Res. 23, 1211–1218.
Lee, D.K., 2007. Achilles tendon repair with acellular tissue graft augmentation in neglected ruptures. J. Foot Ankle Surg. 46, 451–455.
Leigh, D.R., Abreu, E.L., Derwin, K.A., 2008. Changes in gene expression of individual matrix metalloproteinases differ in response to mechanical unloading of tendon fascicles in explant culture. J. Orthop. Res. 26, 1306–1312.
Ljungqvist, A., Schwellnus, M.P., Bachl, N., Collins, M., Cook, J., Khan, K.M., Maffulli, N., Pitsiladis, Y., Riley, G., Golspink, G., Venter, D., Derman, E.W., Engebretsen, L., Volpi, P., 2008. International Olympic Committee consensus statement: molecular basis of connective tissue and muscle injuries in sport. Clin. Sports Med. 27, 231–239.
Manske, P., 2004. Galen and tendon surgery. J. Hand Surg. Am. 29, 547–550.
Matsuda, A., Yoshiki, A., Tagawa, Y., Matsuda, H., Kusakabe, M., 1999. Corneal wound healing in tenascin knockout mouse. Invest Ophthalmol. Vis. Sci. 40, 1071–1080.
McDowell, C.L., Marqueen, T.J., Yager, D., Owen, J., Wayne, J.S., 2002. Characterization of the tensile properties and histologic/biochemical changes in normal chicken tendon at the site of suture insertion. J. Hand Surg. Am. 27, 605–614.
McNeilly, C.M., Banes, A.J., Benjamin, M., Ralphs, J.R., 1996. Tendon cells *in vivo* form a three dimensional network of cell processes linked by gap junctions. J. Anat. 189 (Pt 3), 593–600.
O'Brien, E.T., Kinch, M., Harding, T.W., Epstein, D.L., 1997. A mechanism for trabecular meshwork cell retraction: ethacrynic acid initiates the dephosphorylation of focal adhesion proteins. Exp. Eye Res. 65, 471–483.
Pennington, D.G., 1979. The locking loop tendon suture. Plast. Reconstr. Surg. 63, 648–652.
Poon, I.K., Hulett, M.D., Parish, C.R., 2009. Molecular mechanisms of late apoptotic/necrotic cell clearance. Cell Death Differ.
Ralphs, J.R., Waggett, A.D., Benjamin, M., 2002. Actin stress fibres and cell–cell adhesion molecules in tendons: organisation *in vivo* and response to mechanical loading of tendon cells in vitro. Matrix Biol. 21, 67–74.
Reynolds, B., Wray Jr., R.C., Weeks, P.M., 1976. Should an incompletely severed tendon be sutured? Plast. Reconstr. Surg. 57, 36–38.
Riley, G.P., Curry, V., DeGroot, J., van El, B., Verzijl, N., Hazleman, B.L., Bank, R.A., 2002. Matrix metalloproteinase activities and their relationship with collagen remodelling in tendon pathology. Matrix Biol. 21, 185–195.
Savage, R., 1985. In vitro studies of a new method of flexor tendon repair. J. Hand Surg. Br. 10, 135–141.
Screen, H.R., Lee, D.A., Bader, D.L., Shelton, J.C., 2003. Development of a technique to determine strains in tendons using the cell nuclei. Biorheology 40, 361–368.
Silva, M.J., Boyer, M.I., Ditsios, K., Burns, M.E., Harwood, F.L., Amiel, D., Gelberman, R.H., 2002. The insertion site of the canine flexor digitorum profundus tendon heals slowly following injury and suture repair. J. Orthop. Res. 20, 447–453.
Strickland, J.W., 2000. Development of flexor tendon surgery: twenty-five years of progress. J. Hand Surg. Am. 25, 214–235.
Tang, J.B., 2006. Tendon injuries across the world: treatment. Injury 37, 1036–1042.
Taras, J.S., Raphael, J.S., Marczyk, S.C., Bauerle, W.B., 2001. Evaluation of suture caliber in flexor tendon repair. J. Hand Surg. Am. 26, 1100–1104.
Thurman, R.T., Trumble, T.E., Hanel, D.P., Tencer, A.F., Kiser, P.K., 261-265, 1998. Two-, four-, and six-strand zone II flexor tendon repairs: an in situ biomechanical comparison using a cadaver model. J. Hand Surg. Am. 23, 261–265.
Tilly, J.L., Hsueh, A.J., 1993. Microscale autoradiographic method for the qualitative and quantitative analysis of apoptotic DNA fragmentation. J. Cell. Physiol. 154, 519–526.
Wong, J., Bennett, W., Ferguson, M.W., McGrouther, D.A., 2006. Microscopic and histological examination of the mouse hindpaw digit and flexor tendon arrangement with 3D reconstruction. J. Anat. 209, 533–545.
Wong, J.K., Cerovac, S., Ferguson, M.W., McGrouther, D.A., 2006. The cellular effect of a single interrupted suture on tendon. J. Hand Surg. Br. 31, 358–367.
Wong, J.K., Lui, Y.H., Kapacee, Z., Kadler, K.E., Ferguson, M.W., McGrouther, D.A., 2009. The cellular biology of flexor tendon adhesion formation: an old problem in a new paradigm. Am. J. Pathol. 175, 1938–1951.
Zobitz, M.E., Zhao, C., Amadio, P.C., An, K.N., 2000. Comparison of mechanical properties of various suture repair techniques in a partially lacerated tendon. J. Biomech. Eng. 122, 604–607.

Please cite this article as: Wong, J.K.F., et al., The cell biology of suturing tendons, Matrix Biology (2010), doi:10.1016/j.matbio.2010.06.002

Col4a1 missense mutation reveals a protective role for a novel keratinized simple epithelium in tendon

Susan H. Richardson[a], Sarah Al-Youha[a, b], Tom Van Agtmael[c], Ching-Yan Chloé Yeung[a], Leo Zeef[a], Yinhui Lu[a], Vicky E. Ormston[a], Jason Wong[b], Duncan A. McGrouther[b] and Karl E. Kadler[a, *]

[a]Wellcome Trust Centre for Cell-Matrix Research, Faculty of Life Sciences, Michael Smith Building, and [b]Plastic & Reconstructive Surgery Research, Faculty of Medicine and Human Sciences, University of Manchester, Oxford Road, Manchester M13 9PT UK; [c]Faculty of Biomedical and Life Sciences, University of Glasgow, Dunbarton Road, Glasgow G11 6NU UNITED KINGDOM

*To whom correspondence should be addressed: Fax: +44 161 275 1505, Tel: +44 161 275 5086, Email: karl.kadler@manchester.ac.uk

ABBREVIATIONS

BM, basement membrane, TEM, transmission electron microscopy.

Abstract

The normal ability of tendons to glide smoothly past adjacent tissues during muscle contraction is impaired after injury because of the formation of fibrous adhesions between the tendon and surrounding tissues. To understand more about adhesion formation we embedded artificial and *ex vivo* tendons in fibrin and monitored cell migration. Cells migrated from the artificial tendons thus blurring the well-defined edges of the tissue. In contrast, cells migrated out of ex vivo tendons at injury sites suggesting that the tendon was encapsulated by a cell-retentive layer. We performed a microarray analysis of embryonic and postnatal tendon, and identified genes characteristic of epithelial cells and basement membrane (BM) synthesis. Subsequent experiments showed the presence of a keratin-expressing epithelium at the tendon surface that was in contact with a BM comprising laminin, $\alpha1.\alpha1.\alpha2$ collagen IV, perlecan and nidogen. To establish if BM synthesis occurs at sites of tendon adhesions *in vivo*, we surgically-induced adhesion formation in mouse flexor tendon and showed that the surfaces of the tendon exhibited an uninterrupted layer of laminin that extended throughout the adhesion. Collagen IV is essential for the mechanical stability of BMs. Therefore, we examined the *col4a1*$^{+/Svc}$ mouse that has a range of pathologies resulting from defective BMs caused by a missense mutation in the col4a1 gene encoding collagen IV. The flexor tendons lacked BM and exhibited fibrous adhesions with overlying tissues. In conclusion, tendon is covered by a collagen IV-dependent BM-epithelium that is required for tissue encapsulation, cell retention, and the prevention of adhesion formation.

Introduction

Tendons provide attachment of muscles to bone and are therefore essential for joint movement in vertebrates. The back and forth movement of the tendon during skeletal muscle contraction and relaxation requires that the tendon glides smoothly past adjacent tissues. The properties of the tendon surface that enable tissue encapsulation and gliding, thereby preventing unwanted tissue-tissue adhesions, are poorly understood. Adhesions are a 'hidden disease' with no effective treatment or cure (1). They are fibrous bands of collagenous tissue that form abnormal connections between organs, particularly as a result of trauma, surgery, infection, and inflammatory disease (2, 3). A motivation for our study stemmed from an early observation that artificial tendons embedded in fibrin exhibit extensive cell extravagation whereas ex vivo tendons do not (see below). This preliminary observation led us to study the molecular composition of the cells at the surface of tendons, particularly in the context of the formation of fibrous adhesions in the presence of fibrin.

Cavities and structures within the body are covered by epithelial, endothelial or mesothelial layers that encapsulate and compartmentalise tissues leading to specialized organ function. Furthermore, such cell layers facilitate the movement of nutrients and waste products at cell-air and cell-liquid interfaces. These surface-located cells reside on basement membranes (BMs), which are sheet-like protein structures that are essential for cell differentiation, survival, adhesion, proliferation and migration as well as being important for tissue scaffolding and filtration (for review see (4)). BMs comprise a considerable variety of specialized macromolecules including laminins, which are cruciform-shaped trimeric molecules that provide survival signals to epithelial and endothelial cells (5) and are essential for the formation of BMs (6). The rod-like molecules of collagen IV link together to form a porous scaffold that provides mechanical stability and supports the filtration properties of BMs. Nidogens form protein complexes between laminin and collagen IV. BMs also contain the heparan sulfate proteoglycans perlecan, agrin and collagen XVIII, which have the capacity to bind cytokines and growth factors via their glycosaminoglycan side chains (for review see (7)).

RESULTS

Ex vivo tendons but not artificial tendons have a cell-retentive barrier

We had previously shown that tenocytes isolated from 13-day embryonic chick metatarsal tendons and cultured in 3-dimensional fixed-length fibrin gels synthesize an extracellular matrix that closely resembles that of tendon (8). Here we encased the artificial tendons in a fibrin gel and examined the samples by phase contrast time-lapse light microscopy. The results showed that cells migrated from all surfaces of the artificial tendon to populate the fibrin (Fig. 1A and B). Next, we incubated *ex vivo* mouse tendons in fibrin. Cells migrated from the cut ends but not from the shaft of the tendon during 6 days in culture (Fig. 1C). In a further experiment we produced a 50% tenotomy (prior to incubation in fibrin) and observed cell behaviour in the vicinity of the damaged TE. Time-lapse microscopy showed increased cell migration in the TE (perhaps associated with cell hypertrophy) and cells exiting the injury site (see online movie). The results suggested to us that tendons are encapsulated by a cell-retentive layer that is not recapitulated in artificial tendon.

Microarray analysis of embryonic and postnatal tendon

To identify genes that may be responsible for producing and maintaining the cell-retentive layer we performed a microarray analysis of embryonic and postnatal rat-tail tendon. Rat tendon was used because it offers the opportunity to obtain embryonic and postnatal tendons from the same species without the risk of tissue contamination, which is a problem when dissecting tendons from embryonic mice, and also avoids the complication of postnatal mineralization that can occur in chicken tendon. Analysis showed that between E21 and P42 ~1000 genes decreased in expression by $\geq$2-fold and ~850 genes increased by $\geq$2-fold. Amongst the down-regulated genes were those expressed by epithelial cells (including keratin 1, keratin 5, keratin 10, and keratin 14). Immunofluorescence analyses showed that the outermost layer of cells in the tendon were connected by ZO-1 and claudin-1 tight junctions (Fig. 2A and B) and expressed keratin 1 and 10 (Fig. 2C and D). The expression of keratins indicated the presence of a keratinized epithelium (9). Other genes whose expression decreased between E21 and P42 included cystatin A, stefin A2-like 3, loricrin, and late cornified envelope proteins, which belong to the epidermal differentiation complex (EDC) that is associated with the formation of the stratum corneum (10-17). However, despite the expression of EDC genes, the toluidine blue permeability assay (18) showed that the tendons lacked a cornified barrier layer (Fig. 2E-G).

Identification of a basement-membrane epithelium at the surface of tendon

Transmission electron microscopy (TEM) confirmed the presence of a BM in postnatal mouse and rat tendons (Fig. 3A and B, black arrows). Immunostaining showed that the BM contains α2(IV) collagen, nidogen-1, laminin, and perlecan (Fig. 3C and D). The absence of α3(IV) and α5(IV) collagen suggested that the BM contained the α1.α1.α2 network of type IV collagen (19).

Type IV collagen is needed for laminin deposition in postnatal tendons

Type IV collagen is essential for BM stability (6). Therefore we wanted to know if a mouse with an abnormal type IV collagen would display a tendon phenotype. We examined the *Col4a1*$^{+/Svc}$ mouse that has a G-to-A transition in the *Col4a1* gene producing a G1064D substitution in the α1(IV) chain of type IV collagen (20). Heterozygote mice are viable, which facilitates analysis of tendons at postnatal stages of development. Using immunolocalisation we showed that laminin is expressed in the tendon epithelium of wild-type littermates (Fig. 4A) but not in the tendons of *Col4a1*$^{+/Svc}$ mice (Fig. 4B). Laminin is an essential component of BMs, therefore, the absence of laminin suggested that the integrity of the BM was compromised. Indeed, histological examination of the deep flexor tendons in the hind limbs showed evidence of occasional adhesions (not seen in wild-type mice) between the tendon and the tendon synovium (compare Fig. 4C and 4D). Higher power images of the adhesions show synovial hyperplasia and regions of acellularity in the tendon adjacent to the adhesion (Fig. 4D inset).

Injury to the BM-epithelium can result in tendon adhesions

To test the hypothesis that damage to the BM-epithelium and subsequent cell extravagation might result in adhesions, we severed the flexor tendons of 4 week-old mice and examined the injury site (in separate animals) for up to 21 days post injury. Examination of the mice showed that adhesions had formed between the tendon, the tendon synovium and the skin. The tendon flanking the injury was intact, as shown by the presence of laminin at the intact epithelium (bottom part of Fig 5. A) and laminin occurred throughout the adhesion (Fig. 5B).

DISCUSSION

In this study we show that the surface of the tendon contains a novel BM-epithelium. Damage to the BM-epithelium, either surgically or genetically because of a mutation in the col4a1 gene that encodes the α1(IV) chain of collagen IV, results in adhesion formation. The results are discussed in the context of tendon development, wounding, and adhesions, and highlight the importance of collagen IV in BM synthesis, as well as the need for epithelialisation of tissues in healing and regenerative medicine.

Previous studies have shown that tendon cells cultured in 3D linear fibrin gels synthesise artificial tendons that are similar in ultrastructure to embryonic tendon (8, 21). Our initial studies focused on evaluating the suitability of artificial tendons in tissue engineering applications. As part of these studies the artificial tendons were embedded within a 3D fibrin gel. Fibrin was chosen because it is produced *in vivo* at sites of injury where adhesions are formed (22). During time in culture the artificial tendons gradually became indistinguishable from the fibrin gel as a result of extensive cell migration. In contrast, *ex vivo* tendons incubated in fibrin only lose cells at the site of injury i.e. the cut ends or at sites of injury along the shaft of the tendon. These experiments provided the first indication that native tendons possess a unique property that prevents cell extravagation, especially in the presence of fibrin.

Microarray gene profiling is a powerful approach for performing a genome-wide search for candidate genes involved in cell specialisation. With this in mind, we undertook a microarray comparison of embryonic and postnatal rat tendon. Ranking of the fold changes in gene expression identified genes expressed by keratinized epithelial cells, genes that encode BM components, and genes involved in the formation of the epidermal differentiation complex (EDC). Using antibodies we showed that the BM-epithelium contains both keratin 1 and 10. However, we were unable to confirm the presence of a cornified layer (despite the expression of the genes in embryonic stages) using a toluidine blue barrier assay on whole tendon. We speculate that some cells in tendon might share a common developmental origin with epidermis progenitor cells.

Importantly, the levels of gene expression (as indicated by the microarray analysis) for epithelial cell proteins and BM components were notably higher in embryonic tendon than in adult tendon, suggesting that the BM-epithelium is established during embryonic-to-postnatal development. Electron microscopy showed the presence of flattened cells in embryonic tendon in the absence of an ultrastructurally-distinct BM, which was only apparent in adult tendons. Early studies identified collagen IV in the endotendineum of the extensor carpi radialis muscle with

attached tendon (23). Further studies showed the presence of a thin BM-like layer on both sides of 'flattened fibroblasts' in the peritendineum of adult rat-tail tendon (24, 25). Here we showed that a BM is located at the outermost surface of flexor tendons, which corresponds to the peritendineum according to the nomenclature used by Strocchi and co-workers (25). The results show a delay between the expression of BM genes in embryonic stages and the assembly of the BM in postnatal development. Immunolocalisation showed that the BM in postnatal tendon contains laminin, perlecan, nidogen-1 and the $\alpha1.\alpha1.\alpha2$ network of collagen IV.

Previous studies have highlighted the importance of cell-cell junctions in tendon development. The cells in the core of embryonic tendon are connected via adherens junctions that function to organise the cells and influence the parallelism of the tendon matrix (26). In adult tendon the cells are connected via gap junctions that are involved in intercellular communication in response to mechanical stress (27). We showed here that the epithelial cells at the surface of embryonic tendon are connected by tight junctions, which in other tissues functions as a selective permeability barrier, to maintain apicobasal polarity, and regulate cell behaviour (for example see (28-30)). Staining for tight junction components in embryonic tendon and keratin 1 and 10 in postnatal tendon was a convenient method of visualising the epithelium. Analysis showed that the epithelium in embryonic tendon consisted of several layers of cells whereas in the adult it was a single cell thick. We speculate that the epithelium in embryonic tendon is required to establish the functional BM and to service the cells in the core of the tendon.

Our findings of a BM at the tendon surface prompted us to investigate the requirement of collagen IV in tendon development and injury. ENU-induced mutations in mice had generated the Svc mouse that is small and has vacuolar cataracts (31) resulting from a missense mutation in the col4a1 gene that encodes collagen IV (20). Mice that are heterozygous for the mutation ($col4a1^{+/Svc}$) are viable and develop peripheral iris-corneal adhesions. Studies of the col4a1/col4a2 null mouse has shown that collagen IV is required for mechanical stability of postnatal BMs but is dispensable for BM development (6). Examination of 3 month-old $col4a1^{+/Svc}$ mice showed that, indeed, tendon development was normal in the presence of abnormal collagen IV synthesis. However, the tendons of the mice lacked laminin protein and developed adhesions between the tendon surface and the surrounding tissues. Presumably the absence of laminin and collagen IV in postnatal tendons predisposes the tendon to adhesion formation.

To investigate the role of the epithelium in tendon injury we introduced a partial tenotomy in 4 month-old wild-type mice and analysed the tendons for up to 21 days post injury. Intrasynovial adhesions were evident between the tendon and the tendon sheath. At the sites of adhesion formation the tendons were acellular but the sheath displayed mild hyperplasia. These observations are consistent with cells moving out of the injury site where the BM-epithelium is damaged. Laminin was distributed throughout the adhesion and on its surface. The presence of an intact BM containing a continuous layer of laminin on the surface of the adhesion would explain the long-term stability of these structures.

In conclusion, the results show the importance of the novel BM-epithelium in maintaining the integrity of the tendon. Furthermore, the results suggest that artificial tendons lacking a BM-epithelium might have limited use in tissue engineering applications because of decellularisation of transplanted tissue *in vivo*.

MATERIALS AND METHODS

DMEM (Dulbecco's Modified Eagle's Medium, high glucose), Lascorbic acid 2-phosphate, fetal calf serum (FCS), phosphate buffered saline (PBS) and goat/ donkey anti-rabbit/ mouse Cy3 secondary antibodies were purchased from Invitrogen, UK. Fibrinogen, thrombin, Tween20, bovine serum albumin (BSA), proteinase K, toluidine blue and anti-rabbit laminin antibody were from Sigma Aldrich, UK. Goat anti-mouse/ rabbit Alexa488 secondary antibodies and Vectashield mounting medium with DAPI (4',6-Diamidino-2-phenylindole dihydrochloride) were purchased from Vector labs, Peterborough, UK. Tissue-Tek mounting medium was bought from Fisher Scientific, Loughbourough, UK.

Preparation of artificial tendon

Artificial tendon constructs were prepared as described previously (8). DMEM medium (5 ml) supplemented with L-ascorbic acid 2-phosphate (200 μm) and 10% fetal calf serum was added to each well. The medium was changed and the dishes were scored three times a week until full contraction was achieved.

Artificial tendon culture in a fibrin gel (phase contrast imaging)

At contraction the artificial tendons was encased within a fibrin gel (5 μl thrombin was added, followed by 40 μl fibrinogen) and the tendon cultured for 2 days at 37°C and with 5% CO_2. Phase light and phase contrast microscopy were performed using an Olympus IX51 inverted microscope and images were captured using an Olympus DP70 digital camera.

Artificial tendon culture in a fibrin gel (live cell imaging)

At contraction the artificial tendon was encased within a fibrin gel (5 μl thrombin was added followed by 40 μl fibrinogen) and the tendon cultured for a further 6 days. 2 ml of DMEM medium supplemented with L-ascorbic acid 2-phosphate (200 μm), 10% fetal calf serum and 10 μl calcein AM was used to cover each tendon before incubation at 37ºC for 1 hour. Images were captured using a Leica SP2 Inverted Microscope connected to a personal computer with Leica Confocal Software (Leica Microsystems, Heidelberg, Germany). A heated chamber maintained the tendon at 37°C and with 5% CO_2.

Immunofluorescence

Cryosections of chick tendon (10 μm) were fixed in 100% acetone or methanol at -20°C for 10 min and blocked with 10% normal goat serum or 10% normal donkey serum in PBST (10 mM sodium phosphate, 140 mM NaCl, pH 7.4, 0.1% Tween 20) for 1 hr. Sections were incubated in primary antibody diluted in 5% BSA in PBST overnight at 4°C, washed for 5 x 10 min with PBST and incubated with goat or donkey anti rabbit/mouse-Cy3 (1:100-1000) or goat anti-mouse/rabbit Alexa488 (1:100-1000) for 1 hr at room temperature. Sections were washed for 5 x 10 min with PBST and mounted with Vectashield mounting medium containing DAPI. Control experiments involved omission of the relevant primary antibody and incubation with the appropriate secondary antibody. Little or no fluorescence was detected in control sections. Antibodies used were as follows: Rabbit anti-ZO-1 (1:100, Invitrogen) and rabbit anti-claudin-1 (1:60, Zymed Laboratories). Rabbit polyclonal anti-keratin 1 and 10 were used at 1:100 dilution (Abcam). Secondary goat anti-mouse or goat anti-rabbit Cy3 antibodies were used at 1:1000 dilution. Images were collected on an Olympus BX51 upright microscope using a 20x/ 0.30 Plan Fln objective and captured using a Coolsnap HQ camera through MetaVue Software (Molecular Devices). For analysis of BM components, tail tendons were collected from 20 day old C57BL/6 mice and snap frozen in OCT in liquid nitrogen. Longitudinal cryosections (8 mm) were fixed for 10 min in acetone followed by antigen retrieval using 0.1 M HCl and O.1 M KCl for 10 min. Primary antibodies were incubated overnight. The laminin (1/1000) antibody was a kind gift from Dr. Ulrike Mayer and the H22, H31, H69 antibodies against α2(IV) collagen chain, α3(IV) collagen chain and α6(IV) collagen chain, respectively (1/100), from Dr. Yoshikazu Sadu. The nidogen 1 (1/500) and perlecan (1/500) antibodies were kindly donated by Dr. Rupert Timpl and Dr. Takako Sasaki. Images were captured using a Zeiss LSM510 Meta confocal microscope and Zeiss LSM software. Wax sections of limbs were fixed using a zinc based fixative (32, 33) for 48 hrs at 4ºC, followed by 48 hrs in 50% ethanol. The tendons were then filleted off the bone; wax processed using a Tissue-Tek Vacuum infiltration Processor (Bayer Diagnostics, Newbury, UK) and paraffin embedded. Serial sections (7 μm) were obtained. Sections of tendons were dewaxed and treated for antigen retrieval using proteinase K solution (1 mg/ml in 0.1M Tris-HCl, 50 mM EDTA, pH8) at 37°C for 30 min. Sections were blocked with 10% normal goat serum in PBS-T for 1 hr at room temperature followed by incubation with laminin antibody (1:100) in PBS-T with 5% BSA overnight at 4°C. Sections were rinsed for 5 x 10 min and incubated with goat anti-rabbit Cy3 (1:200), 1 hr at room temperature. Sections were washed for 5 x 10 min. Sections were mounted using Vectashield with DAPI (Vector labs).

Preparation for electron microscopy

Tendons were prepared for transmission electron microscopy as previously described (34, 35). Sections (85 nm thick) were collected and examined in a Tecnai 12 BioTwin transmission electron microscope operated at 100 keV accelerating voltage. Images were collected on film at 2900 x magnification.

Mouse injury model

All animal procedures were approved by the Local Ethical Committee at the University of Manchester and complied with British Home Office regulations on the care and use of laboratory animals. The mice were anaesthetized as described (36). Mice were four-week-old C57/BL6. The flexor digitorum profundus in both hind limbs in the mice were exposed by a skin incision. A 50% laceration was made in the tendon between the A1 and A3 pulley. A proximal tenotomy was made at the ankle joint so the tendons were completely divided distally. This immobilized the limb, promoting adhesion development. The skin incisions were closed using 10/0 polyamide sutures (B Braun Medical, Germany). Six mice were euthanized at each time point: day 3, day 21 post-injury.

Toluidine blue barrier assay

The skin permeability assay was performed as described previously (18). Embryos or dissected mouse flexor tendons were rinsed in PBS and successively immersed in 25, 50, 75, and 100% methanol for 1 min each. They were then rehydrated in PBS and stained with toluidine blue (0.1%) in water for 10 min at room temperature. Samples were briefly washed in PBS and were immediately photographed. Images were taken using a Nikon D200 camera with a 105 mm f2.8 Lens.

Funding

This work was supported by The Wellcome Trust (076939/Z/05/Z) to KEK and The Medical Research Council (G0601268) to TVA. S.A-Y was funded by a grant (aa08961) from the Kuwaiti Ministry of Higher Education. We would like to acknowledge Glaxo-Smith-Kline for the generation of the *Col4a1*$^{+/Svc}$ mice.

SUPPLEMENTARY MATERIAL

A supplementary movie is available at HMG online.

ACKNOWLEDGEMENTS

The authors thank Nicholas Kalson and Zoher Kapacee for help with preparing artificial tendons and live cell imaging, and Glaxo-Smith-Kline for the generation of the *Col4a1*$^{+/Svc}$ mice.

REFERENCES

1 Khanna, A., Friel, M., Gougoulias, N., Longo, U.G. and Maffulli, N. (2009) Prevention of adhesions in surgery of the flexor tendons of the hand: what is the evidence? *Br Med Bull*, **90**, 85-109.

2 Risberg, B. (1997) Adhesions: preventive strategies. *Eur J Surg Suppl*, 32-39.

3 Alpay, Z., Saed, G.M. and Diamond, M.P. (2008) Postoperative adhesions: from formation to prevention. *Semin Reprod Med*, **26**, 313-321.

4 Schwarzbauer, J. (1999) Basement membranes: Putting up the barriers. *Curr Biol*, **9**, R242-244.

5 Aumailley, M., Bruckner-Tuderman, L., Carter, W.G., Deutzmann, R., Edgar, D., Ekblom, P., Engel, J., Engvall, E., Hohenester, E., Jones, J.C. *et al.* (2005) A simplified laminin nomenclature. *Matrix Biol*, **24**, 326-332.

6 Poschl, E., Schlotzer-Schrehardt, U., Brachvogel, B., Saito, K., Ninomiya, Y. and Mayer, U. (2004) Collagen IV is essential for basement membrane stability but dispensable for initiation of its assembly during early development. *Development*, **131**, 1619-1628.

7 Iozzo, R.V., Zoeller, J.J. and Nystrom, A. (2009) Basement membrane proteoglycans: modulators Par Excellence of cancer growth and angiogenesis. *Mol Cells*, **27**, 503-513.

8 Kapacee, Z., Richardson, S.H., Lu, Y., Starborg, T., Holmes, D.F., Baar, K. and Kadler, K.E. (2008) Tension is required for fibripositor formation. *Matrix Biol*, **27**, 371-375.

9 Bragulla, H.H. and Homberger, D.G. (2009) Structure and functions of keratin proteins in simple, stratified, keratinized and cornified epithelia. *J Anat*, **214**, 516-559.

10 Candi, E., Schmidt, R. and Melino, G. (2005) The cornified envelope: a model of cell death in the skin. *Nat Rev Mol Cell Biol*, **6**, 328-340.

11 Steven, A.C. and Steinert, P.M. (1994) Protein composition of cornified cell envelopes of epidermal keratinocytes. *J Cell Sci*, **107 (Pt 2)**, 693-700.

12 Marshall, D., Hardman, M.J., Nield, K.M. and Byrne, C. (2001) Differentially expressed late constituents of the epidermal cornified envelope. *Proc Natl Acad Sci U S A*, **98**, 13031-13036.

13 Mischke, D., Korge, B.P., Marenholz, I., Volz, A. and Ziegler, A. (1996) Genes encoding structural proteins of epidermal cornification and S100 calcium-binding proteins form a gene complex ("epidermal differentiation complex") on human chromosome 1q21. *J Invest Dermatol*, **106**, 989-992.

14 Nemes, Z. and Steinert, P.M. (1999) Bricks and mortar of the epidermal barrier. *Exp Mol Med*, **31**, 5-19.

15 Jackson, B., Tilli, C.M., Hardman, M.J., Avilion, A.A., MacLeod, M.C., Ashcroft, G.S. and Byrne, C. (2005) Late cornified envelope family in differentiating epithelia--response to calcium and ultraviolet irradiation. *J Invest Dermatol*, **124**, 1062-1070.

16 Jensen, J.M. and Proksch, E. (2009) The skin's barrier. *G Ital Dermatol Venereol*, **144**, 689-700.

17 Norlen, L. (2006) Stratum corneum keratin structure, function and formation - a comprehensive review. *Int J Cosmet Sci*, **28**, 397-425.

18 Hardman, M.J., Sisi, P., Banbury, D.N. and Byrne, C. (1998) Patterned acquisition of skin barrier function during development. *Development*, **125**, 1541-1552.

19 Khoshnoodi, J., Pedchenko, V. and Hudson, B.G. (2008) Mammalian collagen IV. *Microsc Res Tech*, **71**, 357-370.

20 Van Agtmael, T., Schlotzer-Schrehardt, U., McKie, L., Brownstein, D.G., Lee, A.W., Cross, S.H., Sado, Y., Mullins, J.J., Poschl, E. and Jackson, I.J. (2005) Dominant mutations of Col4a1 result in basement membrane defects which lead to anterior segment dysgenesis and glomerulopathy. *Hum Mol Genet*, **14**, 3161-3168.

21 Bayer, M.L., Yeung, C.-Y.C., Kadler, K.E., Ovortrup, K., Baar, K., Svensson, R.B., Magnusson, S.P., Krogsgaard, M., Koch, M. and Kjaer, M. (2010) Mature human tendon fibroblasts initiate collagen fibrillogenesis ex vivo. *Biomaterials*, **in press.**

22 Menzies, D. (2004) Adhesions: the cellular science. *Hosp Med*, **65**, 337-339.

23 Duance, V.C., Restall, D.J., Beard, H., Bourne, F.J. and Bailey, A.J. (1977) The location of three collagen types in skeletal muscle. *FEBS Lett*, **79**, 248-252.

24 Guizzardi, S., Foidart, J.M., Leonardi, L., Strocchi, R. and Ruggeri, A. (1987) Evidence for basement membranes in rat tail tendon sheaths. *Basic Appl Histochem*, **31**, 177-181.

25 Strocchi, R., Leonardi, L., Guizzardi, S., Marchini, M. and Ruggeri, A. (1985) Ultrastructural aspects of rat tail tendon sheaths. *J Anat*, **140 (Pt 1)**, 57-67.

26 Richardson, S.H., Starborg, T., Lu, Y., Humphries, S.M., Meadows, R.S. and Kadler, K.E. (2007) Tendon development requires regulation of cell condensation and cell shape via cadherin-11-mediated cell-cell junctions. *Mol Cell Biol*, **27**, 6218-6228.

27 McNeilly, C.M., Banes, A.J., Benjamin, M. and Ralphs, J.R. (1996) Tendon cells in vivo form a three dimensional network of cell processes linked by gap junctions. *J Anat*, **189**, 593-600.

28 Turner, J.R. (2009) Intestinal mucosal barrier function in health and disease. *Nat Rev Immunol*, **9**, 799-809.

29 Furuse, M. and Tsukita, S. (2006) Claudins in occluding junctions of humans and flies. *Trends Cell Biol*, **16**, 181-188.

30 Lee, D.B., Huang, E. and Ward, H.J. (2006) Tight junction biology and kidney dysfunction. *Am J Physiol Renal Physiol*, **290**, F20-34.

31 Thaung, C., West, K., Clark, B.J., McKie, L., Morgan, J.E., Arnold, K., Nolan, P.M., Peters, J., Hunter, A.J., Brown, S.D. *et al.* (2002) Novel ENU-induced eye mutations in the mouse: models for human eye disease. *Hum Mol Genet*, **11**, 755-767.

32 Beckstead, J.H. (1994) A simple technique for preservation of fixation-sensitive antigens in paraffin-embedded tissues. *J Histochem Cytochem*, **42**, 1127-1134.

33 Beckstead, J.H. (1995) A simple technique for preservation of fixation-sensitive antigens in paraffin-embedded tissues: addendum. *J Histochem Cytochem*, **43**, 345.

34 Canty, E.G., Lu, Y., Meadows, R.S., Shaw, M.K., Holmes, D.F. and Kadler, K.E. (2004) Coalignment of plasma membrane channels and protrusions (fibripositors) specifies the parallelism of tendon. *Journal of Cell Biology*, **165**, 553-563.

35 Humphries, S.M., Lu, Y., Canty, E.G. and Kadler, K.E. (2008) Active negative control of collagen fibrillogenesis in vivo: Intracellular cleavage of the type I procollagen propeptides in tendon fibroblasts without intracellular fibrils. *Journal of Biological Chemistry*.

36 Wong, J.K., Cerovac, S., Ferguson, M.W. and McGrouther, D.A. (2006) The cellular effect of a single interrupted suture on tendon. *J Hand Surg Br*, **31**, 358-367.

LEGENDS TO FIGURES

(Please note, the same legends have been placed next to the figures to help the reviewers.)

Figure 1. Ex vivo tendons but not artificial tendons have a cell-retentive barrier. (A) Phase contrast image of an artificial tendon. **(B)** Phase contrast image of an artificial tendon incubated in a fibrin gel. **(C)** Z-stack image of an artificial tendon embedded in a fibrin gel and incubated with Calcein AM. Live cells (green) are apparent in the shaft of the tendon and in the fibrin (top of image). **(D)** Ex vivo mouse flexor tendon embedded in a fibrin gel and incubated with Calcein AM. Live cells exit the tendon at the cut end.

Figure 2. Identification of an epithelium at the surface of tendon. (A-D) Immunofluorescence detection of: ZO-1 (**A**) and claudin-1 **(B)** in transverse sections of day 13 embryonic chick tendon; keratin 1 **(C)** and keratin 10 **(D)** in longitudinal sections of postnatal mouse flexor digitorum superficialis. Blue, DAPI staining. **(E-G)** Toluidine blue barrier assay performed on E15.5 mouse embryo **(E),** P1 newborn moue (**F**), and P28 mouse flexor digitorum superficialis, which was subsequently sectioned (longitudinally) for light microscopy (**G**).

Figure 3. Characterisation of the basement membrane in postnatal mouse and rat tendon. (**A-B**) TEM of mouse and rat tail tendon showing the presence of flat epithelial cells adjacent to a thin BM. (**C**) Immunofluorescence detection of α3(IV) chain of type IV collagen (Col4a3), α2(IV) chain of type IV collagen (Col4a2), and α6(IV) chain of type IV collagen (Col4a6) in longitudinal sections of P28 mouse tail tendon. **(D)** Immunofluorescence detection of nidogen-1 (Nid 1), laminin (Ln), and perlecan (Perl) in longitudinal sections of P28 mouse tail tendon.

Figure 4. Col4$^{+/svc}$ mouse tendons lack a basement membrane and have abnormal adhesions with overlying tissues. (A-B) Immunofluoresence detection of laminin (red) in longitudinal sections of postnatal mouse hind limb showing flexor digitorum profundus (FDP) and flexor digitorum superficialis (FDS) in wild-type **(A)** and Col4a1$^{+/Svc}$ **(B)** mice. **(C-D)** H & E staining of longitudinal sections through a wild-type (**C**) and Col4a1$^{+/Svc}$ (**D**) mouse hind limb. T, tendon. S, synovial space. Insert in (**D**) shows absence of a synovial space and hyperplasia (H) of the tendon synovium. Blue, DAPI. S, synovial space. Arrows, tendon epithelium.

Figure 5. Laminin in tendon adhesions. Immunofluorescence detection of laminin (red) in mouse flexor digitorum profundus 3 days (**A**) and (**B**) 21 days post injury *in vivo*. Blue, DAPI. Arrow, laminin expression at the site of the tenotomy. FDP, flexor digitorum profundus.

FIGURE 1

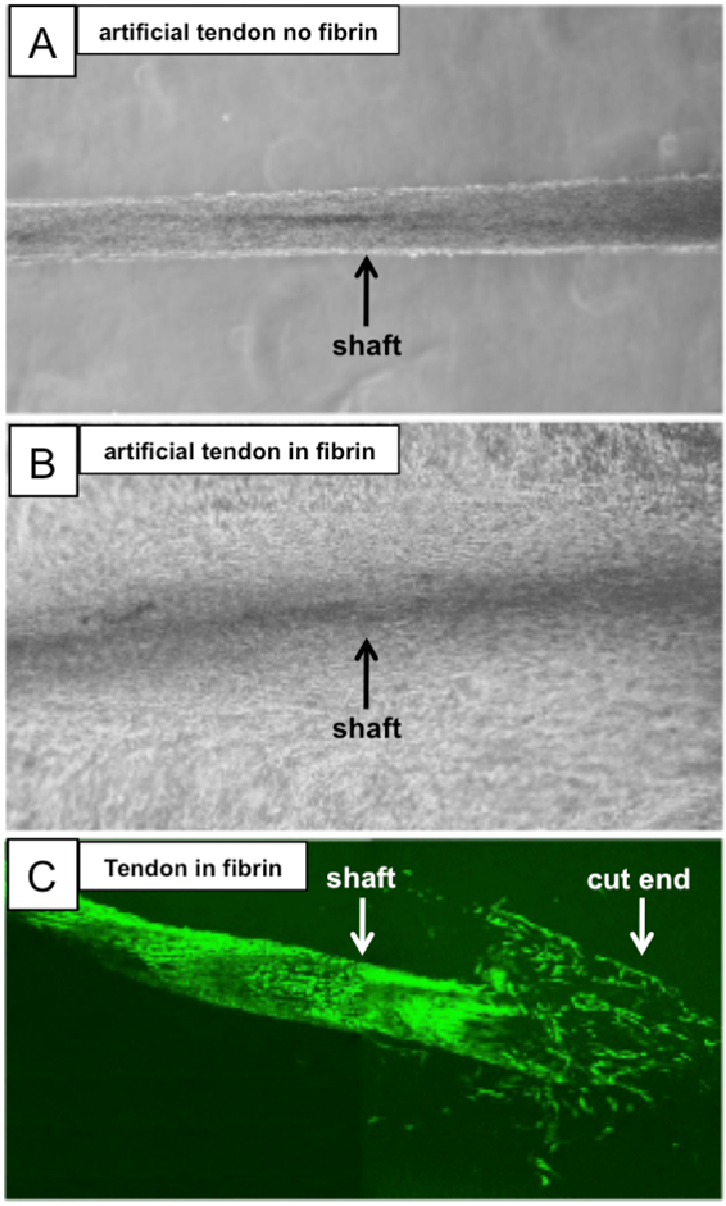

Ex vivo tendons but not artificial tendons have a cell-retentive barrier. (A) Phase contrast image of an artificial tendon. **(B)** Phase contrast image of an artificial tendon incubated in a fibrin gel. **(C)** Z-stack image of an artificial tendon embedded in a fibrin gel and incubated with Calcein AM. Live cells (green) are apparent in the shaft of the tendon and in the fibrin (top of image). **(D)** Ex vivo mouse flexor tendon embedded in a fibrin gel and incubated with Calcein AM. Live cells exit the tendon at the cut end.

FIGURE 2

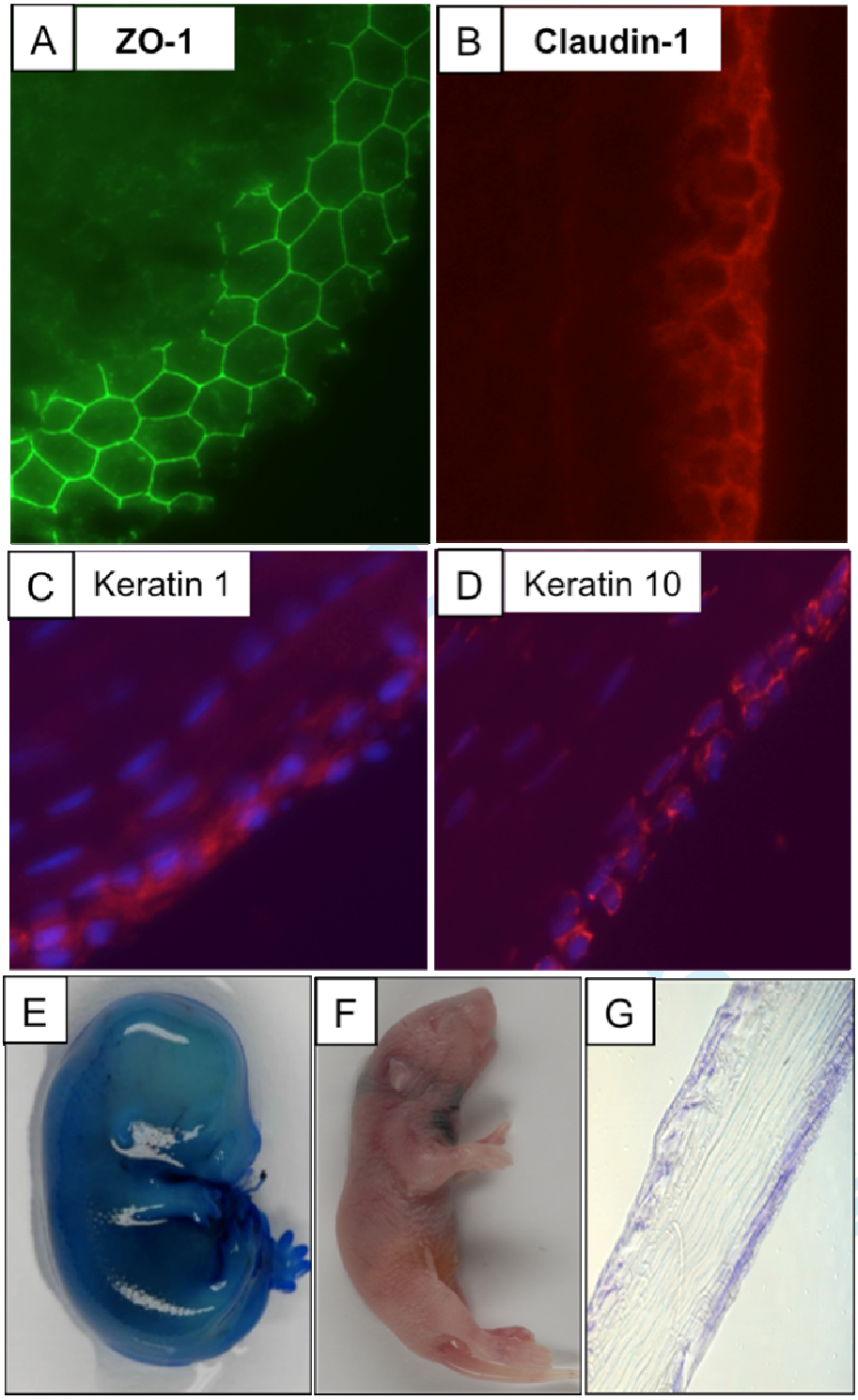

Identification of an epithelium at the surface of tendon. (A-D) Immunofluorescence detection of: ZO-1 (**A**) and claudin-1 **(B)** in transverse sections of day 13 embryonic chick tendon; keratin 1 **(C)** and keratin 10 **(D)** in longitudinal sections of postnatal mouse flexor digitorum superficialis. Blue, DAPI staining. **(E-G)** Toluidine blue barrier assay performed on E15.5 mouse embryo **(E),** P1 newborn moue (**F**), and P28 mouse flexor digitorum superficialis, which was subsequently sectioned (longitudinally) for light microscopy (**G**).

FIGURE 3

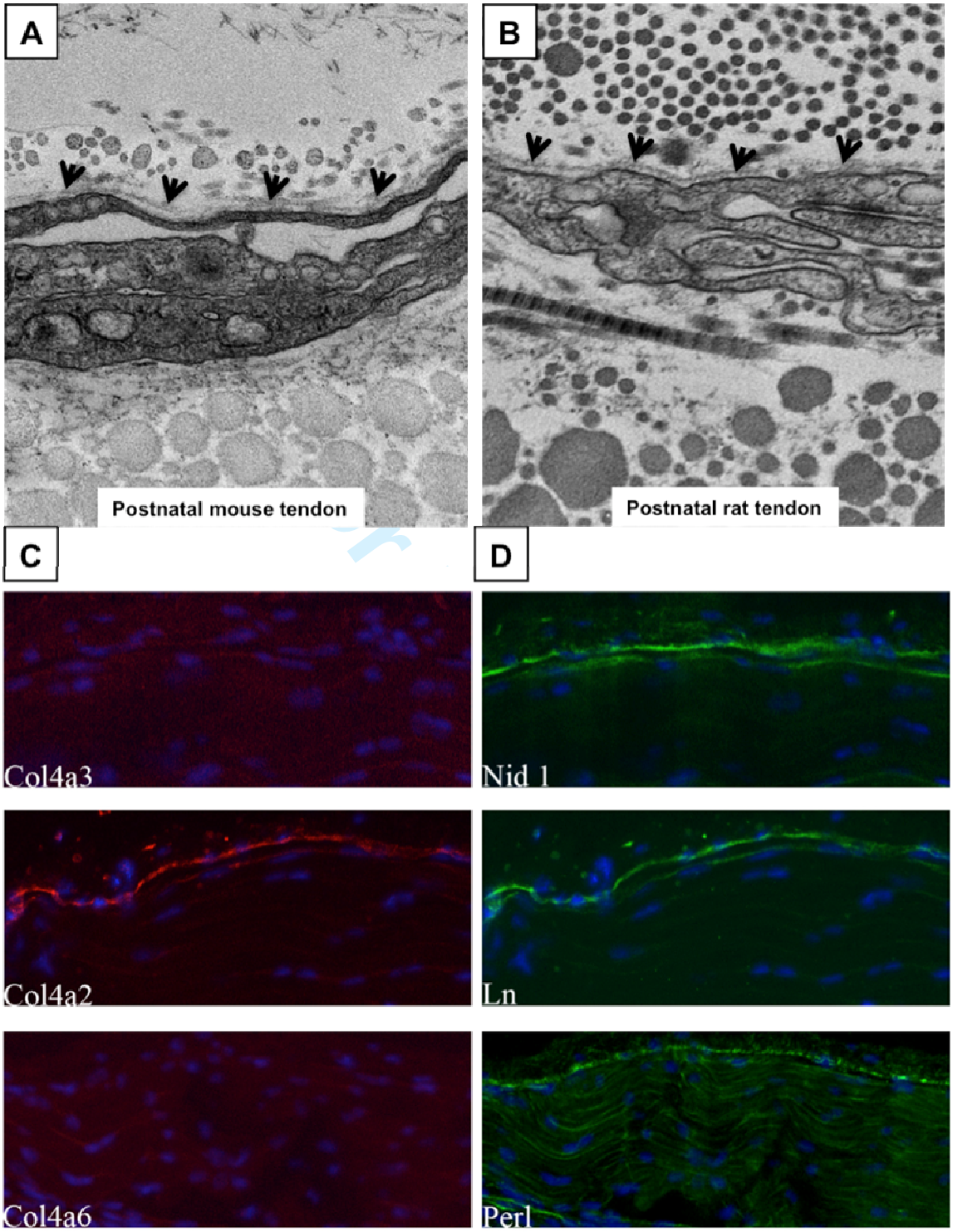

Characterisation of the basement membrane in postnatal mouse and rat tendon. (**A-B**) TEM of mouse and rat tail tendon showing the presence of flat epithelial cells adjacent to a thin BM. (**C**) Immunofluorescence detection of α3(IV) chain of type IV collagen (Col4a3), α2(IV) chain of type IV collagen (Col4a2), and α6(IV) chain of type IV collagen (Col4a6) in longitudinal sections of P28 mouse tail tendon. **(D)** Immunofluorescence detection of nidogen-1 (Nid 1), laminin (Ln), and perlecan (Perl) in longitudinal sections of P28 mouse tail tendon.

FIGURE 4

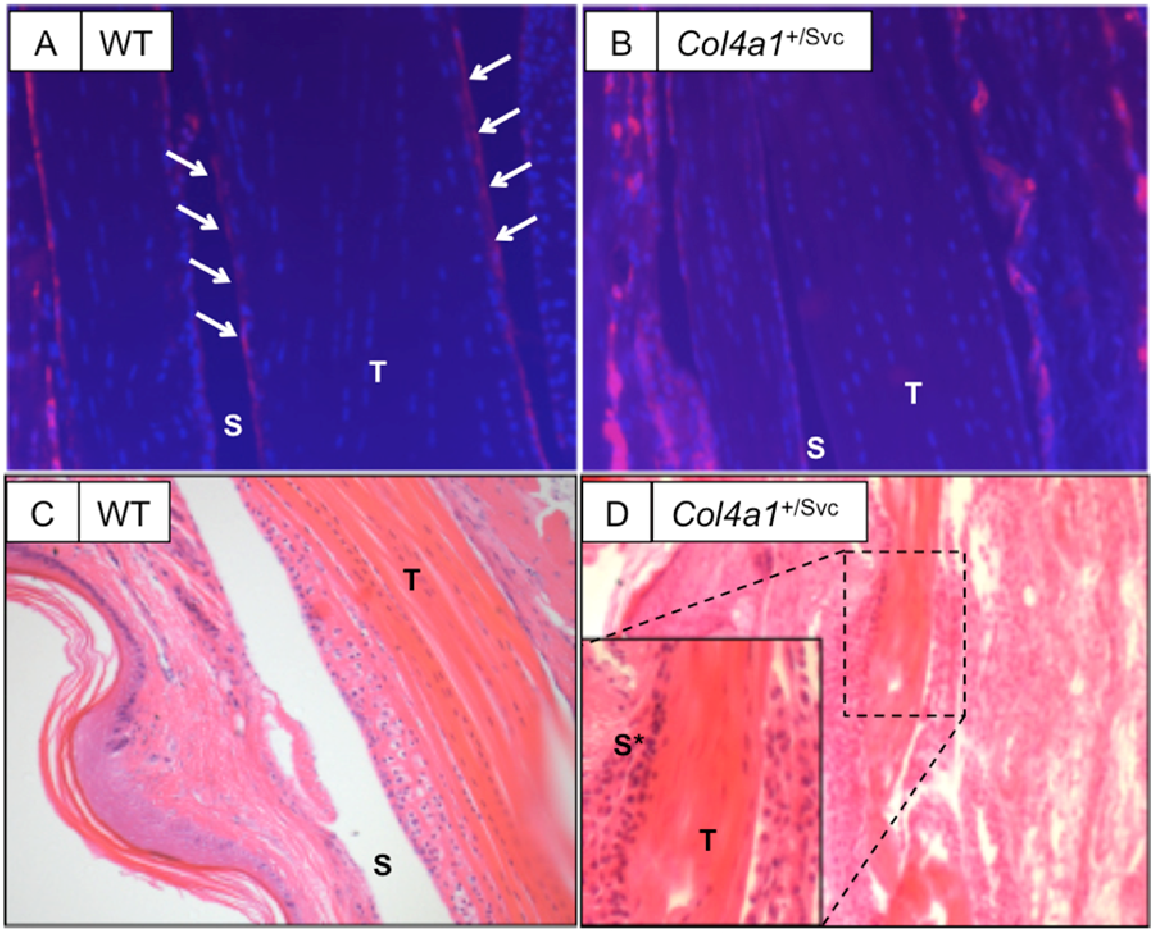

Col4$^{+/SVC}$ mouse tendons lack a basement membrane and have abnormal adhesions with overlying tissues. (A-B) Immunofluoresence detection of laminin (red) in longitudinal sections of postnatal mouse hind limb showing flexor digitorum profundus (FDP) and flexor digitorum superficialis (FDS) in wild-type **(A)** and Col4a1$^{+/Svc}$ **(B)** mice. **(C-D)** H & E staining of longitudinal sections through a wild-type (**C**) and Col4a1$^{+/Svc}$ (**D**) mouse hind limb. T, tendon. S, synovial space. Insert in (**D**) shows absence of a synovial space and hyperplasia (H) of the tendon synovium. Blue, DAPI. S, synovial space. Arrows, tendon epithelium.

FIGURE 5

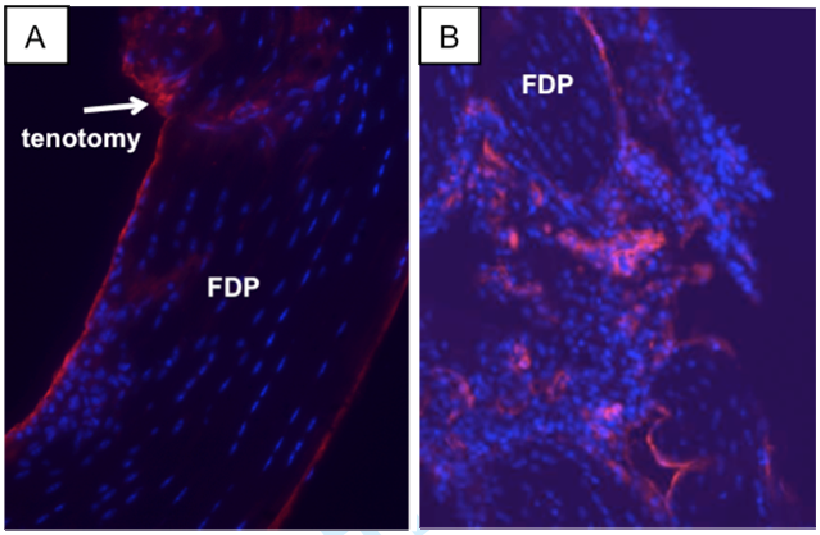

Laminin in tendon adhesions. Immunofluorescence detection of laminin (red) in mouse flexor digitorum profundus 3 days (**A**) and (**B**) 21 days post injury *in vivo*. Blue, DAPI. Arrow, laminin expression at the site of the tenotomy. FDP, flexor digitorum profundus.